Final Report

EFFECT OF CHEMICAL MECHANISM UNCERTAINTY ON AIRSHED MODEL RESULTS

Systems Applications International, Inc.

FEBRUARY 1998

Final Report

EFFECT OF CHEMICAL MECHANISM UNCERTAINTY ON AIRSHED MODEL RESULTS

SYSAPP-97/57

February, 1998

Prepared for

California Air Resources Board
Technical Support Division
2020 L Street
Sacramento, CA 95814

Prepared by

Gary Whitten

Systems Applications International, Inc.
101 Lucas Valley Road
San Rafael, California 94903

and

James Killus
2305 Helena Court
Pinole, California 94564

Copyright 1997 by Systems Applications International, Inc.

DISCLAIMER

The statements and conclusions in this report are those of the Contractor and not necessarily those of the California Air Resources Board (ARB). The mention of commercial products, their source, or their use in connection with material reported herein is not to be construed as actual or implied endorsement of such products.

Contents

EFFECT OF CHEMICAL MECHANISM UNCERTAINTY ON AIRSHED MODEL RESULTS: PHASE I

SUMMARY

The standard Carbon Bond-IV (CB-IV) chemical mechanism is used in the regulatory version of the Urban Airshed Model (UAM) that the U.S. EPA maintains on its internet bulletin board system. This chemical mechanism has been only slightly modified since it was published by Gery et al. (1989). The modifications were considered so minor by the EPA, that a full scale re-evaluation against smog chamber data was not deemed necessary. During Phase I of this study we have addressed the potential effect that uncertainties in the chemistry might have on simulations of ozone formation by developing and testing two alternative forms of the standard CB-IV mechanism: these alternative forms are characterized by either a high or a low radical-flux version of the same chemistry. Phase II is to implement the alternative versions of the chemistry into a UAM and simulate control strategy scenarios that should demonstrate a potential range of uncertainty due to the changes in the chemistry.

As part of Phase I all three versions were tested against a limited set of smog chamber experiments and all three fall within the error bounds published for the original CB-IV by Gery et al. (1989). One development of these tests was that the standard mechanism seems to simulate the smog chamber data better than in 1989 (one exception, discussed below, being newer data with urban mixtures at the lowest VOC-to-NOx ratios). This appears to be due to the use of some newer experiments which have more accurate data and better chamber characterization than existed 10 years ago; that is, a significant fraction of previously poor agreement between data and simulations using the standard mechanism was due to inaccurate data and the use of inadequate chamber characterization parameters.

Box model tests show that the alternative versions do give different control strategy implications when the scenario involves changing the emissions ratio of volatile organic compound (VOC) to nitrogen oxides (NOx). For example, if only VOC emissions are to be reduced, then the effectiveness of such a strategy depends significantly on the mechanism used. Somewhat surprising is the finding that when both VOC and NOx are changed by the same percentage (i.e., when overall emissions are changed but the VOC-to-NOx ratio is held constant) the alternative versions of the chemistry give results very similar to the standard CB-IV.

The construction of the high flux alternative mechanism was done by increasing all radical sources by 30 percent and increasing all radical sinks by the same 30 percent. The low flux alternative reduced these same sources and sinks. These changes produce similar steady-state levels of the various free radicals that control the overall chemistry, but the “flux” of radicals through the system of chain reactions is much higher or lower than for the standard mechanism. The similar levels of radical concentration lead to acceptable simulations of the smog chamber data because one of the important criteria for simulating smog chamber data has always been the decay rate of key VOC species (which, of course, depends strongly on the concentration of radicals, especially the hydroxyl radical [OH]).

The decay of key organic species produces secondary peroxide radicals which immediately convert nitric oxide (NO) to nitrogen dioxide (NO_2), a process that is directly connected to the build-up of ozone. Since this decay of organic species is typically the rate-limiting step for the whole process, it is important to simulate the decay rate accurately in order to achieve acceptable simulations of smog chamber experiments. However, the radical sources tend to come from the organics (e.g., formaldehyde photolysis) while a key radical sink comes from the NOx (i.e., the reaction of OH with NO_2). Hence, it is reasonable to find that the control strategy implications focus on changes in the emissions ratio of VOC-to-NOx. Likewise the fringes of acceptable smog chamber simulation also tend to be those experiments that are at the lowest and highest VOC-to-NOx ratio. Nevertheless the newer experiments, that often have good data for formaldehyde (a key radical source species), also indicate that the standard mechanism still appears to have the "best" radical flux even for the mid-range of VOC-to-NOx ratio experiments. That is, neither the high nor the low flux alternate mechanism appears to fit the smog chamber data better than the standard CB-IV.

Other methods of addressing the uncertainty in UAM simulations due to chemistry are possible. Uncertainty is often assumed to be a fairly random phenomenon and others have addressed the impact of uncertainties by multiple tests using Monte Carlo variations of the key parameters. However, a key ground rule for this particular study has been that the smog chamber tests must still be acceptable for an alternate version of the chemistry to be considered for the UAM tests in Phase II. A comprehensive smog chamber screening of random versions of the mechanism would be costly and there is no indication that randomly selected candidates which passed the smog chamber screening would lead to significantly different control strategy implications than the standard mechanism.

Another source of differences in UAM-based simulations that some might call a form of uncertainty would stem from the use of a newly developed standard chemical mechanism. Such a new mechanism could be developed incorporating the latest scientific information. But this new mechanism would have to be developed in such as way as to still be capable of simulating the same database used to test the original CB-IV, plus any new data that perhaps the original CB-IV cannot simulate acceptably. Another ground rule of the present study has been <u>not</u> to develop a new mechanism but to address the uncertainties in the original CB-IV as still used in regulatory applications of the UAM. There are at least two published studies that have concluded that the CB-IV shows poor simulation performance (low ozone generation compared to observed data) with urban mixtures of VOC at the lowest VOC-to-NOx ratios. An expanded version of the CB-IV that includes the strong photolysis of higher aldehydes is shown in this study to improve performance under such conditions.

INTRODUCTION

Kinetic mechanisms used for simulating photochemical smog formation in regulatory models such as the Urban Airshed Model (UAM) are evaluated using data from smog chamber experiments. Before being published in the *Journal of Geophysical Research* the Carbon Bond mechanism version four (CB-IV) was tested against 170 experiments involving three different smog chambers. The U.S. Environmental Protection Agency, who sponsored the development of the CB-IV, also carefully reviewed the protocols used to evaluate this mechanism before recommending its use in regulatory applications of the UAM.

The California Air Resources Board has designed the present study to develop alternative versions of the CB-IV that, on one hand, fall within the range of published mechanistic uncertainties and still meet some measure of acceptable performance for simulating a smog chamber database, but, on the other hand, provide different estimate of control strategy effectiveness when used in the UAM. These different control strategy estimates will then define a measure of the bounds of uncertainty that might exist in regulatory applications of the UAM, due solely to uncertainties in the CB-IV itself. Therefore, the protocols described in this document play a key role in this project; these protocols are intended to describe the smog chamber database to be used, to outline the procedures to be used to simulate that database, and to define the measures of acceptable simulation performance.

In a previous report (the Task 2 report of 17 January 1997 included here as Appendix B) the development of the alternative mechanisms was described. These alternative versions of the CB-IV are called the high and low radical flux versions. Since the original CB-IV was developed and tested against a smog chamber database using a hierarchical approach, the high and low radical flux alternates to the standard CB-IV are to follow a similar stepwise validation path. Thus, the database must have a sufficient number of experiments at each of these hierarchical steps. In addition to an adequate number of experiments at each step, a reasonable range of VOC-to-NOx precursor ratios also would appear to be important. Finally, a database involving several smog chamber facilities provides more confidence than using data from only one chamber.

Discussions of the currently available database and how it was to be utilized in this project are found in the protocol document included here as Appendix C. The results of the smog chamber modeling follow this section. After the smog chamber tests are discussed, box model tests of potential control strategies are given.

RESULTS

Smog chamber tests were performed on a sample set of the latest available smog chamber data from the University of North Carolina (UNC). The hierarchical approach was used based on the standard mechanism as used by the U.S. EPA in regulatory applications and coded into the Urban Airshed Model (UAM-IV) and available on the internet from the EPA's Bulletin Board System. This version of the CB-IV is reproduced in Table 1a; reaction numbers correspond to those used in UAM code and as referenced below. In order to simulate the smog chamber data, the only modifications made to the chemistry involved using the background VOC, wall effects, and photolysis rates deemed appropriate for the UNC chamber. To create the alternate high and low radical flux versions of the chemistry net radical sources and sinks were increased or decreased by 30 percent, respectively. These net radical sources and sinks affected 16 reactions in the CB-IV mechanism. These 16 reactions are identified below.

The formaldehyde and other photolytic species tests are discussed in Appendix A. Here the smog chamber simulation results for the rest of the hierarchical series are presented. This series begins with ethene as the only VOC. Then propene only, toluene only, and m-xylene only experiments were tested separately. Finally, some experiments using the UNC full urban mixture (SYNURB) were simulated. The smog chamber experiments to be used for testing the mechanisms were prioritized to focus on the latest data available. The number of chamber experiments was determined mainly by the need to demonstrate only that the standard mechanism can still provide adequate reproductions of the new data. As will be seen below, the new data tend to show that the standard mechanism, if anything, tends to work better than the original mechanism of Gery et al. (1989) using the older data.

Reactions Modified

To create the high and low flux alternate versions of the CB-IV chemistry some 16 reactions are involved. In all cases the rate constants, photolysis, or stoichiometric constants relating to net radical sources or sinks were changed by 30 percent. To create the high flux version all changes were 30 percent increases (i.e., times a factor of 1.3) and to create the low flux version all changes were 30 percent decreases (i.e., times a factor of 0.7). The overall differences between the high and low flux changes amount to nearly a factor of two (i.e., 1.86 = 1.3/0.7).

Five photolysis reactions were changed by the appropriate factor. These involved the species ozone (to O^1D, reaction 9), HCHO (to radicals, reaction 38), ALD2 (reaction 45), OPEN (reaction 69), and MGLY (reaction 74). Seven rate constants representing net radical sinks were changed by the appropriate factor. These involved the reaction of OH with NO_2 (reaction 26), and the radical-radical reactions combining HO_2 with itself (reactions 32 and 33), with C_2O_3 (reaction 50), and XO_2 (reaction 86) plus the self-reactions for C_2O_3 (reaction 49) and XO_2 (reaction 80). In the remaining 4 reactions that were affected, only the stoichiometric coefficients leading to radical products were altered. In all 4 cases the reaction of ozone with an olefinic bond is represented; for the species OLE (reaction 58) the radical products of HO_2 and OH were altered, for the species ETH (reaction 62) only the HO_2 product was altered, for the species OPEN (reaction 71) the radical products of C_2O_3, OH, and HO_2 were involved, and for the species ISOP (reaction 77) the radical products of HO_2 and OH were changed.

Three photolysis reactions which were not changed could use some explanation: these three reactions are for the species NO_2 (reaction 1), HONO (reaction 23), and H_2O_2 (reaction 34). The photolysis of NO_2 produces an oxygen atom, O^3P. First of all, O^3P is not one of the HOx radicals, which drive the chain reactions leading to ozone formation through conversions of NO to NO_2. Second, the oxygen atom that does result from NO_2 photolysis, mainly cycles through a well known "do nothing" chain independent of the reactions that involve HOx radicals. This independent "do nothing" chain involves reactions 1, 2, and 3. The photoysis of HONO was not changed because even though the OH produced is indeed part of the HOx group of radicals, this photolysis is also part of a rapid "do nothing" chain cycle that operates independent of the main HOx reactions which govern the production of ozone. This "do nothing" chain involves reactions 22 (which produces HONO from OH and NO) and 23 and unless there is a significant independent source of HONO, there is no net production of OH from reaction 23. The photolysis of H_2O_2 (reaction 34) was not changed first because it is not a significant contribution to HOx in urban atmospheres and second because H_2O_2 formation from the HO_2 self reaction (reactions 32 and 33) sevrves as an important sink for HOx radicals. Furthermore, when H_2O_2 does photolyze it is also part of a minor "do nothing" cycle which works against the radical-sink function of H_2O_2.

The full high and low flux chemical reaction sets are detailed in Tables 1b and 1c.

Ethene

The UNC database lists 51 experiments using only ethene and NOx. Since the CB-IV was published in 1988, there have been 13 new ethene-only experiments; of these, 5 experiments with data in final form were simulated for this project. Table 2 presents a summary of the inputs used and Table 2a presents the comparative ozone peak values and percent differences compared to the observed ozone values. Figures 1 through 15 show the data and simulations in more detail. Data are always shown using only points and simulations are always shown only as lines.

Table 2 -- Ethene Simulation Input Summary.

Date	VOC ppmC	NOx ppm	VOC/ NOx	10^5 wall HONO ppm/min	10^4 wall HCHO ppm/min	initial HONO ppb
ST1995B	4.0	0.651	6.14	5	15	2
ST1295B	2.0	0.647	3.09	5	10	4
AU1688B	1.94	0.408	7.84	5	8	2
JL0688R	3.2	0.344	9.30	5	1.5	1
JL0688B	0.573	0.349	1.64	5	1.5	3

Table 2a -- Ethene Simulation Performance Summary Using Standard and Alternate CB-IV Mechanisms.

Date	Obs. O_3 ppb	Std. O_3 ppb	Error to Obs. %	High Flux ppb	Error to Obs. %	Low Flux ppb	Error to Obs. %
ST1995B	1200	1180	-1.7	1100	-8.3	1177	-1.9
ST1295B	670	590	-11.9	627	-6.4	533	-20.4
AU1688B	1000	990	-1.0	971	-2.9	1037	+3.7
JL0688R	1080	1050	-2.8	1017	-5.8	1112	+3.0
JL0688B	85	84	-2.4	75	-9.6	91	+9.6

These results indicate that the inorganic and ethene reactions can simulate these data fairly well over a rather wide range of VOC/NOx ratios (i.e., from the data of July 6, 1988, a ratio of 1.64 in the blue side and a ratio 9.30 in the red side). With the possible exception of the low flux simulation of the September 12, 1995, experiment, the standard and alternative versions perform similarly. Thus, the radical fluxes appear to be well balanced in spite of nearly a factor of two variation in radical source/sink totals between the high and low flux versions.

Propene

Propene in addition to having its own series of olefinic reactions that are different from those for ethene, adds the important PAN chemistry and acetaldehyde to the hierarchical approach of mechanism validation. In the carbon-bond scheme, propene also brings in paraffin chemistry in that propene is treated as OLE plus PAR. However, the rate constants for OLE use those for propene, which are much greater than any PAR reactions. Hence, the role that PAR plays in propene chemistry is indeed minor.

The UNC database lists over 90 experiments using only propene and NOx. Since the CB-IV was published in 1988, there have been 18 new propene-only experiments; of these, 2 experiments with data in final form were simulated for this project. Table 3 presents a summary of the inputs used and Table 3a presents the comparative ozone peak values and percent differences compared to the observed ozone values. Figures 16 through 24 show the data and simulations in more detail. Data are always shown using only points and simulations are always shown only as lines.

Table 3 -- Propene Simulation Input Summary.

Date	VOC ppmC	NOx ppm	VOC/ NOx	10^5 wall HONO ppm/min	10^4 wall HCHO ppm/min	initial HONO ppb
ST1295R	3.04	0.658	4.62	5	1.5	1
JL0194B	1.46	0.306	4.77	5	1.4	0

Table 3a -- Propene Simulation Performance Summary Using Standard and Alternate CB-IV Mechanisms.

Date	Obs. O_3 ppb	Std. O_3 ppb	Error to Obs. %	High Flux ppb	Error to Obs. %	Low Flux ppb	Error to Obs. %
ST1295R	1105	837	-24.3	846	-23.4	800	-27.6
JL0194B	850	760	-10.6	729	-14.2	800	-5.9

Toluene

The CB-IV uses toluene as a surrogate for mono-substituted aromatic compounds. Toluene smog chamber experiments form the basis for validation and testing of the toluene chemistry. The UNC database lists 18 experiments using only toluene and NOx. Since the CB-IV was published in 1988, there have been 10 new toluene-only experiments; of these, 3 experiments with data in final form were simulated for this project. Table 4 presents a summary of the inputs used and Table 4a presents the comparative simulated ozone peak values using the standard, the high flux, and the low flux chemistries. Percent differences compared to the observed ozone values are also shown. Figures 25 through 33 show the data and simulations in more detail. Data are always shown using only points and simulations are always shown only as lines.

Table 4-- Toluene Simulation Input Summary.

Date	VOC ppmC	NOx ppm	VOC/ NOx	10^5 wall HONO ppm/min	10^4 wall HCHO ppm/min	initial HONO ppb
JL0894B	0.91	0.352	2.59	8	7	6
AU3095B	7.21	0.618	11.67	15	20	6
ST2496B	13.38	0.634	21.1	15	20	3

Table 4a -- Toluene Simulation Performance Summary Using Standard and Alternate CB-IV Mechanisms.

Date	Obs. O_3 ppb	Std. O_3 ppb	Error to Obs. %	High Flux ppb	Error to Obs. %	Low Flux ppb	Error to Obs. %
JL0894B	82	75	-8.5	73	-11.0	87	+6.1
AU3095B	545	514	-5.7	476	-12.7	565	+3.7
ST2496B	593	580	-2.2	540	-8.9	653	+10.1

m-Xylene

The CB-IV uses m-xylene as a surrogate for multi-substituted aromatic compounds. m-Xylene smog chamber experiments form the basis for validation and testing for this type of aromatics chemistry. m-Xylene chemistry differs from that of toluene in two important aspects: the initial reaction with OH is much faster (about a factor of 4) and the aromatic ring appears to fracture more readily to important radical precursor products. The UNC database lists 10 experiments using only m-xylene and NOx. Since the CB-IV was published in 1988, there have been 10 new m-xylene-only experiments; of these, 2 experiments with data in final form were simulated for this project. Table 5 presents a summary of the inputs used and Table 5a presents the comparative ozone peak values and percent differences compared to the observed ozone values. Figures 34 through 40 show the data and simulations in more detail. Data are always shown using only points and simulations are always shown only as lines.

Table 5 -- m-Xylene Simulation Input Summary.

Date	VOC ppmC	NOx ppm	VOC/ NOx	10^5 wall HONO ppm/min	10^4 wall HCHO ppm/min	initial HONO ppb
JL0894R	0.526	0.338	1.56	10	12	4
AU3095R	8.00	0.622	12.9	50	10	1

Table 5a -- m Xylene Simulation Performance Summary Using Standard and Alternate CB-IV Mechanisms.

Date	Obs. O_3 ppb	Std. O_3 ppb	Error to Obs. %	High Flux ppb	Error to Obs. %	Low Flux ppb	Error to Obs. %
JL0894R	390	368	-5.6	392	+0.5	332	-14.9
AU3095R	717	595	-16.8	574	-19.7	615	-14.0

Synthetic Urban (SynUrb) Mixture

UNC developed a mixture (called SynUrb) designed to approximate the spectrum of VOC seen in urban atmospheres. SynUrb contains some 54 different VOC and the mixture has been used in other chambers (e.g., Riverside and TVA). When used with the CB-IV mechanism all the carbon bond species are utilized. The following splits per ppmC of SynUrb are used: OLE at 0.011, PAR at 0.591, HCHO at 0.0093, ALD2 at 0.0174, ETH at 0.0136, NR at 0.0732, TOL at 0.0135, XYL at 0.018, and ISOP at 0.0006.

The UNC database lists 22 experiments using the SynUrb mixture and NOx. Since the CB-IV was published in 1988, there have been 14 new SynUrb experiments; of these, 5 experiments with data in final form were simulated for this project. Table 6 presents a summary of the inputs used and Table 6a presents the comparative ozone peak values and percent differences compared to the observed ozone values. Figures 41 through 64 show the data and simulations in more detail. Data are always shown using only points and simulations are always shown only as lines.

Table 6 -- SynUrb Mixture Simulation Input Summary.

Date	VOC ppmC	NOx ppm	VOC/ NOx	10^5 wall HONO ppm/min	10^4 wall HCHO ppm/min	initial HONO ppb
AU0696R	1.55	0.369	4.2	2	1.3	4
ST1294R	2.00	0.323	6.19	15	3.0	2
ST1194R	2.00	0.346	5.77	15	3.0	4
ST1494B	2.00	0.344	5.81	15	3.0	3
ST1594B	2.00	0.344	5.81	15	3.0	4

Table 6a -- SynUrb Mixture Simulation Performance Summary Using Standard and Alternate CB-IV Mechanisms.

Date	Obs. O_3 ppb	Std. O_3 ppb	Error to Obs. %	High Flux ppb	Error to Obs. %	Low Flux ppb	Error to Obs. %
AU0696R	121	118	-2.5	109	-9.9	122	+0.8
ST1294R	317	315	-0.6	328	+3.5	303	-4.4
ST1194R	332	297	-10.5	249	-25.0	366	+10.2
ST1494B	328	275	-16.2	226	-31.1	338	+3.0
ST1594B	303	240	-20.8	194	-36.0	299	-1.3

With the exception of the September 12, 1994, experiment it is interesting to note that a higher flux of radicals tends to reduce simulated ozone with this mixture. It is unfortunate that the database does not contain a wider range of initial concentrations and concentration ratios to further test the impact of varying the radical flux. The next section deals with this issue at least theoretically.

CONTROL STRATEGY IMPLICATIONS USING A BOX MODEL

The standard OZIPM code (Hogo and Gery, 1988) was used. This software was developed to generate isopleth diagrams for the U.S. EPA control strategy estimation technique known as the Empirical Kinetics Modeling Approach (EKMA). Any chemical mechanism can be used as an input file, and a rather wide range of physical parameters can be introduced. For this project the set of physical parameters used were supplied by W. Carter. This particular set of physical parameters was found by Carter to generate Maximum Incremental Reactivity (MIR) that were very close to the MIRs computed from the average of several box model simulations each using a full set of parameters corresponding to individual cities.

The OZIPM code was first exercised to develop EKMA-type ozone isopleth diagrams for the basic formaldehyde and NOx smog chemistry used in the CB-IV. These diagrams are generated from a matrix of some 120 box model simulations where the only parameters varied are the VOC and NOx inputs. The standard chemistry generates the diagram shown in Figure 65 when contour lines are interpolated between the 120 ozone values. When the radical inputs and sinks are all reduced by 30 percent a similar diagram (not shown) can be generated. Figure 66 shows a diagram generated by first subtracting the ozone generated by the standard chemistry from the reduced radical flux version of the chemistry. That is, contour lines are interpolated through the matrix of the 120 points of ozone difference between the two versions. In Figure 66 the absolute impacts on ozone are shown as the VOC and NOx emissions are varied. For example, it can be seen that starting from the upper right-hand corner (i.e., high VOC and NOx emissions) just reducing VOC (pure formaldehyde) emissions leads first to higher ozone with the low radical flux chemistry followed by lower ozone as compared to the standard chemistry. These differences, which are due to the lower radical flux that was assumed, imply that control strategies based solely on VOC reduction (in this theoretical formaldehyde only system) are uncertain due to the uncertainties in the chemistry associated with reactions involving radical flux (i.e., radical production and loss). Higher radical flux produce similar but opposite differences to the lower radical results shown.

It should be recalled that varying the sources and sinks of HOx radicals simultaneously tends to keep the steady-state concentrations of OH and HO_2 the same even though the flux of radicals through the system changes. Keeping similar steady-state levels of OH and HO_2 is important so that the decay of VOC species and the conversion rate of NO to NO_2 can remain similar enough to maintain acceptable simulations of the smog chamber database. Thus, the significant changes in control strategy which are reflected here (in just the inorganic reaction set plus the formaldehyde chemistry) can be considered as indicative of an uncertainty that exists in “basic” smog chemistry. This is because all the existing chemical mechanisms tend to treat these “basic” inorganic and formaldehyde reactions the same all. Existing smog chemistry mechanisms tend to differ mainly in how the VOC chemistry is treated.

Figure 67 presents the same information as shown in Figure 66, but the differences in ozone are not in absolute parts per billion but in percent of the total ozone generated by the standard mechanism. Figure 68 shows a similar plot to Figure 66, but the high flux chemistry is compared with the standard chemistry instead of the low flux comparison. In the lower right quadrant of these diagrams (i.e., Figures 66 and 68), NOx and VOC (formaldehyde) reductions are seen also seen to be affected by the radical flux changes. However, when other parts of the CB-IV are

included one at a time or all together this region will be seen to be less sensitive to control strategy changes. In the upper left quadrant the results with the full mechanism give essentially the same type of control strategy impact as is shown in the difference diagrams using formaldehyde as the only VOC.

Figures 69, 70, and 71 show isopleth diagrams for the full CB-IV mechanism, plus the low and high flux comparisons as changes in ozone concentration, respectively. Figures 72 and 73 show the results presented in Figures 70 and 71 but expressed as percent changes compared to the base case values shown in Figure 69. The control strategy implications are seen to be roughly similar to what was found using just the formaldehyde and inorganic reactions of the mechanism. The lower right quadrants of the Figures 70 and 71 show very little impact from these variations in radical flux. This region in the diagrams corresponds to conditions with high VOC-to-NOx ratios where NOx control is typically considered preferable to VOC control. Thus, the implication is that uncertainties associated with the high and low flux versions of the chemistry do not appear to have a large impact on NOx control strategies in areas characterized by high VOC-to-NOx ratios. However, it should be noted that the majority of urban areas typically are seen to have fairly low VOC-to-NOx ratios (i.e., in the upper left quadrant of these figures). Thus, the results shown in these diagrams suggest that significant uncertainties in control strategies can occur in many cities due the uncertainties found in the reactions affecting radical flux.

TABLE 1a. EPA UAM (BBN) Carbon Bond 4.3 + UNCCHAM.RXN.

* M E C H A N I S M L I S T I N G * * * * * * * ** * * * * * * * * * * *

1]			NO2	--->	NO	+	O		HVNO2		0.00E+00 /min
2]			O	--->	O3				8.38E+04exp(1175/T)		4.32E+06 /min
3]		O3	+ NO	--->	NO2				2.64E+03exp(-1370/T)		2.66E+01 /(ppm-min)
4]		O	+ NO2	--->	NO				1.38E+04		1.38E+04 /(ppm-min)
5]		O	+ NO2	--->	NO3				2.30E+02exp(687/T)		2.31E+03 /(ppm-min)
6]		O	+ NO	--->	NO2				3.23E+02exp(602/T)		2.44E+03 /(ppm-min)
7]		O3	+ NO2	--->	NO3				1.76E+02exp(-2450/T)		4.73E-02 /(ppm-min)
8]			O3	--->	O				HVO3O3P		0.00E+00 /min
9]			O3	--->	O1D				HVO3O1D*PHOTD		0.00E+00 /min
10]			O1D	--->	O				1.15E+10exp(390/T)*FIC34		4.26E+05 /min
11]		O1D	+ H2O	--->	2.00OH				3.26E+05*FIC34		3.26E+00 /(ppm-min)
12]		O3	+ OH	--->	HO2				2.34E+03exp(-940/T)		1.00E+02 /(ppm-min)
13]		O3	+ HO2	--->	OH				2.10E+01exp(-580/T)		3.00E+00 /(ppm-min)
14A]			NO3	--->	NO				HVNO3NO		0.00E+00 /min
14B]			NO3	--->	NO2	+	O		HVNO3NO2		0.00E+00 /min
15]		NO3	+ NO	--->	2.00NO2				1.91E+04exp(250/T)		4.42E+04 /(ppm-min)
16]		NO3	+ NO2	--->	NO	+	NO2		3.66E+01exp(-1230/T)		5.90E-01 /(ppm-min)
17]		NO3	+ NO2	--->	N2O5				7.85E+02exp(256/T)		1.85E+03 /(ppm-min)
18]		N2O5	+ H2O	--->	2.00HNO3				1.90E-06		1.90E-06 /(ppm-min)
19]			N2O5	--->	NO3	+	NO2		2.11E+16exp(-10897/T)		2.78E+00 /min
20]		NO	+ NO	--->	2.00NO2				2.60E-05exp(530/T)		1.54E-04 /(ppm-min)
21]	NO +	NO2	+ H2O	--->	2.00HONO				1.60E-11		1.60E-11 /(ppm^2-min)
22]		OH	+ NO	--->	HONO				6.56E+02exp(806/T)		9.80E+03 /(ppm-min)
23]			HONO	--->	OH	+	NO		HVNO2*HONO_NO2R		0.00E+00 /min
24]		OH	+ HONO	--->	NO2				9.77E+03		9.77E+03 /(ppm-min)
25]		HONO	+ HONO	--->	NO	+	NO2		1.50E-05		1.50E-05 /(ppm-min)
26]		OH	+ NO2	--->	HNO3				1.54E+03exp(713/T)		1.68E+04 /(ppm-min)
27]		OH	+ HNO3	--->	NO3				7.60E+00exp(1000/T)		2.18E+02 /(ppm-min)
28]		HO2	+ NO	--->	OH	+	NO2		5.48E+03exp(240/T)		1.23E+04 /(ppm-min)
32]		HO2	+ HO2	--->	H2O2				8.74E+01exp(1150/T)		4.14E+03 /(ppm-min)
33]	HO2 +	HO2	+ H2O	--->	H2O2				7.69E-10exp(5800/T)		2.18E-01 /(ppm^2-min)
34]			H2O2	--->	2.00OH				HVH2O2		0.00E+00 /min
35]		OH	+ H2O2	--->	HO2				4.72E+03exp(-187/T)		2.52E+03 /(ppm-min)
36]		OH	+ CO	--->	HO2				3.22E+02		3.22E+02 /(ppm-min)
37]		HCHO	+ OH	--->	HO2	+	CO		1.50E+04		1.50E+04 /(ppm-min)
38]			HCHO	--->	2.00HO2	+	CO		HVHCHOR*PHOTF		0.00E+00 /min
39]			HCHO	--->	CO				HVHCHOS		0.00E+00 /min
40]		HCHO	+ O	--->	OH	+	HO2	+ CO	4.30E+04exp(-1550/T)		2.37E+02 /(ppm-min)

TABLE 1a. (Continued).

41]	HCHO	+ NO3	---> HNO3	+ HO2	+ CO					
						9.30E-01				9.30E-01 /(ppm-min)
42]	ALD2	+ O	---> C2O3	+ OH		1.74E+04exp(-986/T)				6.36E+02 /(ppm-min)
43]	ALD2	+ OH	---> C2O3			1.04E+04exp(250/T)				2.40E+04 /(ppm-min)
44]	ALD2	+ NO3	---> C2O3	+ HNO3		3.70E+00				3.70E+00 /(ppm-min)
45]		ALD2	---> HCHO	+ XO2	+ 2.00HO2	+				
				CO		HVCCHOR*PHOTA				0.00E+00 /min
46]	C2O3	+ NO	---> HCHO	+ XO2	+ HO2	+				
				NO2		5.16E+04exp(-180/T)				2.82E+04 /(ppm-min)
47]	C2O3	+ NO2	---> PAN			3.83E+03exp(380/T)				1.37E+04 /(ppm-min)
48]		PAN	---> C2O3	+ NO2		1.20E+18exp(-13500/T)				2.54E-02 /min
49]	C2O3	+ C2O3	---> 2.00HCHO	+ 2.00XO2		+				
				2.00HO2		3.70E+03				3.70E+03 /(ppm-min)
50]	C2O3	+ HO2	---> 0.79HCHO	+ 0.79XO2		+				
				0.79HO2	+ 0.79OH	9.60E+03				9.60E+03 /(ppm-min)
51]		OH	---> HCHO	+ XO2	+ HO2	6.52E+03exp(-1710/T)				2.10E+01 /min
52]	PAR	+ OH	---> 0.87XO2	+ 0.13XO2N		+				
				0.11HO2	+ 0.11ALD2	+				
				0.76ROR	+ -0.11PAR	1.20E+03				1.20E+03 /(ppm-min)
53]		ROR	---> 1.10ALD2	+ 0.96XO2		+				
				0.94HO2	+ 0.04XO2N	+				
				0.02ROR	+ -2.10PAR	6.25E+16exp(-8000/T)				1.37E+05 /min
54]		ROR	---> HO2			9.55E+04				9.55E+04 /min
55]	ROR	+ NO2	---> NTR			2.20E+04				2.20E+04 /(ppm-min)
56]	O	+ OLE	---> 0.63ALD2	+ 0.38HO2		+				
				0.28XO2	+ 0.30CO	+				
				0.20HCHO	+ 0.02XO2N	+				
				0.22PAR	+ 0.20OH	1.76E+04exp(-324/T)				5.92E+03 /(ppm-min)
57]	OH	+ OLE	---> HCHO	+ ALD2	+ XO2	+				
				HO2	+ -1.00PAR	7.74E+03exp(504/T)				4.20E+04 /(ppm-min)
58]	O3	+ OLE	---> 0.50ALD2	+ 0.74HCHO		+				
				0.33CO	+ 0.44HO2	+				
				0.22XO2	+ 0.10OH	+				
				-1.00PAR		2.10E+01exp(-2105/T)				1.80E-02 /(ppm-min)
59]	NO3	+ OLE	---> 0.91XO2	+ HCHO	+ ALD2	+				
				0.09XO2N	+ NO2	+ -1.00PAR				
						1.13E+01				1.13E+01 /(ppm-min)
60]	O	+ ETH	---> HCHO	+ 0.70XO2	+ CO	+				
				1.70HO2	+ 0.30OH	1.54E+04exp(-792/T)				1.08E+03 /(ppm-min)
61]	OH	+ ETH	---> XO2	+ 1.56HCHO	+ HO2	+				
				0.22ALD2		3.00E+03exp(411/T)				1.19E+04 /(ppm-min)

TABLE 1a. (Continued).

62]	O3	+ ETH	---> HCHO	+ 0.42CO	+ 0.12HO2		
					1.86E+01exp(-2633/T)		2.70E-03 /(ppm-min)
63]	OH	+ TOL	---> 0.08XO2	+ 0.36CRES	+		
			0.44HO2	+ 0.56TO2	3.11E+03exp(322/T)		9.15E+03 /(ppm-min)
64]	TO2	+ NO	---> 0.90NO2	+ 0.90OPEN	+		
			0.90HO2	+ 0.10NTR	1.20E+04		1.20E+04 /(ppm-min)
65]		TO2	---> HO2	+ CRES	2.50E+02		2.50E+02 /min
66]	OH	+ CRES	---> 0.40CRO	+ 0.60XO2	+		
			0.60HO2	+ 0.30OPEN	6.10E+04		6.10E+04 /(ppm-min)
67]	NO3	+ CRES	---> CRO	+ HNO3	3.25E+04		3.25E+04 /(ppm-min)
68]	CRO	+ NO2	---> NTR		2.00E+04		2.00E+04 /(ppm-min)
69]		OPEN	---> C2O3	+ HO2	+ CO		
					HVHCHOR*OPEN_R		0.00E+00 /min
70]	OPEN	+ OH	---> XO2	+ C2O3	+ 2.00CO	+	
			2.00HO2	+ HCHO	4.40E+04		4.40E+04 /(ppm-min)
71]	OPEN	+ O3	---> 0.03ALD2	+ 0.62C2O3	+		
			0.70HCHO	+ 0.03XO2	+		
			0.69CO	+ 0.08OH	+		
			0.76HO2	+ 0.20MGLY	8.03E-02exp(-500/T)		1.50E-02 /(ppm-min)
72]	OH	+ XYL	---> 0.70HO2	+ 0.50XO2	+		
			0.20CRES	+ 0.80MGLY	+		
			1.10PAR	+ 0.30TO2	2.45E+04exp(116/T)		3.62E+04 /(ppm-min)
73]	OH	+ MGLY	---> XO2	+ C2O3	2.60E+04		2.60E+04 /(ppm-min)
74]		MGLY	---> C2O3	+ HO2	+ CO		
					HVHCHOR*MGLY_R		0.00E+00 /min
75]	O	+ ISOP	---> 0.60HO2	+ 0.80ALD2	+		
			0.55OLE	+ 0.50XO2	+		
			0.50CO	+ 0.45ETH	+		
			0.90PAR		2.70E+04		2.70E+04 /(ppm-min)
76]	OH	+ ISOP	---> HCHO	+ XO2	+ 0.67HO2	+	
			0.40MGLY	+ 0.20C2O3	+		
			ETH	+ 0.20ALD2	+ 0.13XO2N		
					1.42E+05		1.42E+05 /(ppm-min)
77]	O3	+ ISOP	---> HCHO	+ 0.40ALD2	+ 0.55ETH	+	
			0.20MGLY	+ 0.06CO	+		
			0.10PAR	+ 0.44HO2	+		
			0.10OH		1.80E-02		1.80E-02 /(ppm-min)
78]	NO3	+ ISOP	---> XO2N		4.70E+02		4.70E+02 /(ppm-min)
79]	XO2	+ NO	---> NO2		1.20E+04		1.20E+04 /(ppm-min)
80]	XO2	+ XO2	--->		2.55E+01exp(1300/T)		2.00E+03 /(ppm-min)
81]	XO2N	+ NO	---> NTR		1.00E+03		1.00E+03 /(ppm-min)

TABLE 1a. (Concluded).

82]	SO2	+ OH	---> HO2	+ SULF			6.49E+02exp(160/T)		1.11E+03 /(ppm-min)
83]		SO2	---> SULF				8.17E-05		8.17E-05 /min
84]	OH	+ MEOH	---> HCHO	+ HO2			1.60E+03		1.60E+03 /(ppm-min)
85]	OH	+ ETOH	---> ALD2	+ HO2			2.38E+03exp(176/T)		4.30E+03 /(ppm-min)
86]	XO2	+ HO2	--->				1.13E+02exp(1300/T)		8.90E+03 /(ppm-min)
XX]		MENO2	---> HO2	+ HCHO	+ NO				
							HVNO2*HONO_NO2R		0.00E+00 /min
ENTRAIN]			--->	0.50CO	+	0.07O3	+		
				0.58H2	+	1.79CH4	+		
				0.00HCHO	+	0.04BVOC	DL*DILUTION		0.00E+00 ppm/min
BCKGND]	OH	+ BVOC	--->	0.67XO2	+	0.67HCHO	+		
				0.67HO2	+	0.17C2O3	+		
				0.00PAR			4.44E+03		4.44E+03 /(ppm-min)
WALLNO2A]		NO2	---> HONO				HVNO2*WALLOH		0.00E+00 /min
WALLNO2B]		NO2	--->	0.50HONO	+	0.50WHNO3	1.60E-04		1.60E-04 /min
WALLNO2C]		WHNO3	---> NO2				HVNO2*WALLNO2		0.00E+00 /min
WALLNO2D]			---> HONO				HVNO2*WALLHONO		0.00E+00 ppm/min
WALLHCHO]			---> HCHO				HVNO2*WALLHCHO		0.00E+00 ppm/min
WALN2O5A]		N2O5	--->	2.00WHNO3			2.50E-03		2.50E-03 /min
WALN2O5B]	N2O5	+ WH2O	--->	2.00WHNO3			2.30E-07exp(2000/T)		1.89E-04 /(ppm-min)
WALLH2O2]		H2O2	--->				KWALLH2O2		4.00E-02 /min
WALLO3]		O3	--->				1.40E-04		1.40E-04 /min
WALLHNO3]		HNO3	---> WHNO3				KWALLHNO3		2.00E-04 /min

TABLE 1b. High Radical Flux EPA UAM (BBN) Carbon Bond 4.3 + UNCCHAM.RXN

```
* * * * * * * * * * * * * * * * * * * * * * * * M E C H A N I S M   L I S T I N G  * * * * * * * * * * * * * * * * * * * * * * *

  1]                  NO2     ---> NO       + O                  HVNO2                                 0.00E+00 /min
  2]                  O       ---> O3                            8.38E+04exp( 1175/T)                  4.32E+06 /min
  3]       O3       + NO      ---> NO2                           2.64E+03exp(-1370/T)                  2.66E+01 /(ppm-min)
  4]       O        + NO2     ---> NO                            1.38E+04                              1.38E+04 /(ppm-min)
  5]       O        + NO2     ---> NO3                           2.30E+02exp(  687/T)                  2.31E+03 /(ppm-min)
  6]       O        + NO      ---> NO2                           3.23E+02exp(  602/T)                  2.44E+03 /(ppm-min)
  7]       O3       + NO2     ---> NO3                           1.76E+02exp(-2450/T)                  4.73E-02 /(ppm-min)
  8]                  O3      ---> O                             HVO3O3P                               0.00E+00 /min
  9]                  O3      ---> O1D                           HVO3O1D*PHOTZ                         0.00E+00 /min
 10]                  O1D     ---> O                             1.15E+10exp(  390/T)*FIC34            4.26E+05 /min
 11]       O1D      + H2O     --->  2.00OH                       3.26E+05*FIC34                        3.26E+00 /(ppm-min)
 12]       O3       + OH      ---> HO2                           2.34E+03exp( -940/T)                  1.00E+02 /(ppm-min)
 13]       O3       + HO2     ---> OH                            2.10E+01exp( -580/T)                  3.00E+00 /(ppm-min)
14A]                  NO3     ---> NO                            HVNO3NO                               0.00E+00 /min
14B]                  NO3     ---> NO2      + O                  HVNO3NO2                              0.00E+00 /min
 15]       NO3      + NO      --->  2.00NO2                      1.91E+04exp(  250/T)                  4.42E+04 /(ppm-min)
 16]       NO3      + NO2     ---> NO       + NO2                3.66E+01exp(-1230/T)                  5.90E-01 /(ppm-min)
 17]       NO3      + NO2     ---> N2O5                          7.85E+02exp(  256/T)                  1.85E+03 /(ppm-min)
 18]       N2O5     + H2O     --->  2.00HNO3                     1.90E-06                              1.90E-06 /(ppm-min)
 19]                  N2O5    ---> NO3      + NO2                2.11E+16exp(-10897/T)                 2.78E+00 /min
 20]       NO       + NO      --->  2.00NO2                      2.60E-05exp(  530/T)                  1.54E-04 /(ppm-min)
 21] NO  + NO2      + H2O     --->  2.00HONO                     1.60E-11                              1.60E-11 /(ppm^2-min)
 22]       OH       + NO      ---> HONO                          6.56E+02exp(  806/T)                  9.80E+03 /(ppm-min)
 23]                  HONO    ---> OH       + NO                 HVNO2*HONO_NO2R                       0.00E+00 /min
 24]       OH       + HONO    ---> NO2                           9.77E+03                              9.77E+03 /(ppm-min)
 25]       HONO     + HONO    ---> NO       + NO2                1.50E-05                              1.50E-05 /(ppm-min)
 26]       OH       + NO2     ---> HNO3                          2.00E+03exp(  713/T)                  2.19E+04 /(ppm-min)
 27]       OH       + HNO3    ---> NO3                           7.60E+00exp( 1000/T)                  2.18E+02 /(ppm-min)
 28]       HO2      + NO      ---> OH       + NO2                5.48E+03exp(  240/T)                  1.23E+04 /(ppm-min)
 32]       HO2      + HO2     ---> H2O2                          1.14E+02exp( 1150/T)                  5.39E+03 /(ppm-min)
 33] HO2 + HO2      + H2O     ---> H2O2                          1.00E-09exp( 5800/T)                  2.84E-01 /(ppm^2-min)
 34]                  H2O2    --->  2.00OH                       HVH2O2                                0.00E+00 /min
 35]       OH       + H2O2    ---> HO2                           4.72E+03exp( -187/T)                  2.52E+03 /(ppm-min)
 36]       OH       + CO      ---> HO2                           3.22E+02                              3.22E+02 /(ppm-min)
 37]       HCHO     + OH      ---> HO2      + CO                 1.50E+04                              1.50E+04 /(ppm-min)
 38]                  HCHO    --->  2.00HO2       + CO           HVHCHOR*PHOTF                         0.00E+00 /min
 39]                  HCHO    ---> CO                            HVHCHOS                               0.00E+00 /min
 40]       HCHO     + O       ---> OH       + HO2       + CO
                                                                 4.30E+04exp(-1550/T)                  2.37E+02 /(ppm-min)
```

TABLE 1b. (Continued).

41]	HCHO	+ NO3	---> HNO3	+ HO2	+ CO			
						9.30E-01		9.30E-01 /(ppm-min)
42]	ALD2	+ O	---> C2O3	+ OH		1.74E+04exp(-986/T)		6.36E+02 /(ppm-min)
43]	ALD2	+ OH	---> C2O3			1.04E+04exp(250/T)		2.40E+04 /(ppm-min)
44]	ALD2	+ NO3	---> C2O3	+ HNO3		3.70E+00		3.70E+00 /(ppm-min)
45]		ALD2	---> HCHO	+ XO2	+ 2.00HO2	+		
				CO		HVCCHOR*PHOTA		0.00E+00 /min
46]	C2O3	+ NO	---> HCHO	+ XO2	+ HO2	+		
				NO2		5.16E+04exp(-180/T)		2.82E+04 /(ppm-min)
47]	C2O3	+ NO2	---> PAN			3.83E+03exp(380/T)		1.37E+04 /(ppm-min)
48]		PAN	---> C2O3	+ NO2		1.20E+18exp(-13500/T)		2.54E-02 /min
49]	C2O3	+ C2O3	---> 2.00HCHO	+ 2.00XO2	+			
				2.00HO2		4.81E+03		4.81E+03 /(ppm-min)
50]	C2O3	+ HO2	---> 0.79HCHO	+ 0.79XO2	+			
				0.79HO2	+ 0.79OH	1.25E+04		1.25E+04 /(ppm-min)
51]		OH	---> HCHO	+ XO2	+ HO2			
						6.52E+03exp(-1710/T)		2.10E+01 /min
52]	PAR	+ OH	---> 0.87XO2	+ 0.13XO2N	+			
				0.11HO2	+ 0.11ALD2	+		
				0.76ROR	+ -0.11PAR	1.20E+03		1.20E+03 /(ppm-min)
53]		ROR	---> 1.10ALD2	+ 0.96XO2	+			
				0.94HO2	+ 0.04XO2N	+		
				0.02ROR	+ -2.10PAR	6.25E+16exp(-8000/T)		1.37E+05 /min
54]		ROR	---> HO2			9.55E+04		9.55E+04 /min
55]	ROR	+ NO2	---> NTR			2.20E+04		2.20E+04 /(ppm-min)
56]	O	+ OLE	---> 0.63ALD2	+ 0.38HO2	+			
				0.28XO2	+ 0.30CO	+		
				0.20HCHO	+ 0.02XO2N	+		
				0.22PAR	+ 0.20OH	1.76E+04exp(-324/T)		5.92E+03 /(ppm-min)
57]	OH	+ OLE	---> HCHO	+ ALD2	+ XO2	+		
				HO2	+ -1.00PAR	7.74E+03exp(504/T)		4.20E+04 /(ppm-min)
58]	O3	+ OLE	---> 0.50ALD2	+ 0.74HCHO	+			
				0.33CO	+ 0.57HO2	+		
				0.22XO2	+ 0.13OH	+		
				-1.00PAR		2.10E+01exp(-2105/T)		1.80E-02 /(ppm-min)
59]	NO3	+ OLE	---> 0.91XO2	+ HCHO	+ ALD2	+		
				0.09XO2N	+ NO2	+ -1.00PAR		
						1.13E+01		1.13E+01 /(ppm-min)
60]	O	+ ETH	---> HCHO	+ 0.70XO2	+ CO	+		
				1.70HO2	+ 0.30OH	1.54E+04exp(-792/T)		1.08E+03 /(ppm-min)
61]	OH	+ ETH	---> XO2	+ 1.56HCHO	+ HO2	+		
				0.22ALD2		3.00E+03exp(411/T)		1.19E+04 /(ppm-min)

TABLE 1b. (Continued).

62]	O3 + ETH	---> HCHO + 0.42CO + 0.16HO2	1.86E+01exp(-2633/T)	2.70E-03 /(ppm-min)		
63]	OH + TOL	---> 0.08XO2 + 0.36CRES + 0.44HO2 + 0.56TO2	3.11E+03exp(322/T)	9.15E+03 /(ppm-min)		
64]	TO2 + NO	---> 0.90NO2 + 0.90OPEN + 0.90HO2 + 0.10NTR	1.20E+04	1.20E+04 /(ppm-min)		
65]	TO2	---> HO2 + CRES	2.50E+02	2.50E+02 /min		
66]	OH + CRES	---> 0.40CRO + 0.60XO2 + 0.60HO2 + 0.30OPEN	6.10E+04	6.10E+04 /(ppm-min)		
67]	NO3 + CRES	---> CRO + HNO3	3.25E+04	3.25E+04 /(ppm-min)		
68]	CRO + NO2	---> NTR	2.00E+04	2.00E+04 /(ppm-min)		
69]	OPEN	---> C2O3 + HO2 + CO	HVHCHOR*OPEN_R	0.00E+00 /min		
70]	OPEN + OH	---> XO2 + C2O3 + 2.00CO + 2.00HO2 + HCHO	4.40E+04	4.40E+04 /(ppm-min)		
71]	OPEN + O3	---> 0.03ALD2 + 0.80C2O3 + 0.70HCHO + 0.03XO2 + 0.69CO + 0.10OH + 0.99HO2 + 0.20MGLY	8.03E-02exp(-500/T)	1.50E-02 /(ppm-min)		
72]	OH + XYL	---> 0.70HO2 + 0.50XO2 + 0.20CRES + 0.80MGLY + 1.10PAR + 0.30TO2	2.45E+04exp(116/T)	3.62E+04 /(ppm-min)		
73]	OH + MGLY	---> XO2 + C2O3	2.60E+04	2.60E+04 /(ppm-min)		
74]	MGLY	---> C2O3 + HO2 + CO	HVHCHOR*MGLY_R	0.00E+00 /min		
75]	O + ISOP	---> 0.60HO2 + 0.80ALD2 + 0.55OLE + 0.50XO2 + 0.50CO + 0.45ETH + 0.90PAR	2.70E+04	2.70E+04 /(ppm-min)		
76]	OH + ISOP	---> HCHO + XO2 + 0.67HO2 + 0.40MGLY + 0.20C2O3 + ETH + 0.20ALD2 + 0.13XO2N	1.42E+05	1.42E+05 /(ppm-min)		
77]	O3 + ISOP	---> HCHO + 0.40ALD2 + 0.55ETH + 0.20MGLY + 0.06CO + 0.10PAR + 0.57HO2 + 0.13OH	1.80E-02	1.80E-02 /(ppm-min)		
78]	NO3 + ISOP	---> XO2N	4.70E+02	4.70E+02 /(ppm-min)		
79]	XO2 + NO	---> NO2	1.20E+04	1.20E+04 /(ppm-min)		
80]	XO2 + XO2	--->	3.31E+01exp(1300/T)	2.60E+03 /(ppm-min)		
81]	XO2N + NO	---> NTR	1.00E+03	1.00E+03 /(ppm-min)		
82]	SO2 + OH	---> HO2 + SULF	6.49E+02exp(160/T)	1.11E+03 /(ppm-min)		

TABLE 1b. (Concluded).

83]		SO2	--->	SULF			8.17E-05		8.17E-05	/min
84]	OH	+ MEOH	--->	HCHO	+ HO2		1.60E+03		1.60E+03	/(ppm-min)
85]	OH	+ ETOH	--->	ALD2	+ HO2		2.38E+03exp(176/T)		4.30E+03	/(ppm-min)
86]	XO2	+ HO2	--->				1.47E+02exp(1300/T)		1.16E+04	/(ppm-min)
XX]		MENO2	--->	HO2	+ HCHO	+ NO				
							HVNO2*HONO_NO2R		0.00E+00	/min
ENTRAIN]			--->	0.50CO	+ 0.07O3	+				
				0.58H2	+ 1.79CH4	+				
				0.00HCHO	+ 0.04BVOC		DL*DILUTION		0.00E+00	ppm/min
BCKGND]	OH	+ BVOC	--->	0.67XO2	+ 0.67HCHO	+				
				0.67HO2	+ 0.17C2O3	+				
				0.00PAR			4.44E+03		4.44E+03	/(ppm-min)
WALLNO2A]		NO2	--->	HONO			HVNO2*WALLOH		0.00E+00	/min
WALLNO2B]		NO2	--->	0.50HONO	+ 0.50WHNO3		1.60E-04		1.60E-04	/min
WALLNO2C]		WHNO3	--->	NO2			HVNO2*WALLNO2		0.00E+00	/min
WALLNO2D]			--->	HONO			HVNO2*WALLHONO		0.00E+00	ppm/min
WALLHCHO]			--->	HCHO			HVNO2*WALLHCHO		0.00E+00	ppm/min
WALN2O5A]		N2O5	--->	2.00WHNO3			2.50E-03		2.50E-03	/min
WALN2O5B]	N2O5	+ WH2O	--->	2.00WHNO3			2.30E-07exp(2000/T)		1.89E-04	/(ppm-min)
WALLH2O2]		H2O2	--->				KWALLH2O2		4.00E-02	/min
WALLO3]		O3	--->				1.40E-04		1.40E-04	/min
WALLHNO3]		HNO3	--->	WHNO3			KWALLHNO3		2.00E-04	/min

TABLE 1c. Low Radical Flux EPA UAM (BBN) Carbon Bond 4.3 + UNCCHAM.TXN

```
* * * * * * * * * * * * * * * * * * * * * * * * M E C H A N I S M   L I S T I N G  * * * * * * * * * * * * * * * * * * * * * * *
  1]                  NO2      ---> NO       + O                    HVNO2                                 0.00E+00 /min
  2]                  O        ---> O3                              8.38E+04exp( 1175/T)                  4.32E+06 /min
  3]       O3       + NO       ---> NO2                             2.64E+03exp(-1370/T)                  2.66E+01 /(ppm-min)
  4]       O        + NO2      ---> NO                              1.38E+04                              1.38E+04 /(ppm-min)
  5]       O        + NO2      ---> NO3                             2.30E+02exp(  687/T)                  2.31E+03 /(ppm-min)
  6]       O        + NO       ---> NO2                             3.23E+02exp(  602/T)                  2.44E+03 /(ppm-min)
  7]       O3       + NO2      ---> NO3                             1.76E+02exp(-2450/T)                  4.73E-02 /(ppm-min)
  8]                  O3       ---> O                               HVO3O3P                               0.00E+00 /min
  9]                  O3       ---> O1D                             HVO3O1D*PHOTZ                         0.00E+00 /min
 10]                  O1D      ---> O                               1.15E+10exp(  390/T)*FIC34            4.26E+05 /min
 11]       O1D      + H2O      --->  2.00OH                         3.26E+05*FIC34                        3.26E+00 /(ppm-min)
 12]       O3       + OH       ---> HO2                             2.34E+03exp( -940/T)                  1.00E+02 /(ppm-min)
 13]       O3       + HO2      ---> OH                              2.10E+01exp( -580/T)                  3.00E+00 /(ppm-min)
14A]                  NO3      ---> NO                              HVNO3NO                               0.00E+00 /min
14B]                  NO3      ---> NO2      + O                    HVNO3NO2                              0.00E+00 /min
 15]       NO3      + NO       --->  2.00NO2                        1.91E+04exp(  250/T)                  4.42E+04 /(ppm-min)
 16]       NO3      + NO2      ---> NO       + NO2                  3.66E+01exp(-1230/T)                  5.90E-01 /(ppm-min)
 17]       NO3      + NO2      ---> N2O5                            7.85E+02exp(  256/T)                  1.85E+03 /(ppm-min)
 18]       N2O5     + H2O      --->  2.00HNO3                       1.90E-06                              1.90E-06 /(ppm-min)
 19]                  N2O5     ---> NO3      + NO2                  2.11E+16exp(-10897/T)                 2.78E+00 /min
 20]       NO       + NO       --->  2.00NO2                        2.60E-05exp(  530/T)                  1.54E-04 /(ppm-min)
 21] NO  + NO2      + H2O      --->  2.00HONO                       1.60E-11                              1.60E-11 /(ppm^2-min)
 22]       OH       + NO       ---> HONO                            6.56E+02exp(  806/T)                  9.80E+03 /(ppm-min)
 23]                  HONO     ---> OH       + NO                   HVNO2*HONO_NO2R                       0.00E+00 /min
 24]       OH       + HONO     ---> NO2                             9.77E+03                              9.77E+03 /(ppm-min)
 25]       HONO     + HONO     ---> NO       + NO2                  1.50E-05                              1.50E-05 /(ppm-min)
 26]       OH       + NO2      ---> HNO3                            1.08E+03exp(  713/T)                  1.18E+04 /(ppm-min)
 27]       OH       + HNO3     ---> NO3                             7.60E+00exp( 1000/T)                  2.18E+02 /(ppm-min)
 28]       HO2      + NO       ---> OH       + NO2                  5.48E+03exp(  240/T)                  1.23E+04 /(ppm-min)
 32]       HO2      + HO2      ---> H2O2                            6.11E+01exp( 1150/T)                  2.90E+03 /(ppm-min)
 33] HO2 + HO2      + H2O      ---> H2O2                            5.38E-10exp( 5800/T)                  1.53E-01 /(ppm^2-min)
 34]                  H2O2     --->  2.00OH                         HVH2O2                                0.00E+00 /min
 35]       OH       + H2O2     ---> HO2                             4.72E+03exp( -187/T)                  2.52E+03 /(ppm-min)
 36]       OH       + CO       ---> HO2                             3.22E+02                              3.22E+02 /(ppm-min)
 37]       HCHO     + OH       ---> HO2      + CO                   1.50E+04                              1.50E+04 /(ppm-min)
 38]                  HCHO     --->  2.00HO2       + CO             HVHCHOR*PHOTF                         0.00E+00 /min
 39]                  HCHO     ---> CO                              HVHCHOS                               0.00E+00 /min
 40]       HCHO     + O        ---> OH       + HO2       + CO
                                                                    4.30E+04exp(-1550/T)                  2.37E+02 /(ppm-min)
 41]       HCHO     + NO3      ---> HNO3     + HO2       + CO
                                                                    9.30E-01                              9.30E-01 /(ppm-min)
```

TABLE 1c. (Continued).

42]	ALD2	+ O	---> C2O3	+ OH		1.74E+04exp(-986/T)	6.36E+02	/(ppm-min)
43]	ALD2	+ OH	---> C2O3			1.04E+04exp(250/T)	2.40E+04	/(ppm-min)
44]	ALD2	+ NO3	---> C2O3	+ HNO3		3.70E+00	3.70E+00	/(ppm-min)
45]		ALD2	---> HCHO	+ XO2	+ 2.00HO2	+		
				CO		HVCCHOR*PHOTA	0.00E+00	/min
46]	C2O3	+ NO	---> HCHO	+ XO2	+ HO2	+		
				NO2		5.16E+04exp(-180/T)	2.82E+04	/(ppm-min)
47]	C2O3	+ NO2	---> PAN			3.83E+03exp(380/T)	1.37E+04	/(ppm-min)
48]		PAN	---> C2O3	+ NO2		1.20E+18exp(-13500/T)	2.54E-02	/min
49]	C2O3	+ C2O3	---> 2.00HCHO	+ 2.00XO2		+		
				2.00HO2		2.59E+03	2.59E+03	/(ppm-min)
50]	C2O3	+ HO2	---> 0.79HCHO	+ 0.79XO2		+		
				0.79HO2	+ 0.79OH	6.72E+03	6.72E+03	/(ppm-min)
51]		OH	---> HCHO	+ XO2	+ HO2			
						6.52E+03exp(-1710/T)	2.10E+01	/min
52]	PAR	+ OH	---> 0.87XO2	+ 0.13XO2N		+		
				0.11HO2	+ 0.11ALD2	+		
				0.76ROR	+ -0.11PAR	1.20E+03	1.20E+03	/(ppm-min)
53]		ROR	---> 1.10ALD2	+ 0.96XO2		+		
				0.94HO2	+ 0.04XO2N	+		
				0.02ROR	+ -2.10PAR	6.25E+16exp(-8000/T)	1.37E+05	/min
54]		ROR	---> HO2			9.55E+04	9.55E+04	/min
55]	ROR	+ NO2	---> NTR			2.20E+04	2.20E+04	/(ppm-min)
56]	O	+ OLE	---> 0.63ALD2	+ 0.38HO2		+		
				0.28XO2	+ 0.30CO	+		
				0.20HCHO	+ 0.02XO2N	+		
				0.22PAR	+ 0.20OH	1.76E+04exp(-324/T)	5.92E+03	/(ppm-min)
57]	OH	+ OLE	---> HCHO	+ ALD2	+ XO2	+		
				HO2	+ -1.00PAR	7.74E+03exp(504/T)	4.20E+04	/(ppm-min)
58]	O3	+ OLE	---> 0.50ALD2	+ 0.74HCHO		+		
				0.33CO	+ 0.31HO2	+		
				0.22XO2	+ 0.07OH	+		
				-1.00PAR		2.10E+01exp(-2105/T)	1.80E-02	/(ppm-min)
59]	NO3	+ OLE	---> 0.91XO2	+ HCHO	+ ALD2	+		
				0.09XO2N	+ NO2	+ -1.00PAR		
						1.13E+01	1.13E+01	/(ppm-min)
60]	O	+ ETH	---> HCHO	+ 0.70XO2	+ CO	+		
				1.70HO2	+ 0.30OH	1.54E+04exp(-792/T)	1.08E+03	/(ppm-min)
61]	OH	+ ETH	---> XO2	+ 1.56HCHO	+ HO2	+		
				0.22ALD2		3.00E+03exp(411/T)	1.19E+04	/(ppm-min)
62]	O3	+ ETH	---> HCHO	+ 0.42CO	+ 0.08HO2			
						1.86E+01exp(-2633/T)	2.70E-03	/(ppm-min)

TABLE 1c. (Continued).

63]	OH	+ TOL	--->	0.08XO2 + 0.44HO2	+ 0.36CRES + 0.56TO2	3.11E+03exp(322/T)	9.15E+03 /(ppm-min)	
64]	TO2	+ NO	--->	0.90NO2 + 0.90HO2	+ 0.90OPEN + 0.10NTR	1.20E+04	1.20E+04 /(ppm-min)	
65]		TO2	--->	HO2	+ CRES	2.50E+02	2.50E+02 /min	
66]	OH	+ CRES	--->	0.40CRO + 0.60HO2	+ 0.60XO2 + 0.30OPEN	6.10E+04	6.10E+04 /(ppm-min)	
67]	NO3	+ CRES	--->	CRO	+ HNO3	3.25E+04	3.25E+04 /(ppm-min)	
68]	CRO	+ NO2	--->	NTR		2.00E+04	2.00E+04 /(ppm-min)	
69]		OPEN	--->	C2O3	+ HO2 + CO	HVHCHOR*OPEN_R	0.00E+00 /min	
70]	OPEN	+ OH	--->	XO2 + 2.00HO2	+ C2O3 + 2.00CO + HCHO	4.40E+04	4.40E+04 /(ppm-min)	
71]	OPEN	+ O3	--->	0.03ALD2 + 0.70HCHO + 0.69CO + 0.53HO2	+ 0.43C2O3 + 0.03XO2 + 0.06OH + 0.20MGLY	8.03E-02exp(-500/T)	1.50E-02 /(ppm-min)	
72]	OH	+ XYL	--->	0.70HO2 + 0.20CRES + 1.10PAR	+ 0.50XO2 + 0.80MGLY + 0.30TO2	2.45E+04exp(116/T)	3.62E+04 /(ppm-min)	
73]	OH	+ MGLY	--->	XO2	+ C2O3	2.60E+04	2.60E+04 /(ppm-min)	
74]		MGLY	--->	C2O3	+ HO2 + CO	HVHCHOR*MGLY_R	0.00E+00 /min	
75]	O	+ ISOP	--->	0.60HO2 + 0.55OLE + 0.50CO + 0.90PAR	+ 0.80ALD2 + 0.50XO2 + 0.45ETH	2.70E+04	2.70E+04 /(ppm-min)	
76]	OH	+ ISOP	--->	HCHO + 0.40MGLY ETH	+ XO2 + 0.67HO2 + 0.20C2O3 + 0.20ALD2	+ 0.13XO2N 1.42E+05	1.42E+05 /(ppm-min)	
77]	O3	+ ISOP	--->	HCHO + 0.20MGLY + 0.10PAR + 0.07OH	+ 0.40ALD2 + 0.55ETH + 0.06CO + 0.31HO2	1.80E-02	1.80E-02 /(ppm-min)	
78]	NO3	+ ISOP	--->	XO2N		4.70E+02	4.70E+02 /(ppm-min)	
79]	XO2	+ NO	--->	NO2		1.20E+04	1.20E+04 /(ppm-min)	
80]	XO2	+ XO2	--->			1.79E+01exp(1300/T)	1.40E+03 /(ppm-min)	
81]	XO2N	+ NO	--->	NTR		1.00E+03	1.00E+03 /(ppm-min)	
82]	SO2	+ OH	--->	HO2	+ SULF	6.49E+02exp(160/T)	1.11E+03 /(ppm-min)	
83]		SO2	--->	SULF		8.17E-05	8.17E-05 /min	
84]	OH	+ MEOH	--->	HCHO	+ HO2	1.60E+03	1.60E+03 /(ppm-min)	

TABLE 1c. (Concluded).

85]	OH	+ ETOH	---> ALD2	+ HO2			2.38E+03exp(176/T)		4.30E+03 /(ppm-min)
86]	XO2	+ HO2	--->				7.94E+01exp(1300/T)		6.23E+03 /(ppm-min)
XX]		MENO2	---> HO2	+ HCHO	+ NO				
							HVNO2*HONO_NO2R		0.00E+00 /min
ENTRAIN]			--->	0.50CO	+	0.07O3	+		
				0.58H2	+	1.79CH4	+		
				0.00HCHO	+	0.04BVOC	DL*DILUTION		0.00E+00 ppm/min
BCKGND]	OH	+ BVOC	--->	0.67XO2	+	0.67HCHO	+		
				0.67HO2	+	0.17C2O3	+		
				0.00PAR			4.44E+03		4.44E+03 /(ppm-min)
WALLNO2A]		NO2	---> HONO				HVNO2*WALLOH		0.00E+00 /min
WALLNO2B]		NO2	--->	0.50HONO	+	0.50WHNO3	1.60E-04		1.60E-04 /min
WALLNO2C]		WHNO3	---> NO2				HVNO2*WALLNO2		0.00E+00 /min
WALLNO2D]			---> HONO				HVNO2*WALLHONO		0.00E+00 ppm/min
WALLHCHO]			---> HCHO				HVNO2*WALLHCHO		0.00E+00 ppm/min
WALN2O5A]		N2O5	--->	2.00WHNO3			2.50E-03		2.50E-03 /min
WALN2O5B]	N2O5	+ WH2O	--->	2.00WHNO3			2.30E-07exp(2000/T)		1.89E-04 /(ppm-min)
WALLH2O2]		H2O2	--->				KWALLH2O2		4.00E-02 /min
WALLO3]		O3	--->				1.40E-04		1.40E-04 /min
WALLHNO3]		HNO3	---> WHNO3				KWALLHNO3		2.00E-04 /min

FIGURE 1.

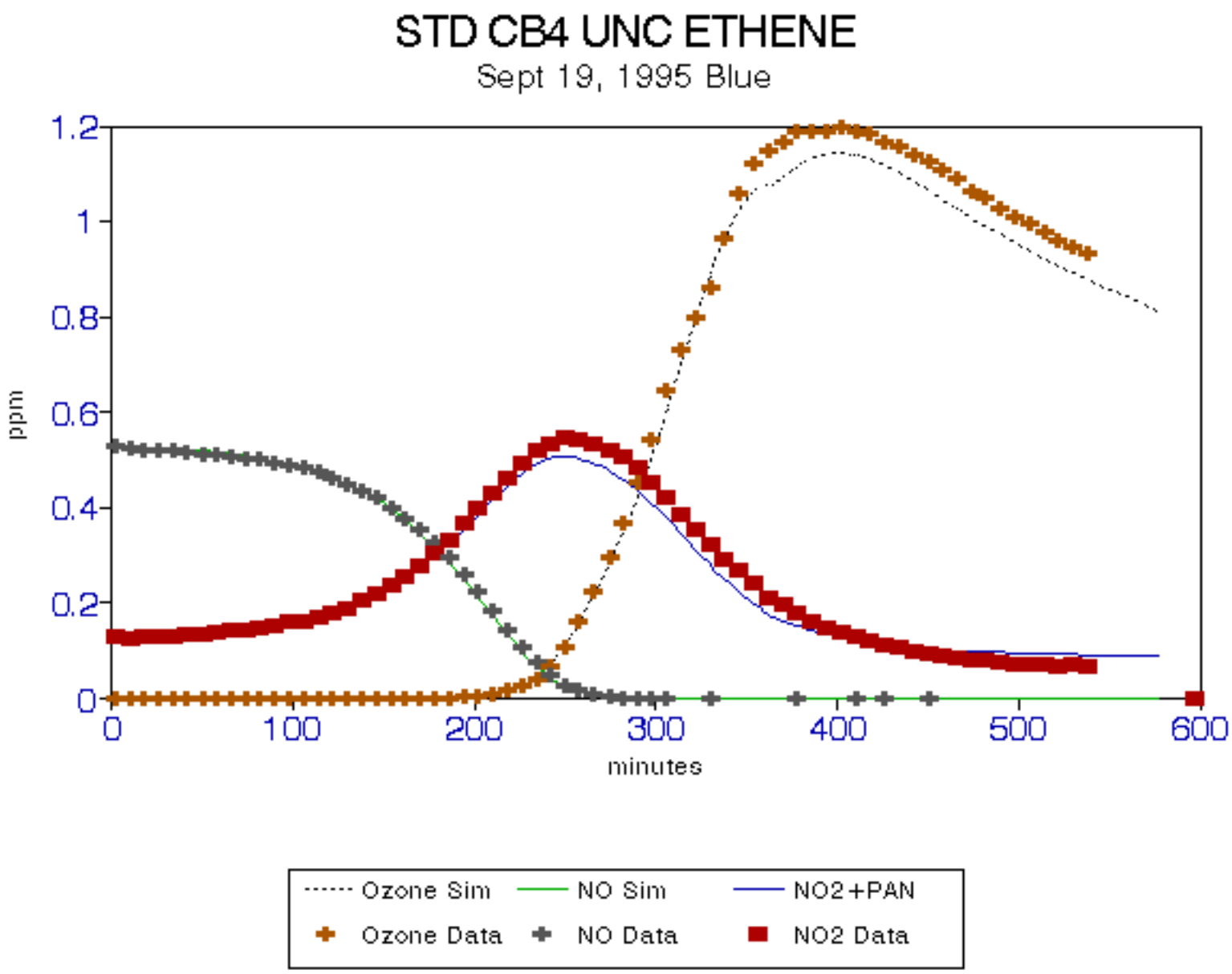
STD CB4 UNC ETHENE
Sept 19, 1995 Blue
ppm
1.2
1
0.8
0.6
0.4
0.2
0
0
100
200
300
400
500
600
minutes
Ozone Sim
NO Sim
NO2+PAN
Ozone Data
NO Data
NO2 Data

FIGURE 2.

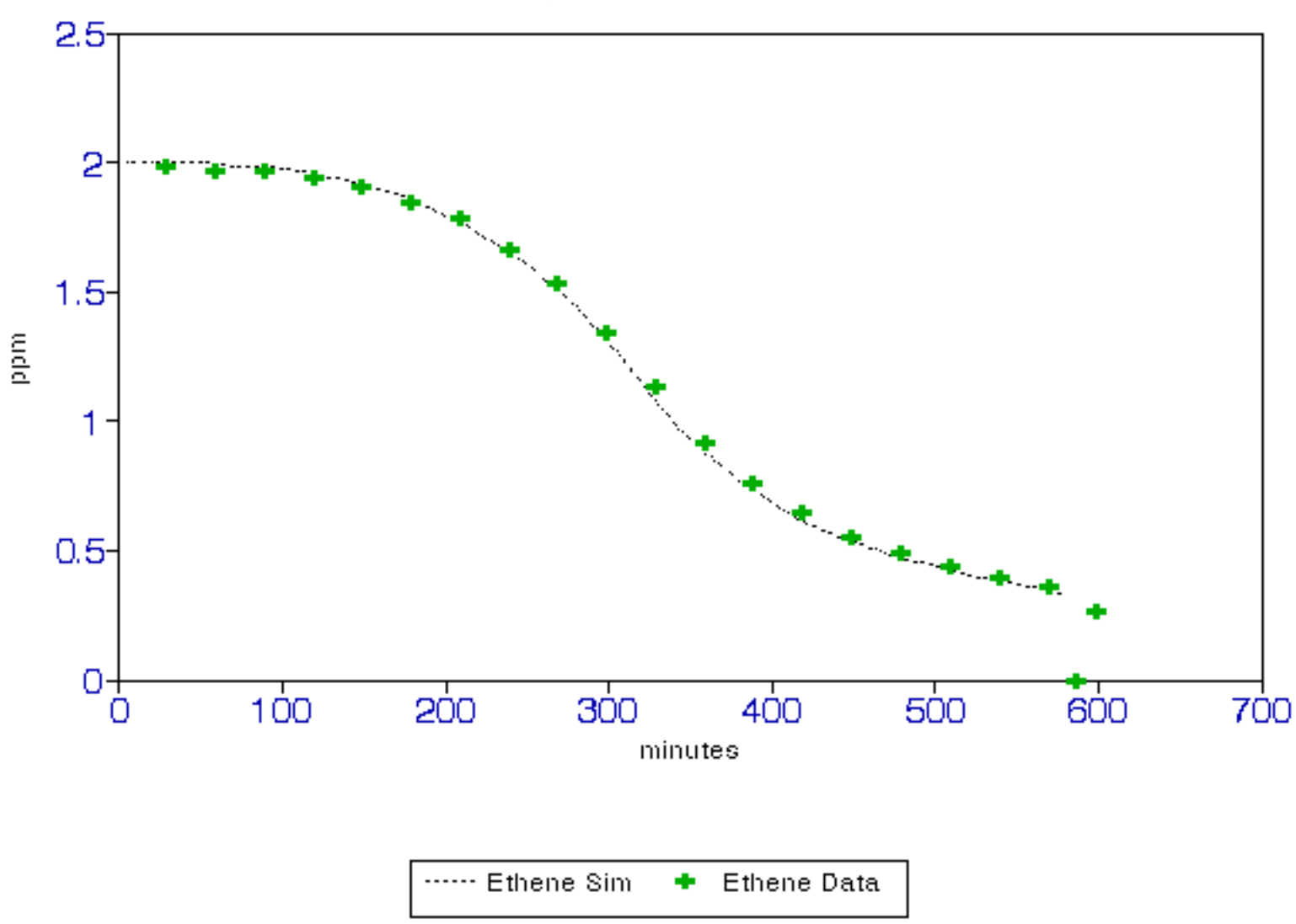
STD CB4 UNC ETHENE
Sept 19, 1995 Blue
2.5
2
1.5
1
0.5
0
ppm
0
100
200
300
400
500
600
700
minutes
Ethene Sim
Ethene Data

FIGURE 3.

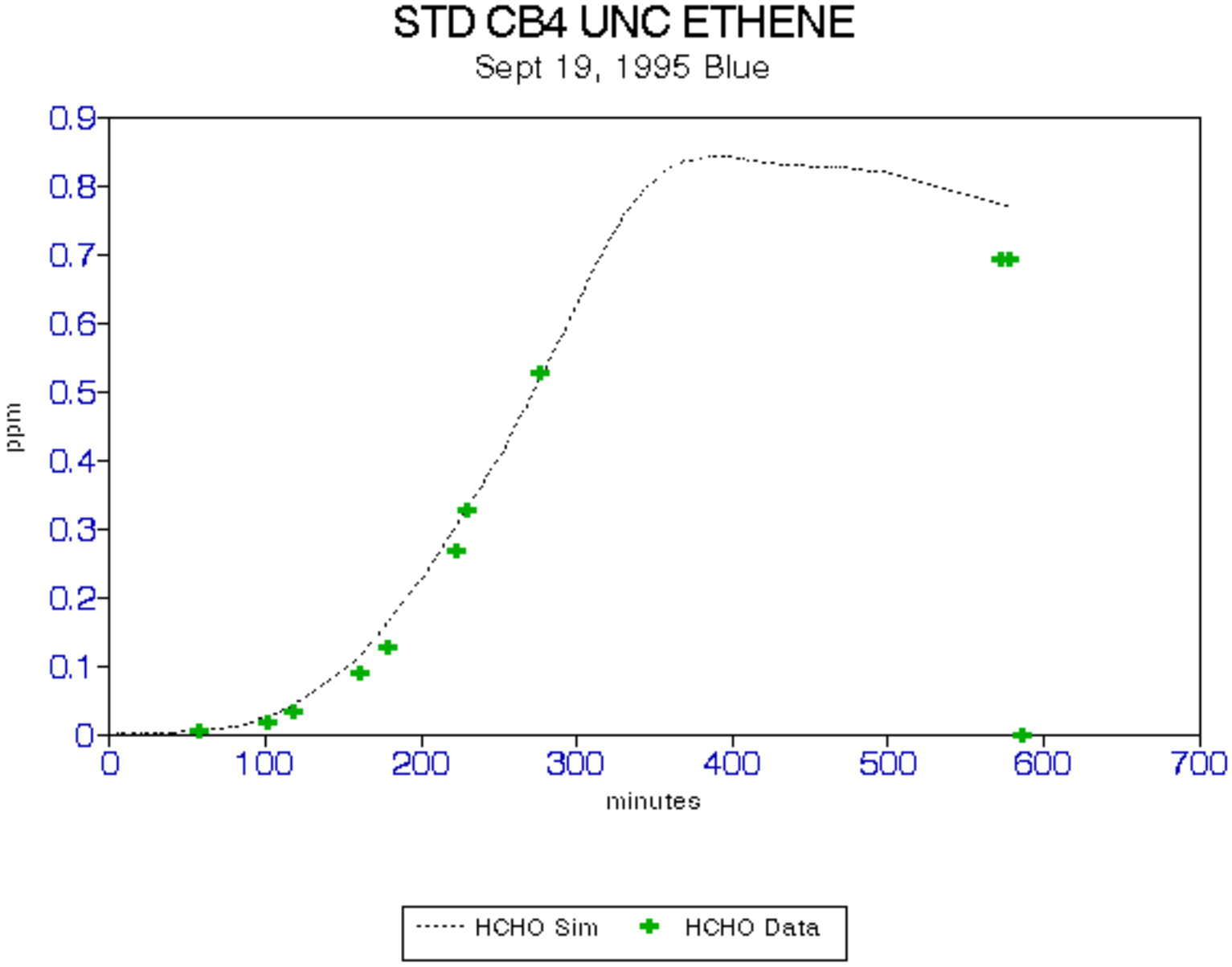
STD CB4 UNC ETHENE
Sept 19, 1995 Blue
ppm
0.9
0.8
0.7
0.6
0.5
0.4
0.3
0.2
0.1
0
0
100
200
300
400
500
600
700
minutes
HCHO Sim
HCHO Data

FIGURE 4.

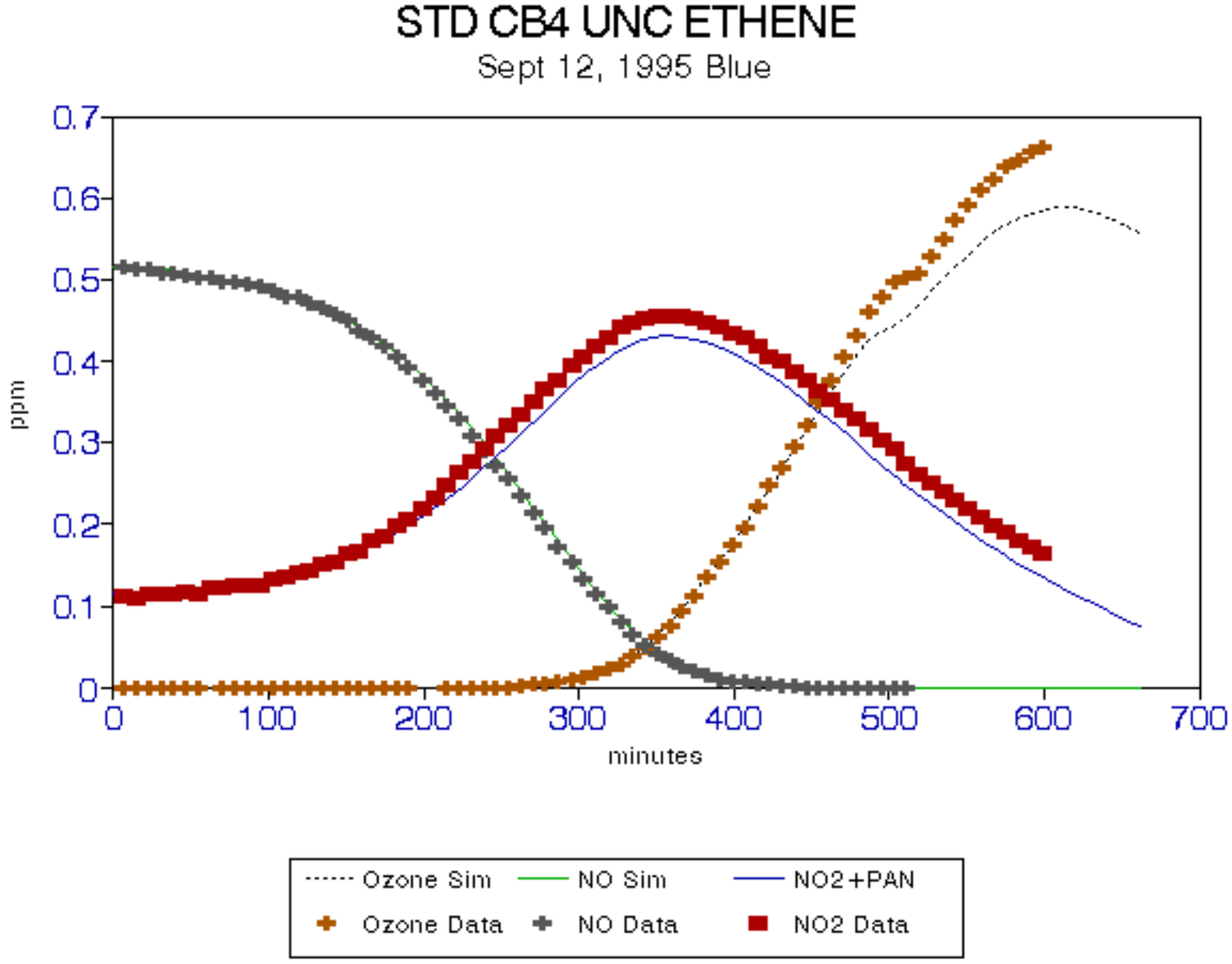
STD CB4 UNC ETHENE
Sept 12, 1995 Blue
0.7
0.6
0.5
0.4
0.3
0.2
0.1
0
ppm
0
100
200
300
400
500
600
700
minutes
Ozone Sim
NO Sim
NO2+PAN
Ozone Data
NO Data
NO2 Data

FIGURE 5.

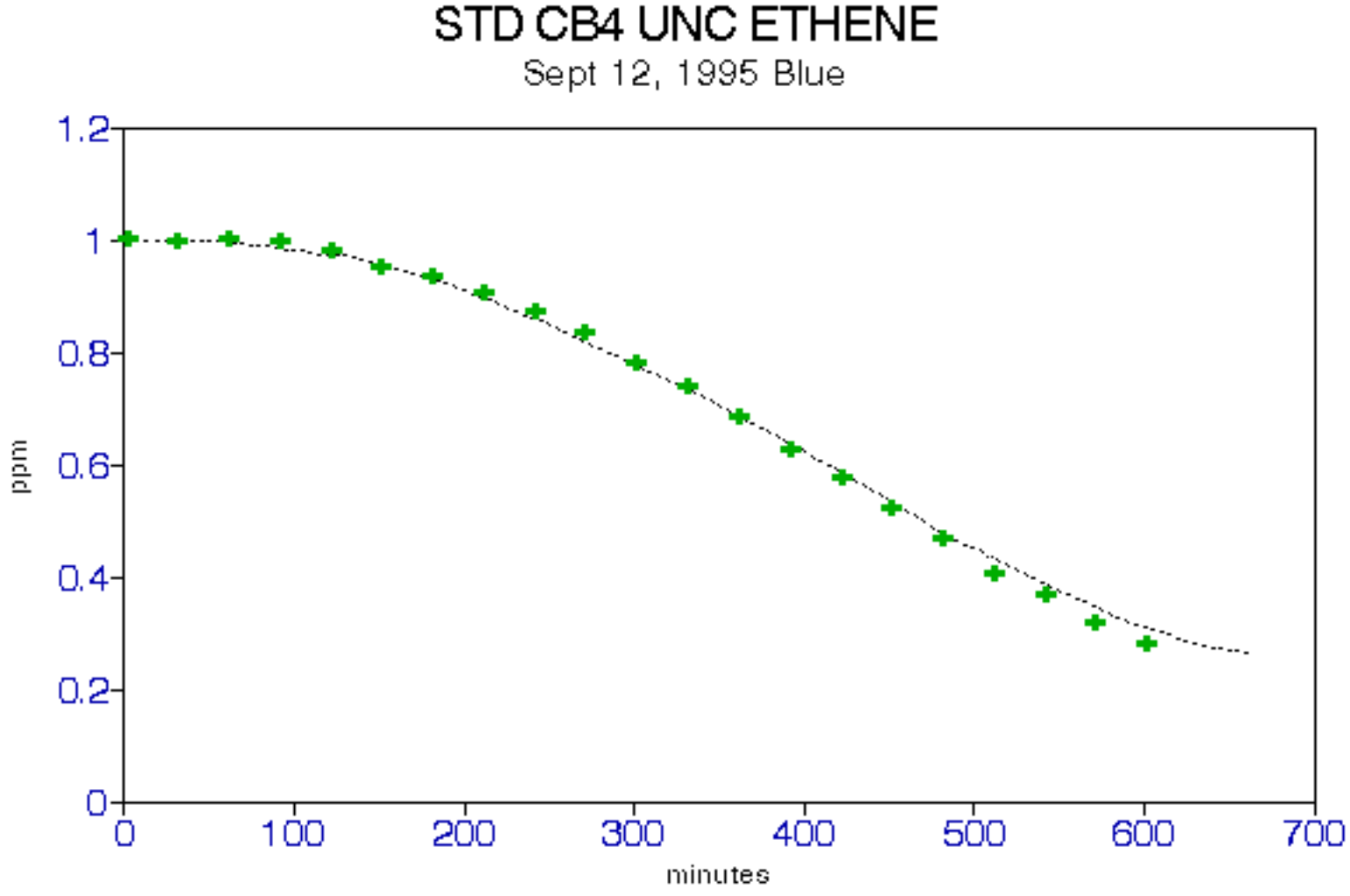
STD CB4 UNC ETHENE
Sept 12, 1995 Blue
1.2
1
0.8
0.6
0.4
0.2
0
ppm
0
100
200
300
400
500
600
700
minutes
Ethene Sim
Ethene Data

FIGURE 6.

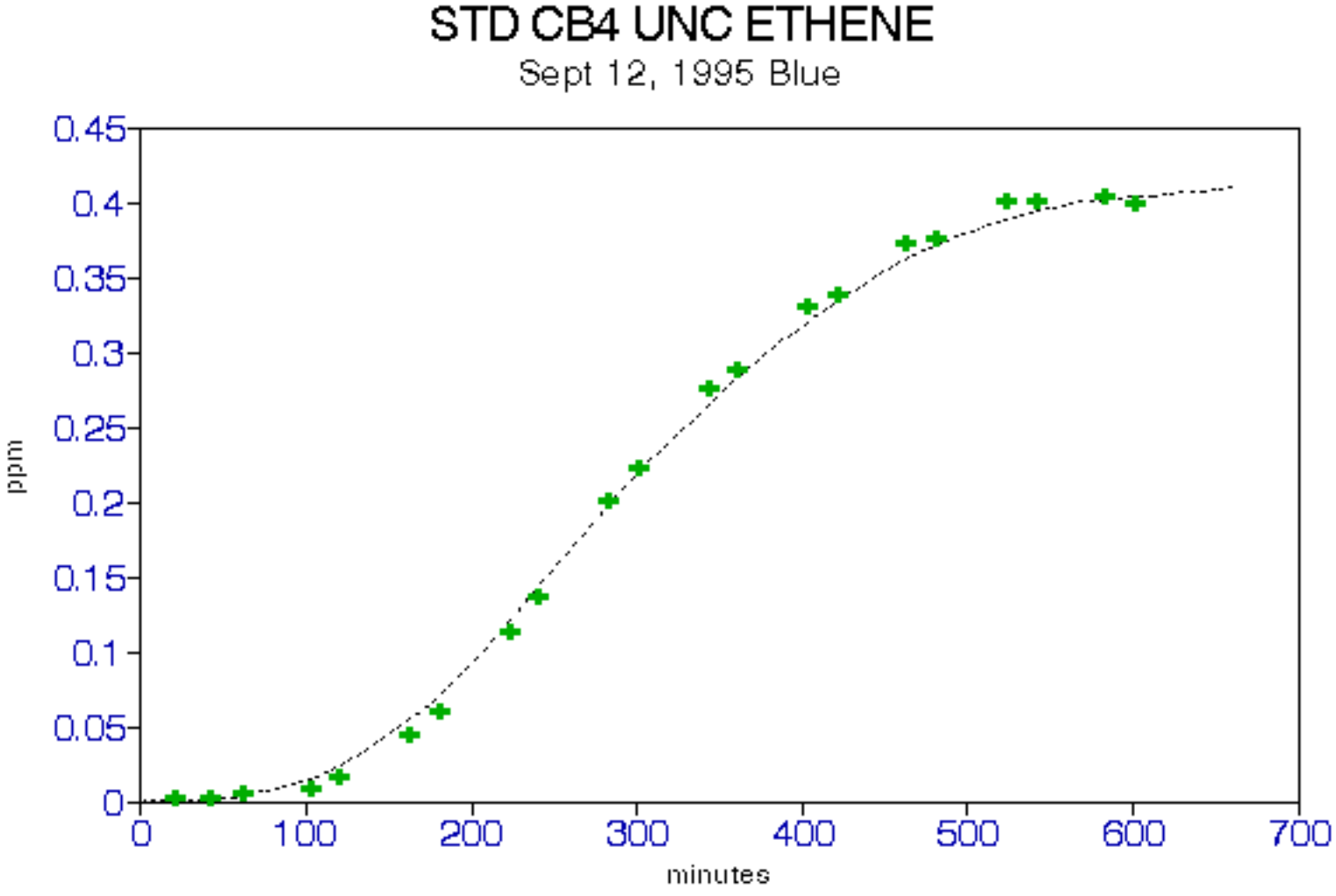
STD CB4 UNC ETHENE
Sept 12, 1995 Blue
0.45
0.4
0.35
0.3
0.25
0.2
0.15
0.1
0.05
0
ppm
0
100
200
300
400
500
600
700
minutes
HCHO Sim
HCHO Data

FIGURE 7.

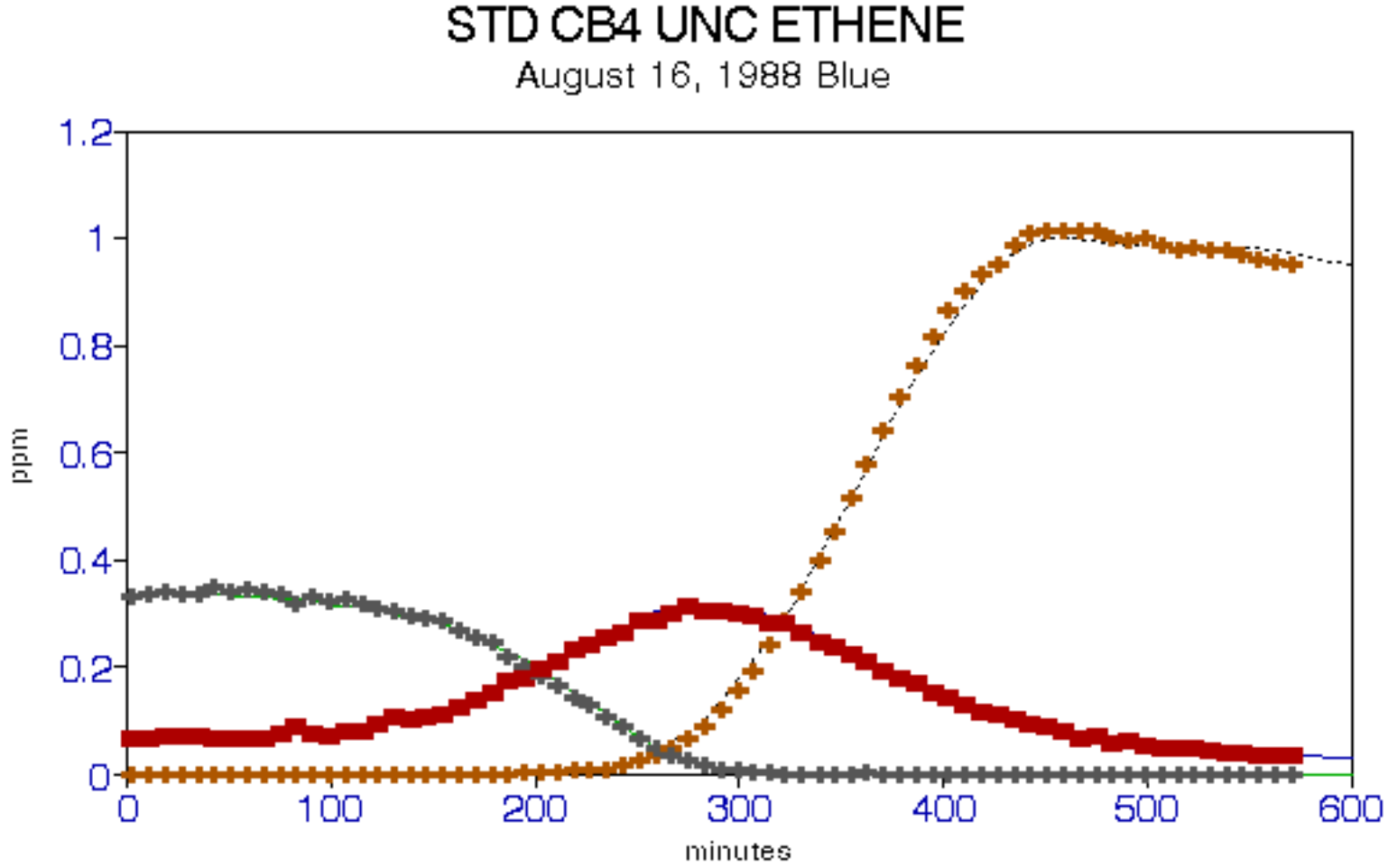
STD CB4 UNC ETHENE
August 16, 1988 Blue
1.2
1
0.8
0.6
0.4
0.2
0
ppm
0
100
200
300
400
500
600
minutes
Ozone Sim
NO Sim
NO2+PAN
Ozone Data
NO Data
NO2 Data

FIGURE 8.

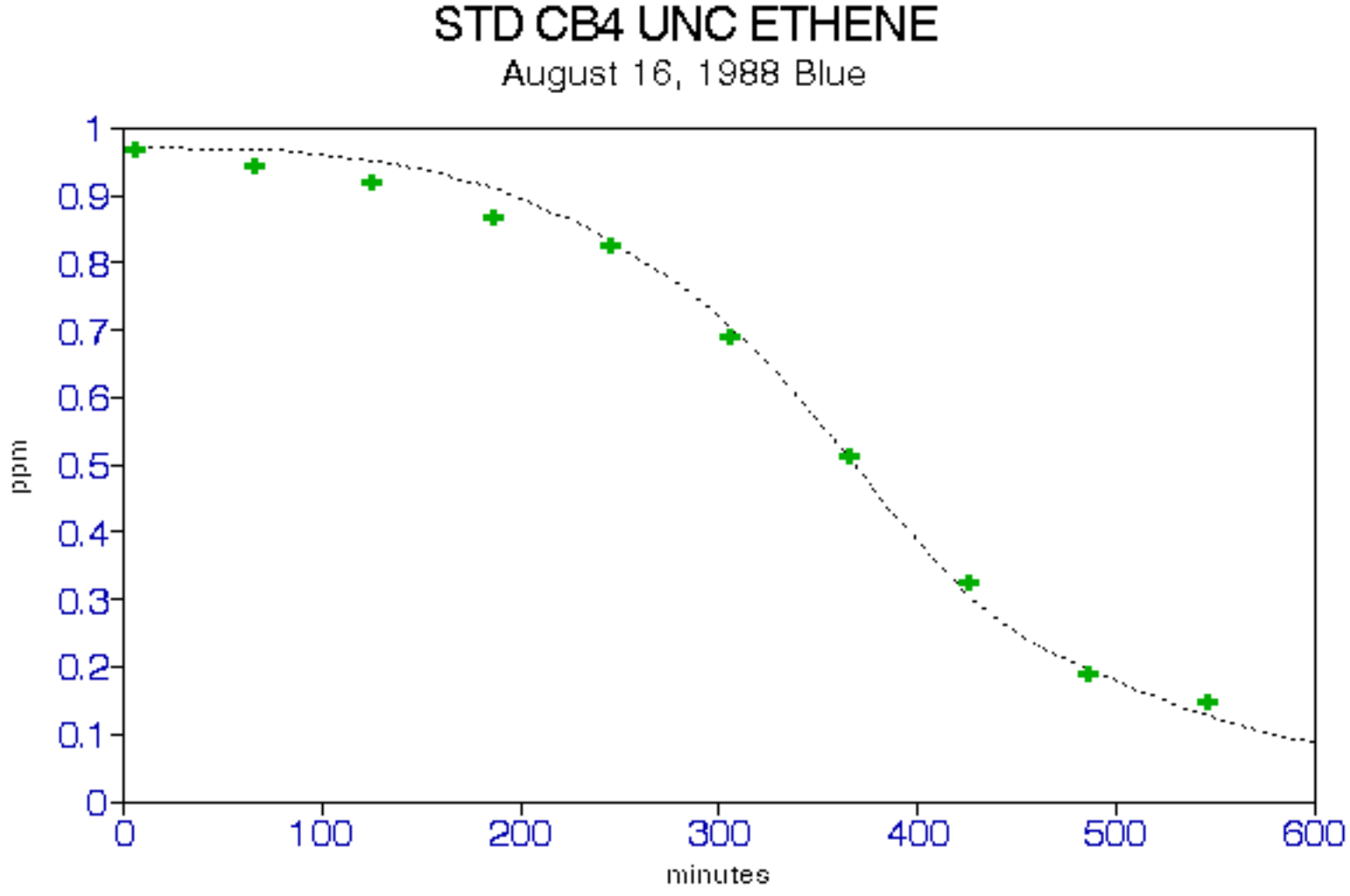
STD CB4 UNC ETHENE
August 16, 1988 Blue
ppm
1
0.9
0.8
0.7
0.6
0.5
0.4
0.3
0.2
0.1
0
0
100
200
300
400
500
600
minutes
Ethene Sim
Ethene Data

FIGURE 9.

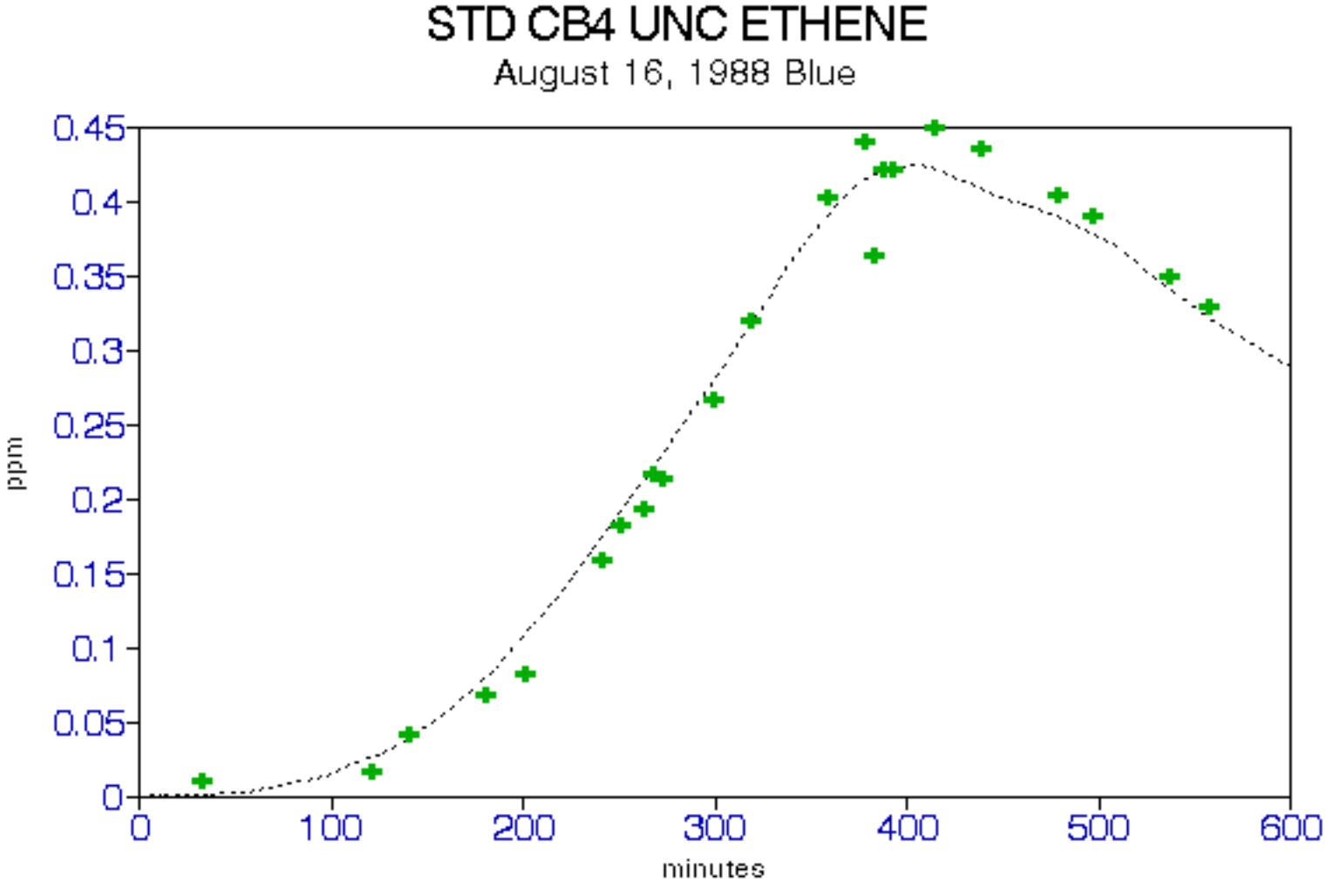
STD CB4 UNC ETHENE
August 16, 1988 Blue
0.45
0.4
0.35
0.3
0.25
0.2
0.15
0.1
0.05
0
ppm
0
100
200
300
400
500
600
minutes
HCHO Sim
HCHO Data

FIGURE 10.

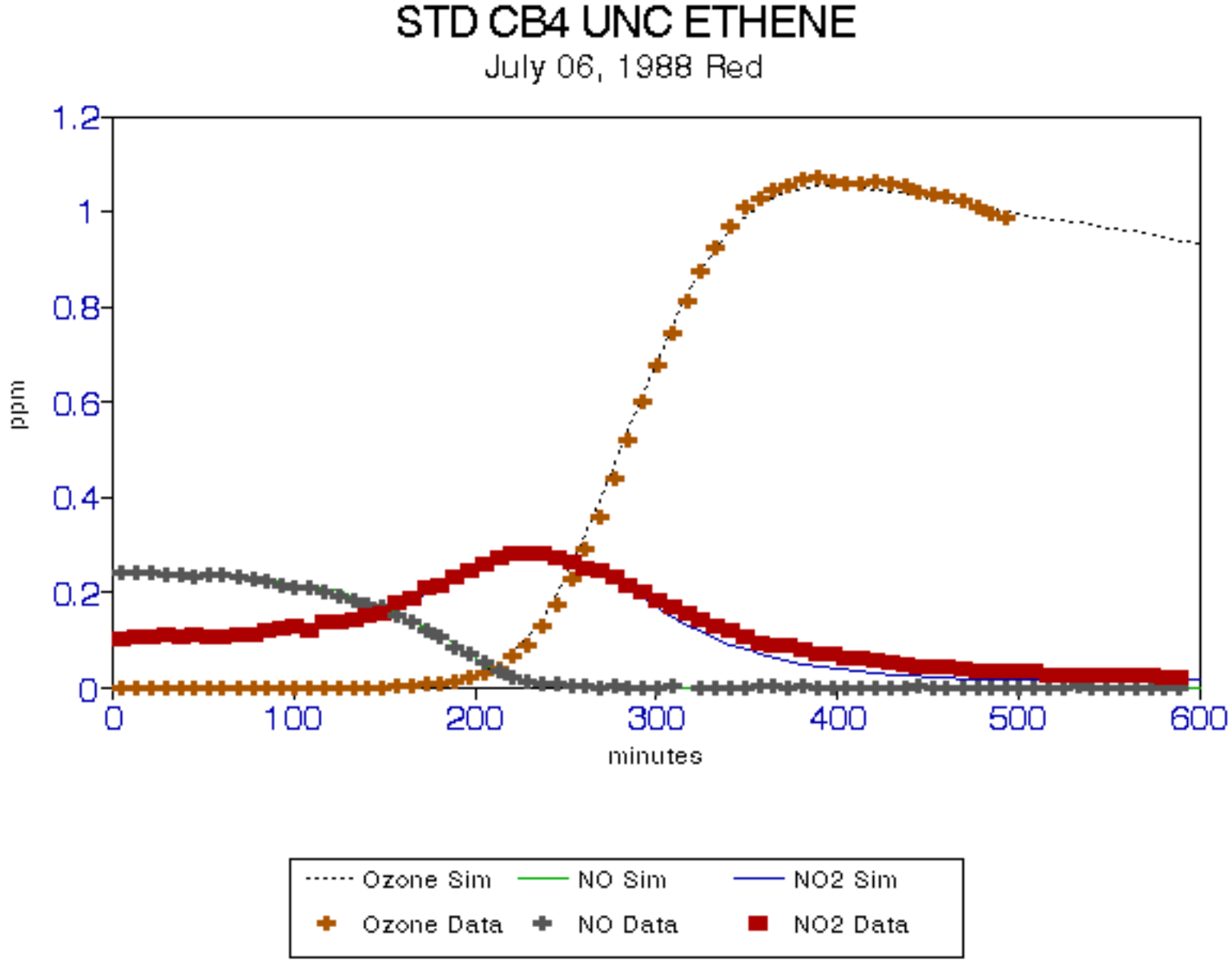
STD CB4 UNC ETHENE
July 06, 1988 Red
1.2
1
0.8
0.6
0.4
0.2
0
ppm
0
100
200
300
400
500
600
minutes
Ozone Sim
NO Sim
NO2 Sim
Ozone Data
NO Data
NO2 Data

FIGURE 11.

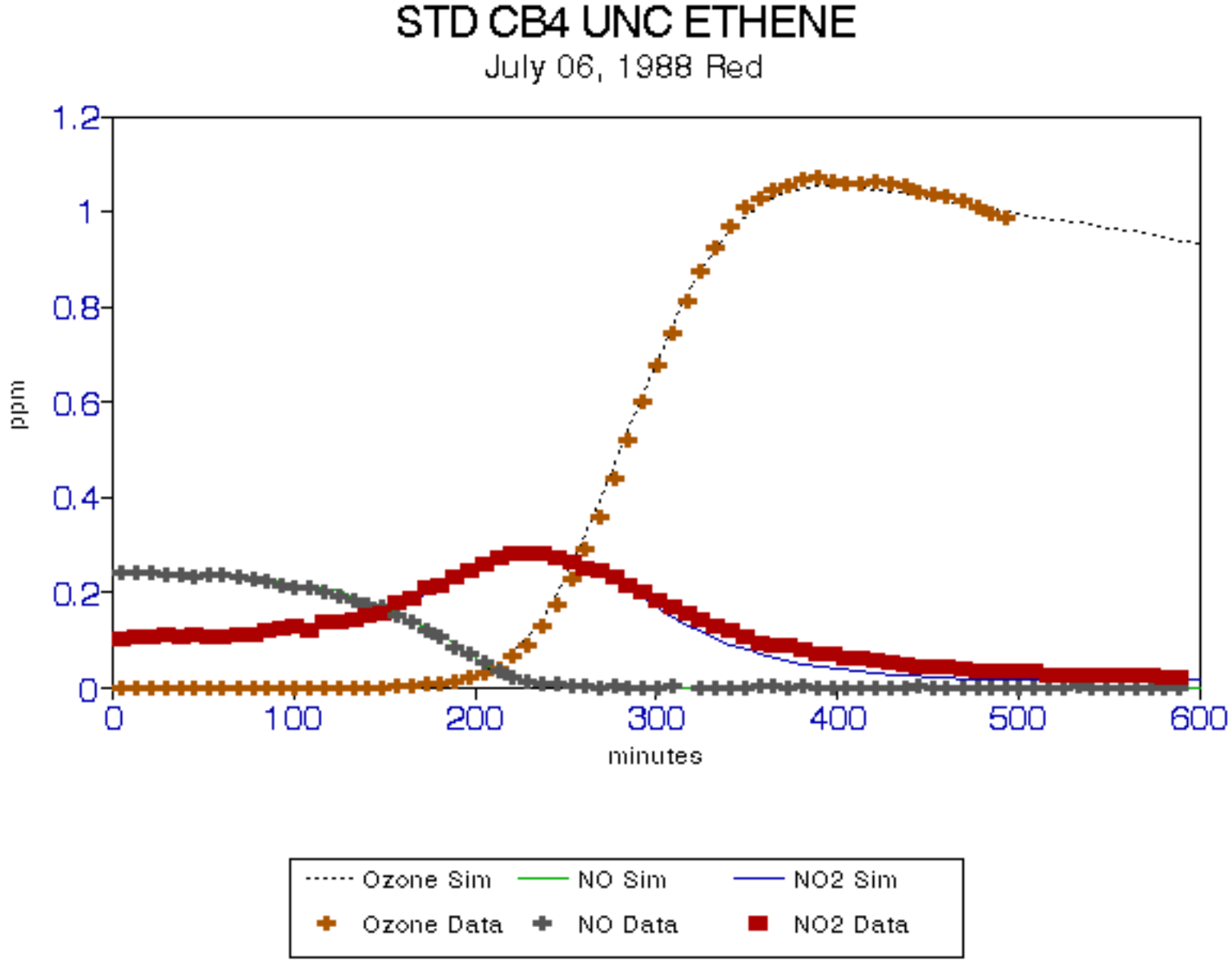
STD CB4 UNC ETHENE
July 06, 1988 Red
1.2
1
0.8
0.6
0.4
0.2
0
ppm
0
100
200
300
400
500
600
minutes
Ozone Sim
NO Sim
NO2 Sim
Ozone Data
NO Data
NO2 Data

FIGURE 12.

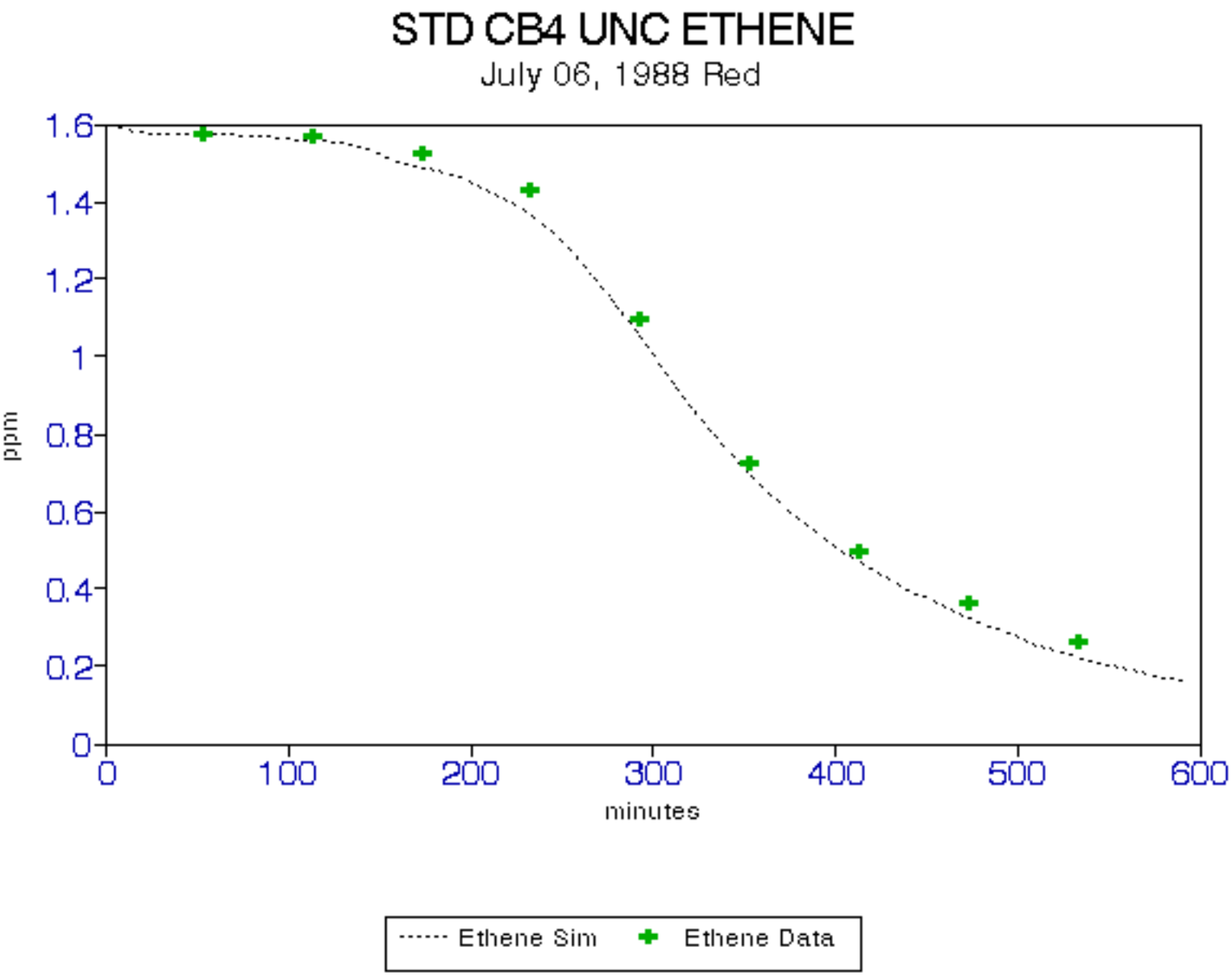
STD CB4 UNC ETHENE
July 06, 1988 Red
ppm
1.6
1.4
1.2
1
0.8
0.6
0.4
0.2
0
0
100
200
300
400
500
600
minutes
Ethene Sim
Ethene Data

FIGURE 13.

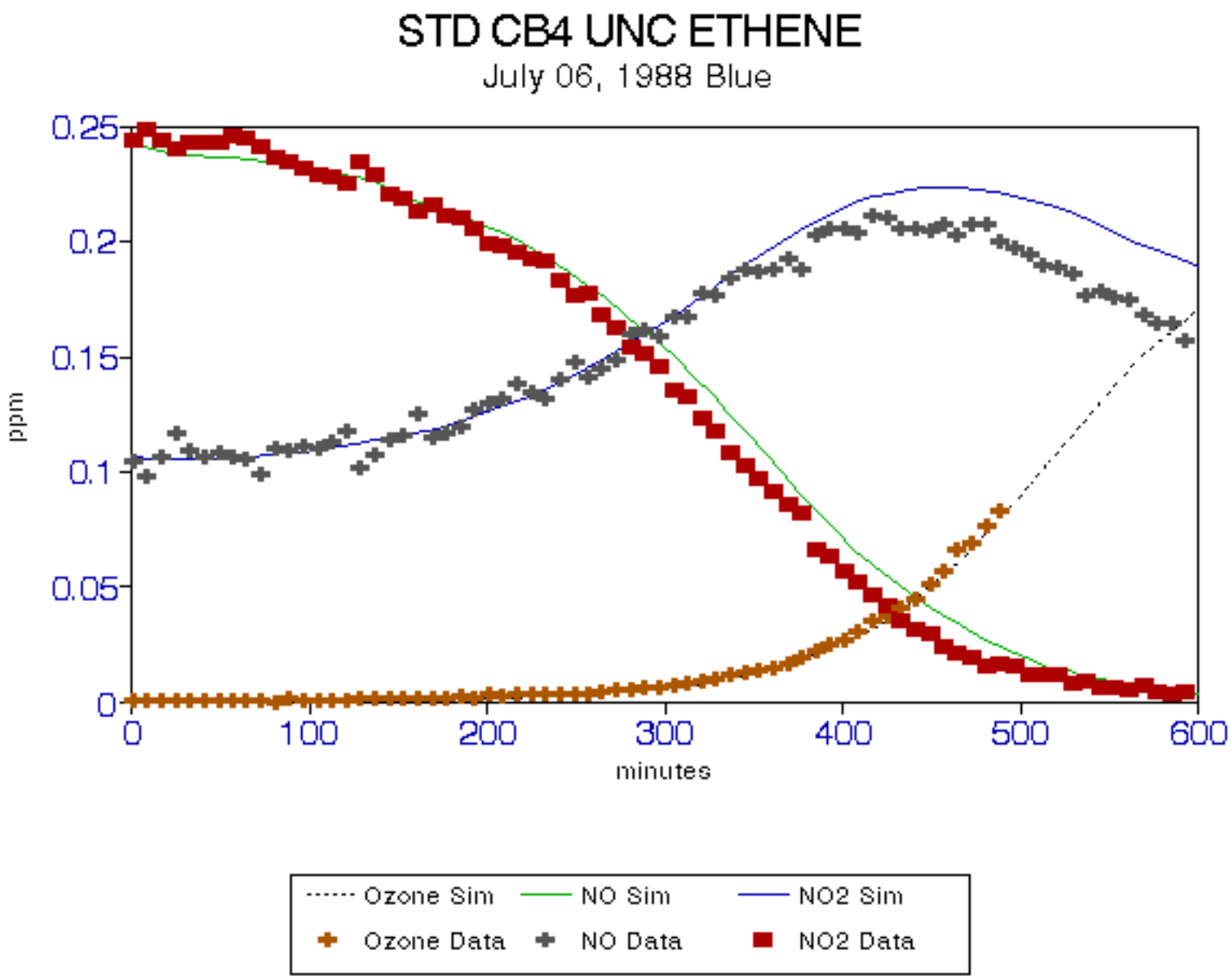
STD CB4 UNC ETHENE
July 06, 1988 Blue
ppm
0.25
0.2
0.15
0.1
0.05
0
0
100
200
300
400
500
600
minutes
Ozone Sim
NO Sim
NO2 Sim
Ozone Data
NO Data
NO2 Data

FIGURE 14.

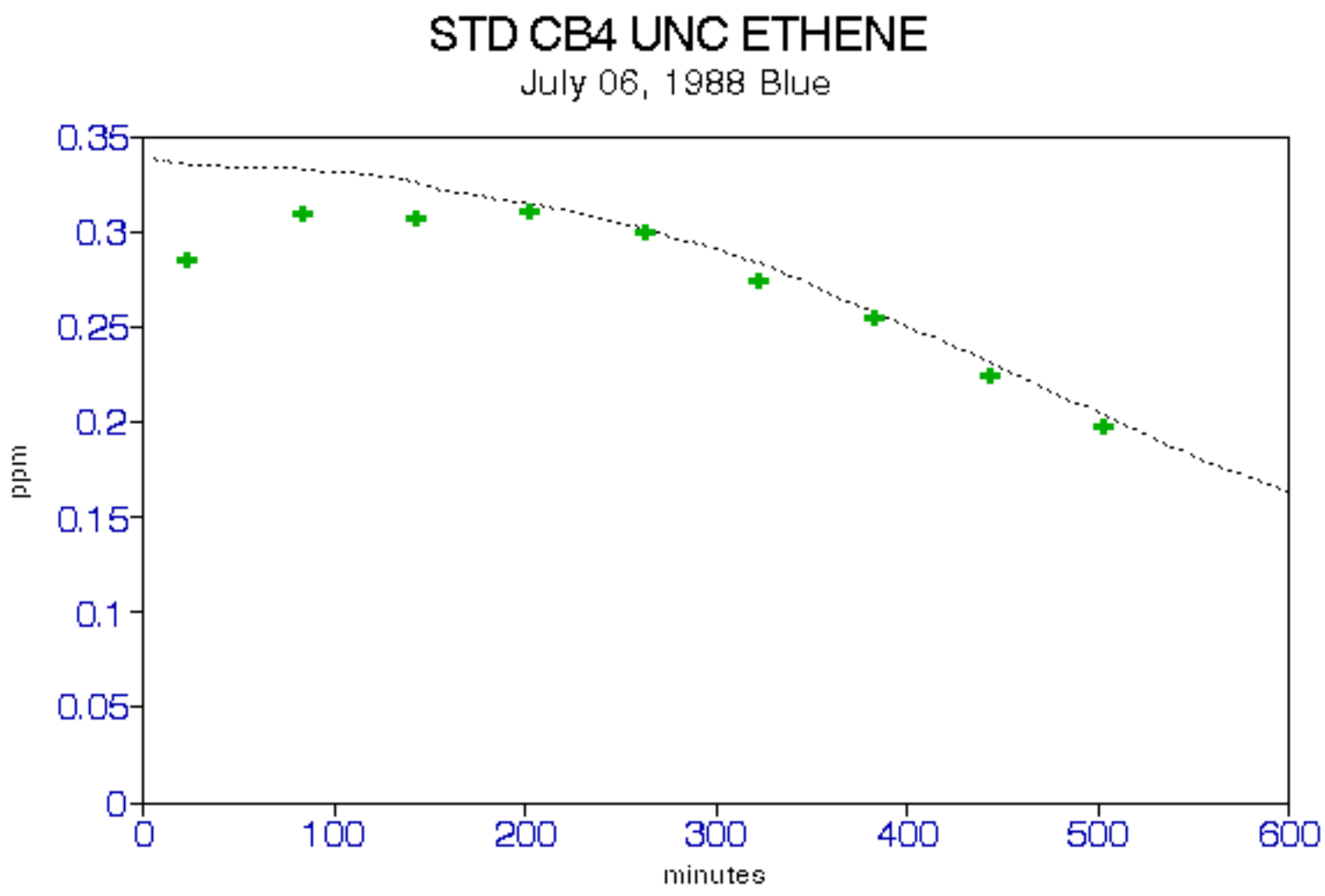
STD CB4 UNC ETHENE
July 06, 1988 Blue
0.35
0.3
0.25
0.2
0.15
0.1
0.05
0
ppm
0
100
200
300
400
500
600
minutes
Ethene Sim
Ethene Data

FIGURE 15.

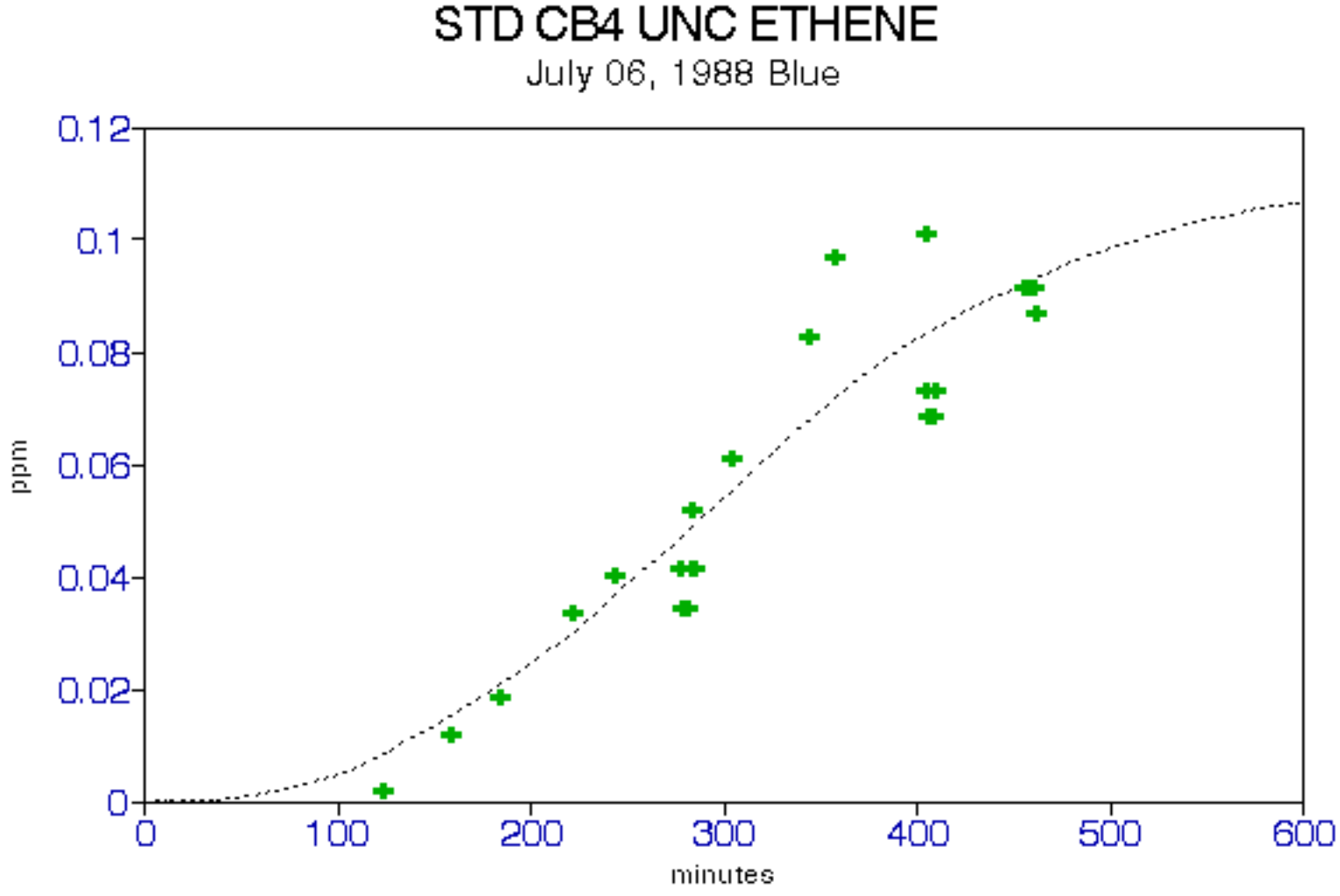
STD CB4 UNC ETHENE
July 06, 1988 Blue
0.12
0.1
0.08
0.06
0.04
0.02
0
ppm
0
100
200
300
400
500
600
minutes
HCHO Sim
HCHO Data

FIGURE 16.

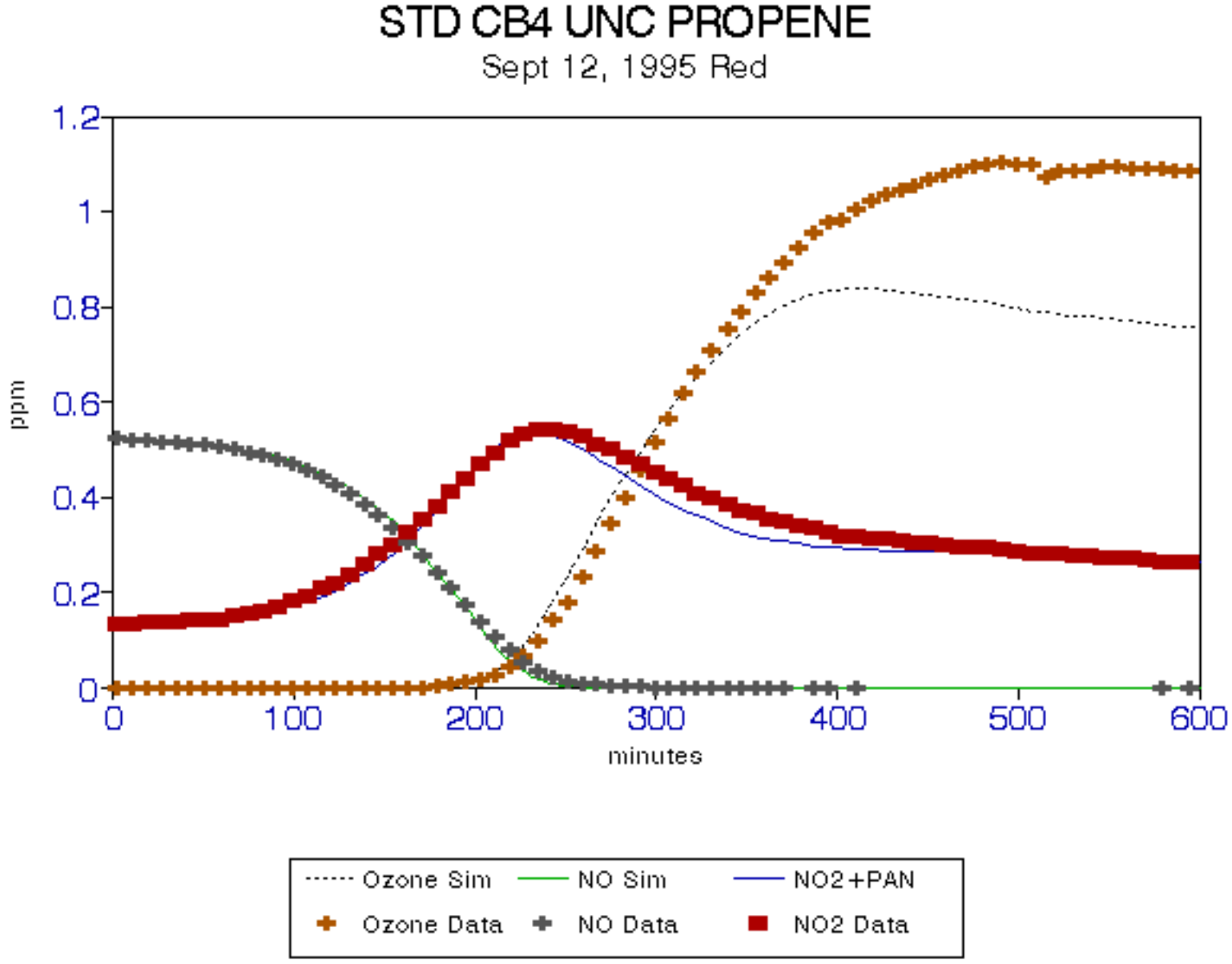
STD CB4 UNC PROPENE
Sept 12, 1995 Red
1.2
1
0.8
0.6
0.4
0.2
0
ppm
0
100
200
300
400
500
600
minutes
Ozone Sim
NO Sim
NO2+PAN
Ozone Data
NO Data
NO2 Data

FIGURE 17.

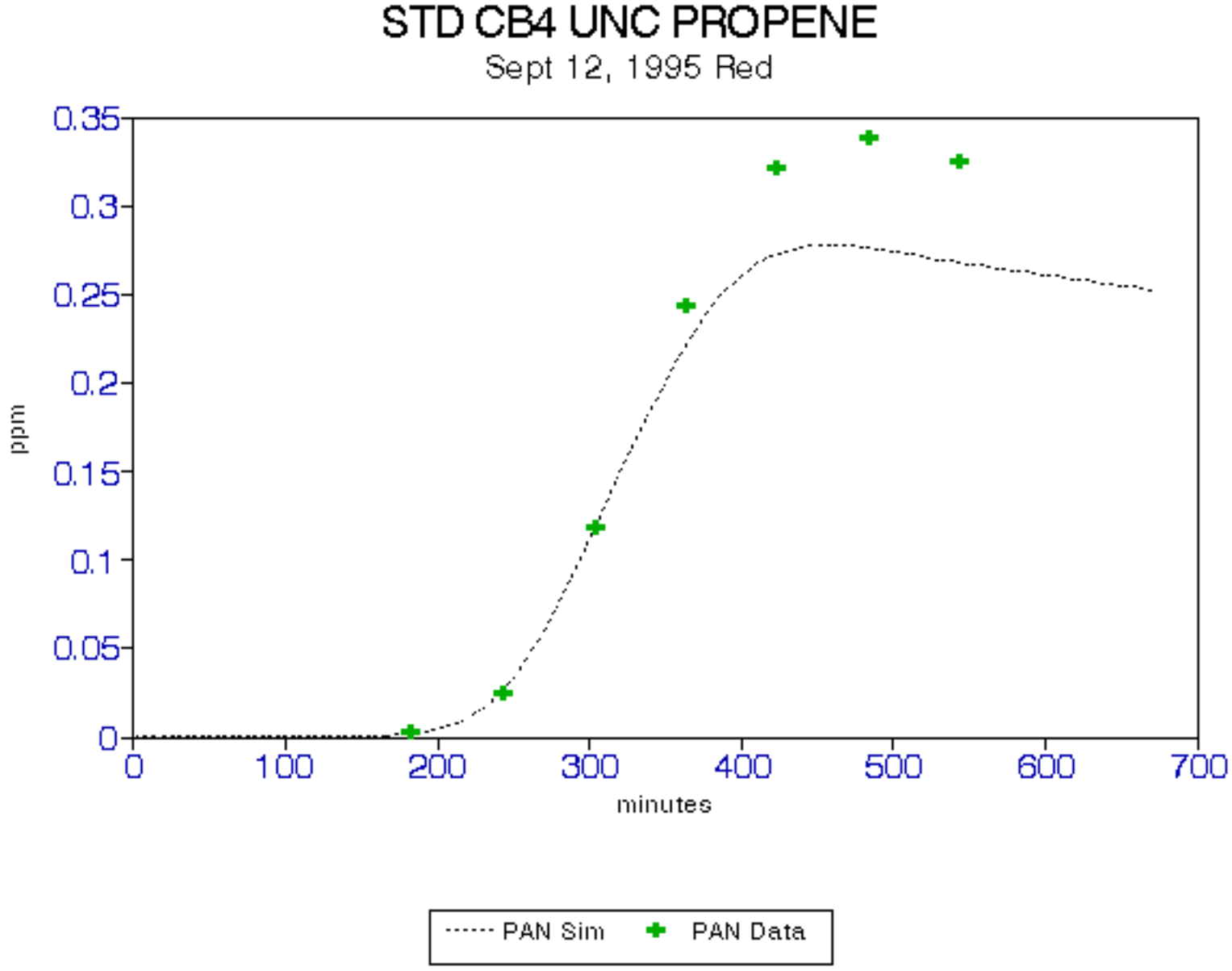
STD CB4 UNC PROPENE
Sept 12, 1995 Red
0.35
0.3
0.25
0.2
0.15
0.1
0.05
0
ppm
0
100
200
300
400
500
600
700
minutes
PAN Sim
PAN Data

FIGURE 18.

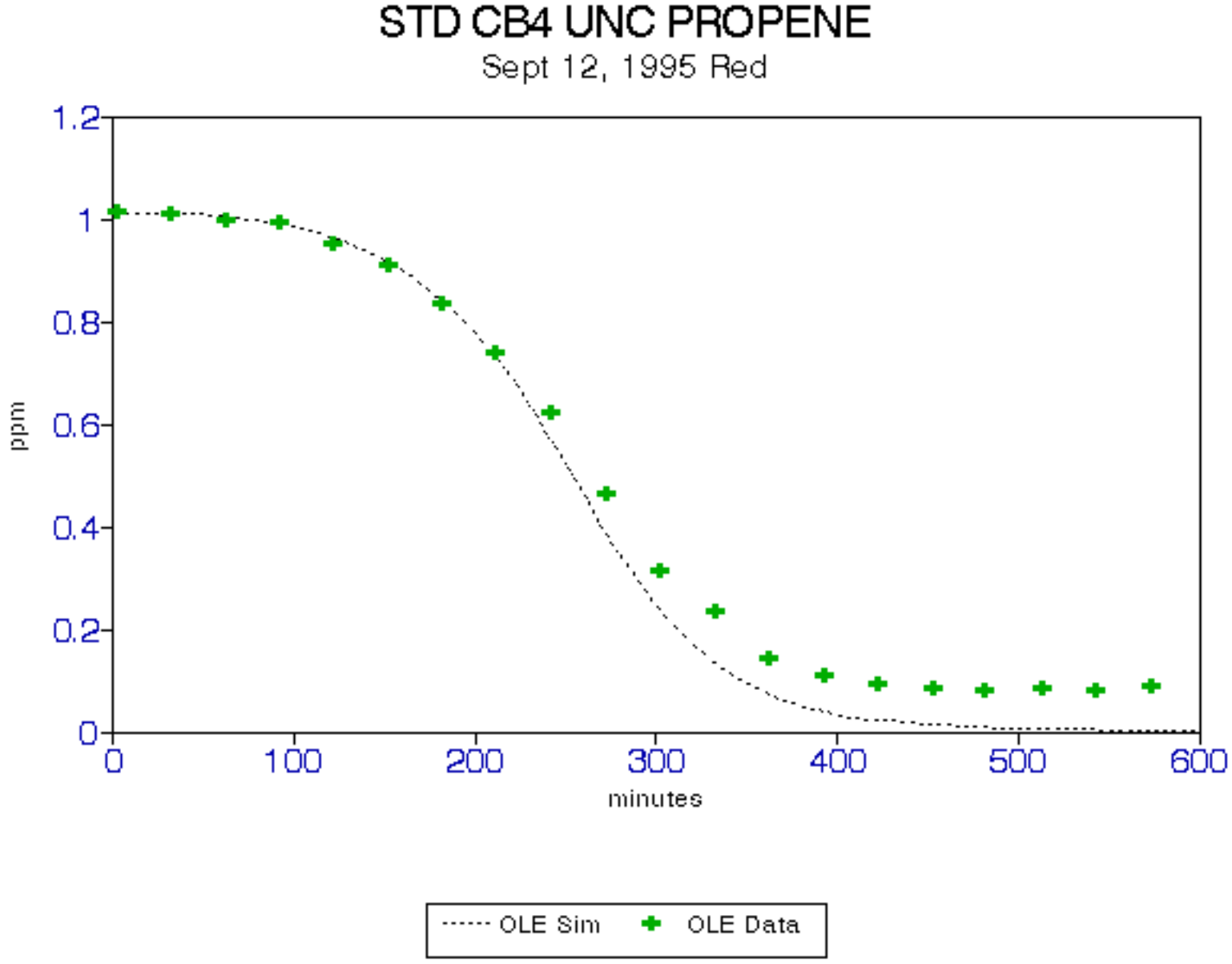
STD CB4 UNC PROPENE
Sept 12, 1995 Red
1.2
1
0.8
0.6
0.4
0.2
0
ppm
0
100
200
300
400
500
600
minutes
OLE Sim
OLE Data

FIGURE 19.

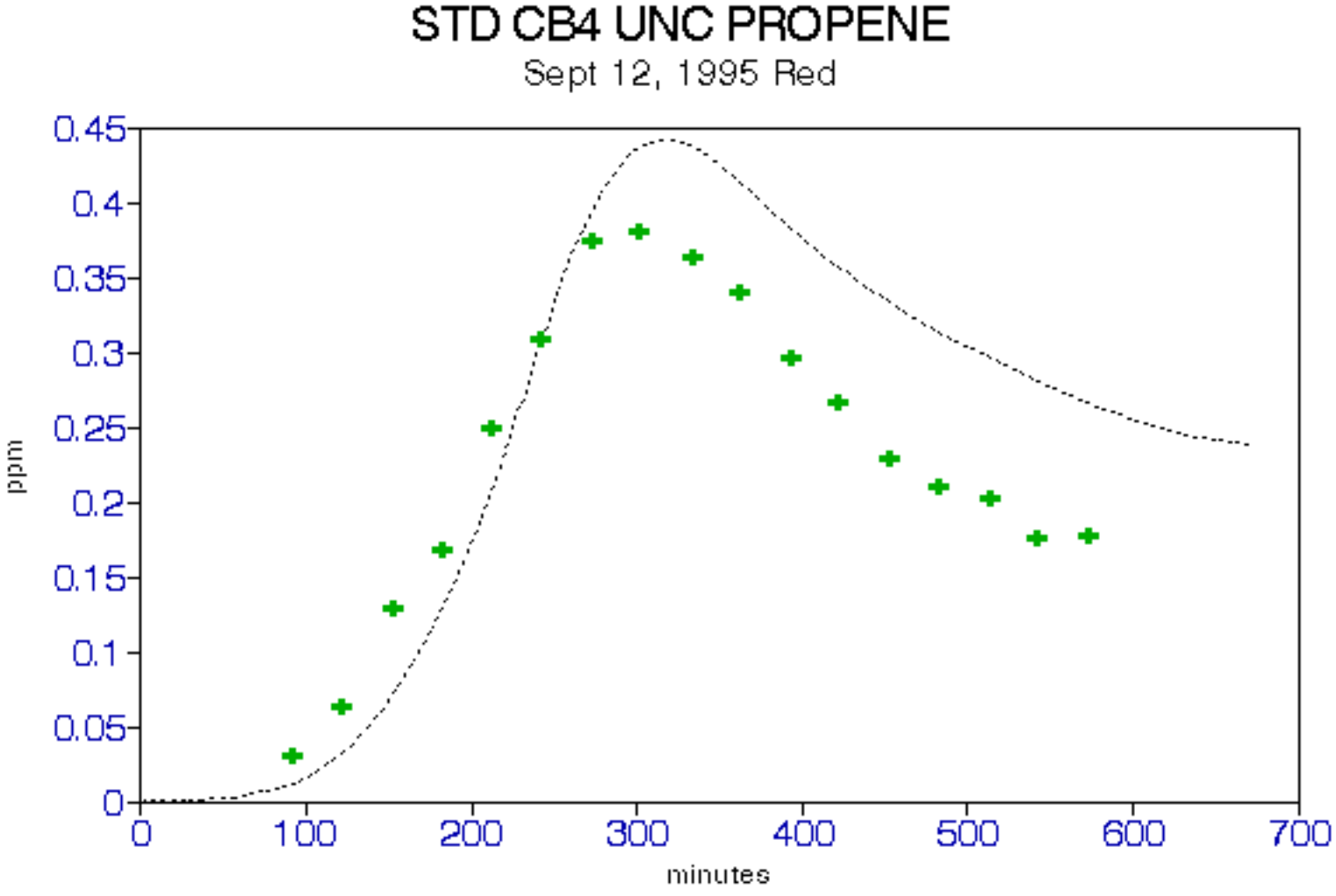
STD CB4 UNC PROPENE
Sept 12, 1995 Red
ppm
0.45
0.4
0.35
0.3
0.25
0.2
0.15
0.1
0.05
0
0
100
200
300
400
500
600
700
minutes
ALD2 Sim
ALD2 Data

FIGURE 20.

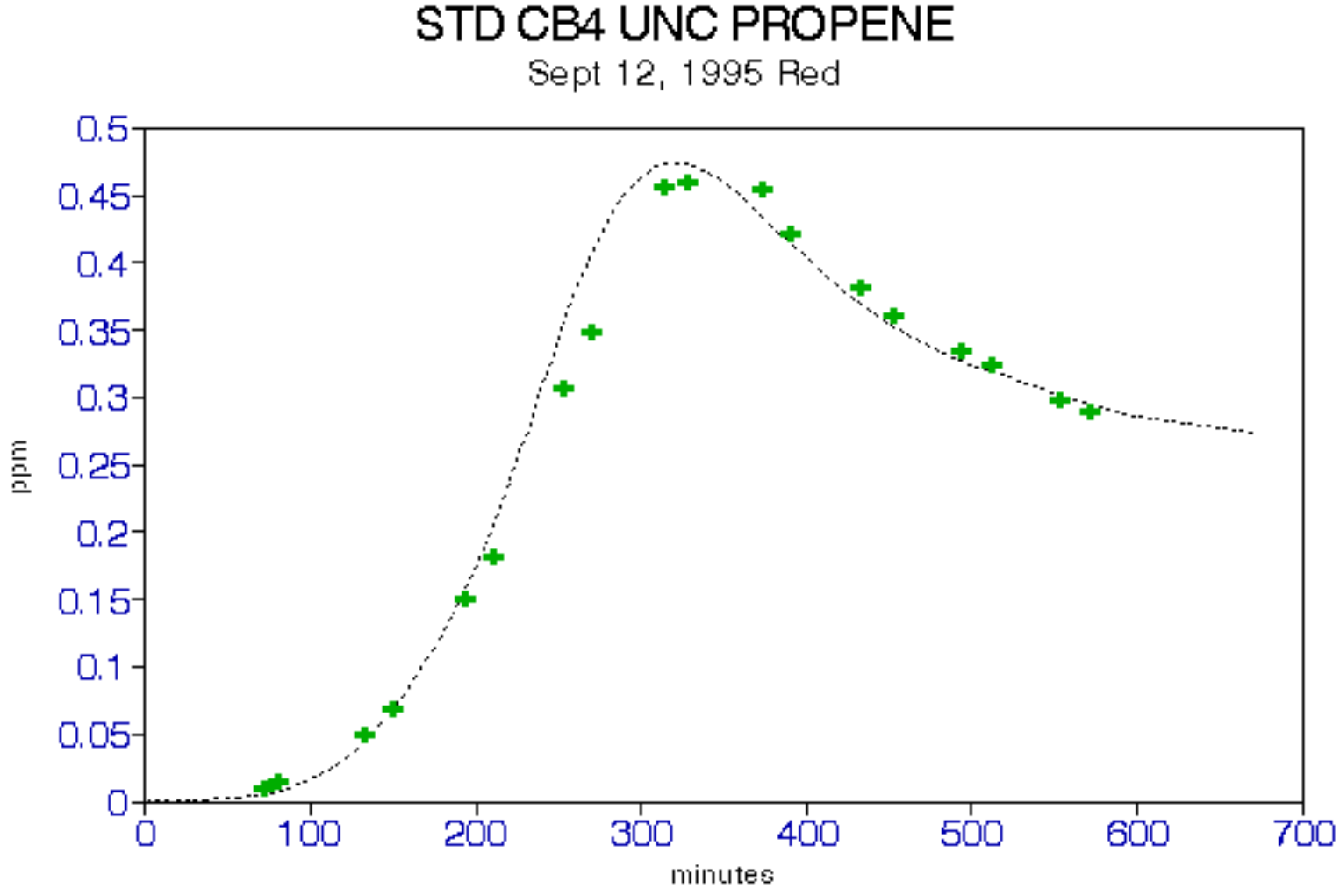
STD CB4 UNC PROPENE
Sept 12, 1995 Red
ppm
0.5
0.45
0.4
0.35
0.3
0.25
0.2
0.15
0.1
0.05
0
0
100
200
300
400
500
600
700
minutes
HCHO Sim
HCHO Data

FIGURE 21.

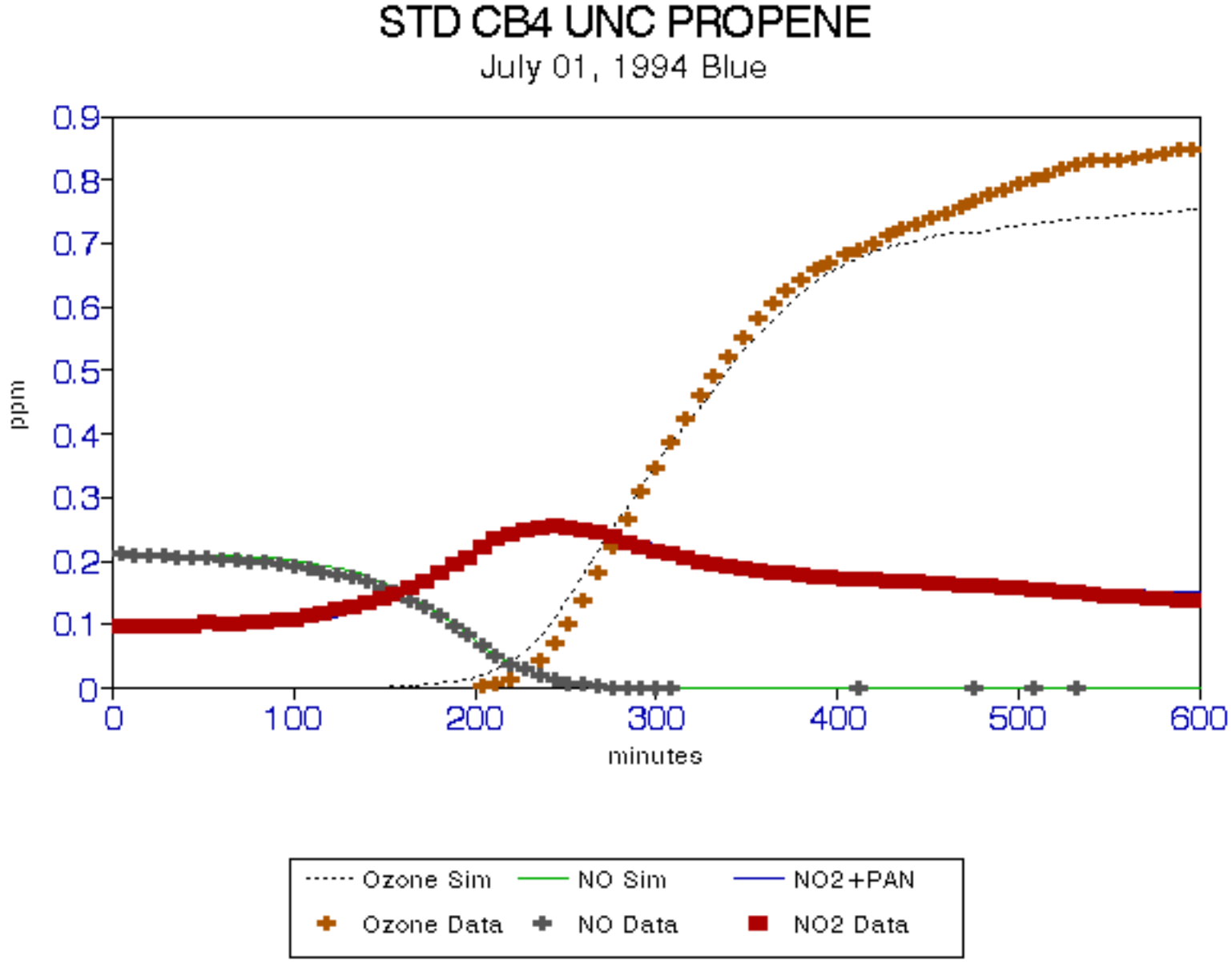
STD CB4 UNC PROPENE
July 01, 1994 Blue
ppm
0.9
0.8
0.7
0.6
0.5
0.4
0.3
0.2
0.1
0
0
100
200
300
400
500
600
minutes
Ozone Sim
NO Sim
NO2+PAN
Ozone Data
NO Data
NO2 Data

FIGURE 22.

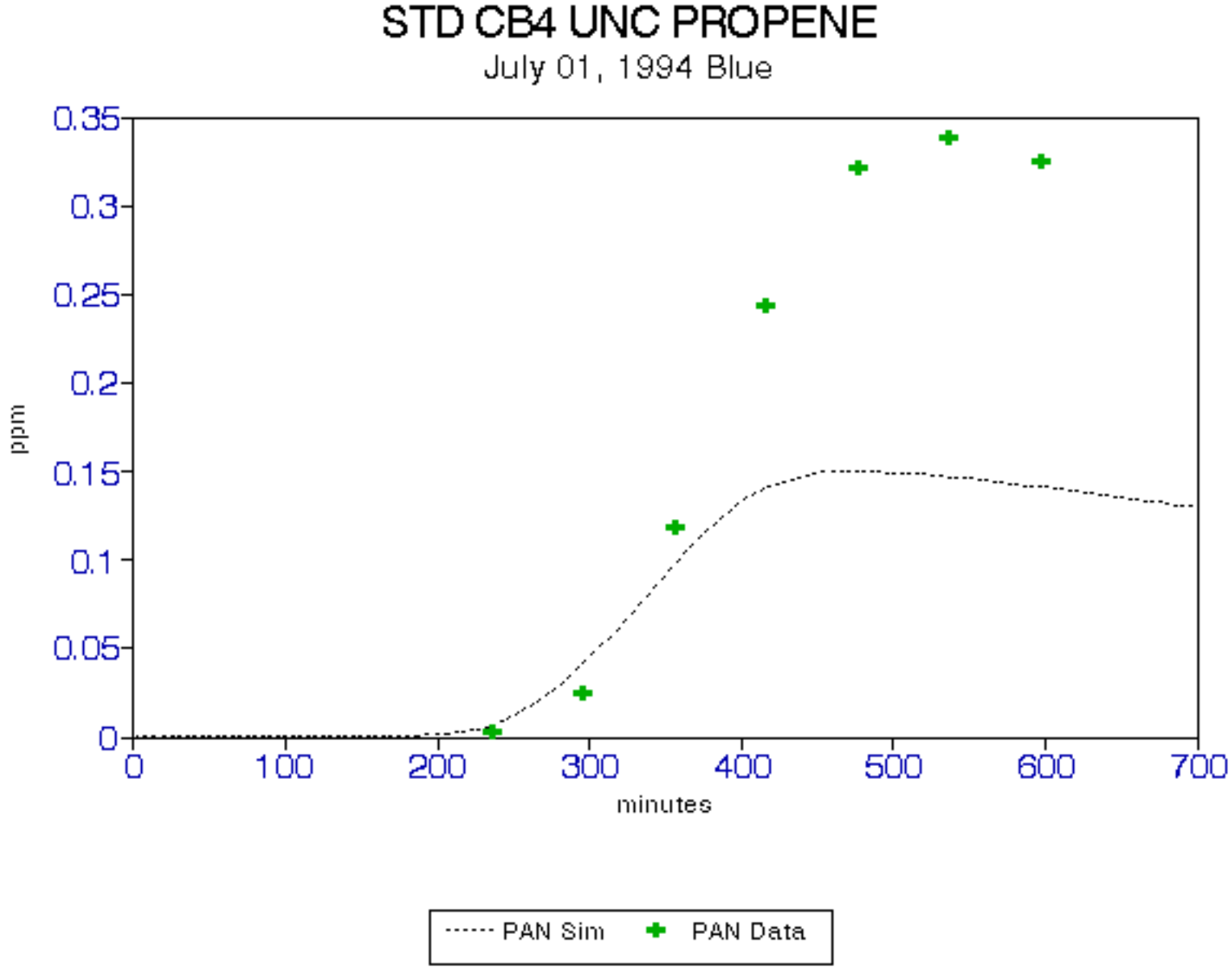
STD CB4 UNC PROPENE
July 01, 1994 Blue
0.35
0.3
0.25
0.2
0.15
0.1
0.05
0
ppm
0
100
200
300
400
500
600
700
minutes
PAN Sim
PAN Data

FIGURE 23.

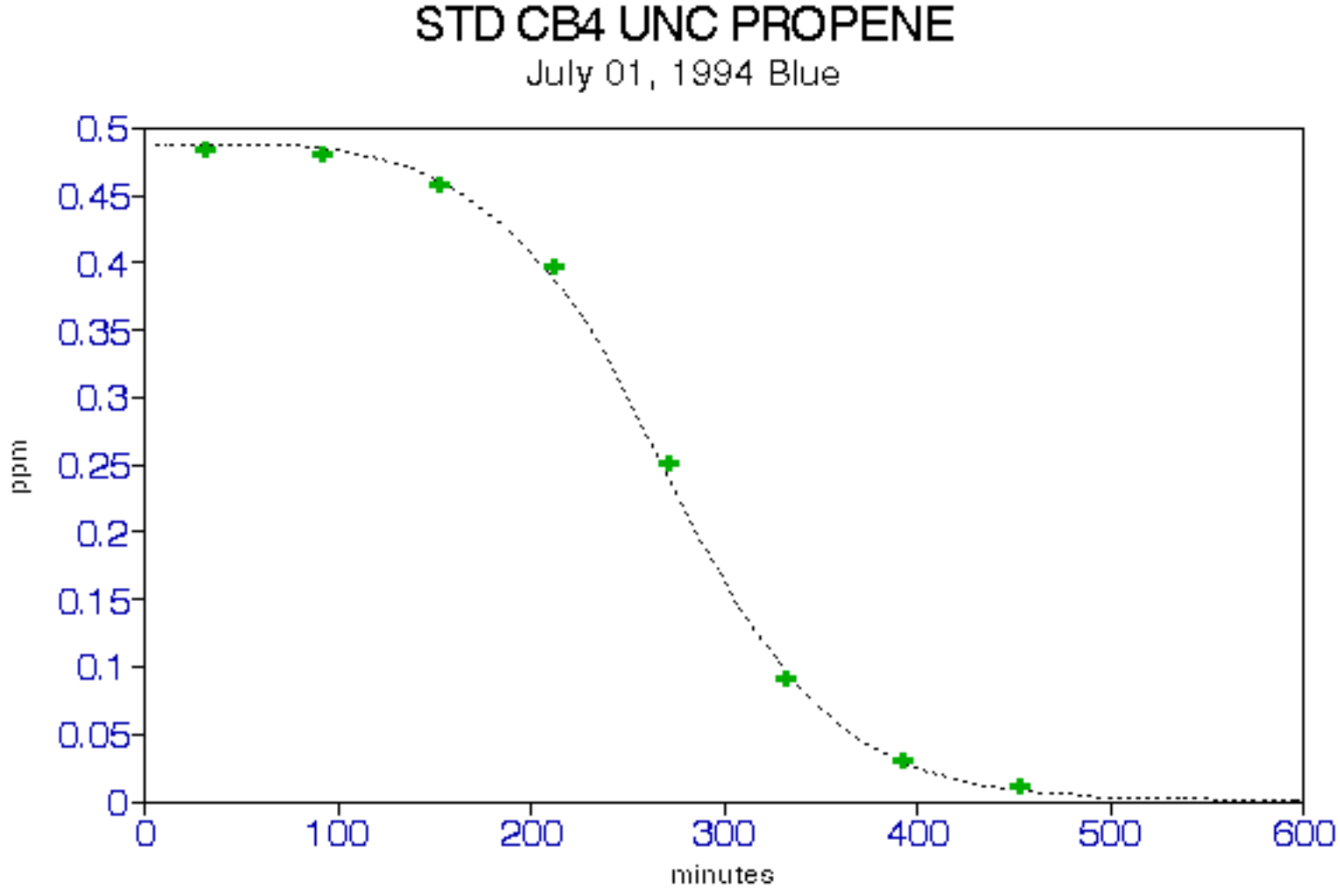
STD CB4 UNC PROPENE
July 01, 1994 Blue
0.5
0.45
0.4
0.35
0.3
0.25
0.2
0.15
0.1
0.05
0
ppm
0
100
200
300
400
500
600
minutes
OLE Sim
OLE Data

FIGURE 24.

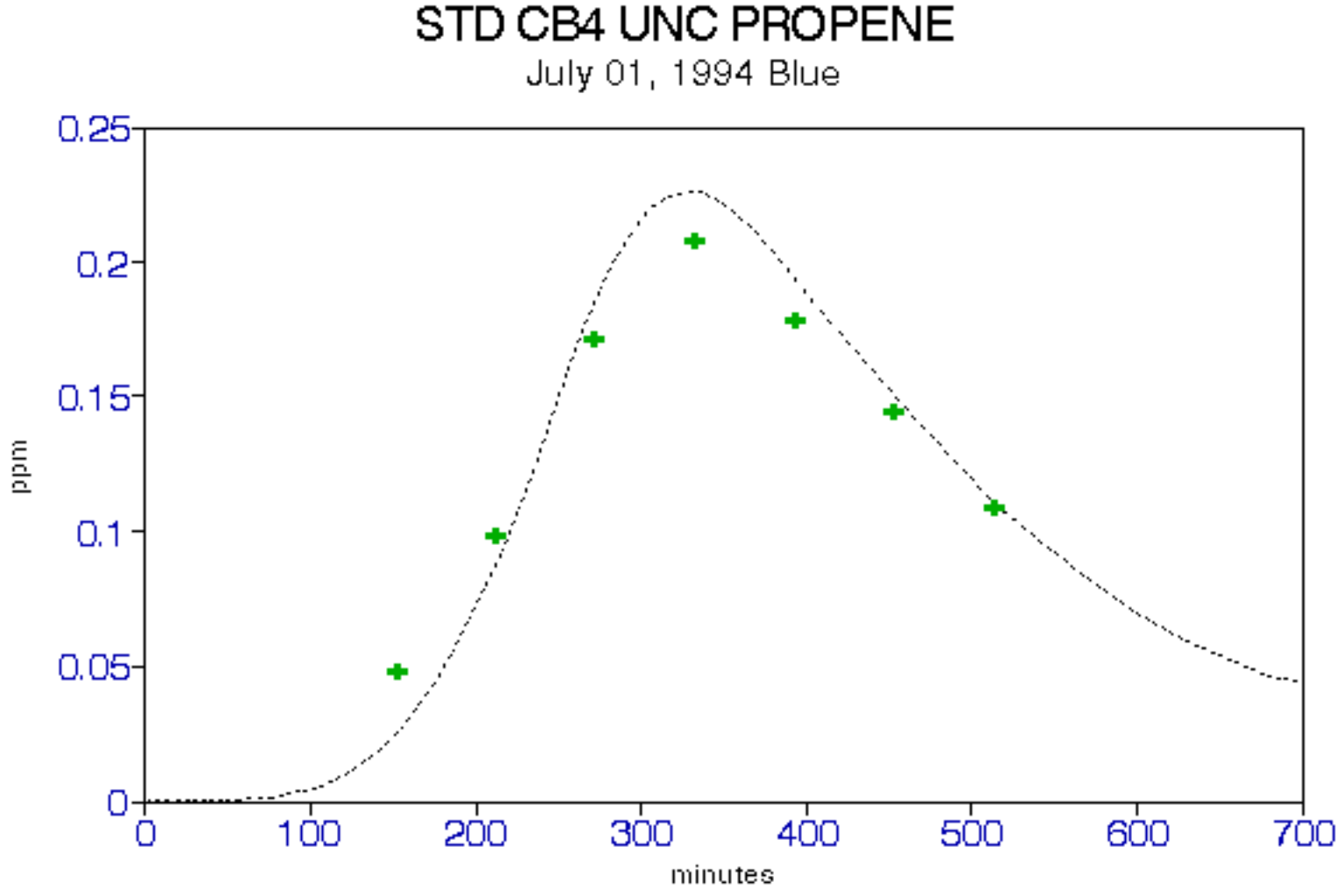
STD CB4 UNC PROPENE
July 01, 1994 Blue
0.25
0.2
0.15
0.1
0.05
0
ppm
0
100
200
300
400
500
600
700
minutes
ALD2 Sim
ALD2 Data

FIGURE 25.

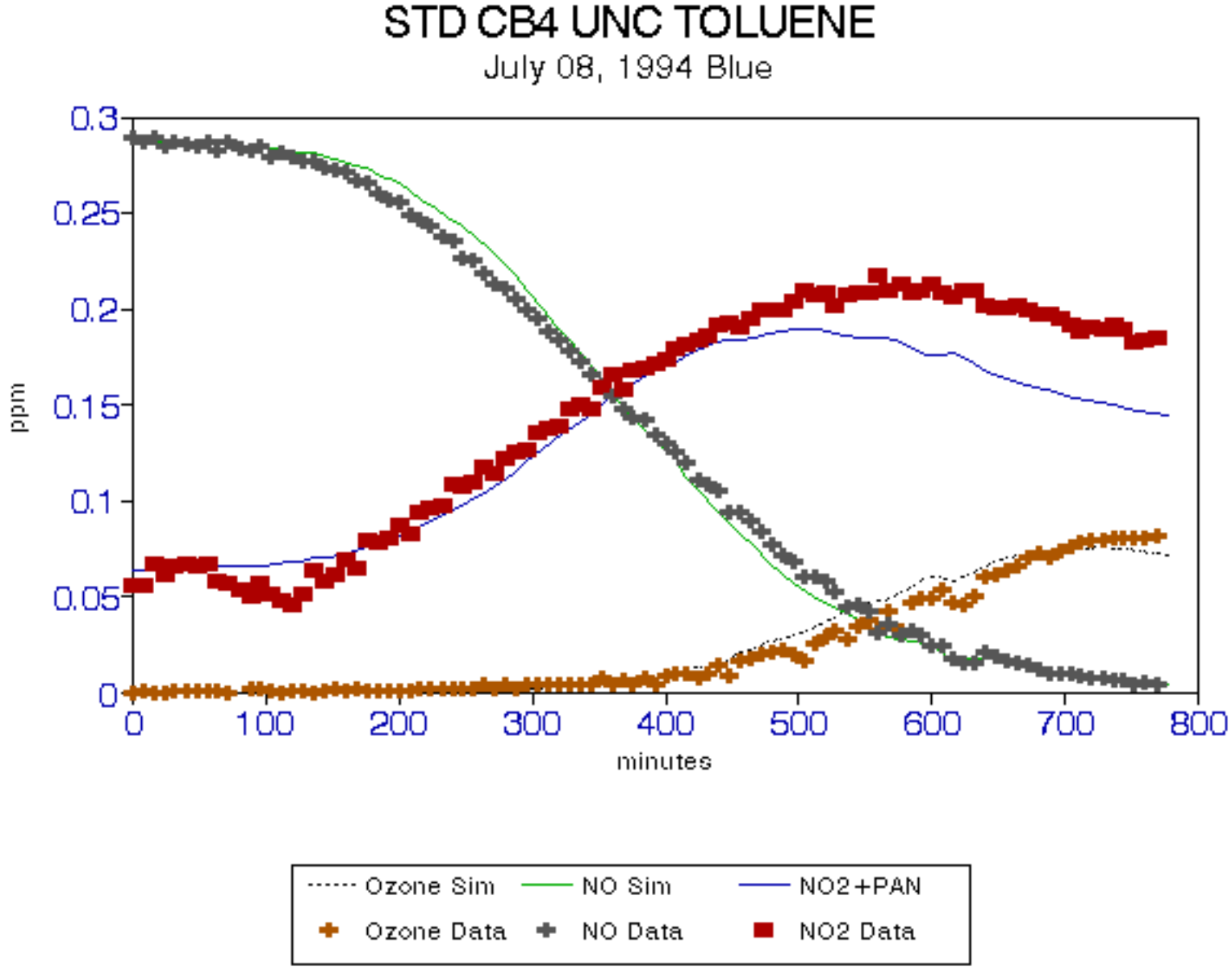
STD CB4 UNC TOLUENE
July 08, 1994 Blue
0.3
0.25
0.2
0.15
0.1
0.05
0
ppm
0
100
200
300
400
500
600
700
800
minutes
Ozone Sim
NO Sim
NO2+PAN
Ozone Data
NO Data
NO2 Data

FIGURE 26.

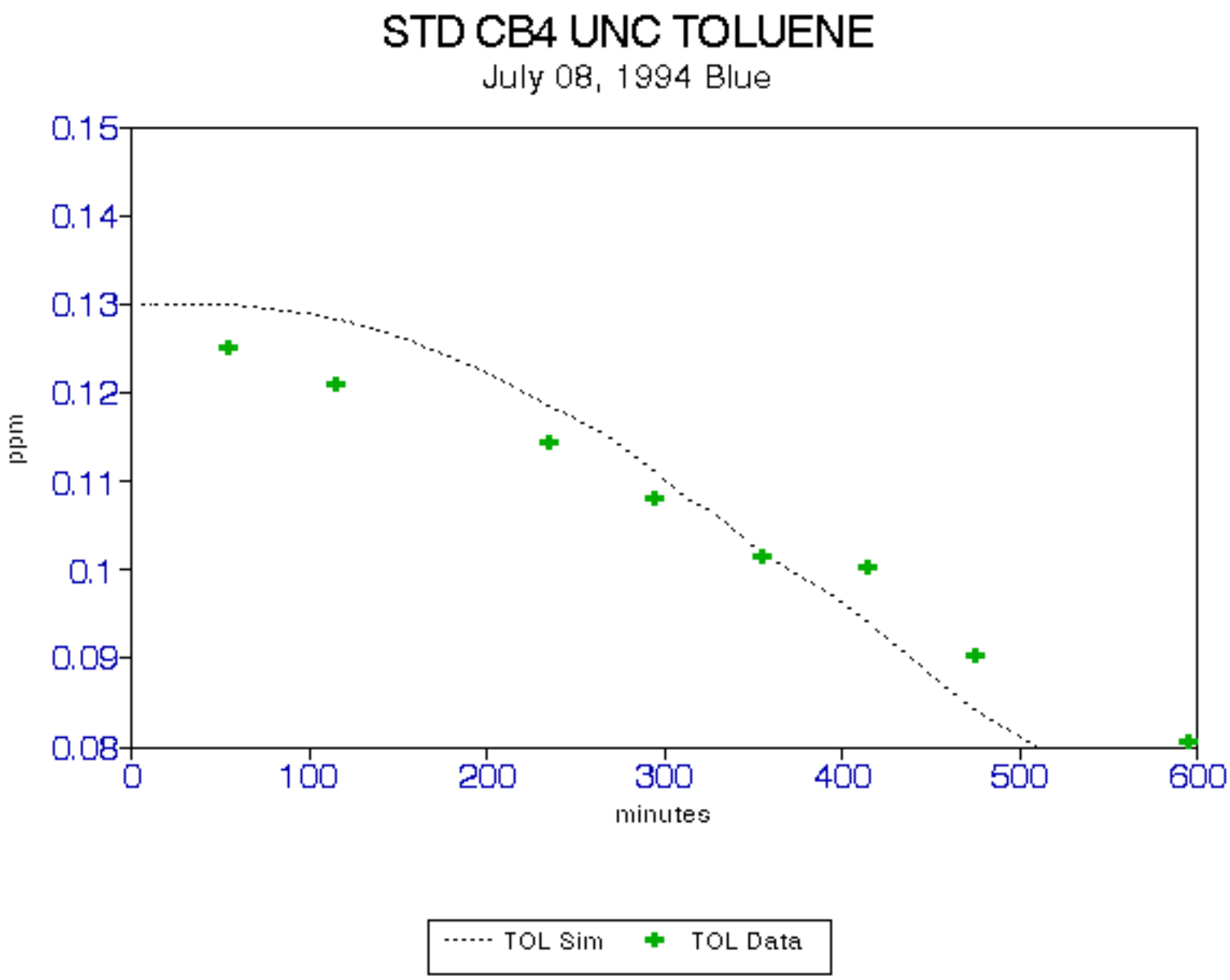
STD CB4 UNC TOLUENE
July 08, 1994 Blue
ppm
0.15
0.14
0.13
0.12
0.11
0.1
0.09
0.08
0
100
200
300
400
500
600
minutes
TOL Sim
TOL Data

FIGURE 27.

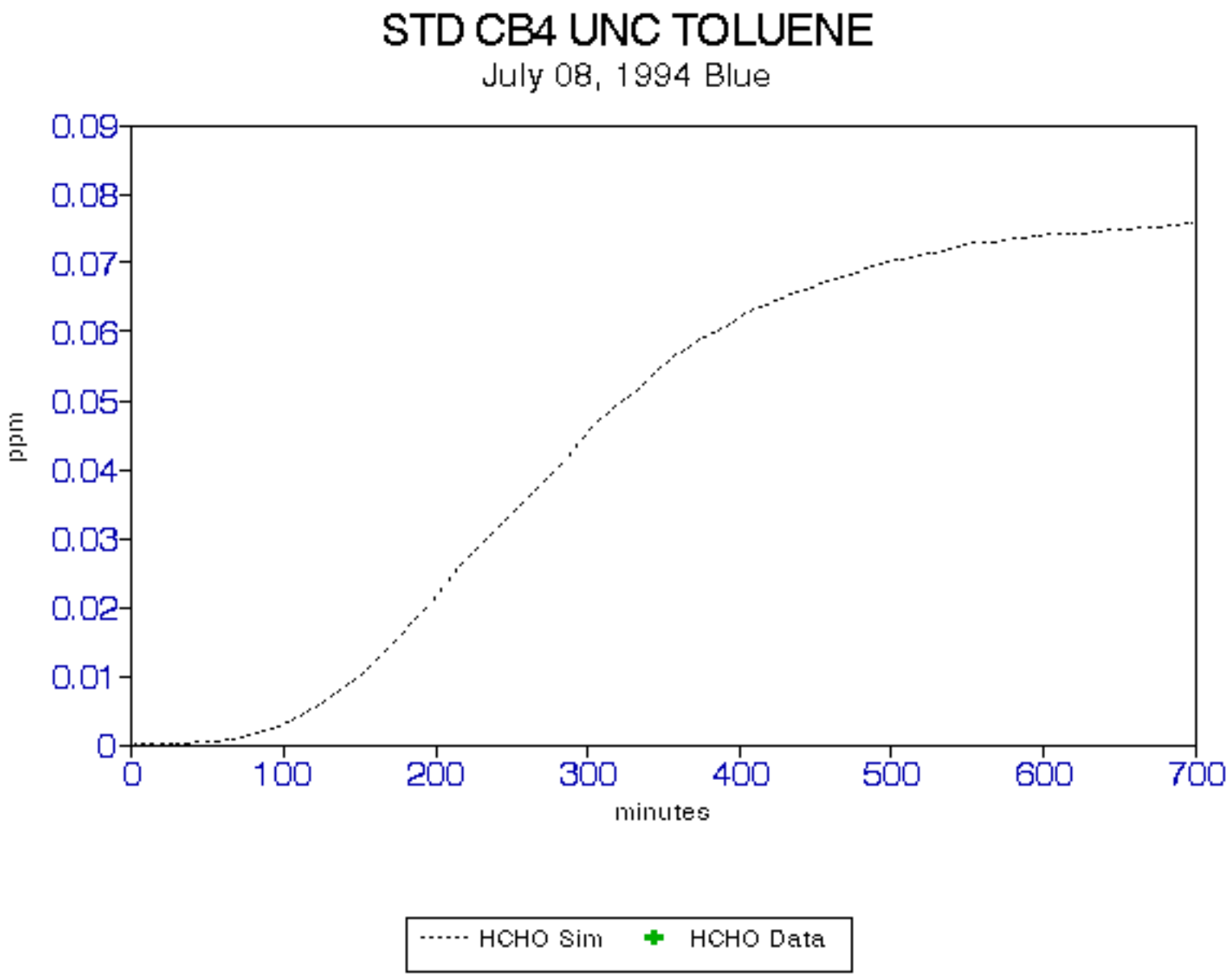
STD CB4 UNC TOLUENE
July 08, 1994 Blue
0.09
0.08
0.07
0.06
0.05
0.04
0.03
0.02
0.01
0
ppm
0
100
200
300
400
500
600
700
minutes
HCHO Sim
HCHO Data

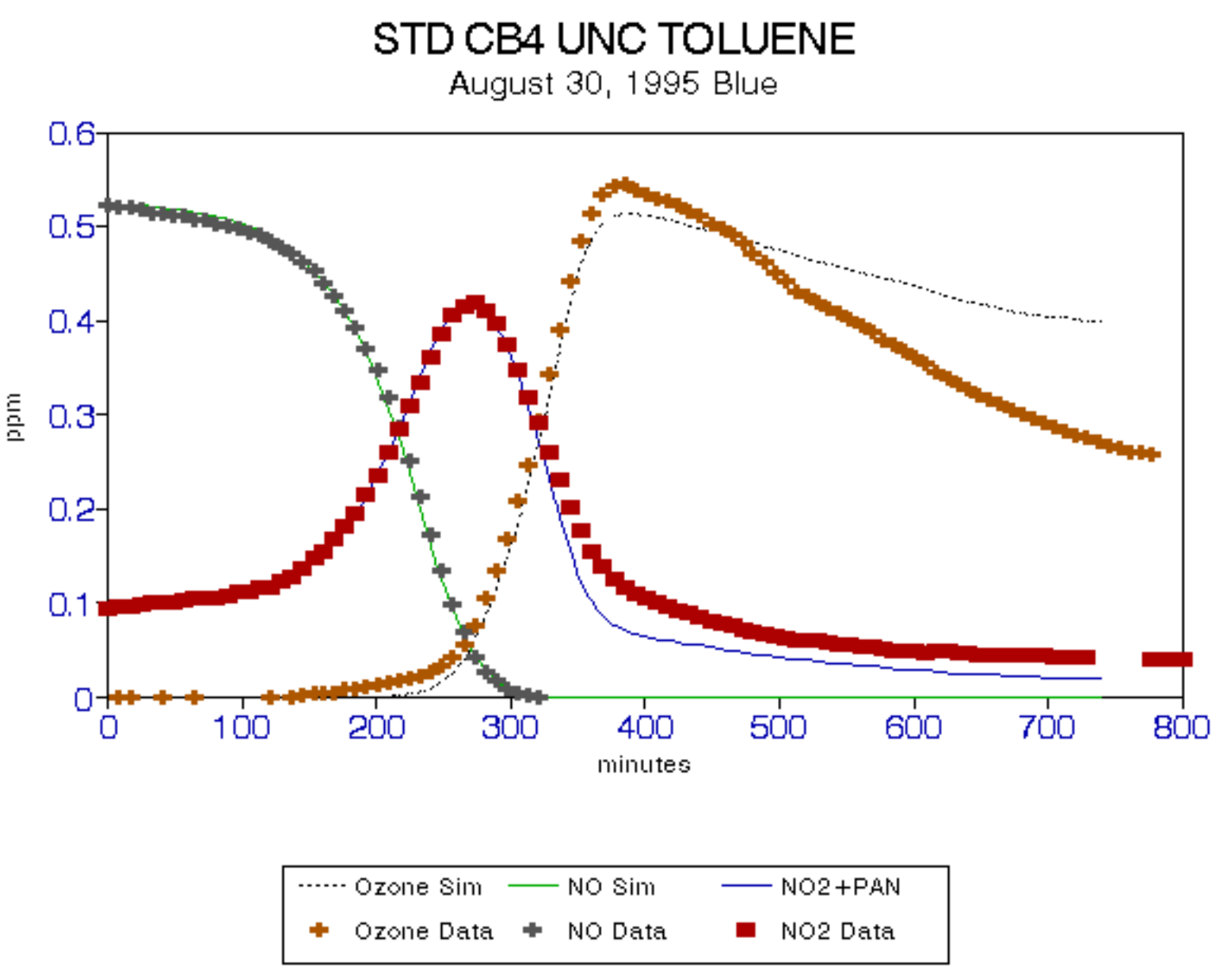
STD CB4 UNC TOLUENE
August 30, 1995 Blue
0.6
0.5
0.4
0.3
0.2
0.1
0
ppm
0
100
200
300
400
500
600
700
800
minutes
Ozone Sim
NO Sim
NO2+PAN
Ozone Data
NO Data
NO2 Data

FIGURE 29.

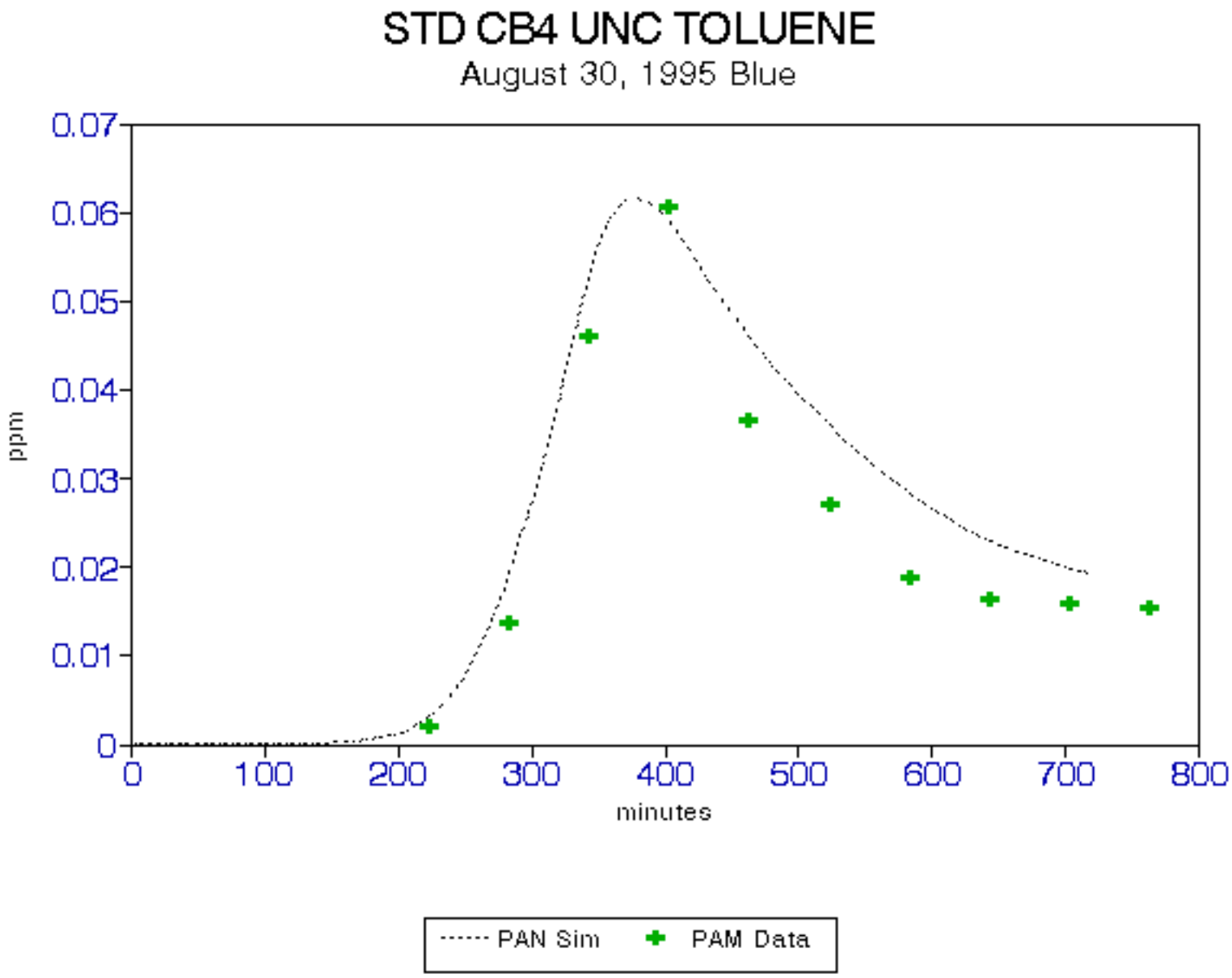
STD CB4 UNC TOLUENE
August 30, 1995 Blue
0.07
0.06
0.05
0.04
0.03
0.02
0.01
0
ppm
0
100
200
300
400
500
600
700
800
minutes
PAN Sim
PAM Data

FIGURE 30.

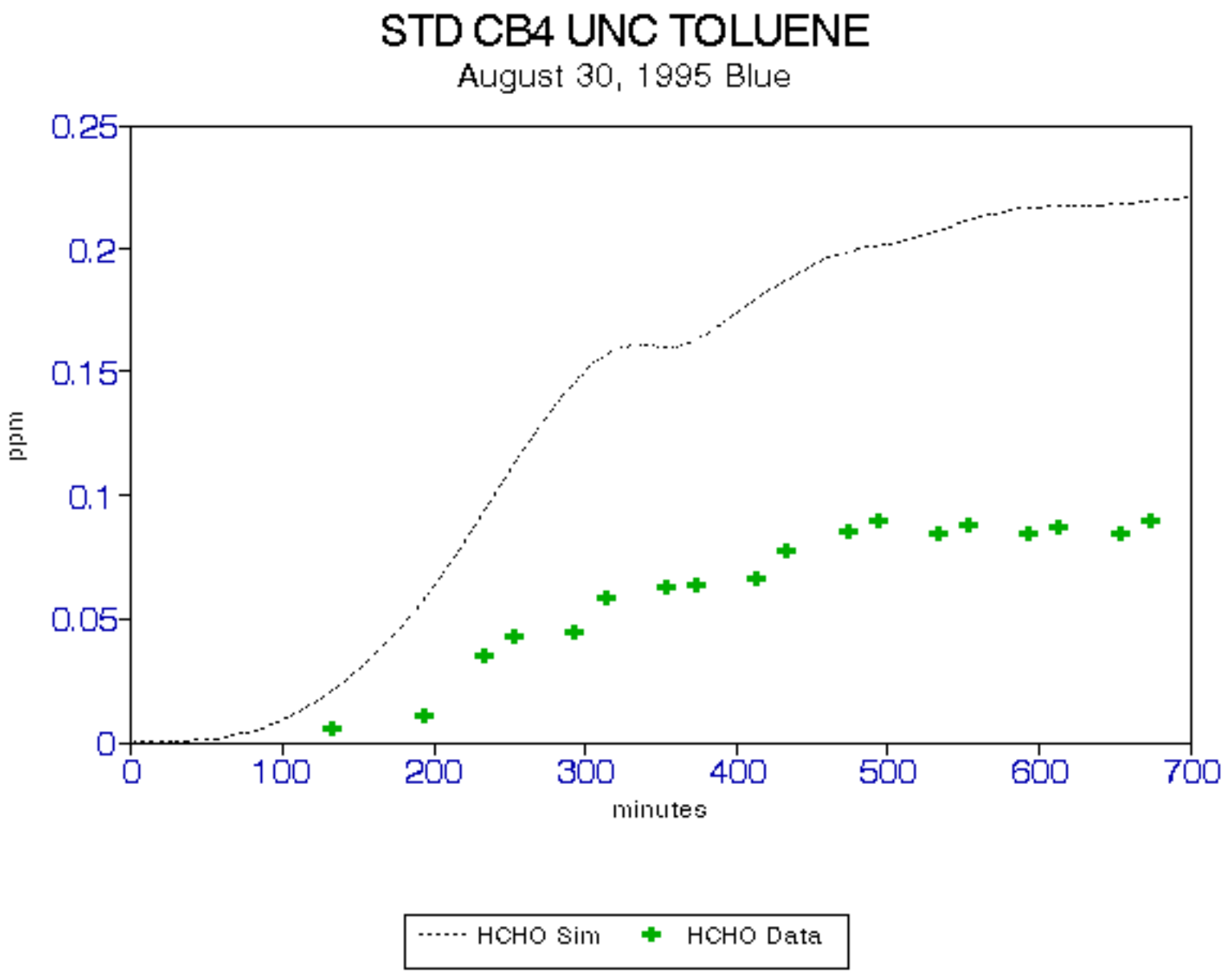
STD CB4 UNC TOLUENE
August 30, 1995 Blue
0.25
0.2
0.15
0.1
0.05
0
ppm
0
100
200
300
400
500
600
700
minutes
HCHO Sim
HCHO Data

FIGURE 31.

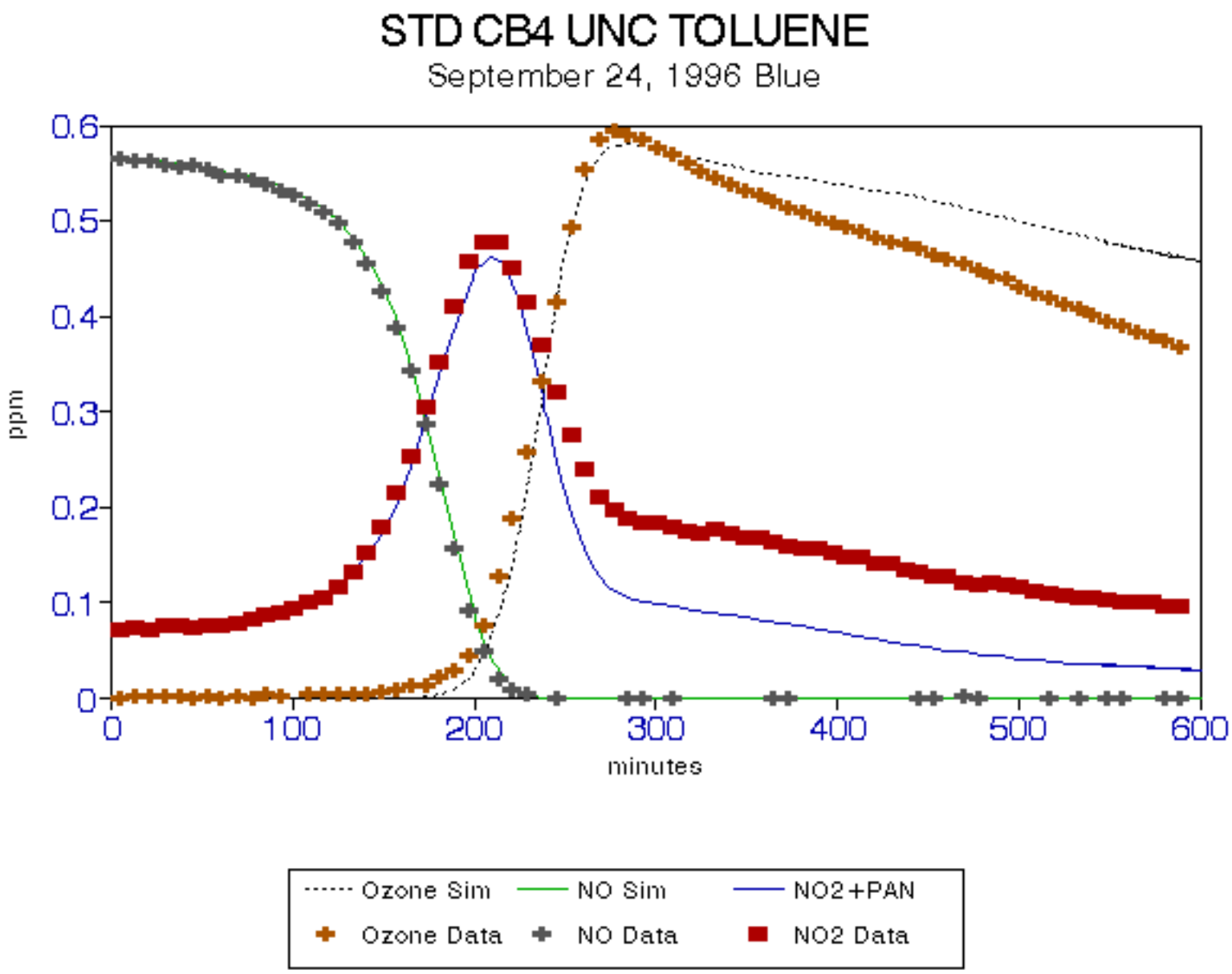
STD CB4 UNC TOLUENE
September 24, 1996 Blue
ppm
0.6
0.5
0.4
0.3
0.2
0.1
0
0
100
200
300
400
500
600
minutes
Ozone Sim
NO Sim
NO2+PAN
Ozone Data
NO Data
NO2 Data

FIGURE 32.

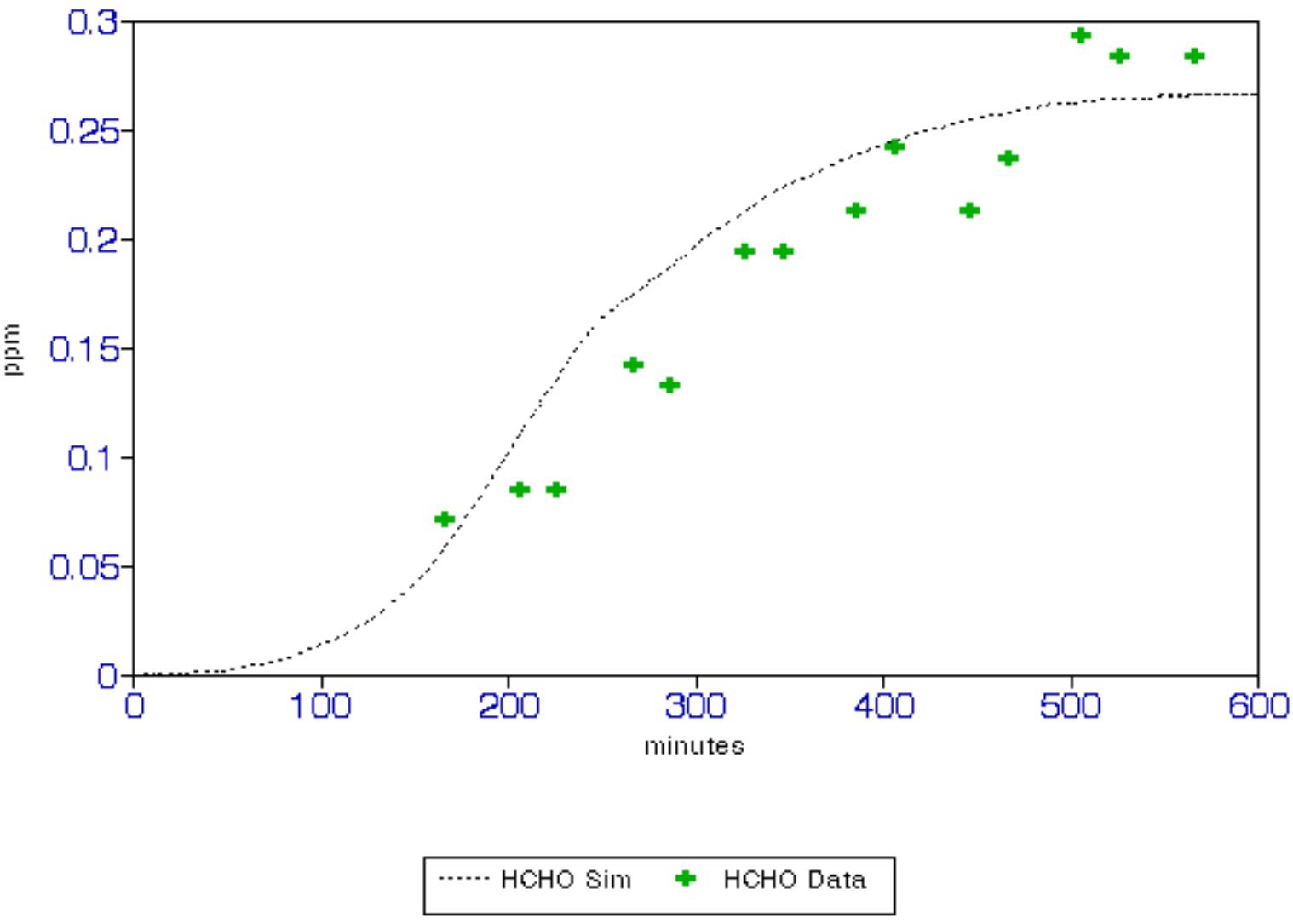
STD CB4 UNC TOLUENE
September 24, 1996 Blue
0.3
0.25
0.2
0.15
0.1
0.05
0
ppmC
0
100
200
300
400
500
600
minutes
HCHO Sim
HCHO Data

FIGURE 33.

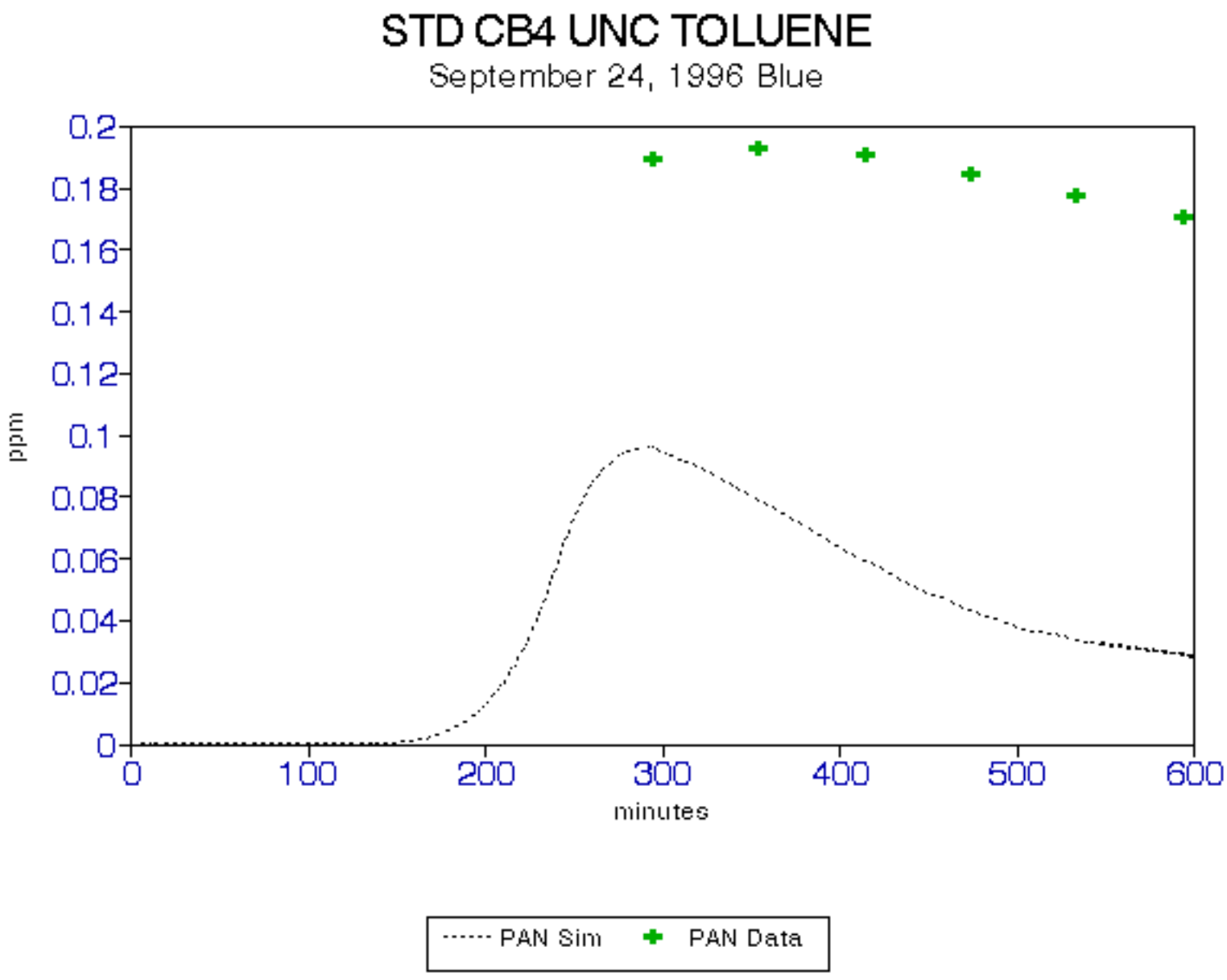
STD CB4 UNC TOLUENE
September 24, 1996 Blue
0.2
0.18
0.16
0.14
0.12
0.1
0.08
0.06
0.04
0.02
0
ppm
0
100
200
300
400
500
600
minutes
PAN Sim
PAN Data

FIGURE 34.

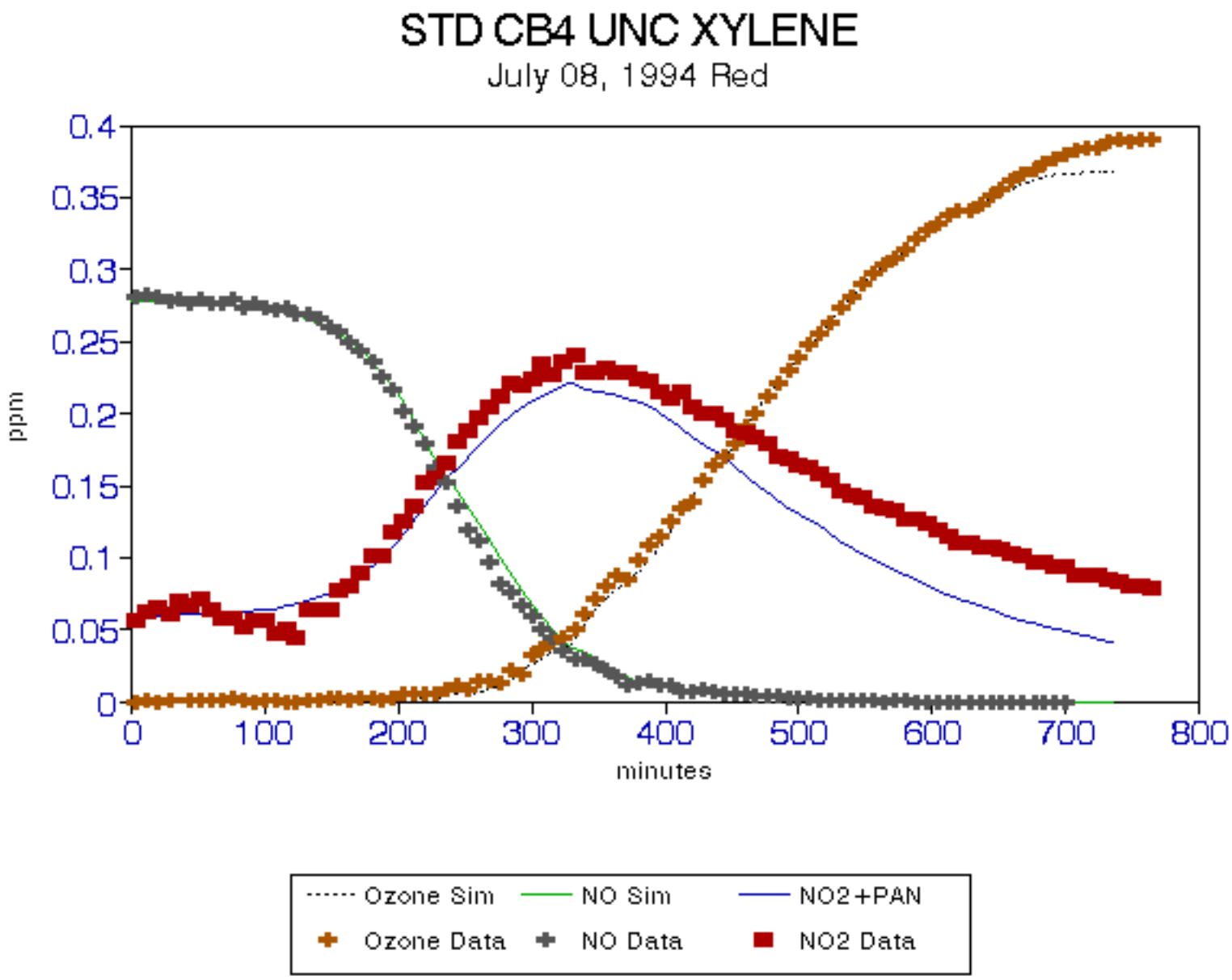
STD CB4 UNC XYLENE
July 08, 1994 Red
ppm
0.4
0.35
0.3
0.25
0.2
0.15
0.1
0.05
0
0
100
200
300
400
500
600
700
800
minutes
Ozone Sim
NO Sim
NO2+PAN
Ozone Data
NO Data
NO2 Data

FIGURE 35.

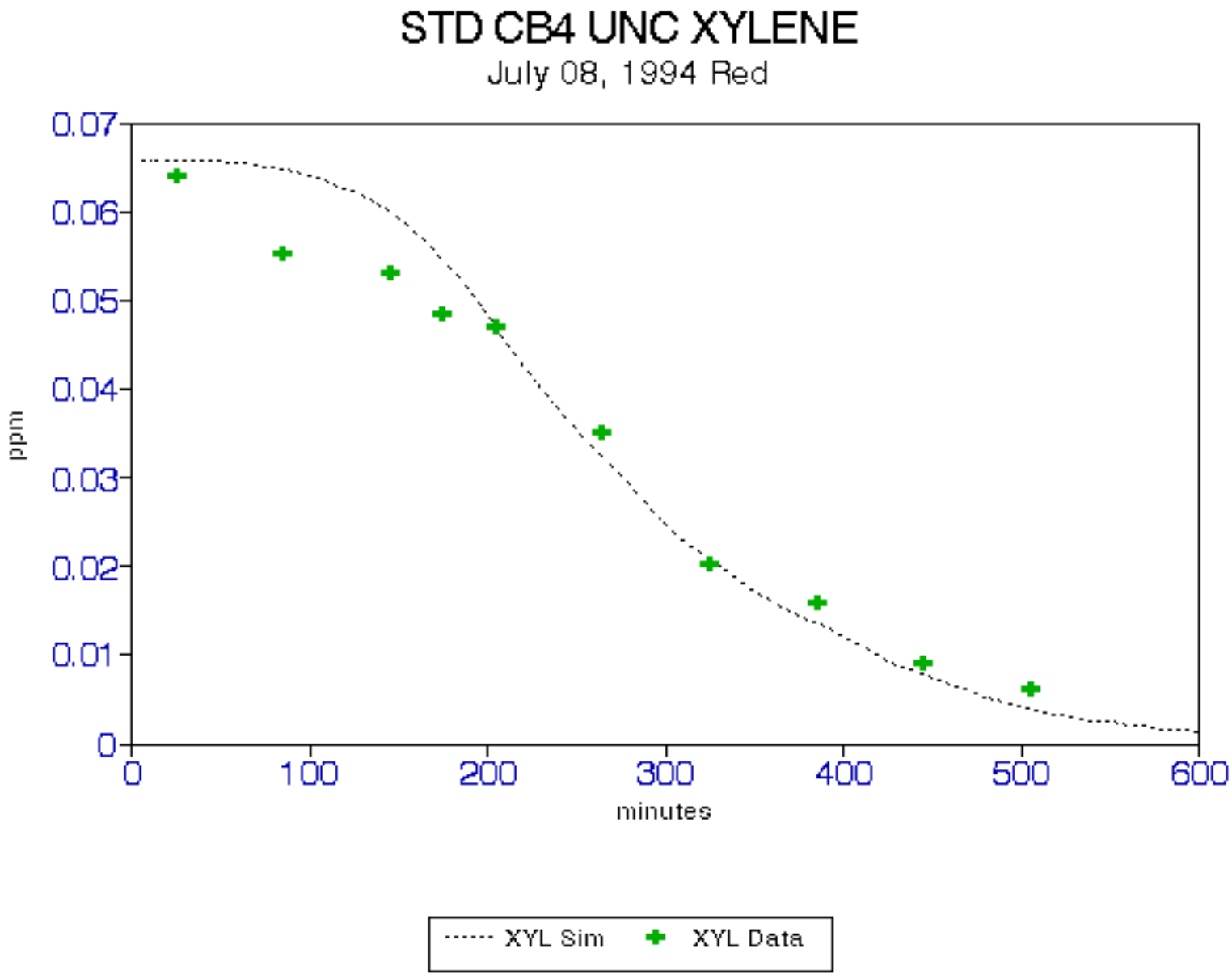
STD CB4 UNC XYLENE
July 08, 1994 Red
0.07
0.06
0.05
0.04
0.03
0.02
0.01
0
ppm
0
100
200
300
400
500
600
minutes
XYL Sim
XYL Data

FIGURE 36.

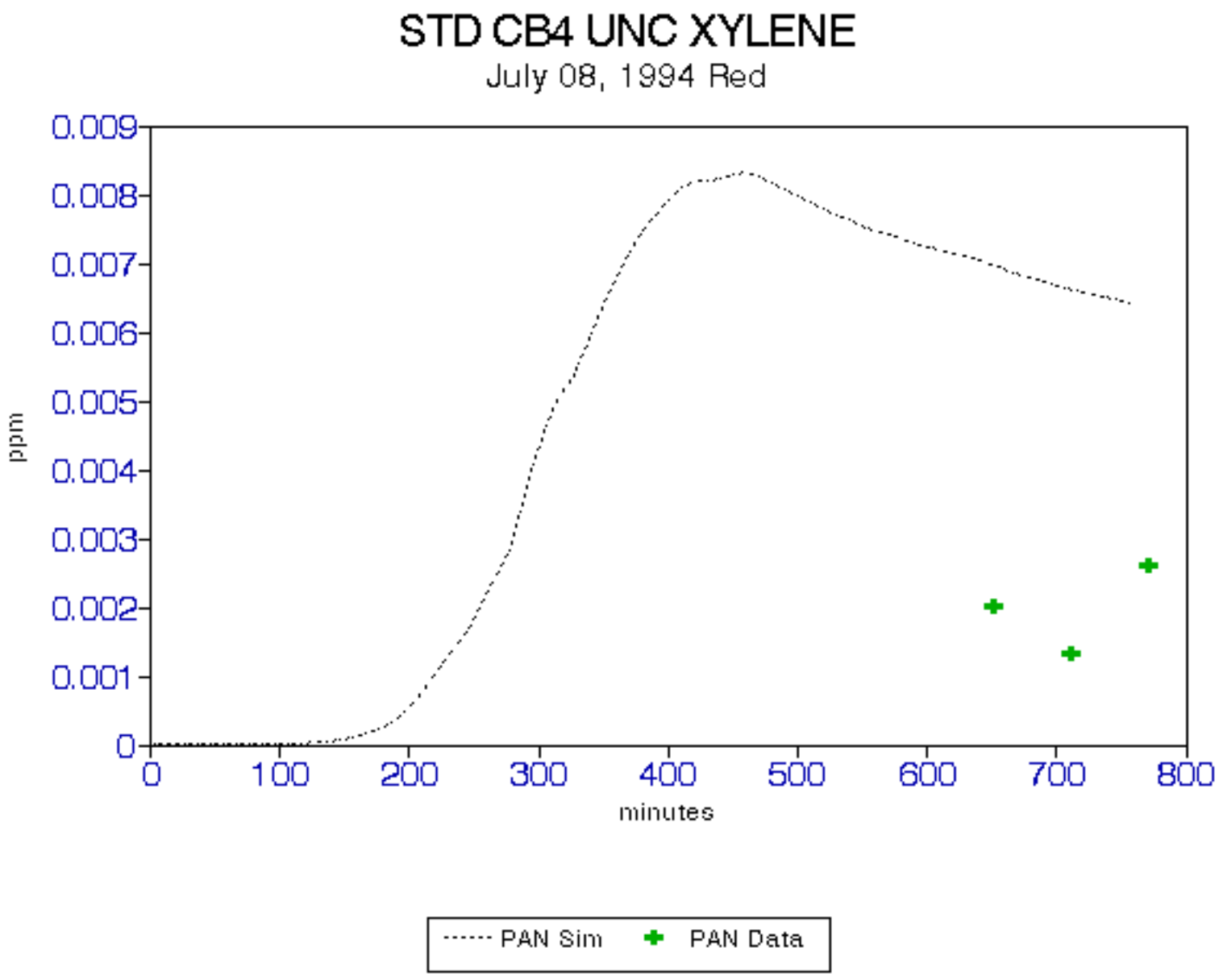
STD CB4 UNC XYLENE
July 08, 1994 Red
0.009
0.008
0.007
0.006
0.005
0.004
0.003
0.002
0.001
0
ppm
0
100
200
300
400
500
600
700
800
minutes
PAN Sim
PAN Data

FIGURE 37.

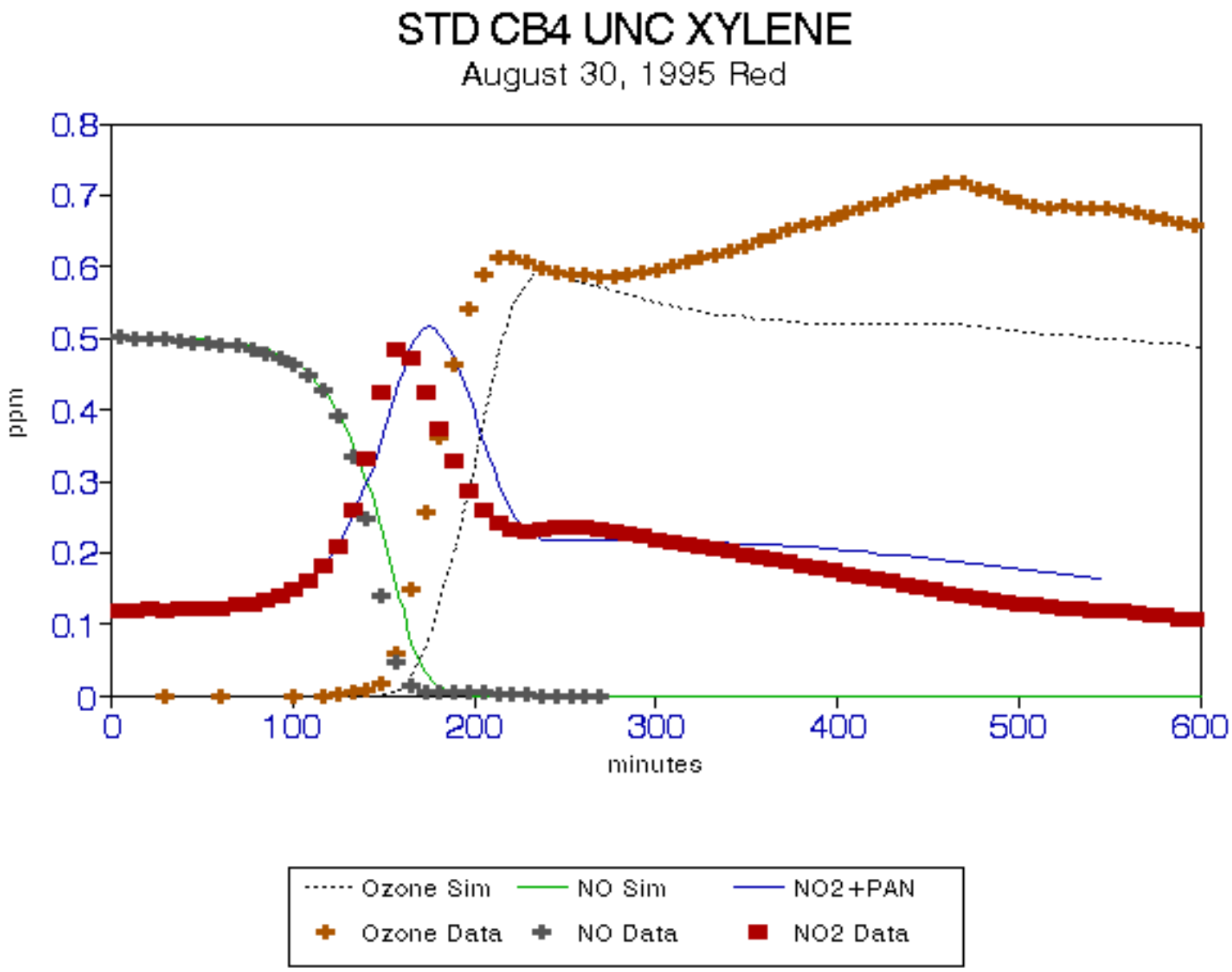
STD CB4 UNC XYLENE
August 30, 1995 Red
ppm
0.8
0.7
0.6
0.5
0.4
0.3
0.2
0.1
0
0
100
200
300
400
500
600
minutes
Ozone Sim
NO Sim
NO2+PAN
Ozone Data
NO Data
NO2 Data

FIGURE 38.

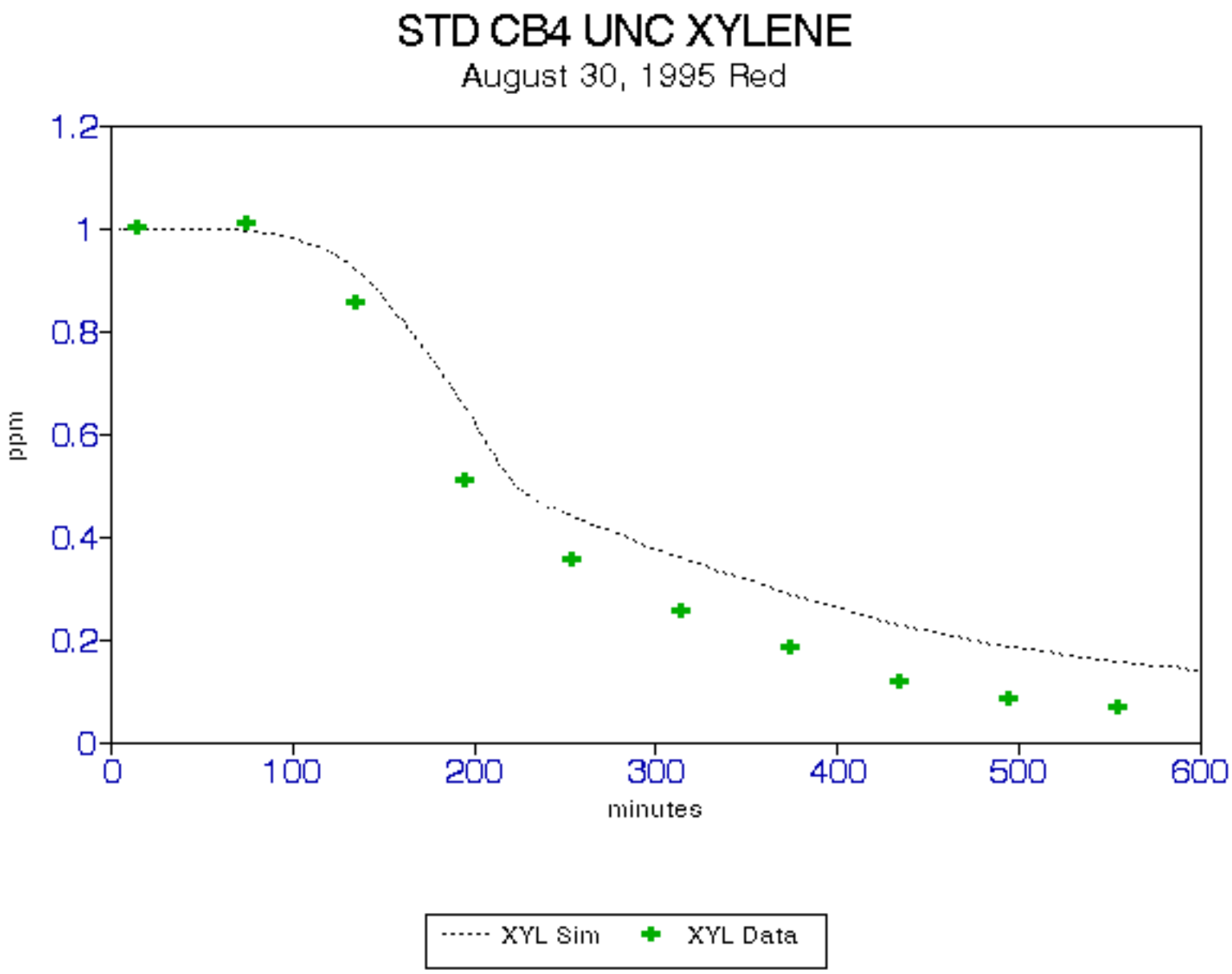
STD CB4 UNC XYLENE
August 30, 1995 Red
1.2
1
0.8
0.6
0.4
0.2
0
ppm
0
100
200
300
400
500
600
minutes
XYL Sim
XYL Data

FIGURE 39.

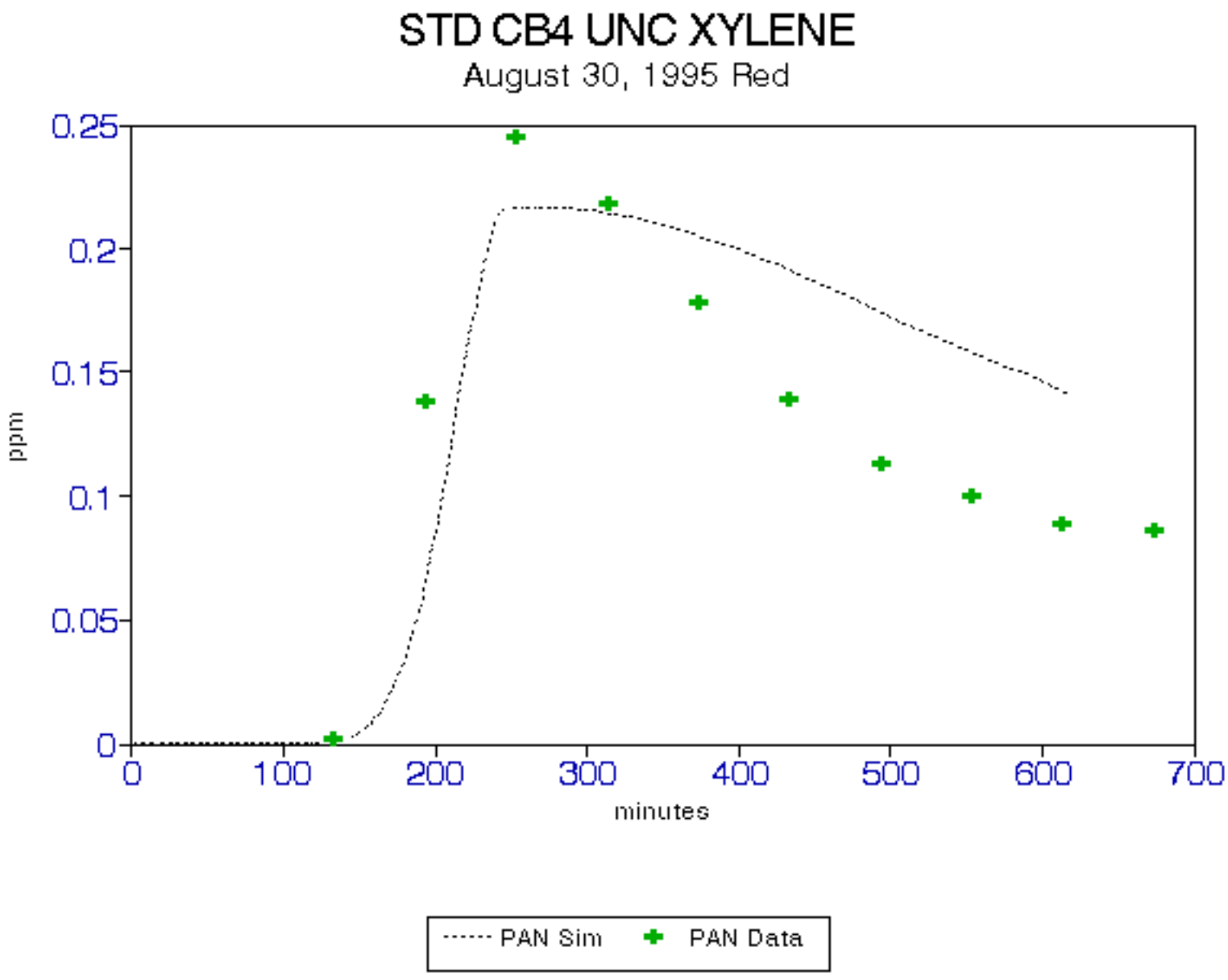
STD CB4 UNC XYLENE
August 30, 1995 Red
0.25
0.2
0.15
0.1
0.05
0
ppm
0
100
200
300
400
500
600
700
minutes
PAN Sim
PAN Data

FIGURE 40.

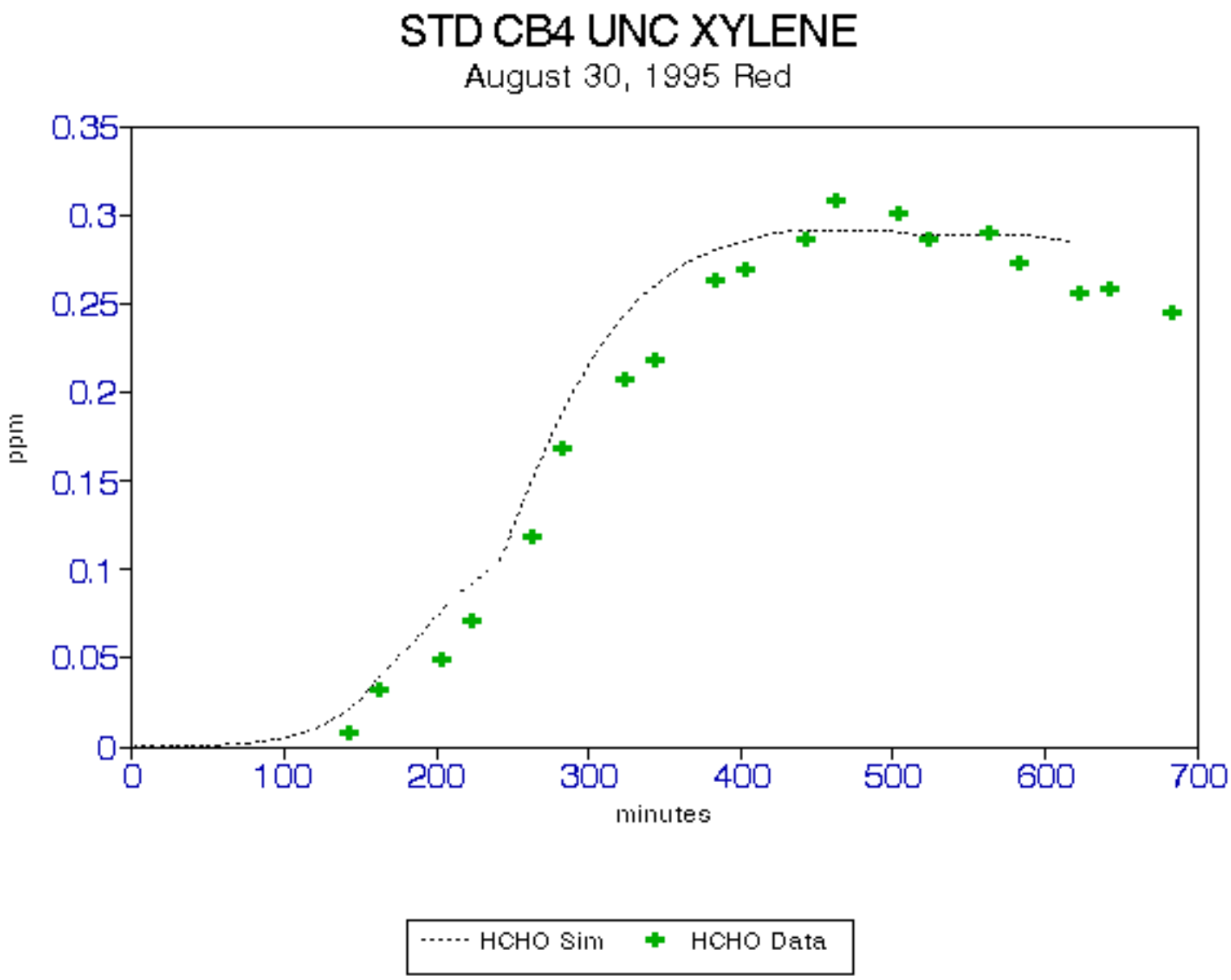
STD CB4 UNC XYLENE
August 30, 1995 Red
ppm
0.35
0.3
0.25
0.2
0.15
0.1
0.05
0
0
100
200
300
400
500
600
700
minutes
HCHO Sim
HCHO Data

FIGURE 41.

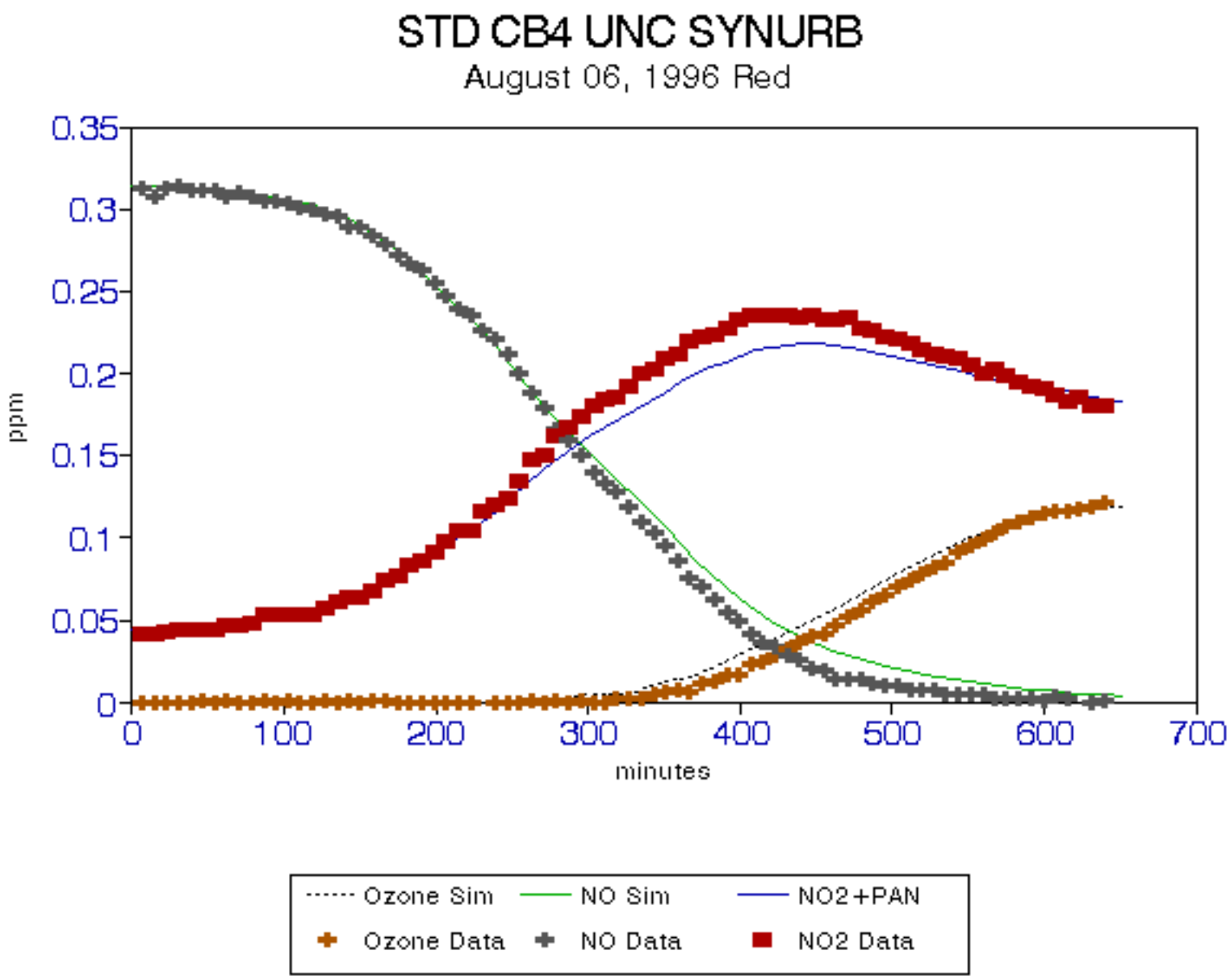
STD CB4 UNC SYNURB
August 06, 1996 Red
ppm
0.35
0.3
0.25
0.2
0.15
0.1
0.05
0
0
100
200
300
400
500
600
700
minutes
Ozone Sim
NO Sim
NO2+PAN
Ozone Data
NO Data
NO2 Data

FIGURE 42.

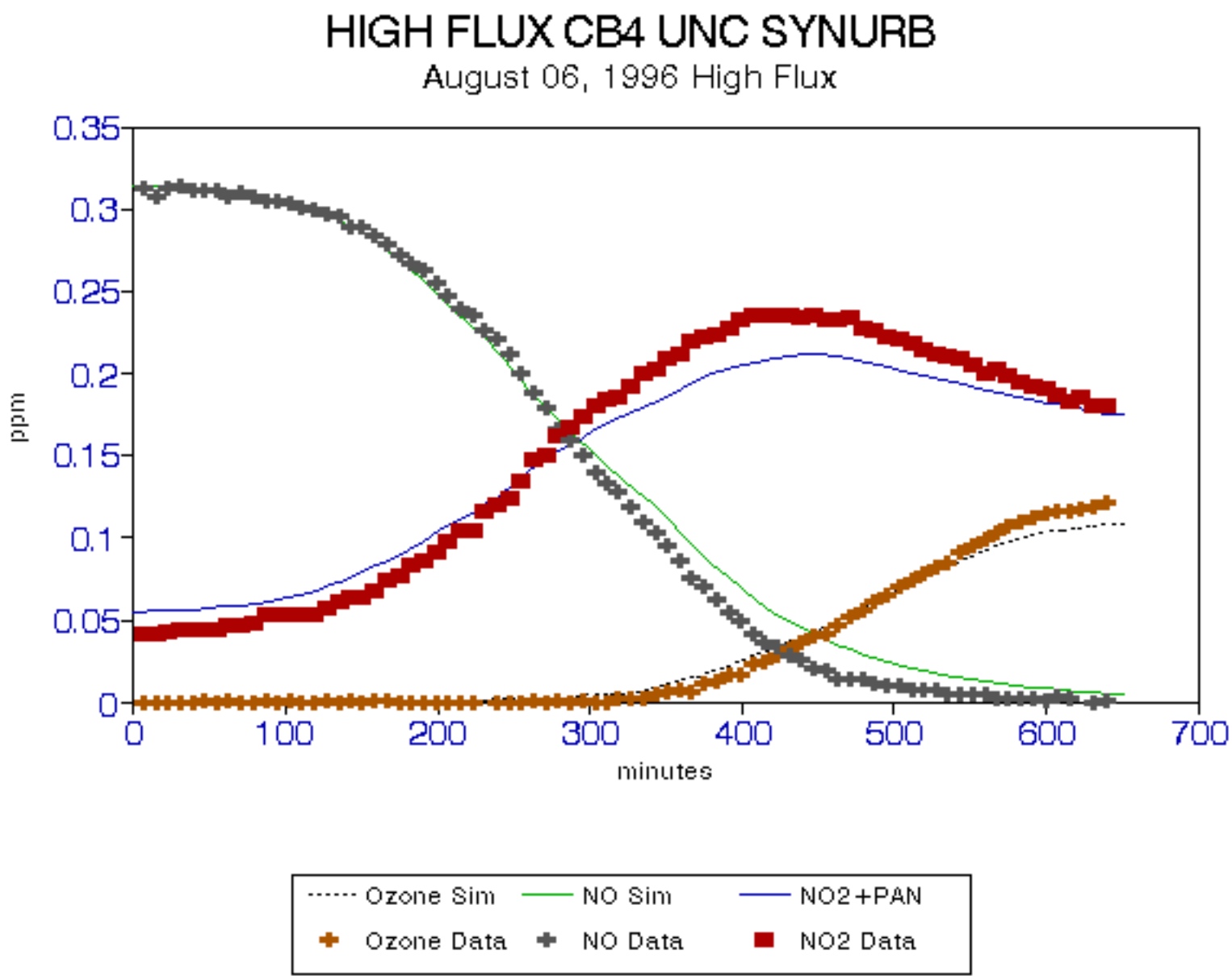
HIGH FLUX CB4 UNC SYNURB
August 06, 1996 High Flux
ppm
0.35
0.3
0.25
0.2
0.15
0.1
0.05
0
0
100
200
300
400
500
600
700
minutes
Ozone Sim
NO Sim
NO2+PAN
Ozone Data
NO Data
NO2 Data

FIGURE 43.

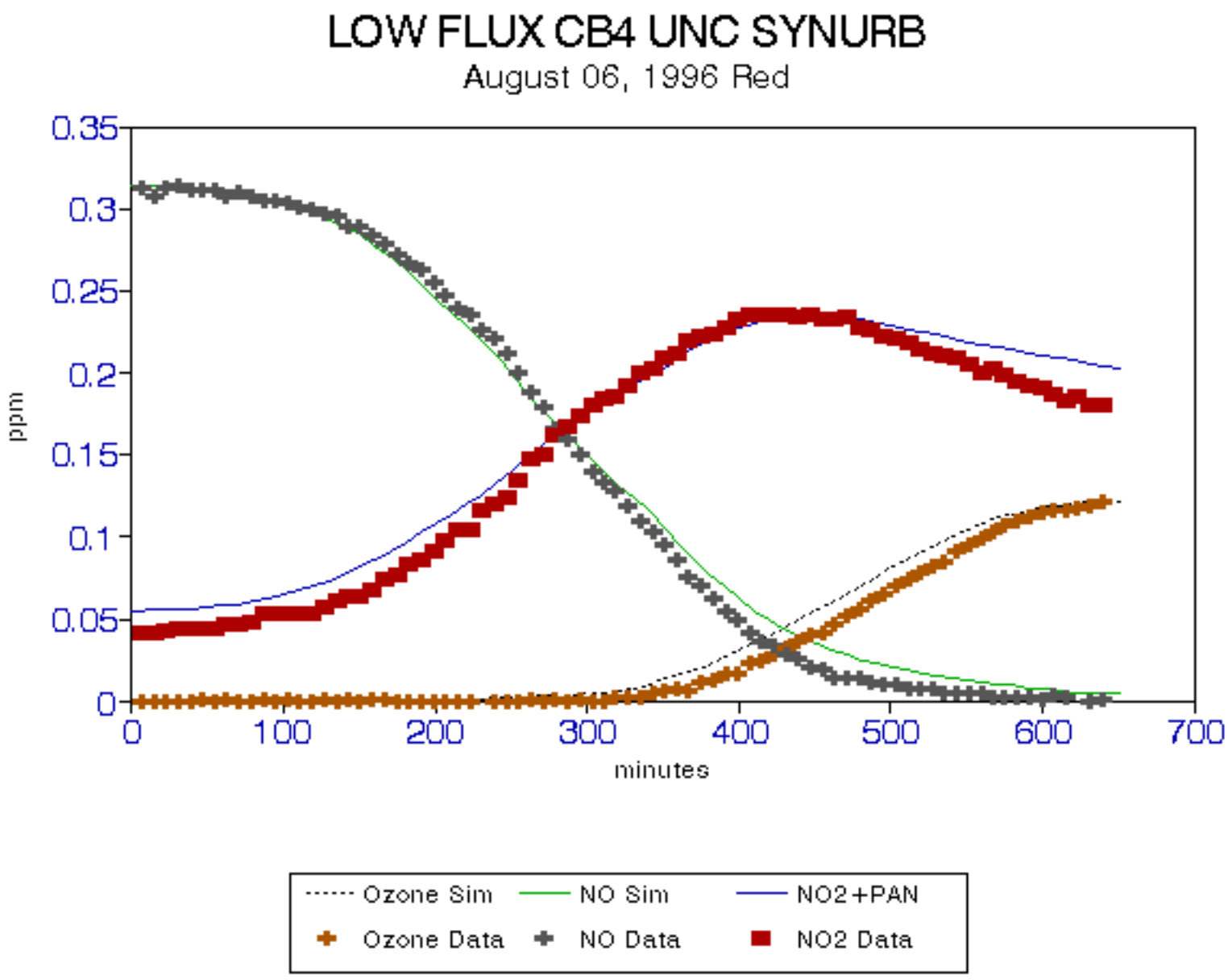
LOW FLUX CB4 UNC SYNURB
August 06, 1996 Red
ppm
0.35
0.3
0.25
0.2
0.15
0.1
0.05
0
0
100
200
300
400
500
600
700
minutes
Ozone Sim
NO Sim
NO2+PAN
Ozone Data
NO Data
NO2 Data

FIGURE 44.

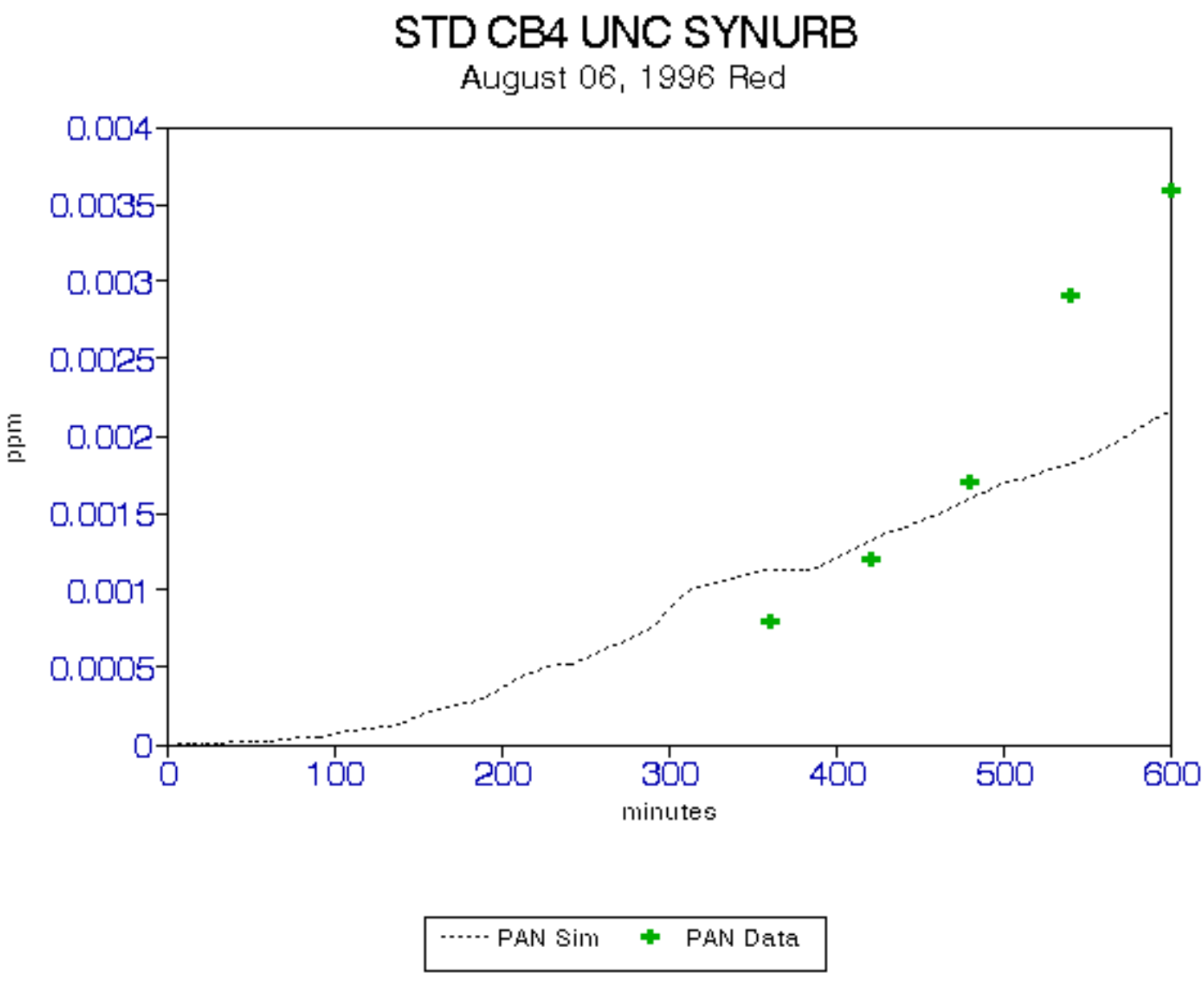
STD CB4 UNC SYNURB
August 06, 1996 Red
ppm
0.004
0.0035
0.003
0.0025
0.002
0.0015
0.001
0.0005
0
0
100
200
300
400
500
600
minutes
PAN Sim
PAN Data

FIGURE 45.

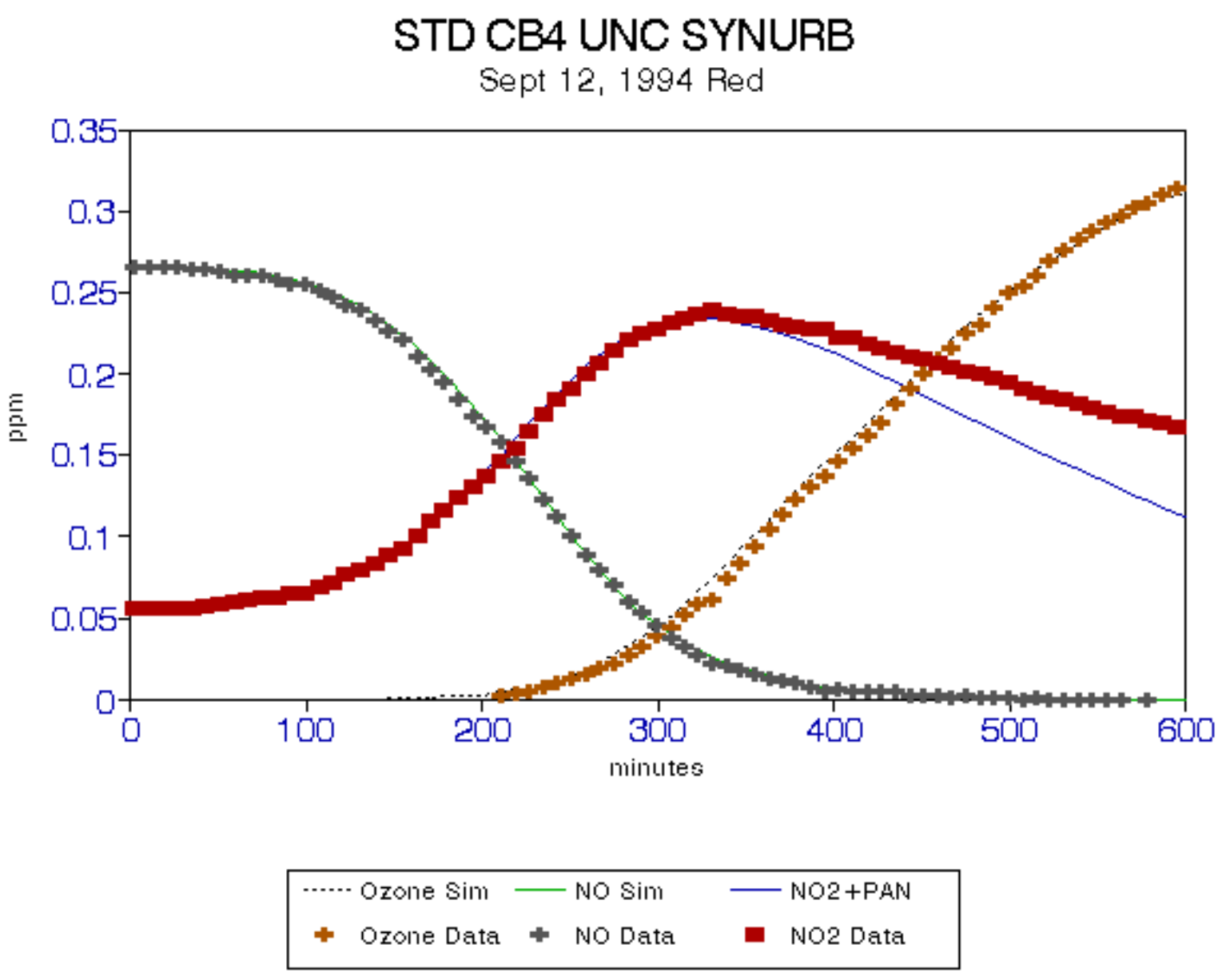
STD CB4 UNC SYNURB
Sept 12, 1994 Red
ppm
0.35
0.3
0.25
0.2
0.15
0.1
0.05
0
0
100
200
300
400
500
600
minutes
Ozone Sim
NO Sim
NO2+PAN
Ozone Data
NO Data
NO2 Data

FIGURE 46.

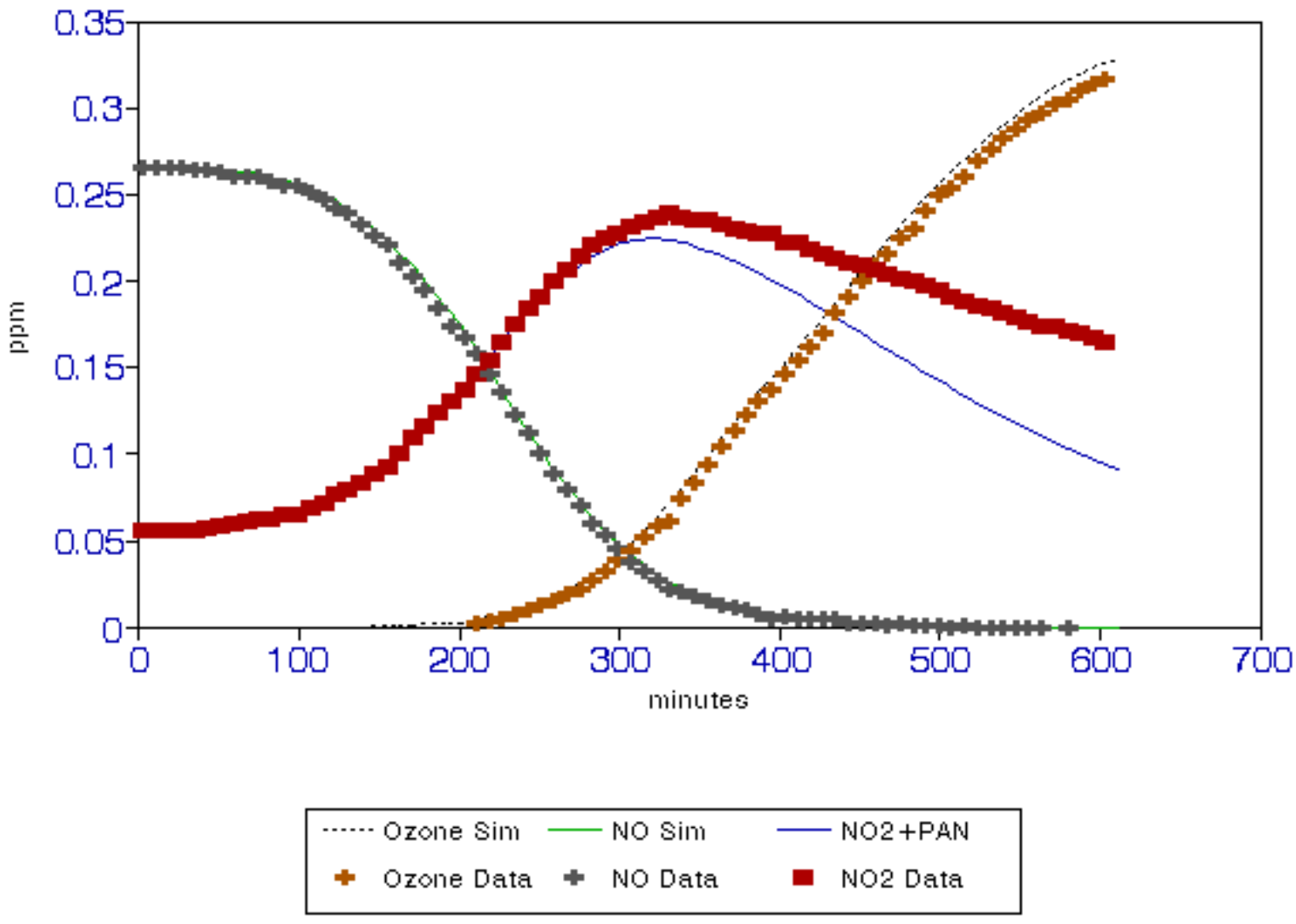
HIGH FLUX CB4 UNC SYNURB
Sept 12, 1994 Red
ppm
0.35
0.3
0.25
0.2
0.15
0.1
0.05
0
0
100
200
300
400
500
600
700
minutes
Ozone Sim
NO Sim
NO2+PAN
Ozone Data
NO Data
NO2 Data

FIGURE 47.

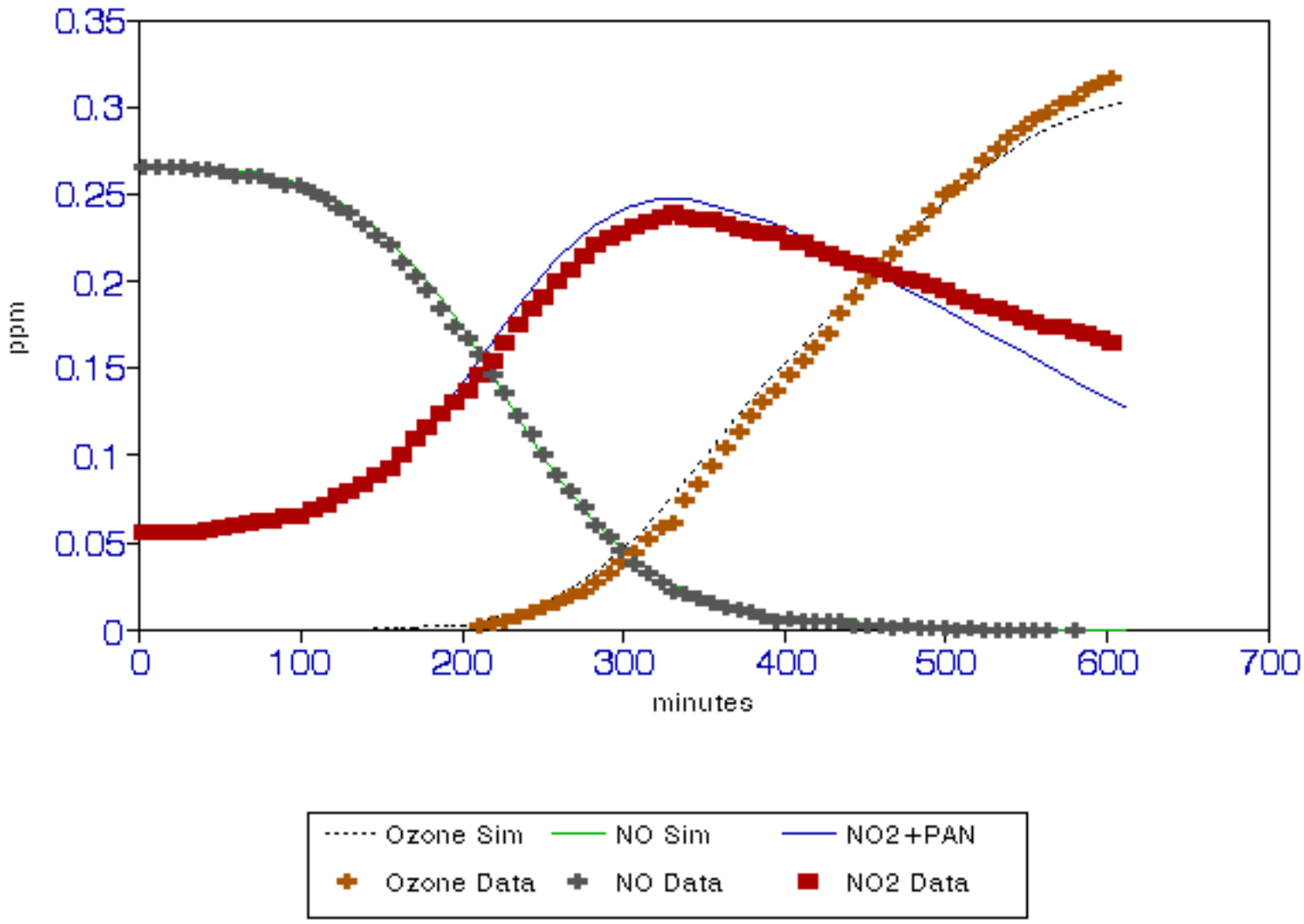
LOW FLUX CB4 UNC SYNURB
Sept 12, 1994 Red
ppm
0.35
0.3
0.25
0.2
0.15
0.1
0.05
0
0
100
200
300
400
500
600
700
minutes
Ozone Sim
NO Sim
NO2+PAN
Ozone Data
NO Data
NO2 Data

FIGURE 48.

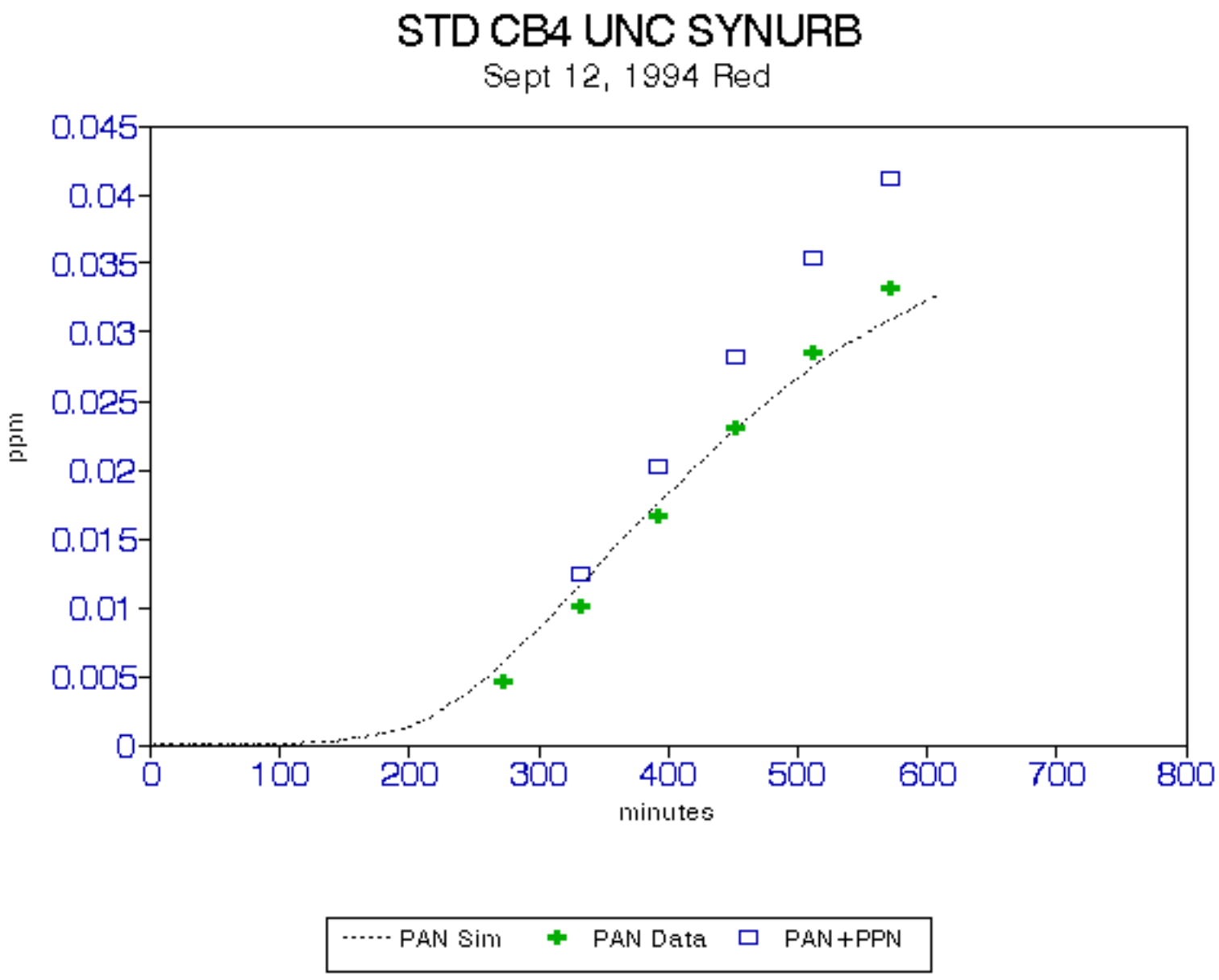
STD CB4 UNC SYNURB
Sept 12, 1994 Red
0.045
0.04
0.035
0.03
0.025
0.02
0.015
0.01
0.005
0
ppm
0
100
200
300
400
500
600
700
800
minutes
PAN Sim
PAN Data
PAN+PPN

FIGURE 49.

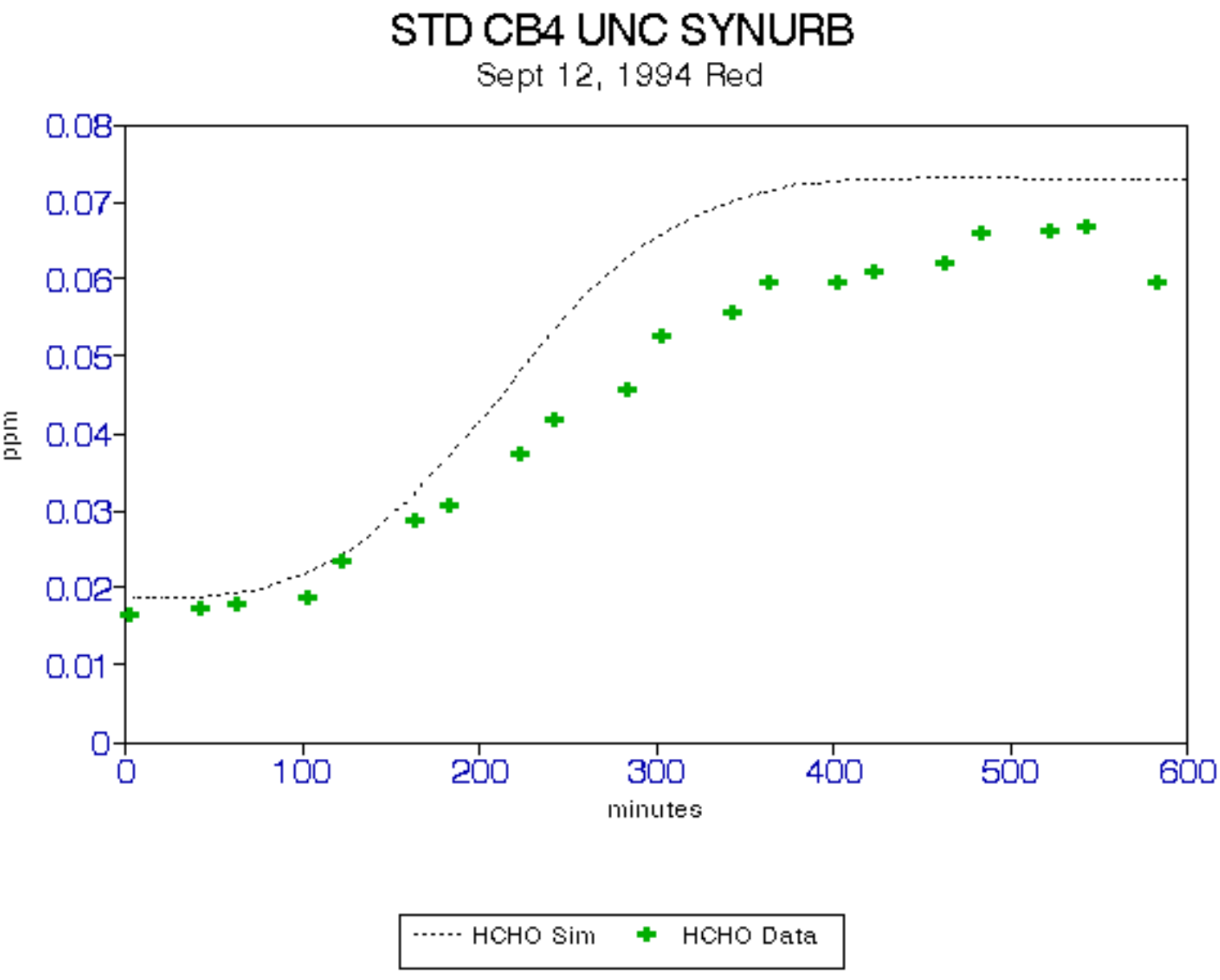
STD CB4 UNC SYNURB
Sept 12, 1994 Red
ppm
0.08
0.07
0.06
0.05
0.04
0.03
0.02
0.01
0
0
100
200
300
400
500
600
minutes
HCHO Sim
HCHO Data

FIGURE 50.

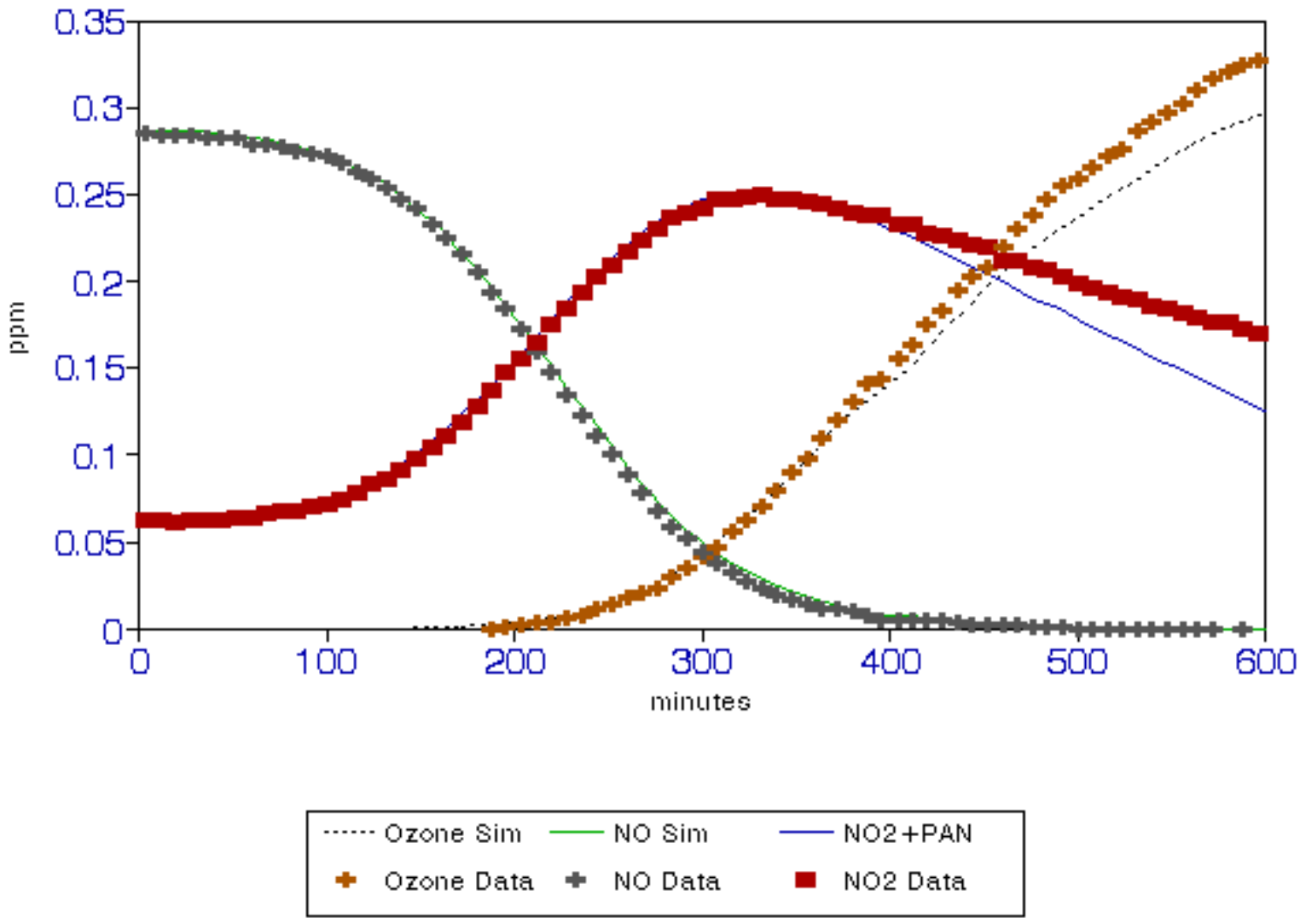
STD CB4 UNC SYNURB
Sept 11, 1994 Red
ppm
0.35
0.3
0.25
0.2
0.15
0.1
0.05
0
0
100
200
300
400
500
600
minutes
Ozone Sim
NO Sim
NO2+PAN
Ozone Data
NO Data
NO2 Data

FIGURE 51.

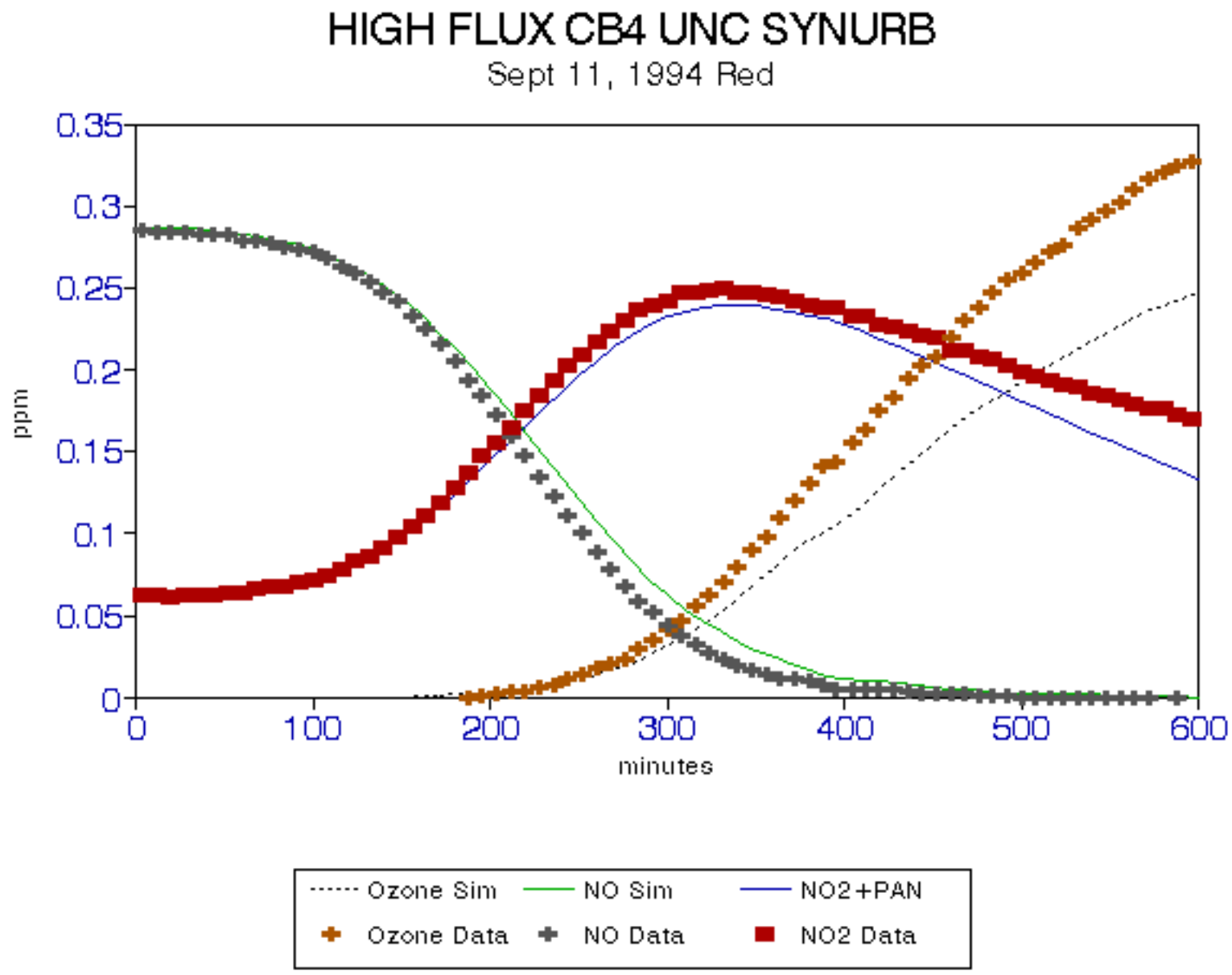
HIGH FLUX CB4 UNC SYNURB
Sept 11, 1994 Red
ppm
0.35
0.3
0.25
0.2
0.15
0.1
0.05
0
0
100
200
300
400
500
600
minutes
Ozone Sim
NO Sim
NO2+PAN
Ozone Data
NO Data
NO2 Data

FIGURE 52.

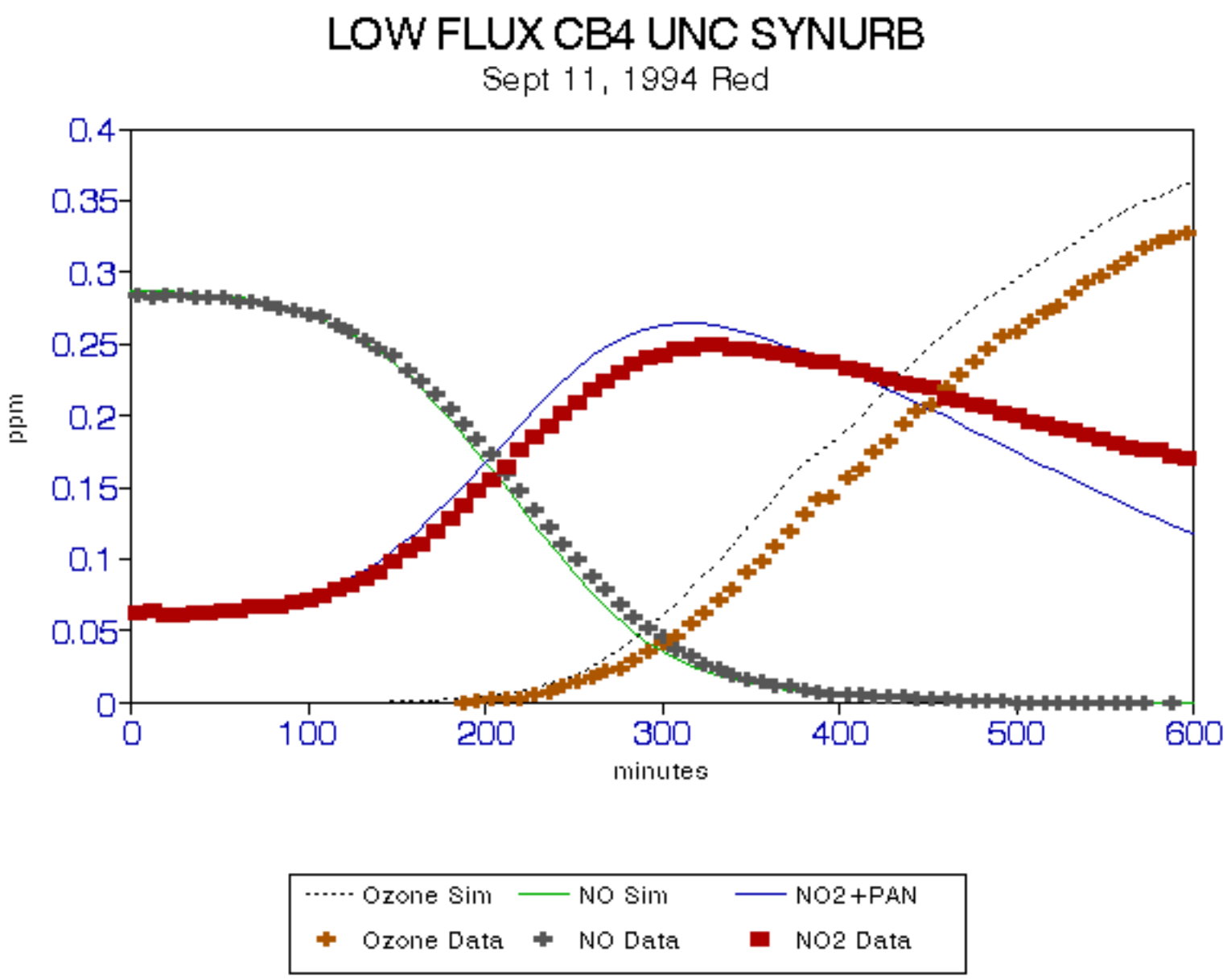
LOW FLUX CB4 UNC SYNURB
Sept 11, 1994 Red
ppm
0.4
0.35
0.3
0.25
0.2
0.15
0.1
0.05
0
0
100
200
300
400
500
600
minutes
Ozone Sim
NO Sim
NO2+PAN
Ozone Data
NO Data
NO2 Data

FIGURE 53.

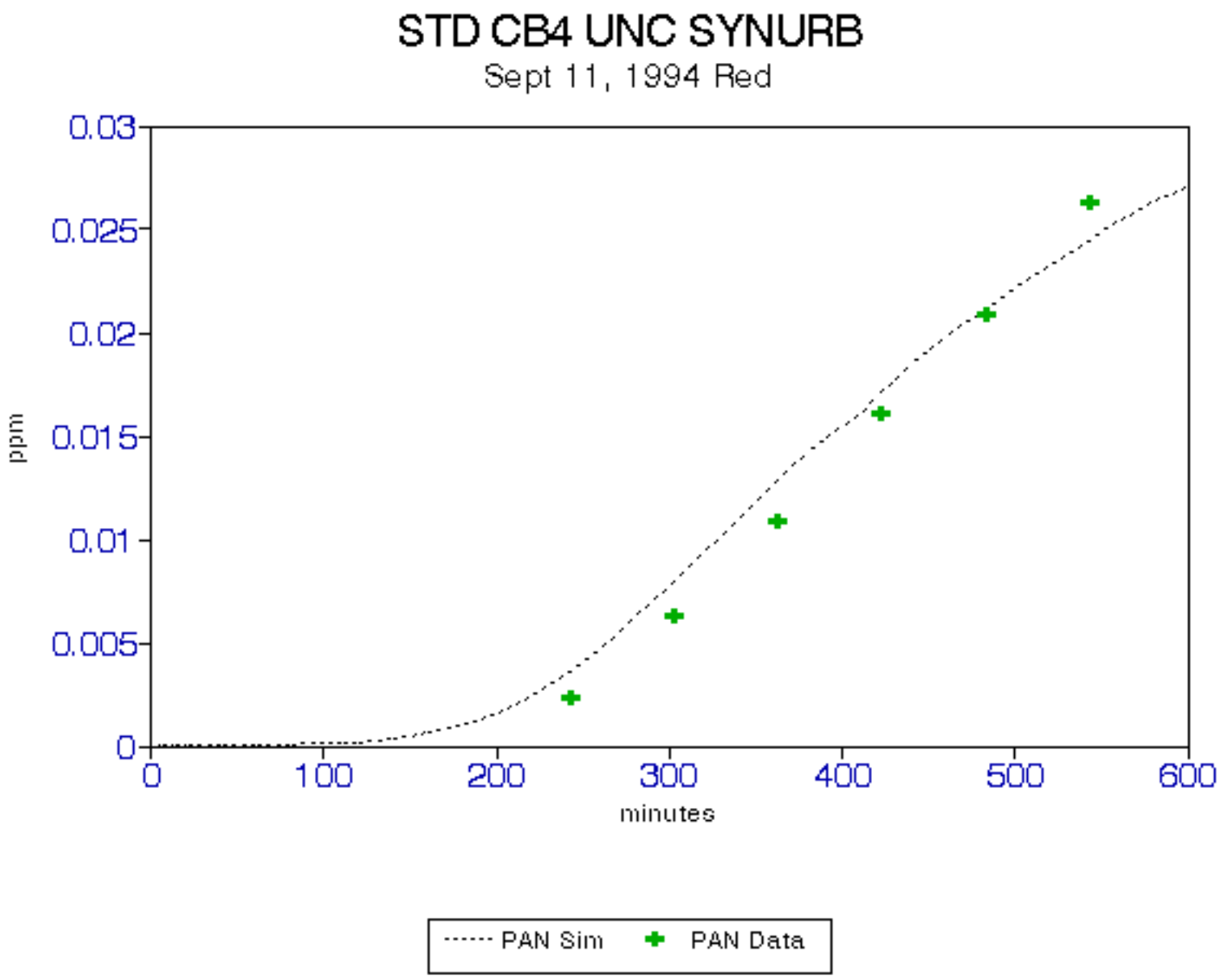
STD CB4 UNC SYNURB
Sept 11, 1994 Red
ppm
0.03
0.025
0.02
0.015
0.01
0.005
0
0
100
200
300
400
500
600
minutes
PAN Sim
PAN Data

FIGURE 54.

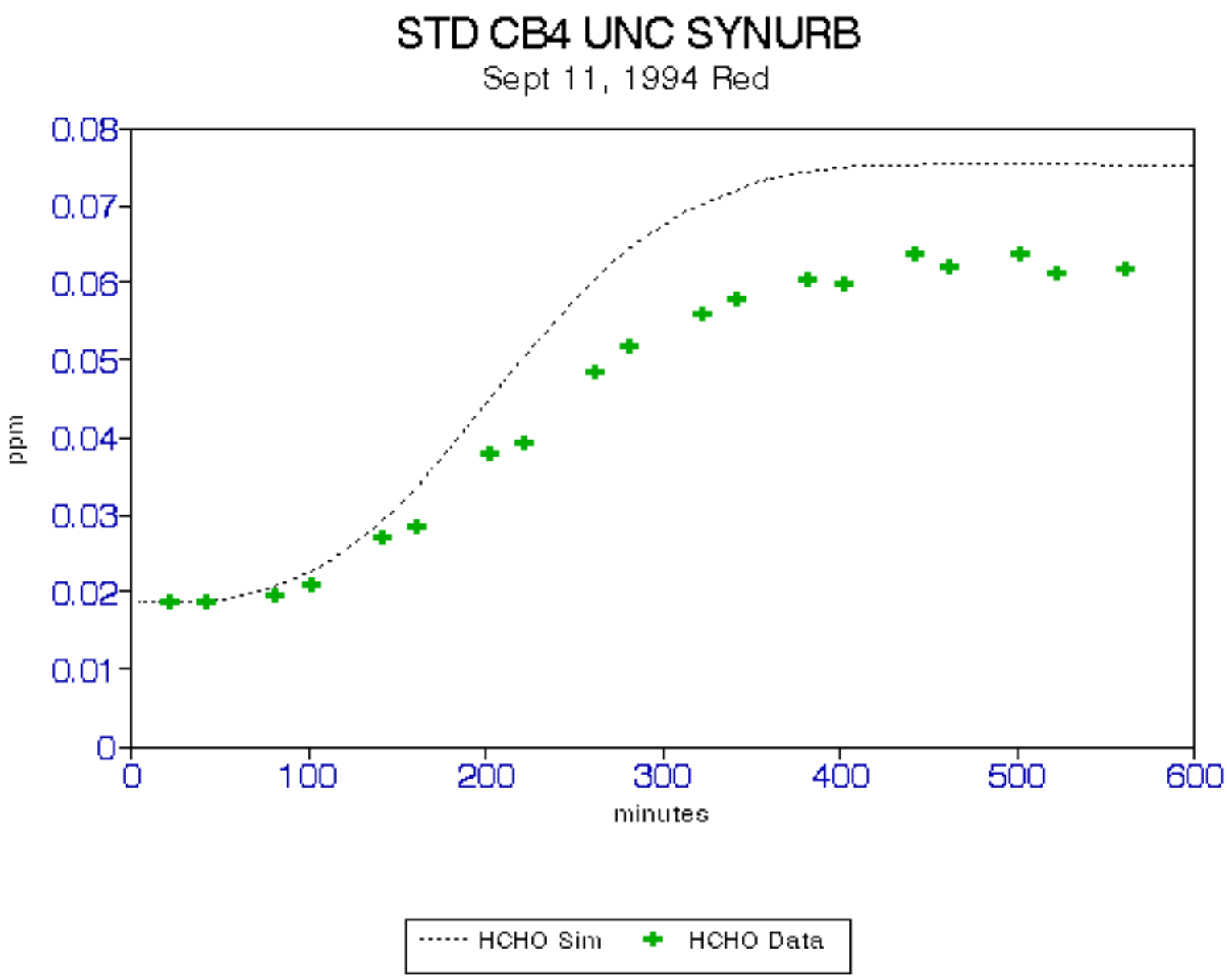
STD CB4 UNC SYNURB
Sept 11, 1994 Red
ppm
0.08
0.07
0.06
0.05
0.04
0.03
0.02
0.01
0
0
100
200
300
400
500
600
minutes
HCHO Sim
HCHO Data

FIGURE 55.

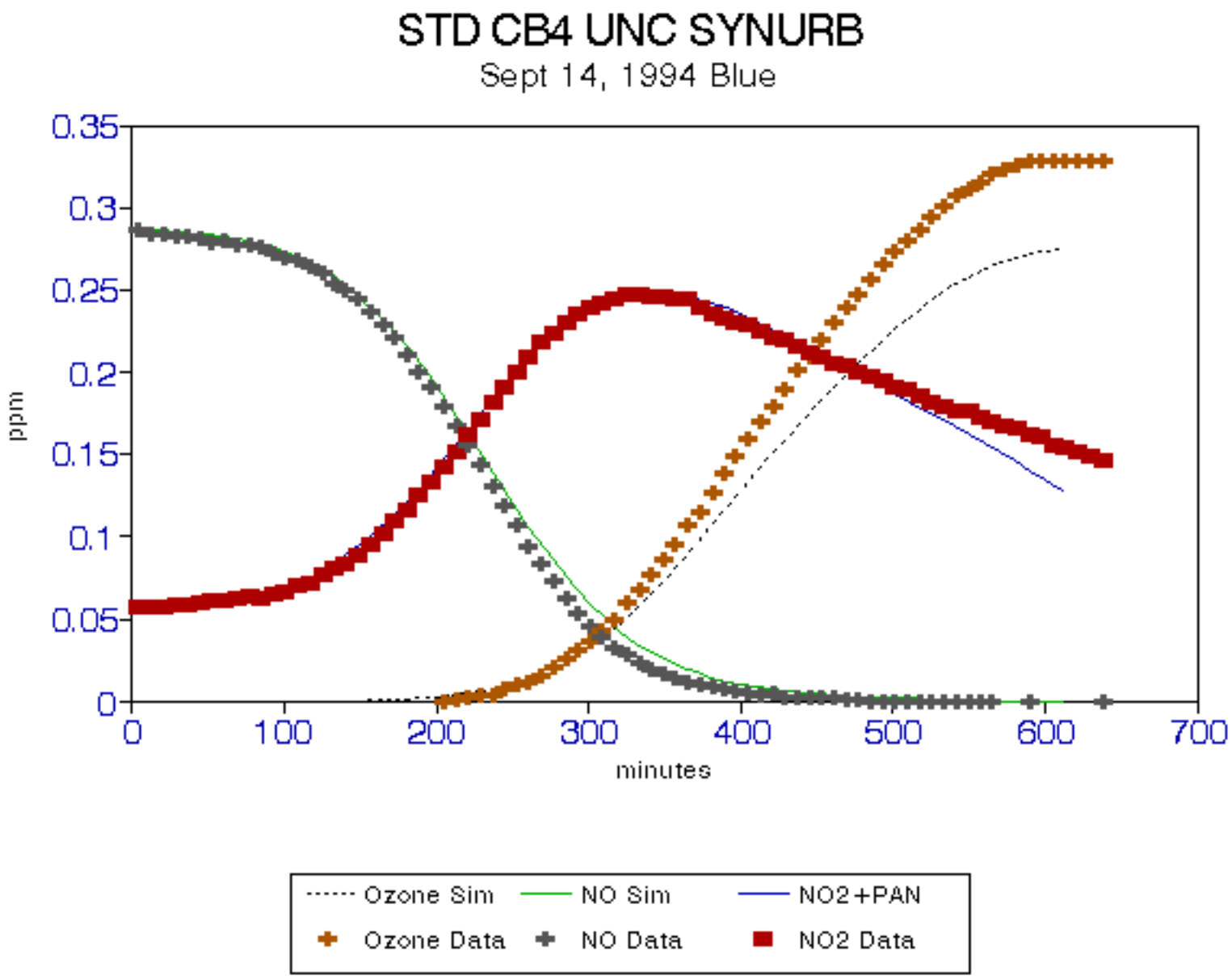
STD CB4 UNC SYNURB
Sept 14, 1994 Blue
ppm
0.35
0.3
0.25
0.2
0.15
0.1
0.05
0
0
100
200
300
400
500
600
700
minutes
Ozone Sim
NO Sim
NO2+PAN
Ozone Data
NO Data
NO2 Data

FIGURE 56.

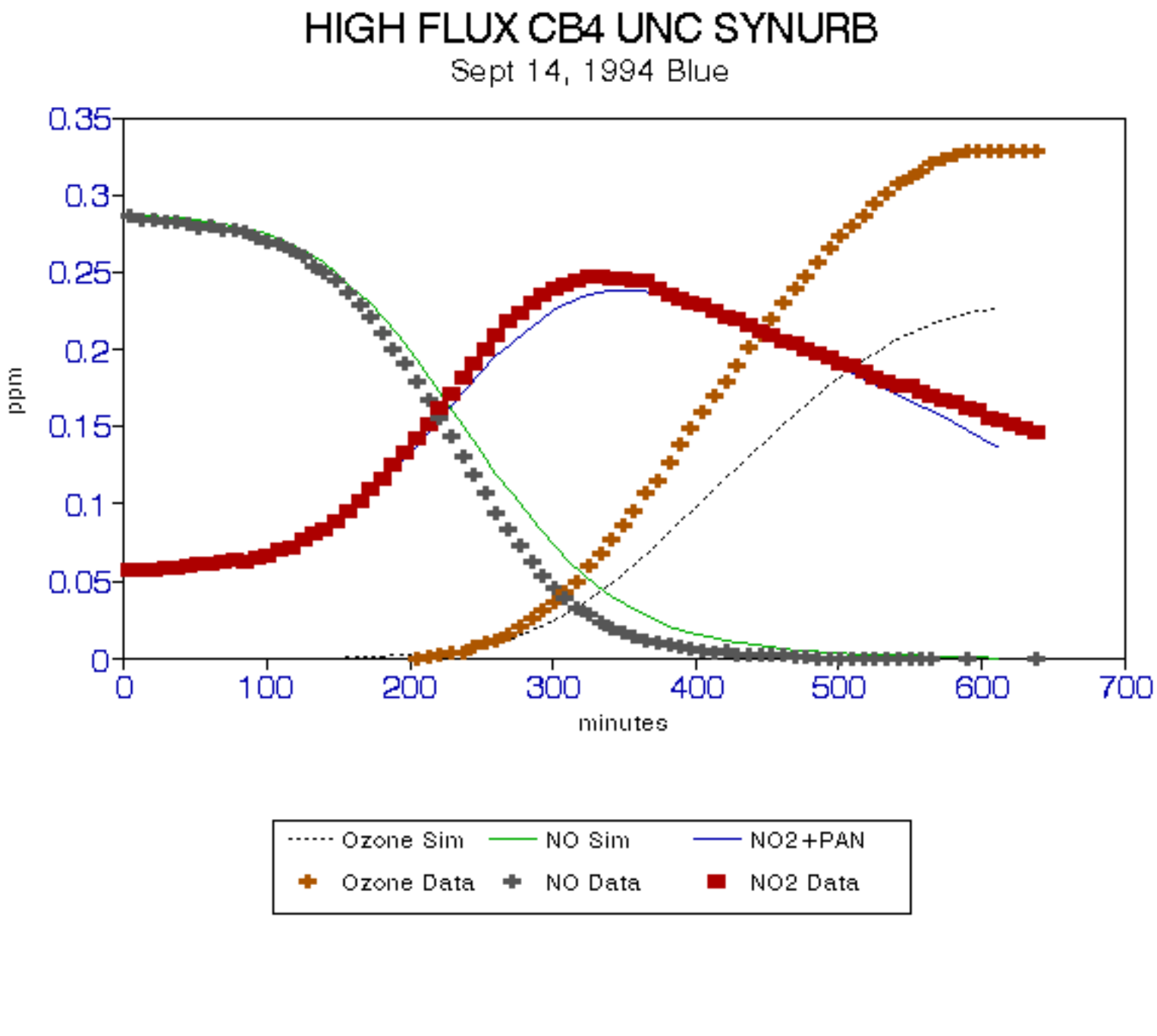
HIGH FLUX CB4 UNC SYNURB
Sept 14, 1994 Blue
ppm
0.35
0.3
0.25
0.2
0.15
0.1
0.05
0
0
100
200
300
400
500
600
700
minutes
Ozone Sim
NO Sim
NO2+PAN
Ozone Data
NO Data
NO2 Data

FIGURE 57.

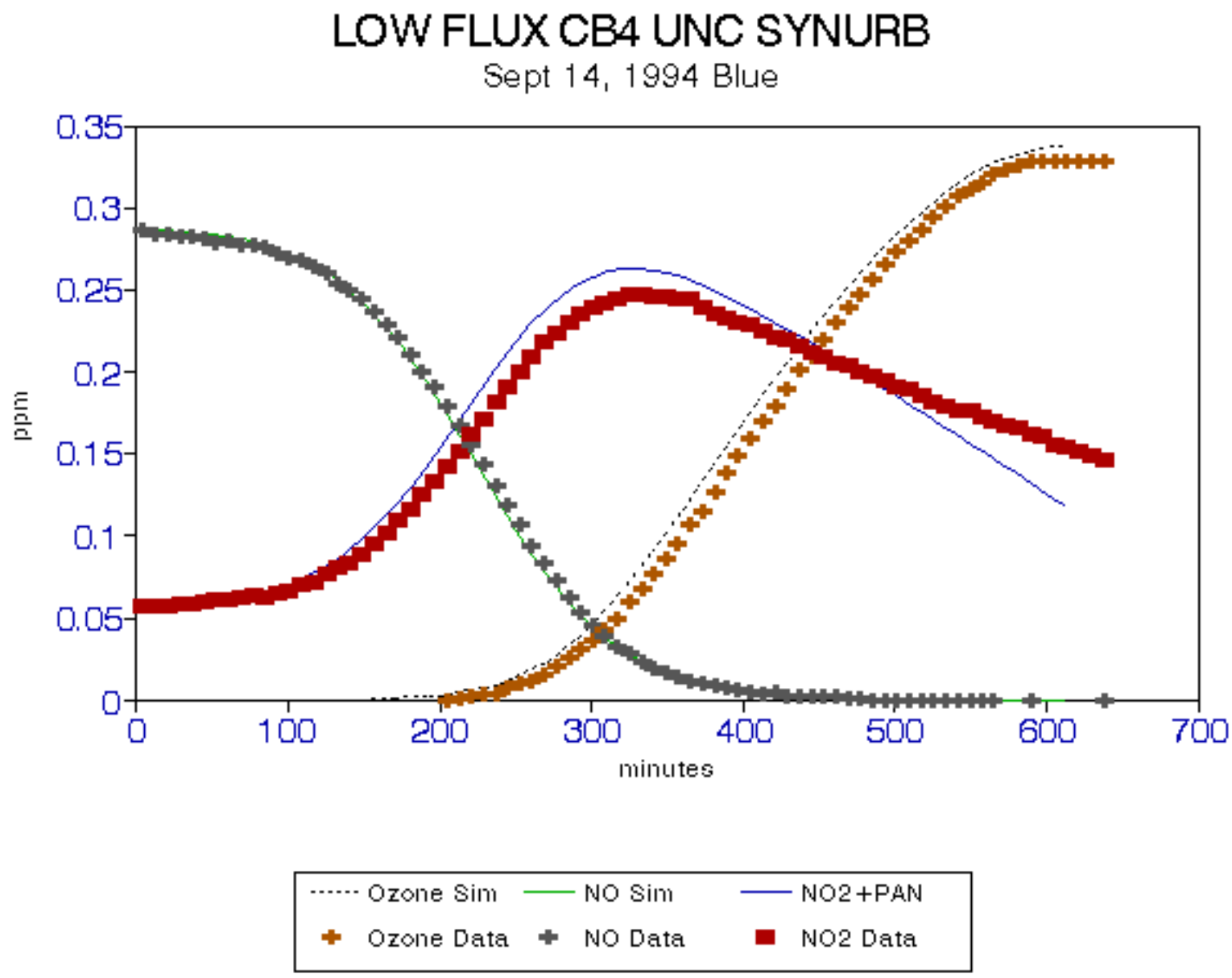
LOW FLUX CB4 UNC SYNURB
Sept 14, 1994 Blue
ppm
0.35
0.3
0.25
0.2
0.15
0.1
0.05
0
0
100
200
300
400
500
600
700
minutes
Ozone Sim
NO Sim
NO2+PAN
Ozone Data
NO Data
NO2 Data

FIGURE 58.

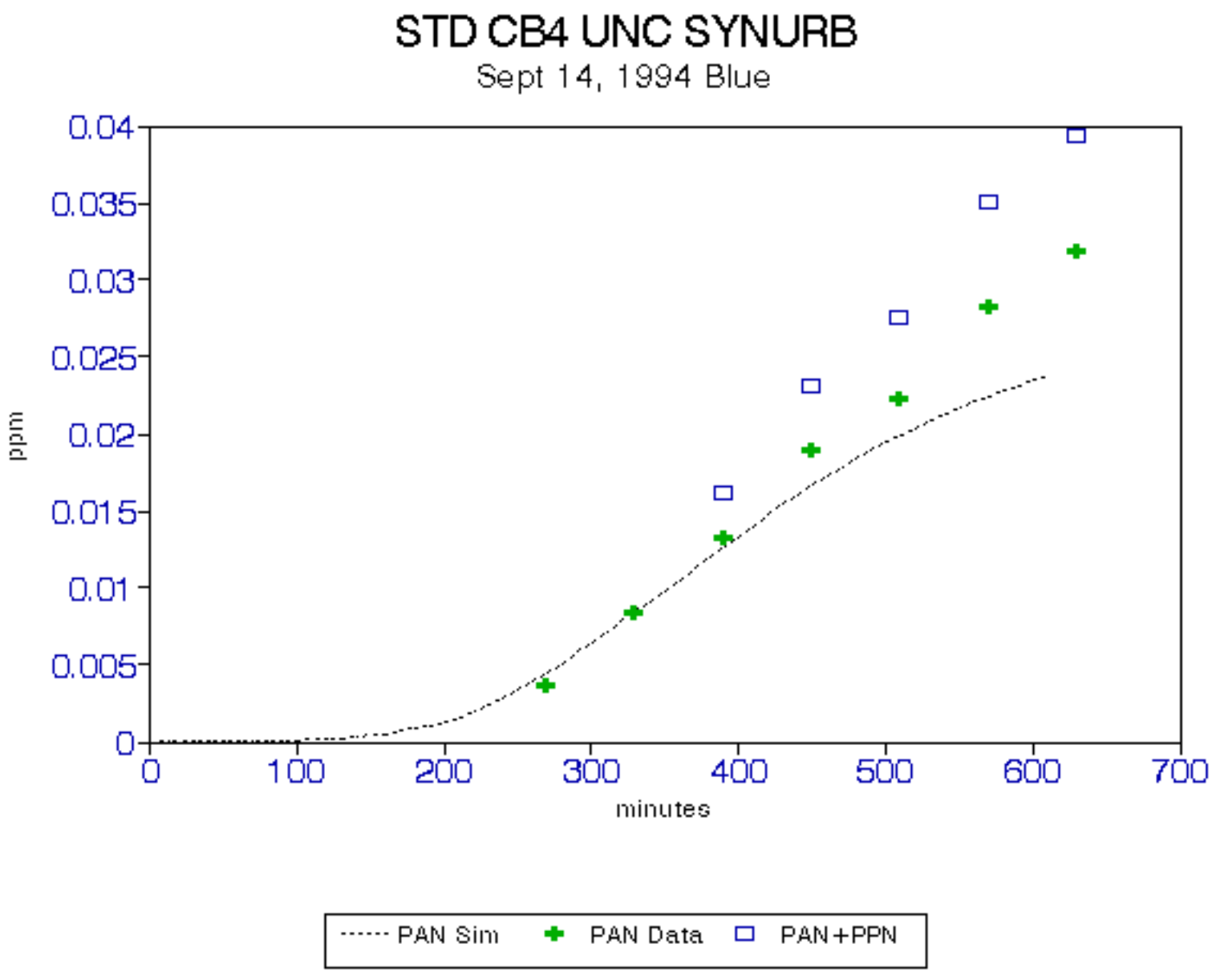
STD CB4 UNC SYNURB
Sept 14, 1994 Blue
ppm
0.04
0.035
0.03
0.025
0.02
0.015
0.01
0.005
0
0
100
200
300
400
500
600
700
minutes
PAN Sim
PAN Data
PAN+PPN

FIGURE 59.

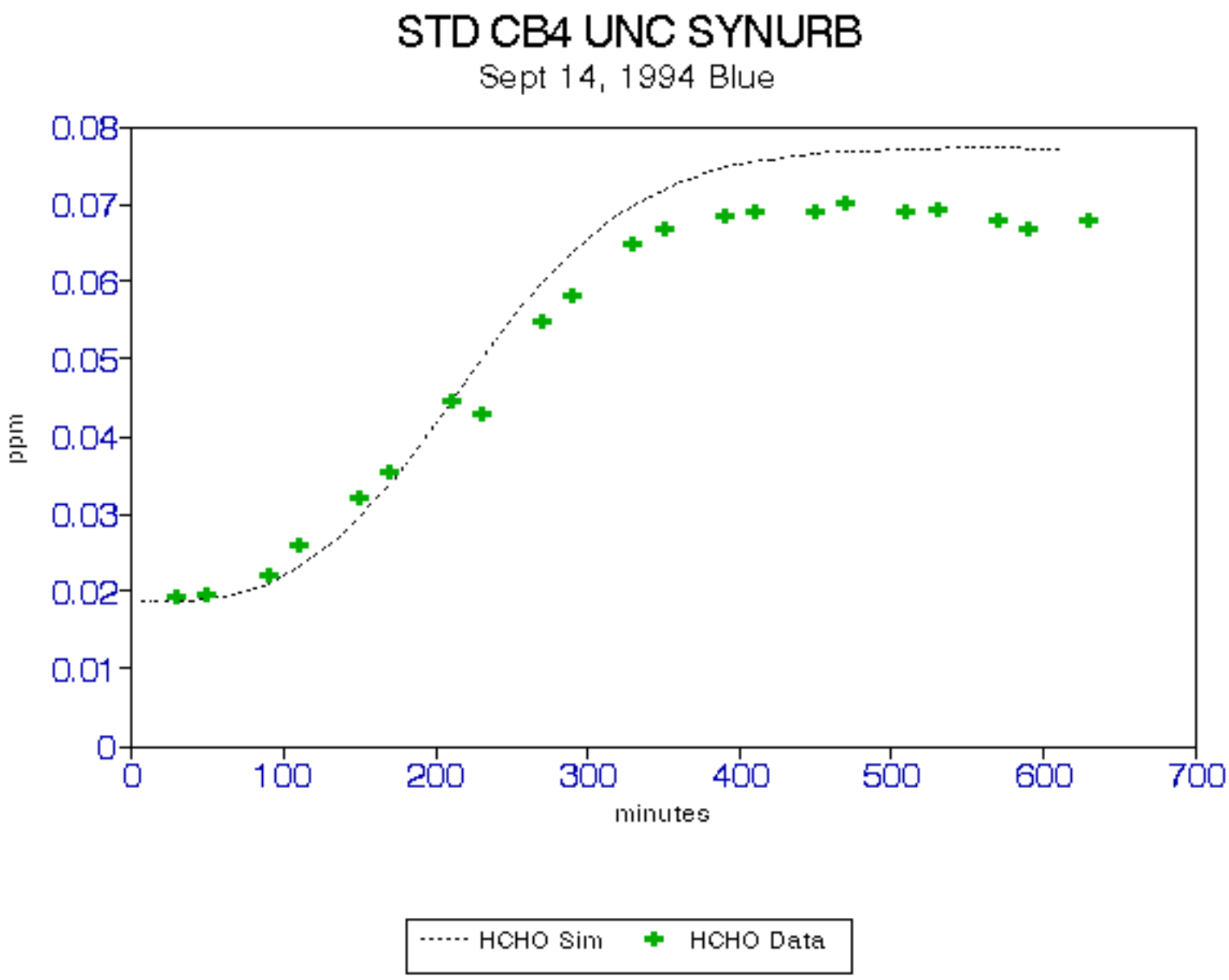
STD CB4 UNC SYNURB
Sept 14, 1994 Blue
ppm
0.08
0.07
0.06
0.05
0.04
0.03
0.02
0.01
0
0
100
200
300
400
500
600
700
minutes
HCHO Sim
HCHO Data

FIGURE 60.

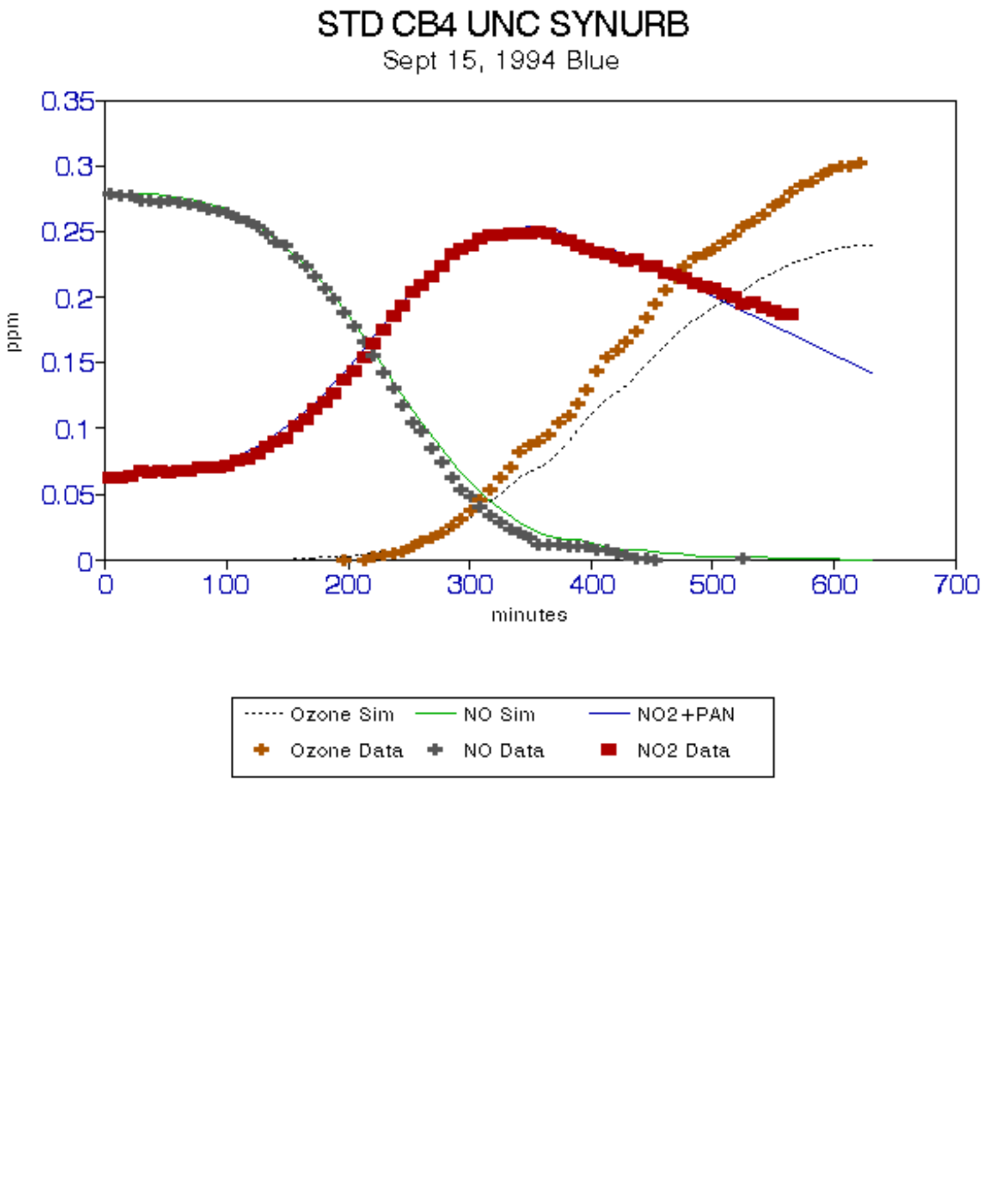
STD CB4 UNC SYNURB
Sept 15, 1994 Blue
ppm
0.35
0.3
0.25
0.2
0.15
0.1
0.05
0
0
100
200
300
400
500
600
700
minutes
Ozone Sim
NO Sim
NO2+PAN
Ozone Data
NO Data
NO2 Data

FIGURE 61.

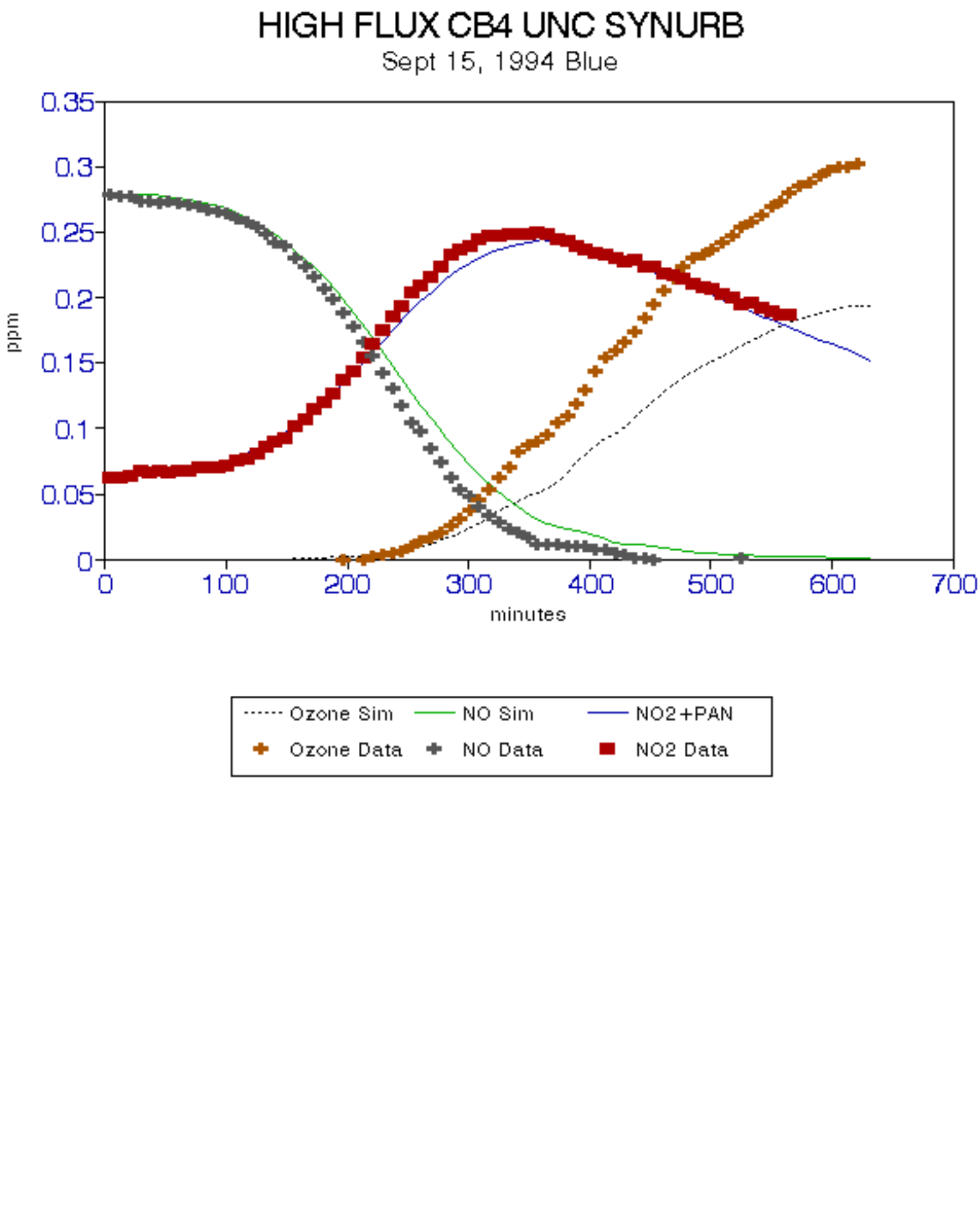
HIGH FLUX CB4 UNC SYNURB
Sept 15, 1994 Blue
0.35
0.3
0.25
0.2
0.15
0.1
0.05
0
ppm
0
100
200
300
400
500
600
700
minutes
Ozone Sim
NO Sim
NO2+PAN
Ozone Data
NO Data
NO2 Data

FIGURE 62.

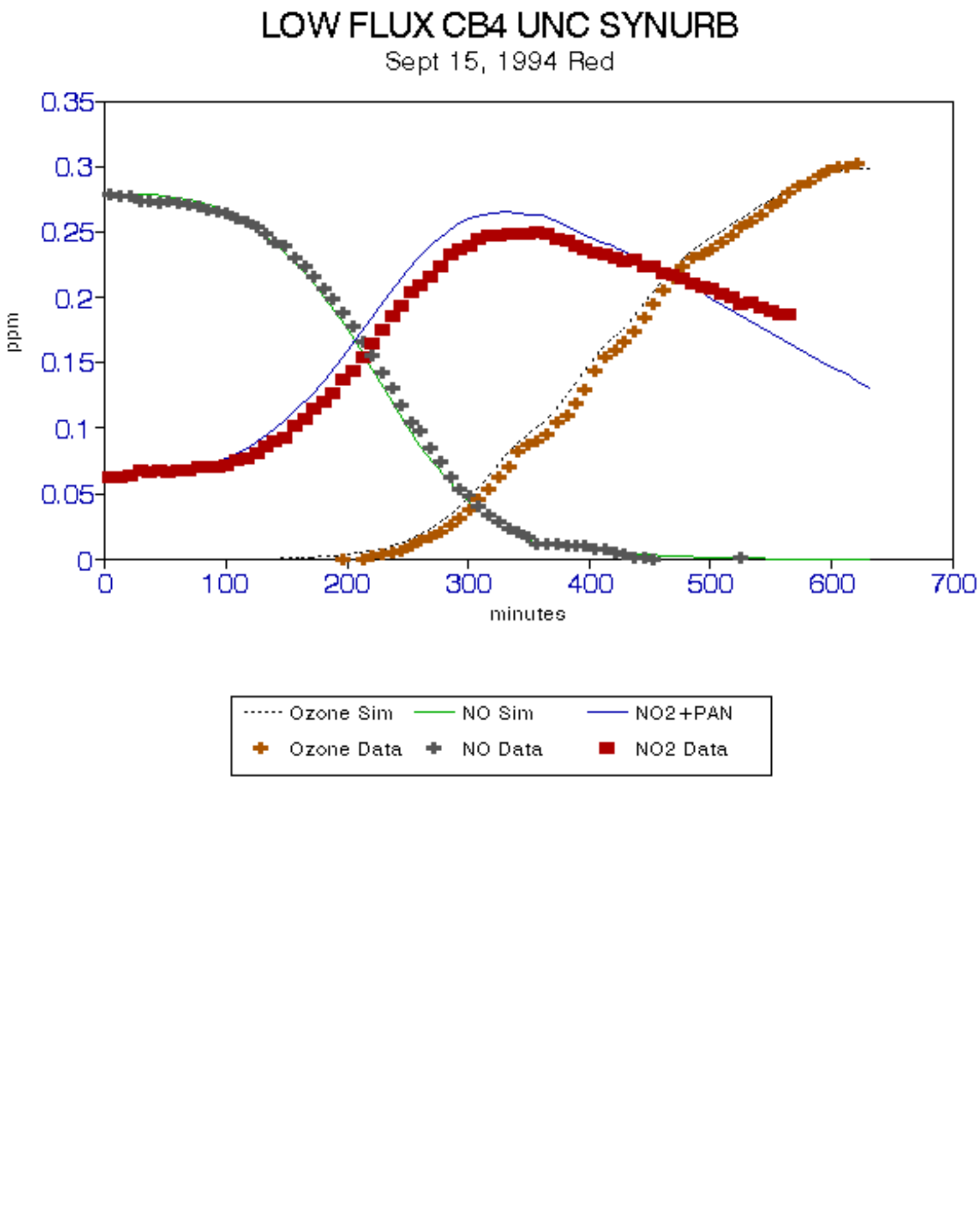
LOW FLUX CB4 UNC SYNURB
Sept 15, 1994 Red
ppm
0.35
0.3
0.25
0.2
0.15
0.1
0.05
0
0
100
200
300
400
500
600
700
minutes
Ozone Sim
NO Sim
NO2+PAN
Ozone Data
NO Data
NO2 Data

FIGURE 63.

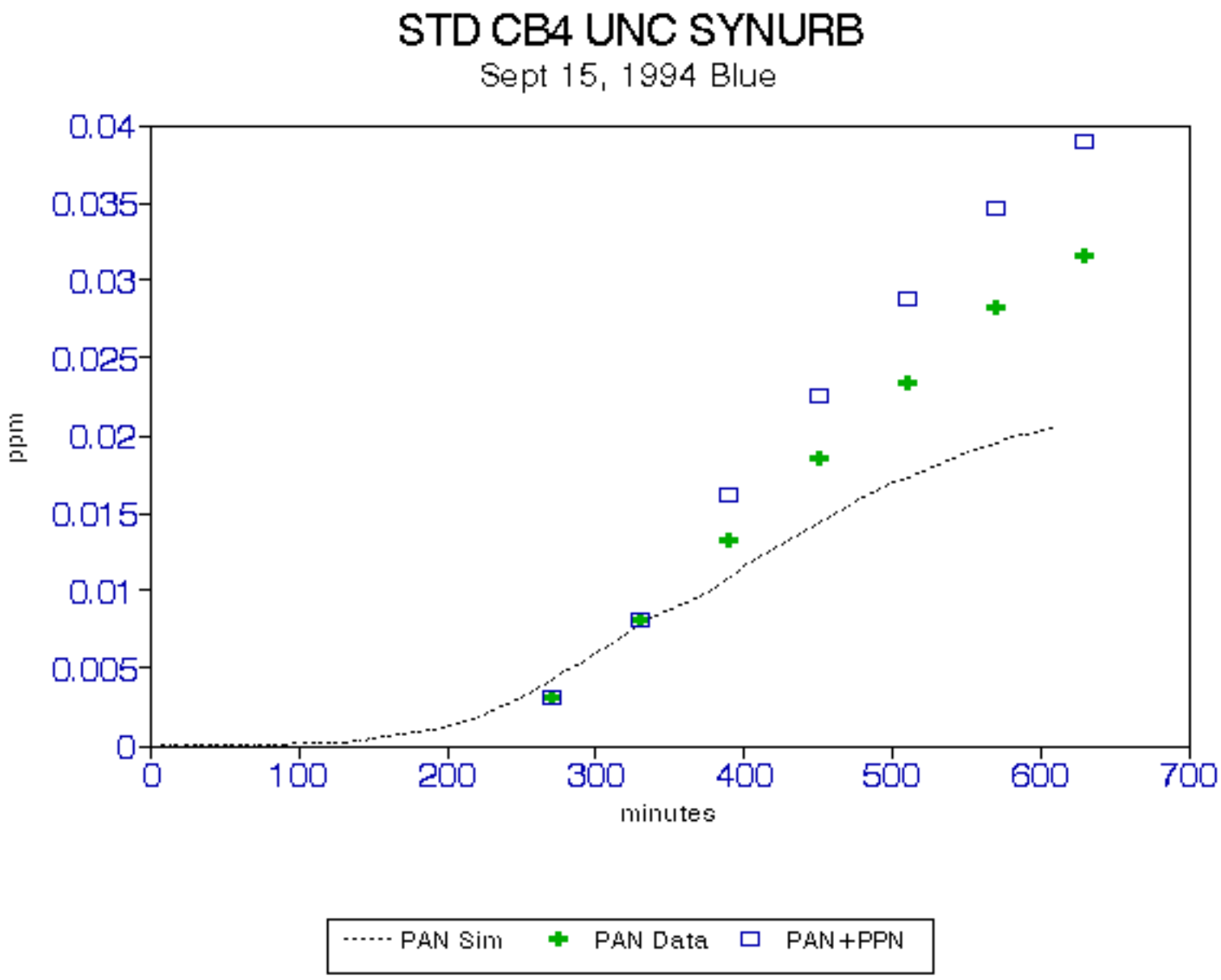
STD CB4 UNC SYNURB
Sept 15, 1994 Blue
ppm
0.04
0.035
0.03
0.025
0.02
0.015
0.01
0.005
0
0
100
200
300
400
500
600
700
minutes
PAN Sim
PAN Data
PAN+PPN

FIGURE 64.

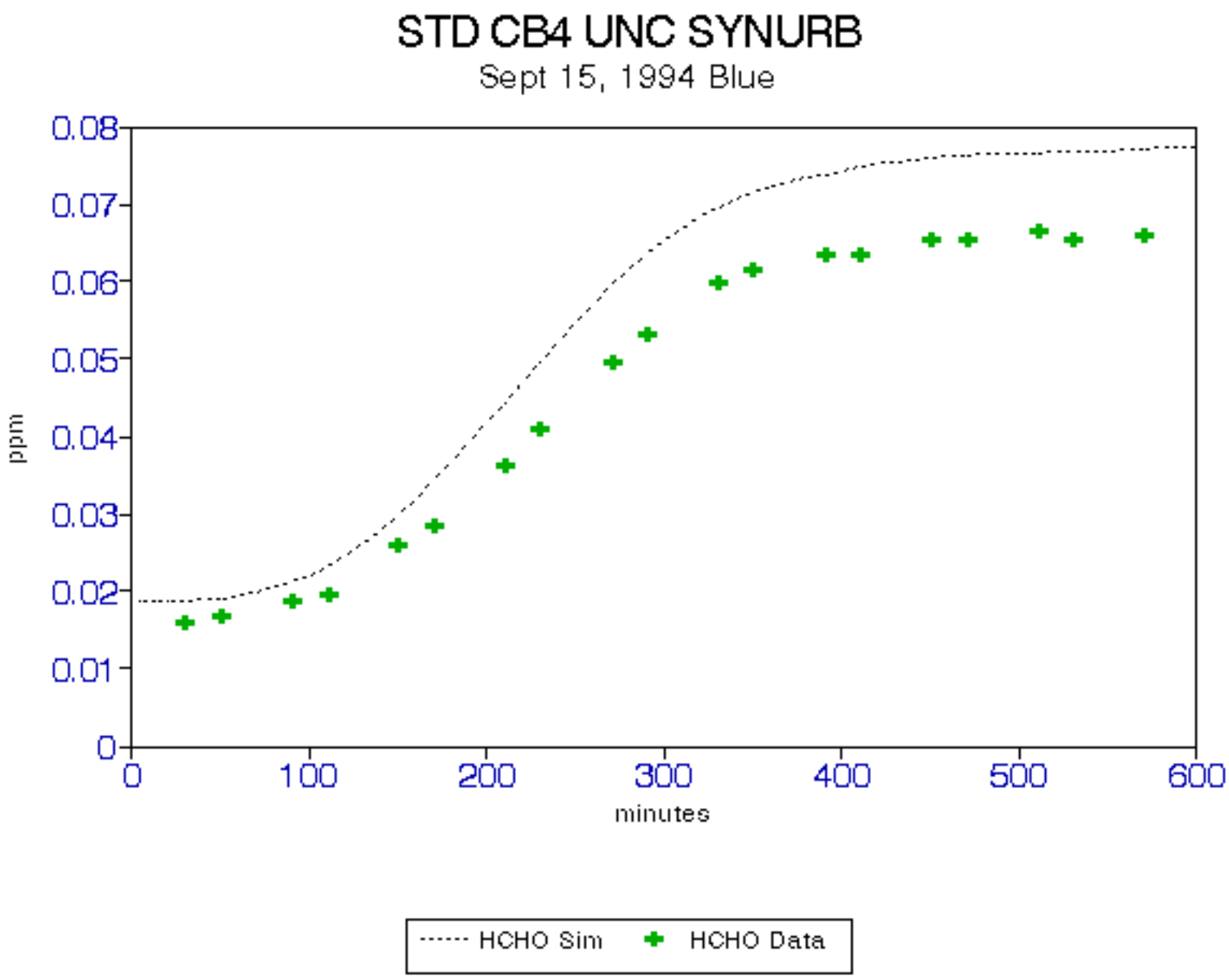
STD CB4 UNC SYNURB
Sept 15, 1994 Blue
ppm
0.08
0.07
0.06
0.05
0.04
0.03
0.02
0.01
0
0
100
200
300
400
500
600
minutes
HCHO Sim
HCHO Data

FIGURE 65.

STANDARD FORMALDEHYDE

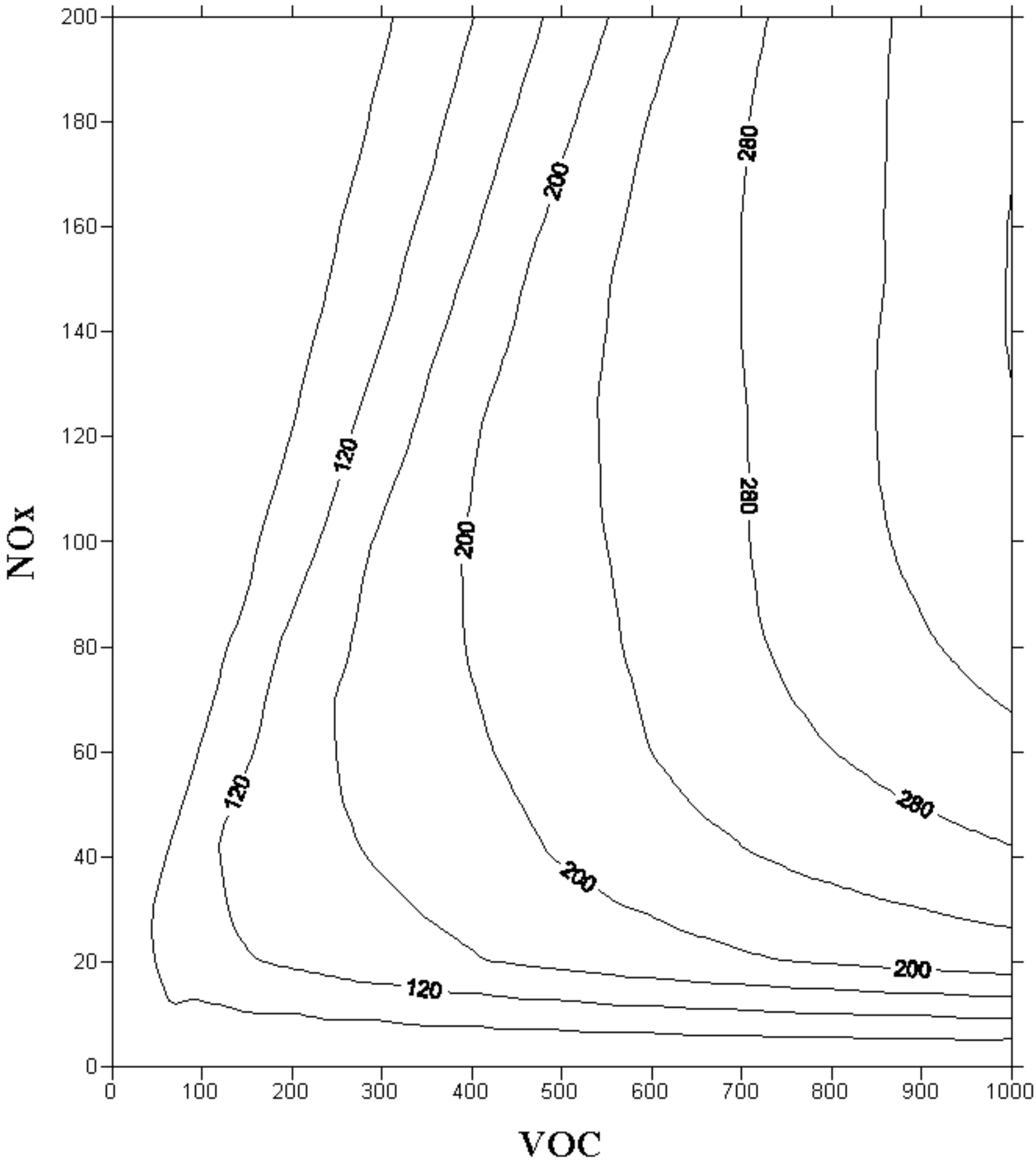

FIGURE 66.

LOW FLUX DIFFERENCES

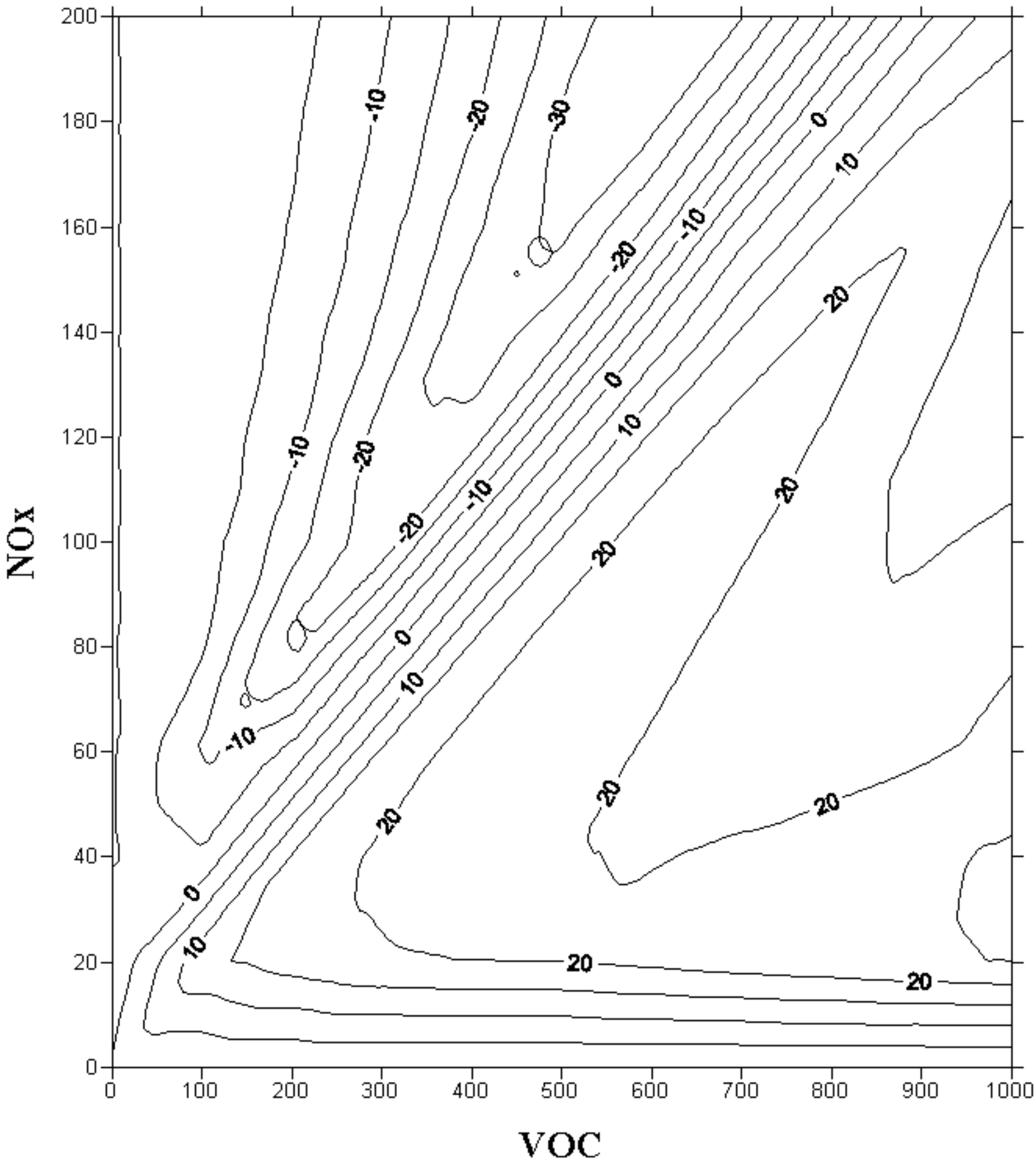

FIGURE 67.

LOW FLUX PERCENT DIFFERENCES

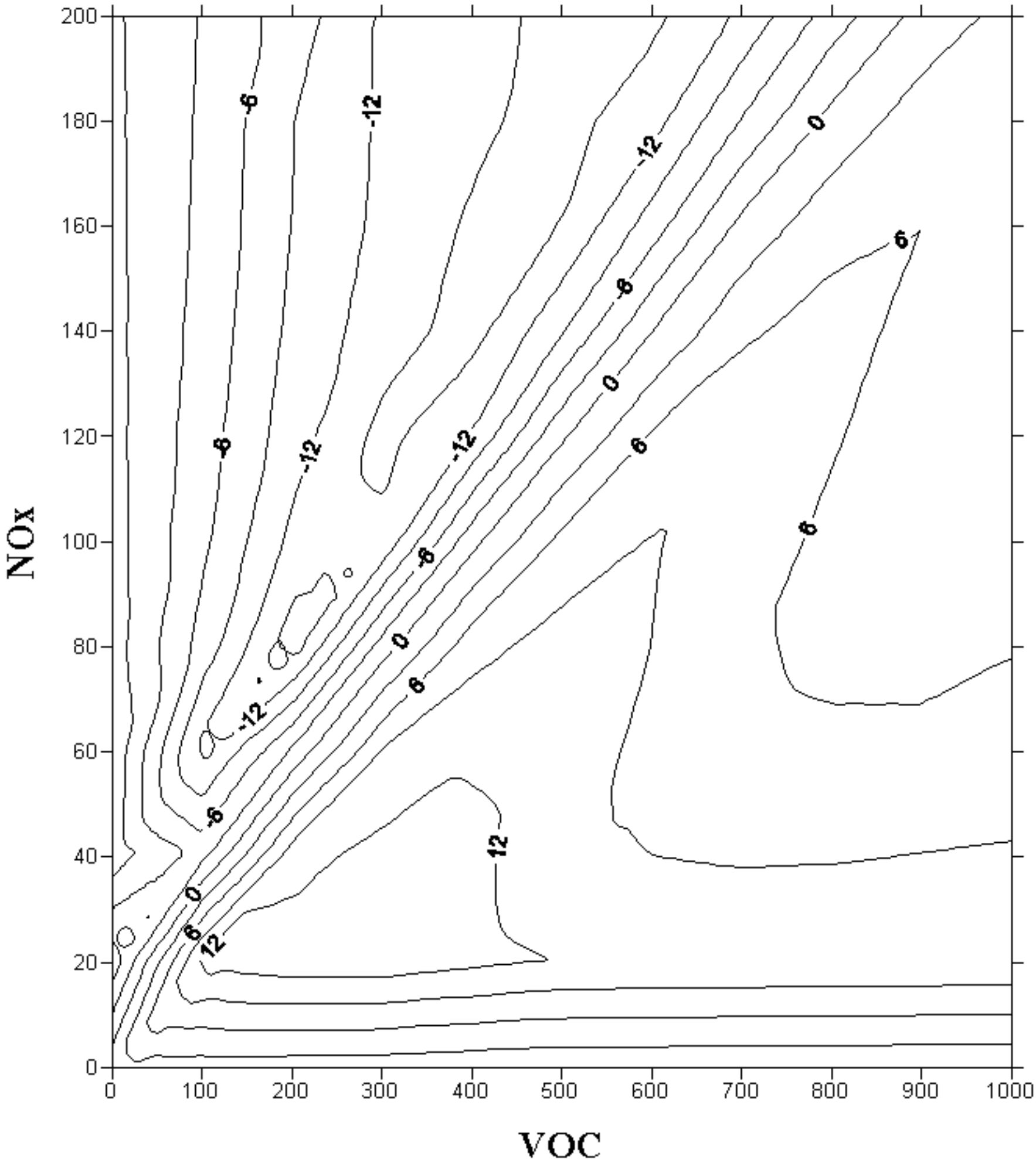

FIGURE 68.

HIGH FLUX DIFFERENCES

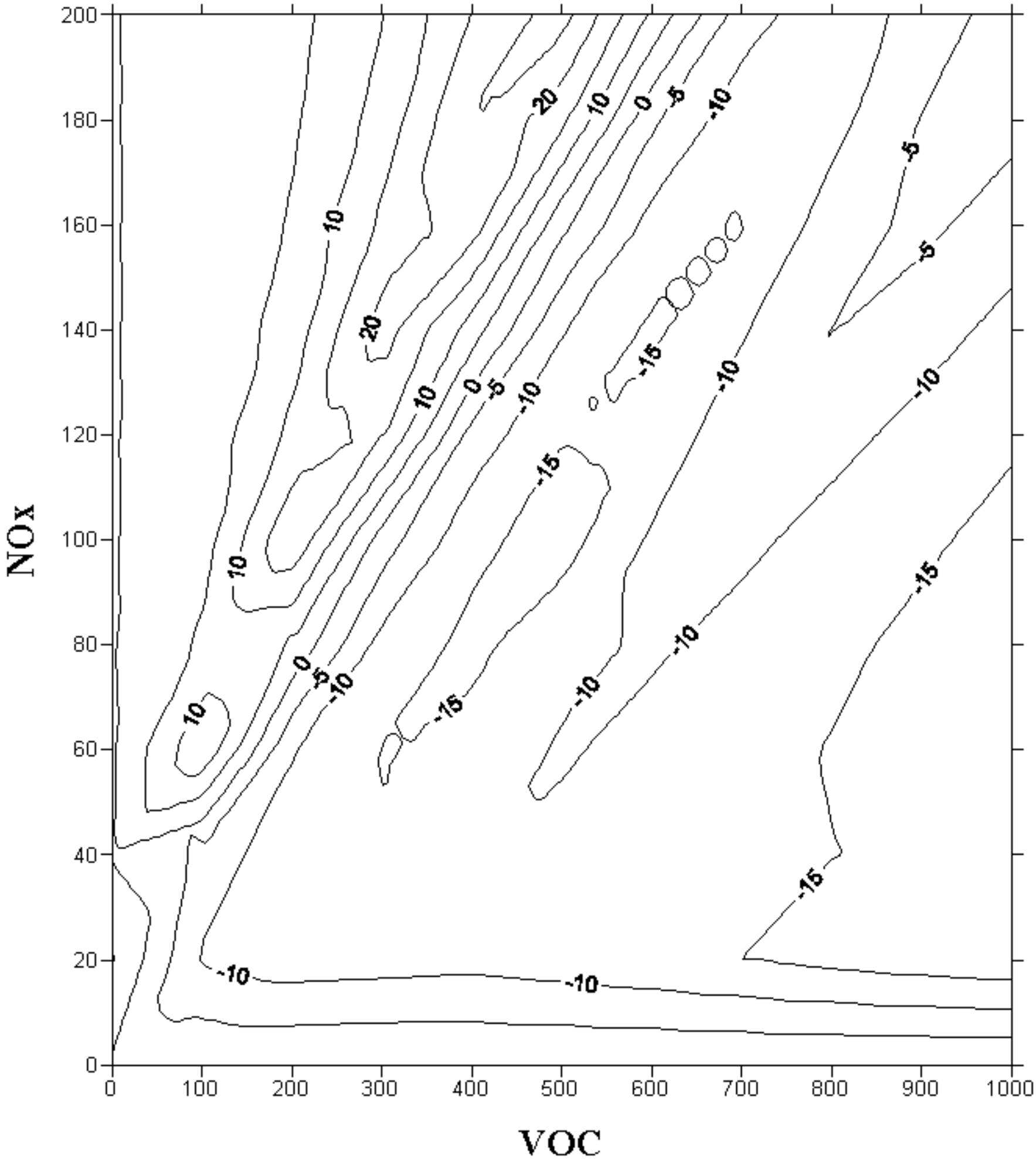

FIGURE 69.

STANDARD CB4

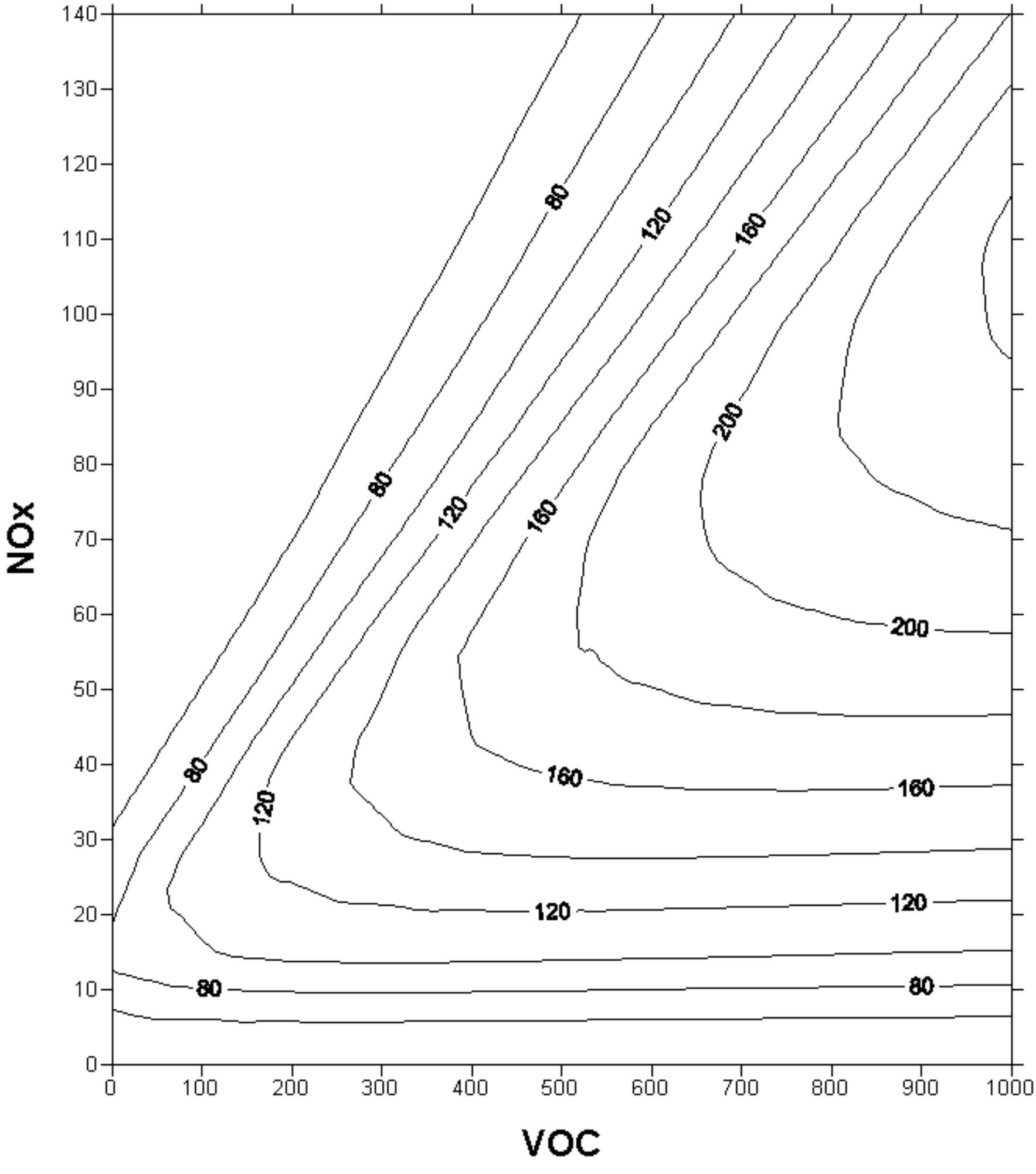

FIGURE 70.

LOW FLUX CB4 IMPACT

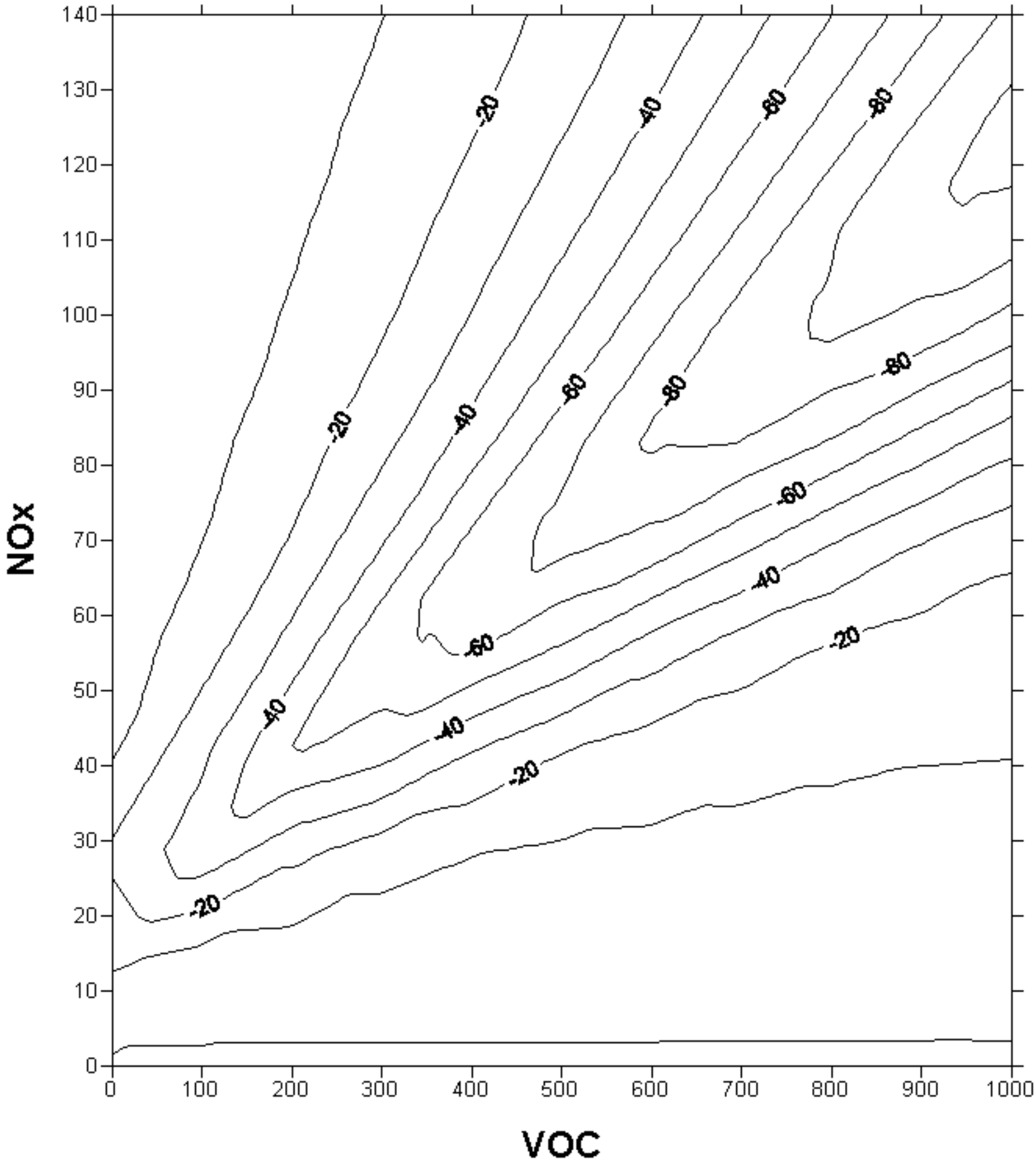

FIGURE 71.

HIGH FLUX CB4 IMPACT

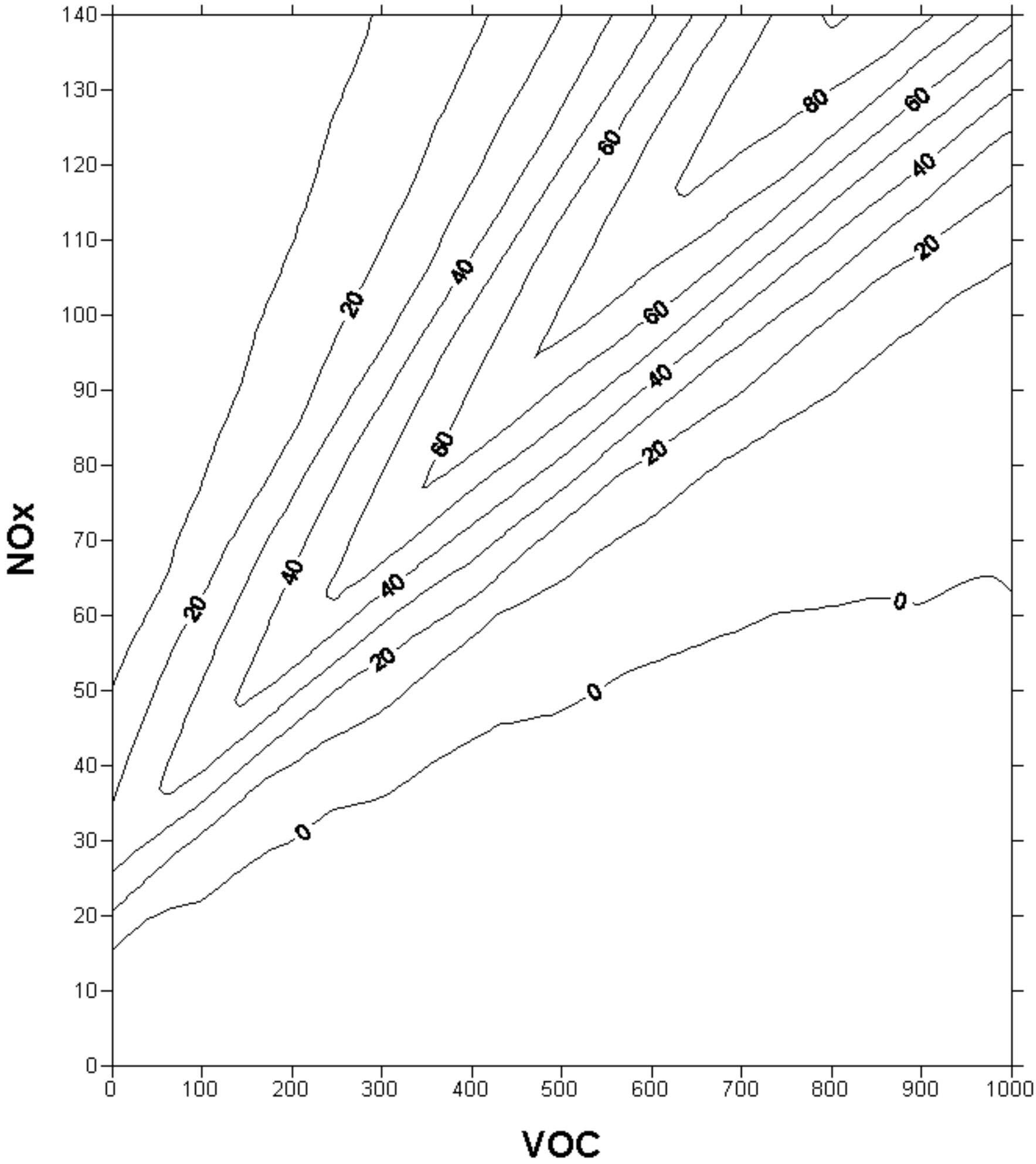

FIGURE 72.

PERCENT IMPACTS OF HIGH FLUX CB4

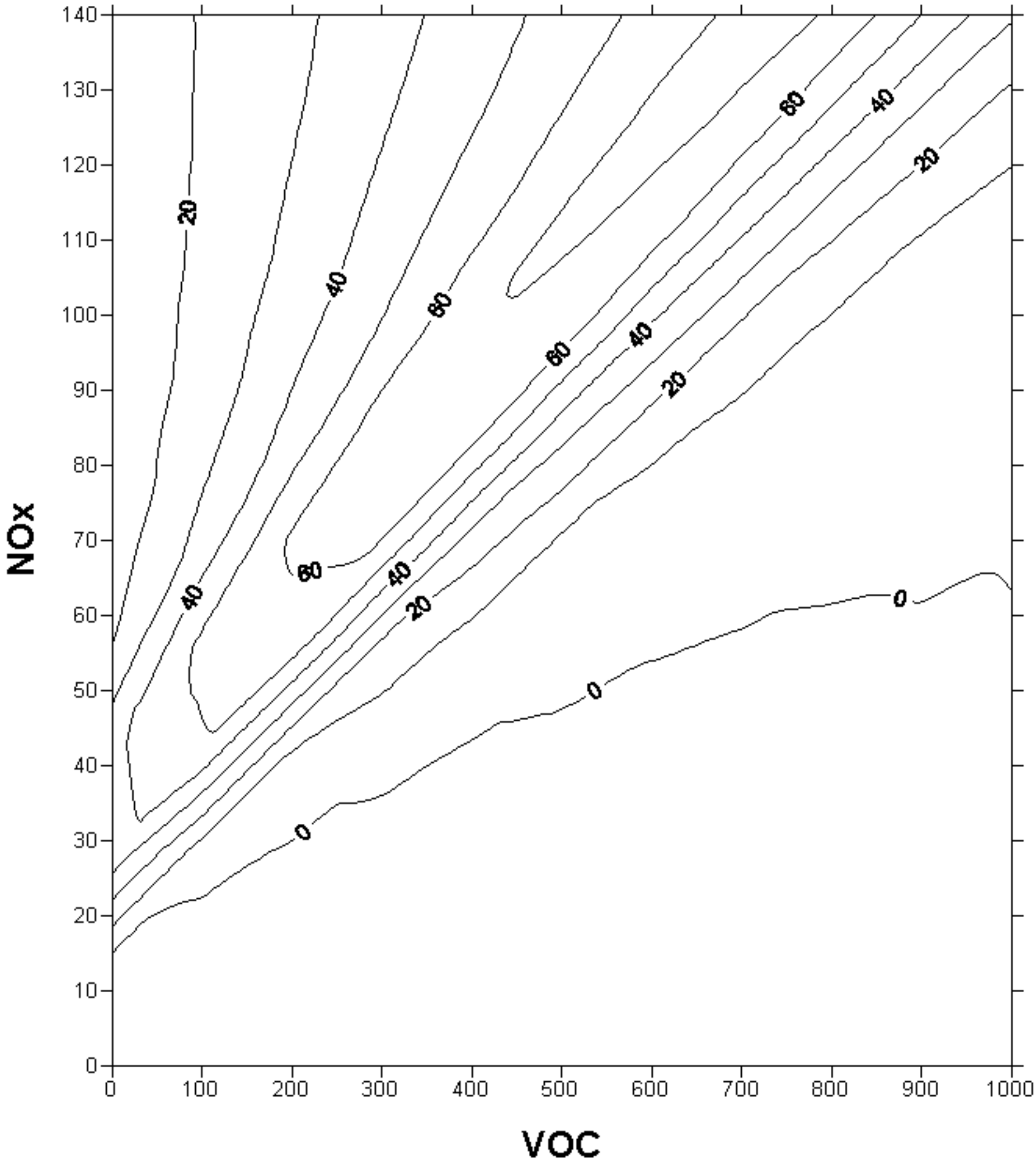

FIGURE 73.

PERCENT IMPACTS OF LOW FLUX CB4

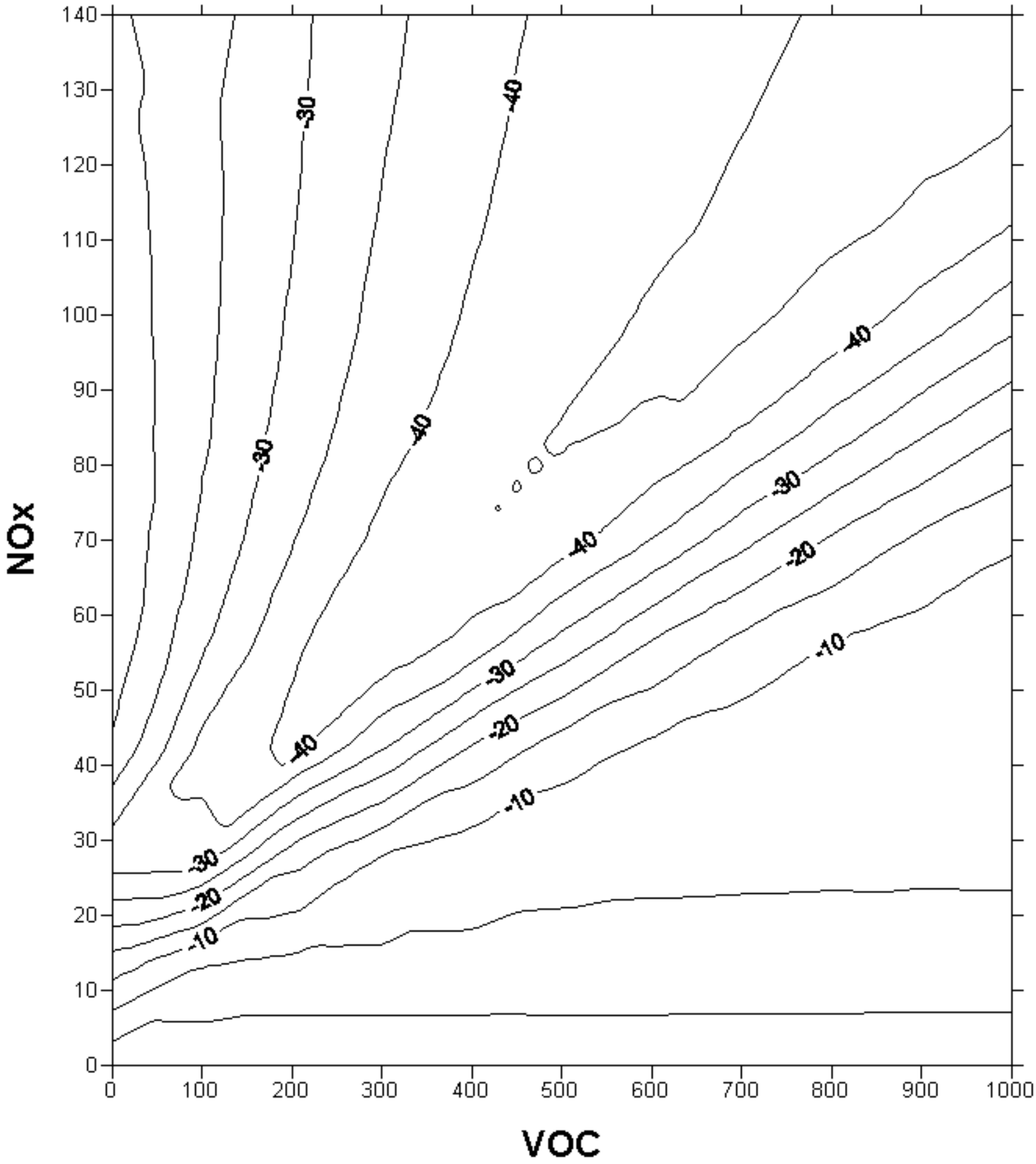

APPENDIX A

APPENDIX A

Chamber modeling in support of mechanism sensitivity studies -- Photolysis effects

by

James Killus

Review

In the Appendix to the Task 2 report, it was noted that the greatest uncertainty in photochemical modeling lay in the estimation of photolysis rates for the photolytic species important to the atmospheric chemistry of smog formation. In general, photolytic rates are estimated by a combination of measurements and modeling procedures, using absorption cross sections and quantum yields that are established in laboratory kinetic experiments (of various sorts), followed by the use of radiative transfer models to calculate the actinic flux in the atmosphere. This entire sequence of cross section, quantum yield, and actinic flux calculations will be abbreviated as QYCSAF in this report, with QYCSAFa representing an atmospheric estimate and QYCSAFc representing a chamber estimate.

For smog chambers that use natural sunlight, an additional model is used to calculate the effect of the chamber itself on the actinic flux. Smog chambers that use artificial light introduce yet another set of uncertainties in the characterization of the light source and do nothing to resolve the problems associated with the characterization of atmospheric actinic flux. For that reason, a natural light chamber was chosen for modeling in this project.

The most studied rate is the photolysis of NO_2 (K1), whose absorption cross section and quantum yield characteristics are known to a fair degree of accuracy; uncertainties in NO_2 photolysis, therefore, lie primarily in the estimation of actinic flux. NO_2 photolysis is also unique in that there are methods for its straightforward derivation from in situ chamber data, thus allowing a direct comparison of QYCSAFc calculations to a chamber observation of NO_2 photolysis.

Atmospheric estimates of NO_2 photolysis via QYCSAF calculations have been compared to actinometric measurements of K1 in a number of studies, but it should be noted that there are also uncertainties introduced by the actinometric device itself. Lantz et al., for example, estimated error limits of approximately 5% (1 standard deviation) for the absolute error of their NO_2 actinometer (owing to potential errors in calibration standards, temperature measurements, etc.), and a measurement error (noise in the data collected over a 30 minute period) of approximately 2% for midday readings during all four seasons at a Mauna Loa site. However, measurements during that study, MLOPEX 2, differed from NO_2 actinometry from a previous study at the same location, MLOPEX 1, by 37%, reasons which Lantz et al. were explicitly unable to explain.

The MLOPEX 2 study also compared the results of chemical actinometric measurements of ozone photolysis to $O(^1D)$ to QYCSAFa calculations (Shetter et al. 1996) and found that the latter overestimated the former by about 18%, even after the modification of standard quantum yield estimates in the 312-320 nm region to better fit the slant ozone column dependence of this photolysis rate. Overall uncertainty in the actinometer was estimated at 11% (1 standard deviation). It seems doubtful, therefore, that the QYCSAFa estimates for ozone photolysis are certain to better than 30%. Indeed a comparison of various actinometric measurements of ozone photolysis (as a function of slant ozone column thickness) indicated error limits (from the highest 1_ to lowest 1_ limit) of a factor of two (see Figure 1). It is also worth noting that the photolysis estimates for some studies were often outside the error limits for the estimates of other studies.

The other photolysis rates important to smog photochemistry usually involve oxygenated hydrocarbons whose photolysis generates hydrogen containing radicals that feed the hydroxyl-catalyzed radical oxidation cycle that is central to the smog formation process. A list of such photolysis rates would include:

1 > Formaldehyde photolysis to radical products (another pathway to molecular hydrogen and CO is less important)

2 > Acetaldehyde (radical products only)

3 > Propionaldehyde

4 > C4+ aldehydes

5 > Methyl glyoxal (formed from both aromatic and isoprene oxidation)

6 > Biacetyl (biacetyl formation is lumped with methyl glyoxal in the Carbon Bond mechanism)

7 > Unknown photolytic products of aromatics oxidation (OPEN in the CB-IV, several species labeled "AFG" in SAPRC chemistry)

This is, of course, only a partial list, since there are a large number of trace species in hydrocarbon oxidation product chemistry. Generally, however, any tractable kinetic mechanism must, at some point, cease treating every compound explicitly and begin to lump trace species into categories containing similar species.

The QYCSAF photolytic calculations for the compounds on the above list are uncertain to varying degrees. In some cases, the compounds themselves are unknown, and no such calculations are possible. In such cases, the only reasonable method of estimation appears to be pure empiricism: in chamber oxidation experiments, any gap between known radical sources and what is needed to explain the radical flux in the experiment is usually

attributable to unknown products having an unknown photolysis rate. Obviously, the potential error is large.

In the task 2 report, it was suggested that estimates of QYCSAFc for known compounds might be tested in chamber experiments involving those compounds themselves. It was also suggested that prior modeling studies should be representative of such "actinometric" chamber experiments, and, therefore, that variations in estimates that have been used for such experiments might serve as a first guess as to the uncertainty involved in QYCSAFc calculations.

The variations of previous photolysis estimates occurred because of a variety of phenomena, some real, and some that are artifacts of the QYCSAFc procedure. For example, changes in estimates due to changes in measurements of, or assumptions about, quantum yields or absorption cross sections are an artifact, as are differences due to changes in calculations (or measurements) of actinic flux. In Task 2, it was found that there had been several such artifactal changes in photolysis estimates over the past 15 years, resulting in variations of 10-25% which went largely unnoticed in smog chamber modeling studies. Thus, variations of this degree would not be expected to be sufficient for calling a particular simulation "erroneous" or to consider it to be evidence of a flaw in the modeling process. After a number of experiments were modeled under Task 3, this conjecture was, if anything, found to be too cautious, and that variations of 30-50% might easily be considered within the range of experimental uncertainty for most photolytic compounds.

Sidebar: Background Chamber Reactivity

A confounding factor in the use of smog chambers to assess reactivity, especially radical initiation reactivity is the matter of chamber background reactivity. "Blank" chambers (those with no intentionally added smog precursors) are known to emit various reactive species including organics, nitrogen oxides and nitrous acid. Some of the chamber contaminant species exhibit radical initiation behavior, and this is a confounding element in any attempt to infer radical initiation from chamber experiments.

At the outset of this round of modeling the UNC chamber data, it was the intention to use the "chamber background model" that is currently used by UNC investigators (the UNC chamber background reaction set has also been used by Bill Carter of SAPRC when modeling UNC data). However, after some examination of a variety of simulation artifacts, the UNC chamber model reactions were found not to give an accurate representation of the background reactivity of the UNC chamber. This is particularly true of the "WallOH" model, which represents a substantial fraction of the chamber-derived radical initiation processes in the UNC chamber model. The reaction used in the UNC modeling considers the "WallOH" phenomenon as a photoenhanced conversion of NO_2 to HONO. This has a number of specific features that may be tested against a variety of characterization experiments, the most important feature being an increase in the "chamber radicals" when NO_2 increases. A number of experiments had previously been examined

from teflon bag experiments (see "Background Reactivity in Smog Chambers," by Killus and Whitten, 1990) and no good evidence was found to support such an NO_2-linked increase in radical inputs. Evidence was found that the radical inputs from chamber background were linked to sunlight, and that a portion of such inputs were linked to NOx inputs into the chamber. Taken together, the most plausible source of chamber reactivity appeared to be a light enhanced chamber emission of HONO (independent of NO_2 levels, but greatly enhanced by liquid water condensation events), and a background of photolytic hydrocarbons equivalent to some 5-20 ppb of HCHO.

An example of the difference between these two methods of assessing chamber reactivity can be seen in Figure 2, which shows a methane-NOx run on a day with sufficient clouds to reduce the reactivity of the photochemistry -- which highlights the background reactivity assumptions. Experimental data for NOx also showed a substantial dilution effect during the day (10-20%), and there was no measured dilution tracer, so dilution must be estimated.

The two simulation line sets show the difference between the effect of two different sets of chamber radical assumptions. The closest fit line is for a direct emission of HONO and HCHO amounting to K1 times 0.15 ppb/min of HONO and K1 times 0.22 ppb/min of HCHO (the simulation is not very sensitive to the last parameter), with dilution being fit to match the total NOx decay behavior. The less well-fitted line is for the UNC chamber model, a combination of NO_2-to-HONO, plus a wall source of NO_2. The wall source of NO_2 is critical to the UNC chamber effects model, because without this reaction, NOx decays too rapidly during the afternoon, even if dilution is set to zero. However, there was no combination of NO_2-to-HONO, NO_2 emission, and dilution that would match the behavior of the system, although, as can be seen, the results are good enough that one might accept them as reasonable. However, the effort involved in tuning the three variables in the UNC chamber effects model (dilution, "WallOH", and "WallNO2"), was much greater than in the simpler wall source.

The fact that both the "WallOH" parameter and the "WallNO2" parameter have a significant effect on NOx behavior (the former reducing NOx and the latter increasing it) in the chamber makes joint use of these reactions cumbersome. Moreover, there are no good guidelines for their application other than what works on any given day. Since there is some evidence against the "WallOH" source model, and since it appears to be more difficult to use, the previously published wall effects model was chosen for these simulations.

Formaldehyde simulations

Formaldehyde (HCHO) would seem to be the best candidate for a smog chamber validation of the QYCSAFc calculations, since formaldehyde is a fairly strong radical source with no photolytic products to interfere with the estimation of photolysis for HCHO itself. However, there is the caveat that HCHO is strongly reactive to OH, so photolysis and OH reaction compete with each other in causing HCHO decay. For that

reason, plus the fact that HCHO also photolyzes to stable products, HCHO decay itself cannot be used to estimate HCHO photolysis to radicals.

There have been two previous modeling sets for UNC formaldehyde experiments within the last 10 years, the CB-IV validation set by Gery et al., 1988, and the study of Jeffries et al. (1989). The former used different QYCSAFc calculations than those currently used by UNC and in this study. However, as noted in the Task 2 report, changes in the absorption cross section data for HCHO have apparently been offset by changes in the assumed actinic flux in the UNC chamber, resulting in HCHO photolysis rates that are similar (generally within 15%).

A careful examination of the HCHO simulations from the CBMIV validation series shows a persistent underprediction of ozone, combined with an overprediction of HCHO decay. This was masked by the presence of two HCHO/CO/NOx experiments (figures 6-1 and 6-2 from Gery et al. 1988), which showed an overprediction of ozone, indicating that the overprediction of HCHO decay was due to an overprediction of HCHO photolysis, which led to an overestimate of radical reactivity. In the HCHO/NOx experiments, (figures 6-3 to 6-7, ibid), the larger portion of HCHO had been oxidized by the end of the experiment, leaving little leeway for further oxidation and ozone production, even if the photolysis of HCHO were to be increased. For that reason, in many of the HCHO experiments, peak ozone is not very sensitive to HCHO photolysis, because the ozone precursors are largely gone when ozone peaks, and altering photolysis rates only changes the timing of the ozone peak.

Figure 3 shows the simulation for the HCHO-NOx experiment of October 9, 1984, using the current QYCSAFc estimates from UNC and two simulations using 90 percent and 80 percent of the base case HCHO photolysis to radicals. This experiment is one of the experimental set that is sensitive to ozone photolysis, and the simulation using 90 percent HCHO photolysis gives the closest match to the 1988 validation set, as well as the closest agreement with peak ozone. However, HCHO decay is substantially overestimated (as was the case in the 1988 validation series), which suggests that a limitation of HCHO oxidation chemistry is being compensated by an overestimation of radical photolysis from HCHO.

This conjecture is supported by the parallel experiment in the Red chamber for October 9 (Figure 4), where 50 ppm CO was added to an otherwise identical HCHO experiment. The results are the same as those in the 1988 validation series -- a substantial overestimation of ozone. It is necessary to reduce HCHO photolysis to radicals by 35 percent to fit the ozone production seen in this experiment, although it should be noted that this results in an underestimation of NOx decay, and even this reduction in photolysis still somewhat overestimates the decay of HCHO. A substantial increase in the chamber parameter for the hydrolysis of N_2O_5 might reduce these disparities somewhat, but variation tests for this reaction were not performed.

It should be emphasized that the simulation results described here are not unique to the Carbon Bond Mechanism, since the CB-IV uses a standard, explicit formulation for HCHO and inorganic compounds. This may be seen in Figure 5, which shows simulation results for the July 15, 1986, Red experiment. In addition to the CB-IV mechanism results for 100 percent (base case) HCHO photolysis, the UNC explicit mechanism results are shown -- barely separable from the CB-IV results for ozone, and only slightly more separated for NO_2.

In "A Chamber and Modeling Study to Assess the Photochemistry of Formaldehyde," by Jeffries et al. (1989) simulation results are presented for a total of 7 HCHO-NOx experiments on 5 days (on two of the days both the Red and Blue chamber were HCHO-NOx experiments). These days were

May 18, 1977 (one side HCHO)
July 18, 1977 (one side HCHO)
July 8, 1986 (both sides HCHO)
July 15, 1988 (both sides HCHO)
August 16, 1988 (one side HCHO)

On the May 18, 1977 day, water condensed on the chamber walls, which results in a temporary loss of HCHO from the gas phase due to wall absorption of HCHO, followed by a return of HCHO to the gas phase when the water evaporates. There are a number of similar days (i.e. days that involved condensed water interference with the introduction of HCHO into the gas phase) that have been modeled in previous simulation studies at SAI (see Whitten, Killus, and Johnson, 1984). It is doubtful that meaningful conclusions concerning HCHO photolysis can be drawn from such circumstances. In any case, the UNC simulations underpredict ozone substantially. (Figures 71 and 72 from Jeffries et al.).

The July 18, 1977 modeled by UNC day did not have condensed water. The experiment showed a substantial underprediction of ozone, however, similar to those simulations described above for the CB-IV validation series, except that HCHO decay was properly simulated (Figures 69 and 70).

The simulation results reported by Jeffries et al. for the remaining HCHO-NOx experiments are excellent (Figures 65-68;95 and 96). However, except for the July 15, 1988 experiments, discussed below, these simulations could not be reproduced using the normal chamber effect model. For the August 16, 1988 Red case, Jeffries et al. report the use of 200 ppb of background VOC for the HCHO-NOx experiment only, and the simulation of this experiment done for this study shows a similar response to BVOC (see Figure 6), although this new simulation slightly overpredicts ozone with the 200 ppb BVOC input. However, Jeffries et al. (1989) report a more typical value of 55 ppb BVOC for their simulations of the Blue chamber (an ethene experiment), and it must be concluded that the good simulations obtained for the July 15 HCHO-NOx experiment may only be a matter of curve fitting, with no application to the present study.

The excellent fits of Jeffries et al. (1989) for the July 8, 1986 experiments (Figures 7 and 8) could not be reproduced. Also, some sensitivity tests indicate that the peak ozone in these particular experiments is relatively insensitive to changes in HCHO photolysis (Figure 8), so altering the experimental inputs to fit the ozone (e.g. by increasing BVOC) would serve no useful purpose.

Figures 5, 9, 10 and 11 show the simulation results for July 15, 1988, and September 23, 1996. These are the only experiments in the UNC data set that appear to be well simulated by the kinetic mechanisms and nominal chamber effects models. For July 15, ozone, NOx, and HCHO are all well simulated, with a small positive error indicated for the rate of oxidation in the morning (less than 10%), and a similar, negative error indicated for the rate of oxidation in the afternoon. It should be noted, however, that the afternoon of this experiment was cloudy. Figure 9 also shows a test of the sensitivity of an HCHO experiment to the chamber model using wall emissions of HONO. Paradoxically, the elimination of the HONO input results in a small «MDUL»increase«MDNM» in ozone.

HCHO measurements

In the July 15, 1988 experiments, UNC was operating two HCHO measurement instruments, a device from CEA Instruments, and a Dasgupta diffusion scrubber system (PKD). While the two instruments were equivalently calibrated and tended to give similar results during most of an experiment, they differed substantially at the beginning of the July 15 experiment (Figures 5b and 9b). Moreover, HCHO data at the beginning of these experiments was very noisy, resulting in a substantial range of plausible initial conditions. For the Red side of this experiment, initial HCHO might have been set at anywhere from 0.67 to 0.87 ppm, given the range of early measurement. It may be noted that the intended injection was for 1 ppm. On the Blue side, with an intended injection of 0.5 ppm, early measurements ranged from 0.39 to 0.43 ppm.

For the September 23, 1996 experiment, only the PKD instrument was in operation, and the instrument was noisy during the morning, giving measurements that ranged from 0.85 to 1.07 ppm on the 1 ppm injection side, and 0.44 to 0.54 on the 0.5 ppm injection side. While these measurements can plausibly support the claim of a quantitative injection of HCHO, they may just as easily be seen as a «MDUL»+«MDNM»10 percent uncertainty in initial conditions, which is similar to the uncertainty noted by Jeffries et al. (1989) for HCHO measurements generally.

An uncertainty of 10 percent (or greater) in HCHO initial conditions translates into a substantially greater uncertainty for HCHO photolysis, since NOx oxidation responds to both radical inputs and the quantity of HCHO reacting with OH to yield oxidizing radicals.

Summary of HCHO results

To summarize the present findings for simulations of HCHO-NOx experiments, for most of the UNC experiments, there is a persistent inability of the HCHO mechanism to predict peak ozone for these experiments. The question is whether this is due to an analytical shortcoming (negative bias in HCHO measurements), a mechanistic shortcoming (the existence of some additional NOx oxidation mechanism in HCHO photochemistry), or a feature of the UNC chamber itself.

If the flaw is in the UNC chamber model, the problem appears to occur only for HCHO experiments, and not for other types of experiments, including HCHO experiments with CO added. This seems unlikely. A mechanistic explanation also seems unlikely, given the simplicity of the oxidation mechanism for HCHO; a compound whose only known products are CO, HO_2, and H_2 (from photolysis) does not seem a likely candidate for product yield uncertainties.

The most likely shortcoming in these data lies in analytical difficulties for HCHO measurement; Jeffries et al. (1989) note several cases in which they suspected calibration problems for HCHO, although those difficulties were cases where a positive bias or interference was suspected and the nature of the observed simulation shortcomings are more consistent with a negative bias. Moreover, the differences between two HCHO monitoring methods, plus data scatter in the morning, when initial conditions are established, makes this the most attractive explanation.

Only two days (four experiments) in the current database seems to allow the accurate simulation of ozone and HCHO decay. For the July 1988, Red side, a standard HCHO-NOx and chamber model gives a peak ozone of 0.42, versus 0.454 for a 30 percent increase in HCHO photolysis and 0.358 for a 30 percent decrease; peak measured ozone for that experiment was 0.437 ppm ozone. For the Blue side, the standard model gives 0.129 peak ozone, versus 0.17 for a 30 percent increase in HCHO photolysis, and 0.084 ppm ozone for a 30 percent decrease in HCHO photolysis. Measured peak ozone was 0.14 ppm. "Tuning" the photolysis rate for this day would suggest an increase of about 10 percent for both sides. However, none of the sensitivity tests, i.e. plus or minus 30 percent give simulation fits that are worse than other days and other experiments using the standard HCHO model.

For the September 23, 1996 day, peak ozone on the Blue side was 0.485, with a base case simulation peak of 0.5 ppm. An increase of 20 percent in HCHO photolysis resulted in peak ozone of 0.53 ozone, while a decrease of 20 percent gave ozone at 0.458 ppm. On the Red side, measured peak ozone was 0.14 ppm with an identical base case simulation peak. Modifications of HCHO photolysis by 20 percent gave simulation peaks of 0.167 and 0.108 ppm. It seems likely that HCHO photolysis could not be reliably established to within 20 percent on the basis of these experiments.

Given the sensitivity that was found in HCHO-NOx experiments to uncertainties in initial chamber loading of NOx, plus the insensitivity of many experiments to variations in HCHO photolysis, an uncertainty of «MDUL» cannot be ruled out within-chamber

«MDNM»HCHO photolysis of 20 percent-30 percent from plausibility. Given the inevitable uncertainty of going from a within-chamber estimate of photolysis to an atmospheric estimate, plus the normal day-to-day variations in such important parameters as atmospheric haze and cloud cover, as well as site specific inputs such as ground albedo, it seems clear that atmospheric estimates of photolysis are uncertain to an even greater degree.

Higher aldehydes

As discussed in the Task 2 report, there is a significant difference (factor of 4) between the QYCSAF photolytic rates of acetaldehyde and propionaldehyde (Ald2 and Ald3). There are two UNC experiments which compare these two compounds, and on the basis of those experiments, it can tentatively be concluded that there is a substantial difference between the photolytic rates of the two compounds. However, there are substantial caveats.

For the August 24, 1982 experiments, neither the acetaldehyde nor the propionaldehyde experiments are sufficiently well simulated to allow fine discrimination of the uncertainties of photolysis (Figures 12 and 13). Moreover, substantial variations in photolysis (+ or - 50 percent) for Ald2 and Ald3 do not substantially alter the goodness of fit. Moreover, neither PPN nor PAN was well simulated for either experiment on this day.

It is worth noting that in the development and testing of the CB-IV mechanism on the August 24 day, both the Ald2 and Ald3 experiments were much better simulated than in the simulations displayed here, and in those simulations Ald2 was simply used as a surrogate for Ald3. However, it is apparent that this was partly a matter of compensating errors, since the total measured concentration of PAN plus PPN was considerably greater than that of the simulation surrogate i.e. PAN only. The confounding effects of PaNs are discussed below.

The June 14, 1982 day was initially very poorly simulated using UNC default inputs. However, on closer examination, it was determined that the dilution curve calculated by UNC based upon the CCl_4 tracer data was problematic; the CCl_4 instrument showed a great deal of noise in the morning data, making the total dilution for the day very uncertain. Also, the UNC dilution calculation does not seem to handle circumstances where the tracer data show a significant increase. Therefore, following UNC protocols, dilution for another day was used, and the simulation improved markedly (Figure 13 and 14). However, the lack of adequate day-specific dilution data greatly increases the uncertainty of the results, and the fact that PAN is substantially underpredicted also indicates considerable uncertainty.

Were the June 14 experiments considered to be definitive, a probable conclusion would be that photolysis of both Ald2 and Ald3 were substantially overpredicted, though this conclusion would be tempered by the observation that PAN is underpredicted, which would indicate that actually more radicals were present than simulated.

A more recent experiment at UNC (October 4, 1996) compared a 1 ppm (volumetric) loading of acetaldehyde to a "half and half" mixture of acetaldehyde and propionaldehyde (0.5 ppm and 0.5 ppm volumetric). Figures 15 and 16 give simulations for the acetaldehyde and propionaldehyde mechanisms for that matched experiment. One complicating factor in this experiment was that there seems to have been a high rate of dilution in the chamber, roughly 30 percent over the course of the experiment according to the CCl_4 data, although UNC investigators have questioned the temperature calibration for the CCl_4 measurements on this day. The situation for the October 4 experiments is similar to the June 14 experiments in that the ozone profiles would seem to call for lower rates of aldehyde photolysis, whereas data for PANs suggest that the radical inputs are underpredicted.

The importance of PAN measurements for the higher aldehyde experiments brings up a general question pertaining to radical balances in experiments where PAN is a significant product. Since PAN is a major radical sink, uncertainties in radical inputs from photolytic species may be reflected in PAN (and PPN) product yields rather than in NOx oxidation and ozone formation. Conversely, uncertainties in PAN measurements result in uncertainties in determining radical source behavior from chamber data.

The substantial discrepancies between model predictions and observations, along with the problems noted above, suggest the need for substantial mechanism (re)development efforts for propionaldehyde, its product PPN, and perhaps for acetaldehyde and PAN as well. It is suggested that, if such development efforts were undertaken, the most appropriate method would be the use of a series of experiments in constant light type reaction vessels at different temperatures and light intensities, since the variation of these inputs seems to have a marked impact on photooxidation behavior and the degree to which the kinetic mechanisms achieve good simulations.

In any case, the uncertainties in photolysis rates for higher aldehydes obviously exceed those for HCHO, and deviations of more than 50 percent do not produce simulations that are notably less accurate than the base case runs.

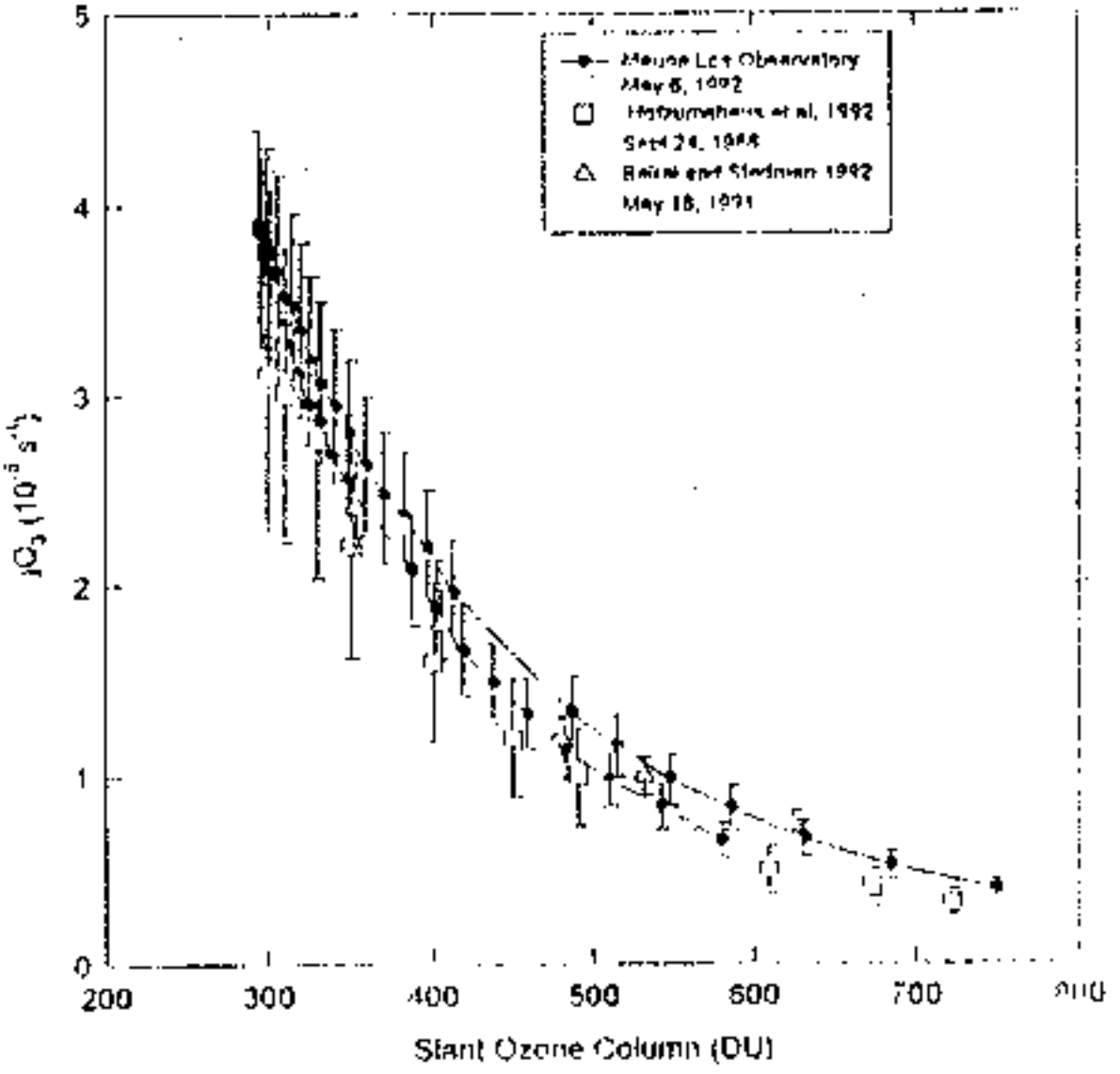

Figure 1 Measured jO_1 as a function of ozone slant path. Actinometer data from Mauna Loa on May 6, 1992 (filled circles with connecting lines), filter radiometer data from the Atlantic Ocean on September 24, 1988 [*Hofzumahaus et al.*, 1992] (open squares), and actinometer data from Denver, Colorado, on May 18, 1991 [*Bairai and Stedman*, 1992] (open triangles) Error bars represent measurement error estimated by each author.

Figure 2: September 20, 1993

Methane-NOx (chamber reactivity)

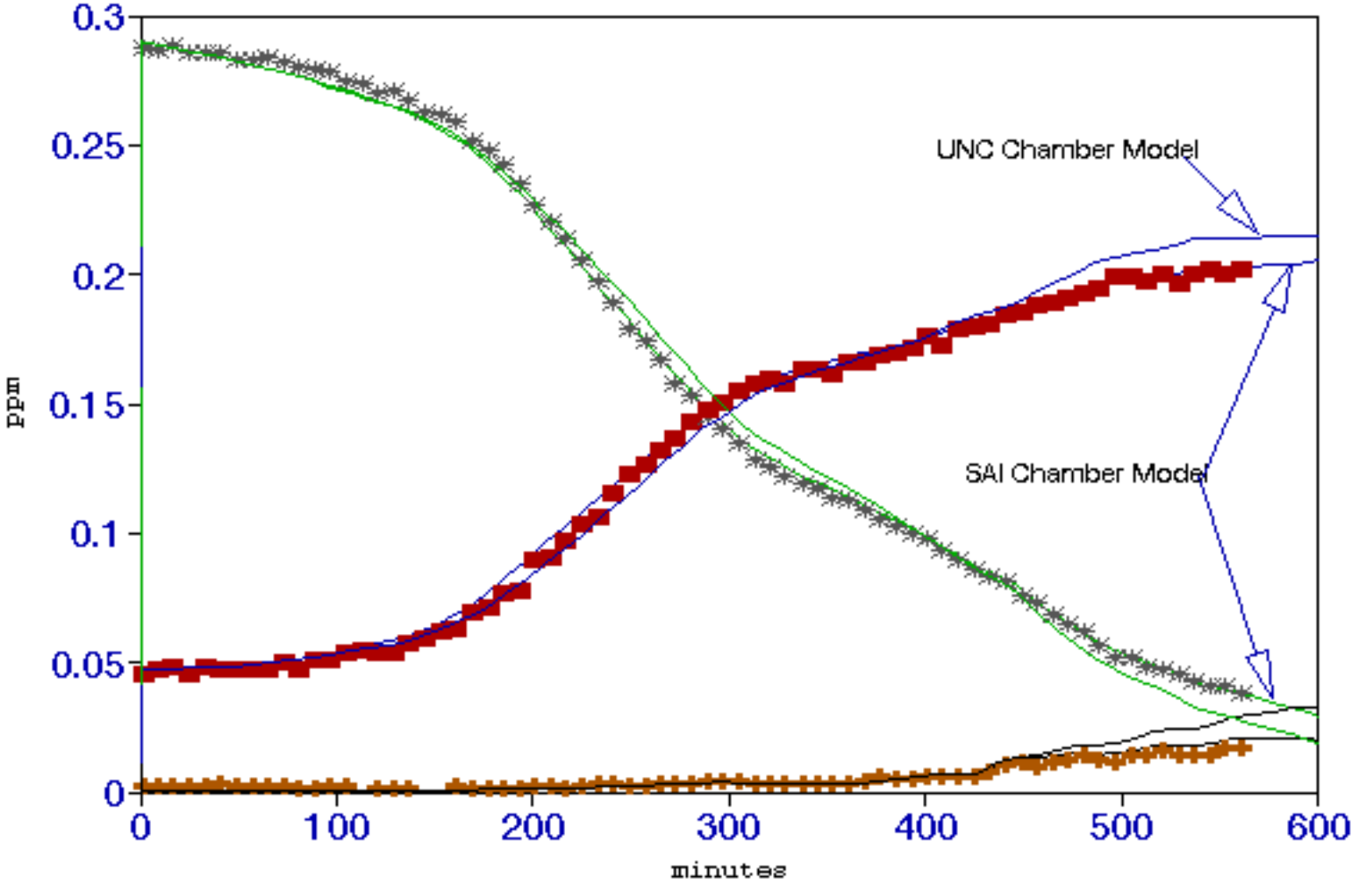

Figure 3a: October 9, 1984 Blue

HCHO-NOx (80%, 90%, 100% photolysis)

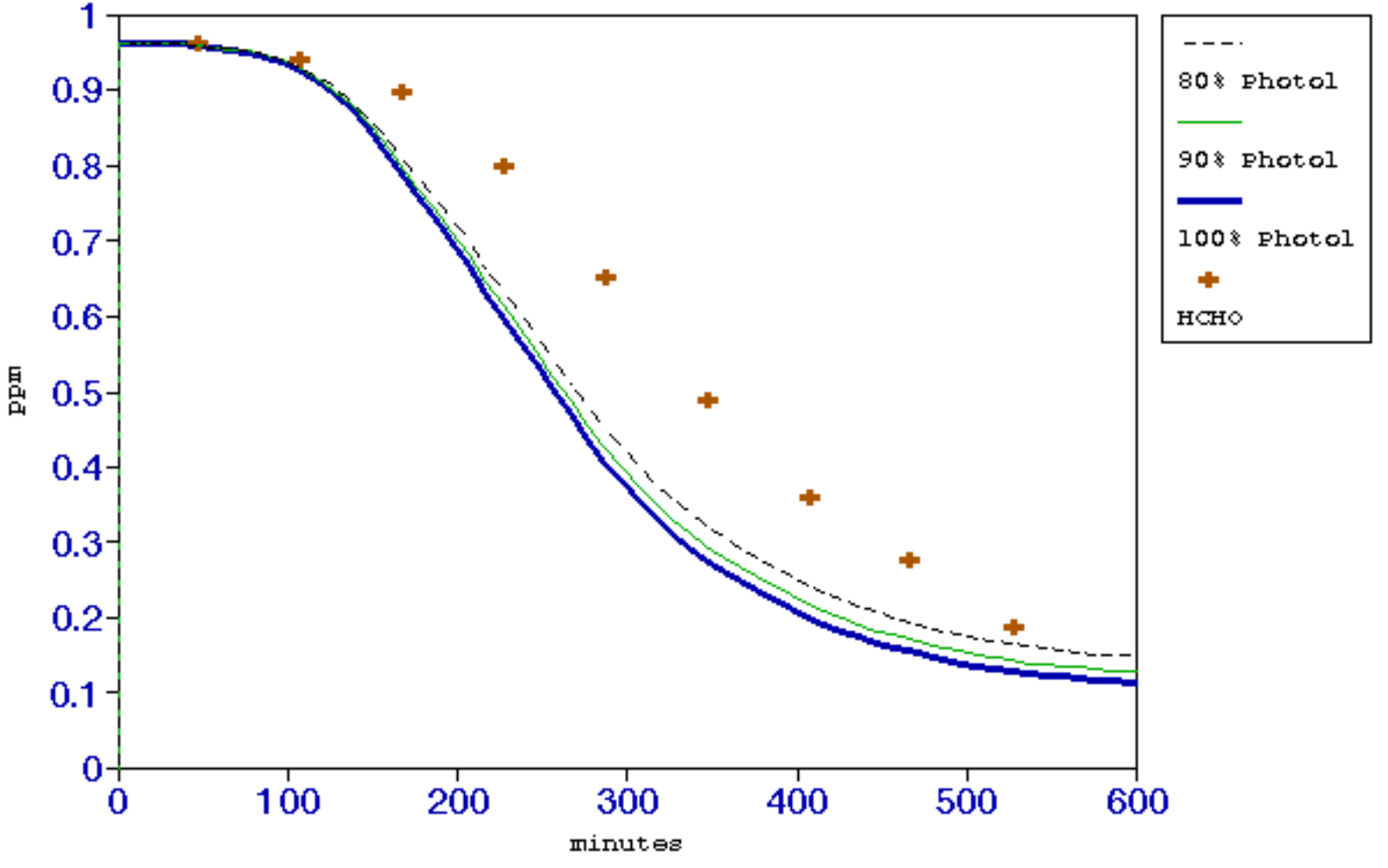

Figure 3b: October 9, 1984 Blue

HCHO-NOx (80%, 90%, 100% photolysis)

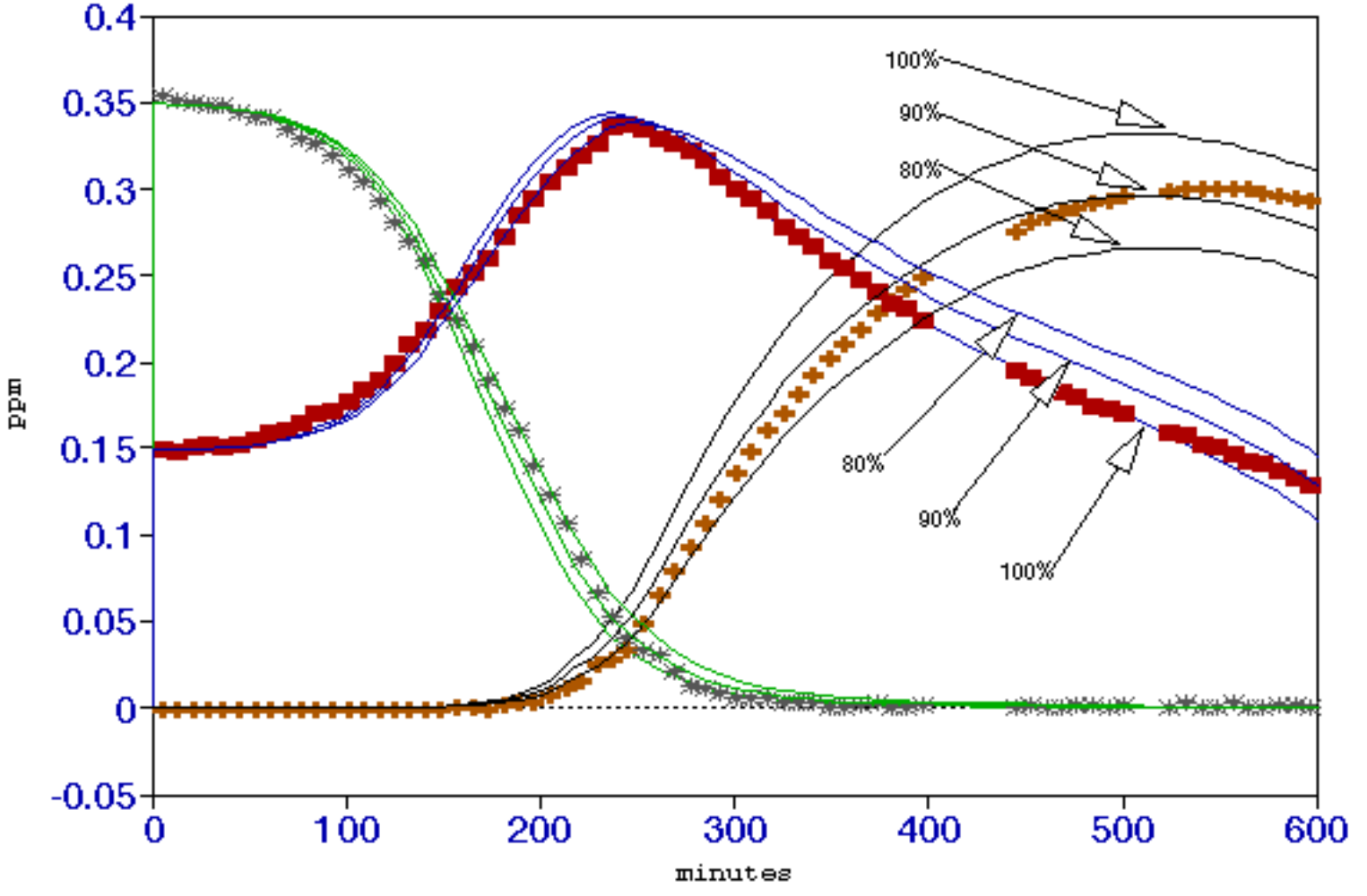

Figure 4a: October 9, 1984 Red

HCHO-NOx (100%, 65% photolysis)

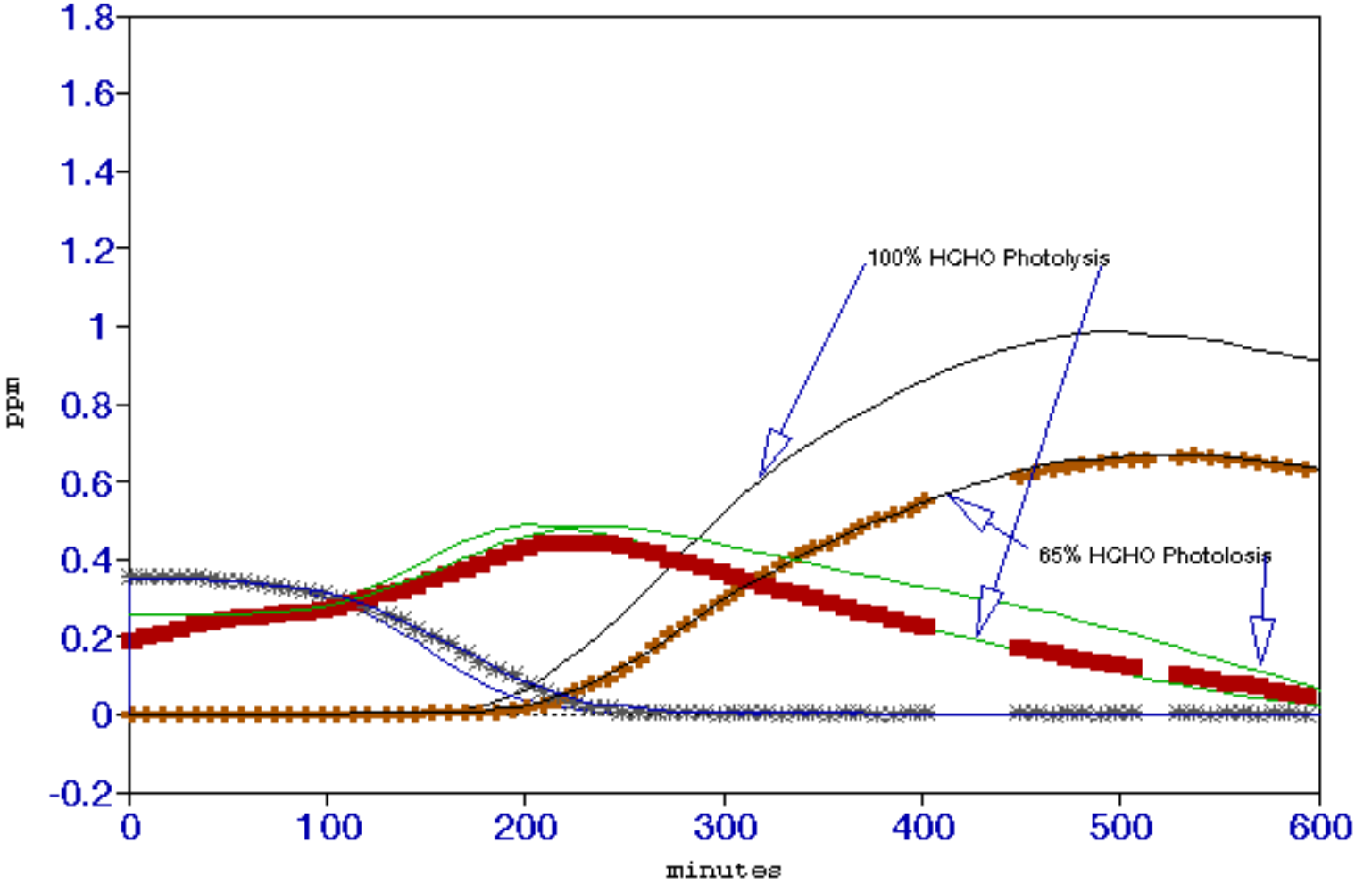

Figure 4b: October 9, 1984

HCHO-NOx (100%, 65% photolysis)

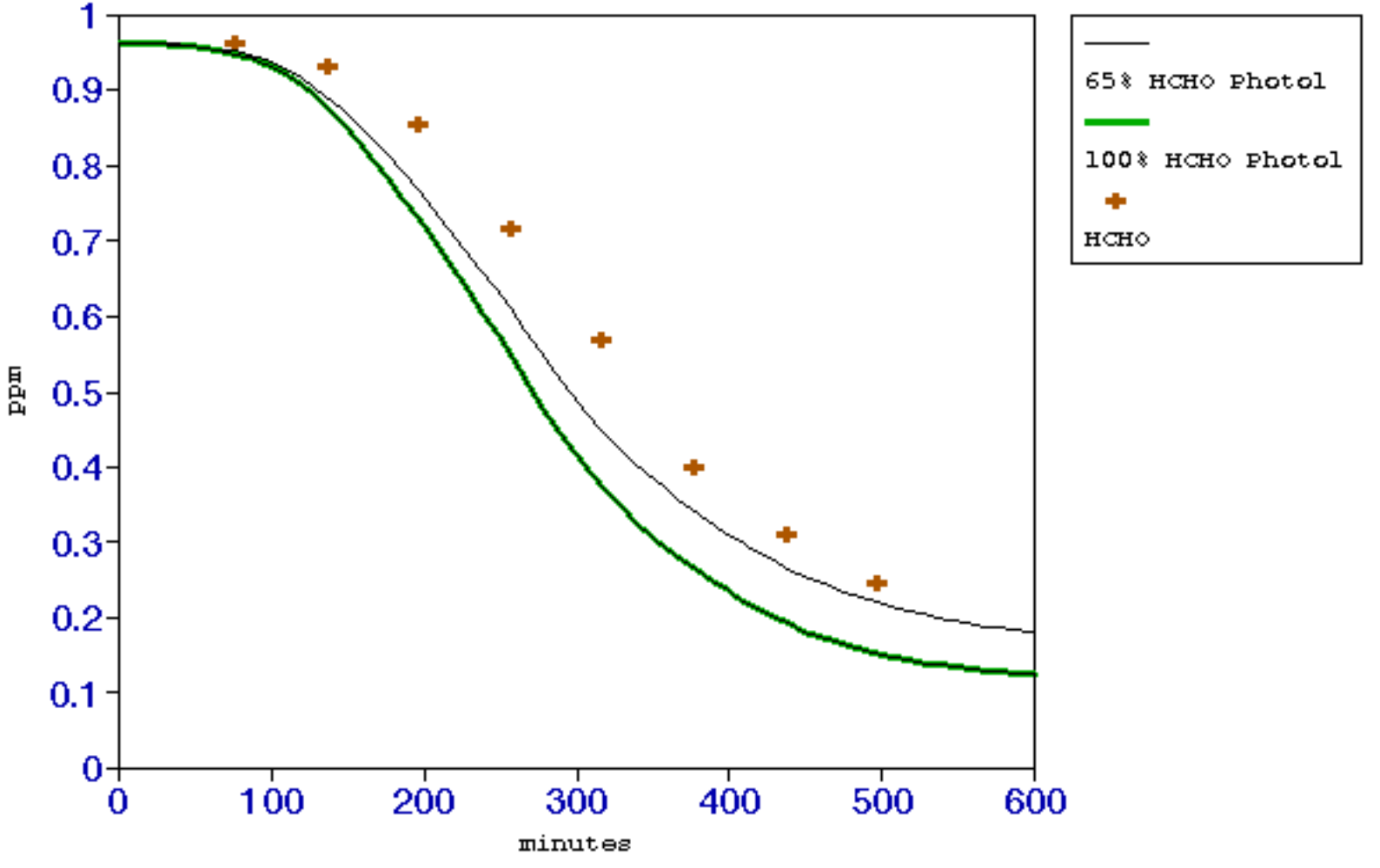

Figure 5a: July 15, 1988 Red

HCHO-NOx (130%, 100%, 70% photolysis)

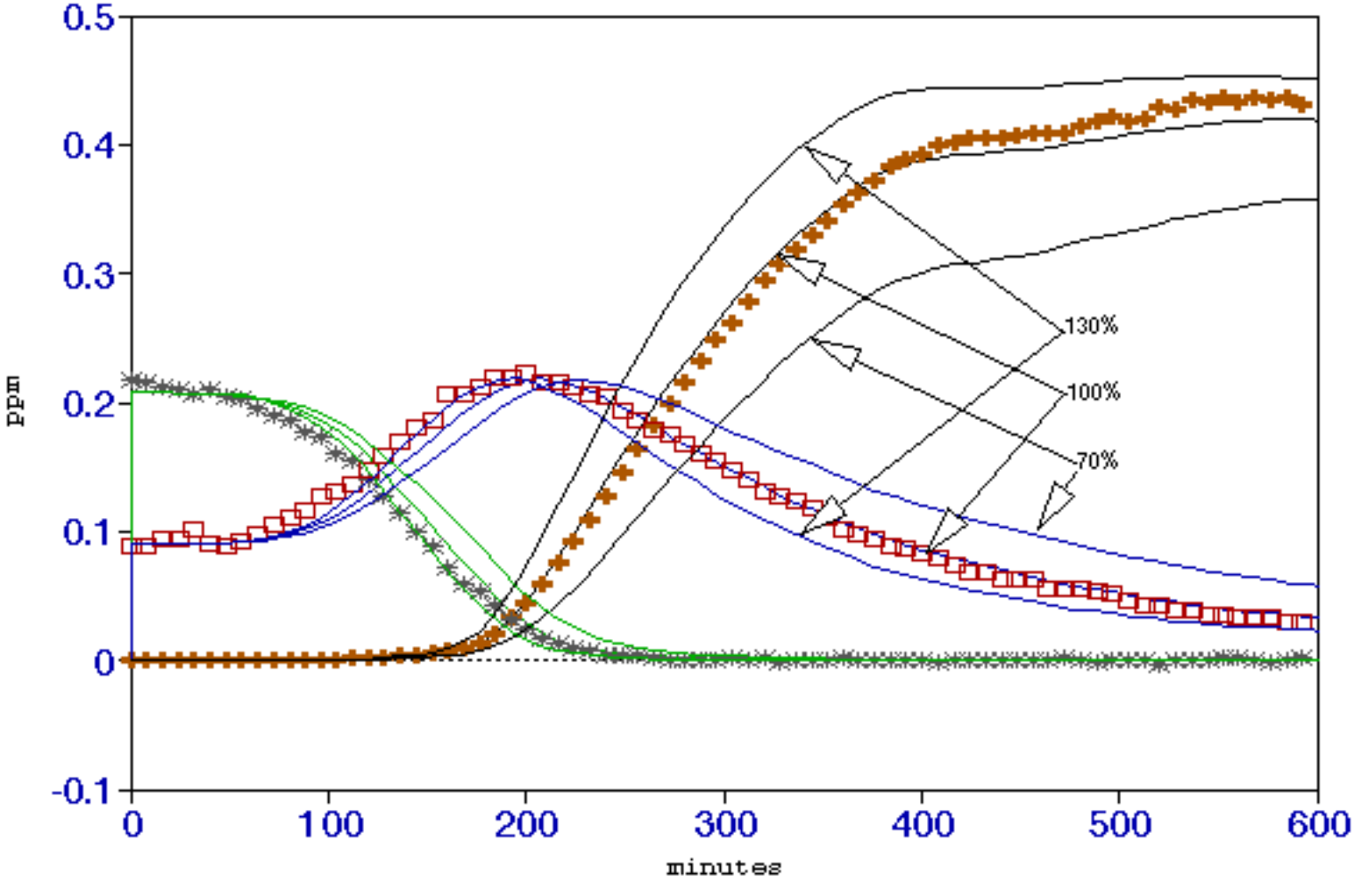

Figure 5b: July 15, 1988 Red

HCHO-NOx

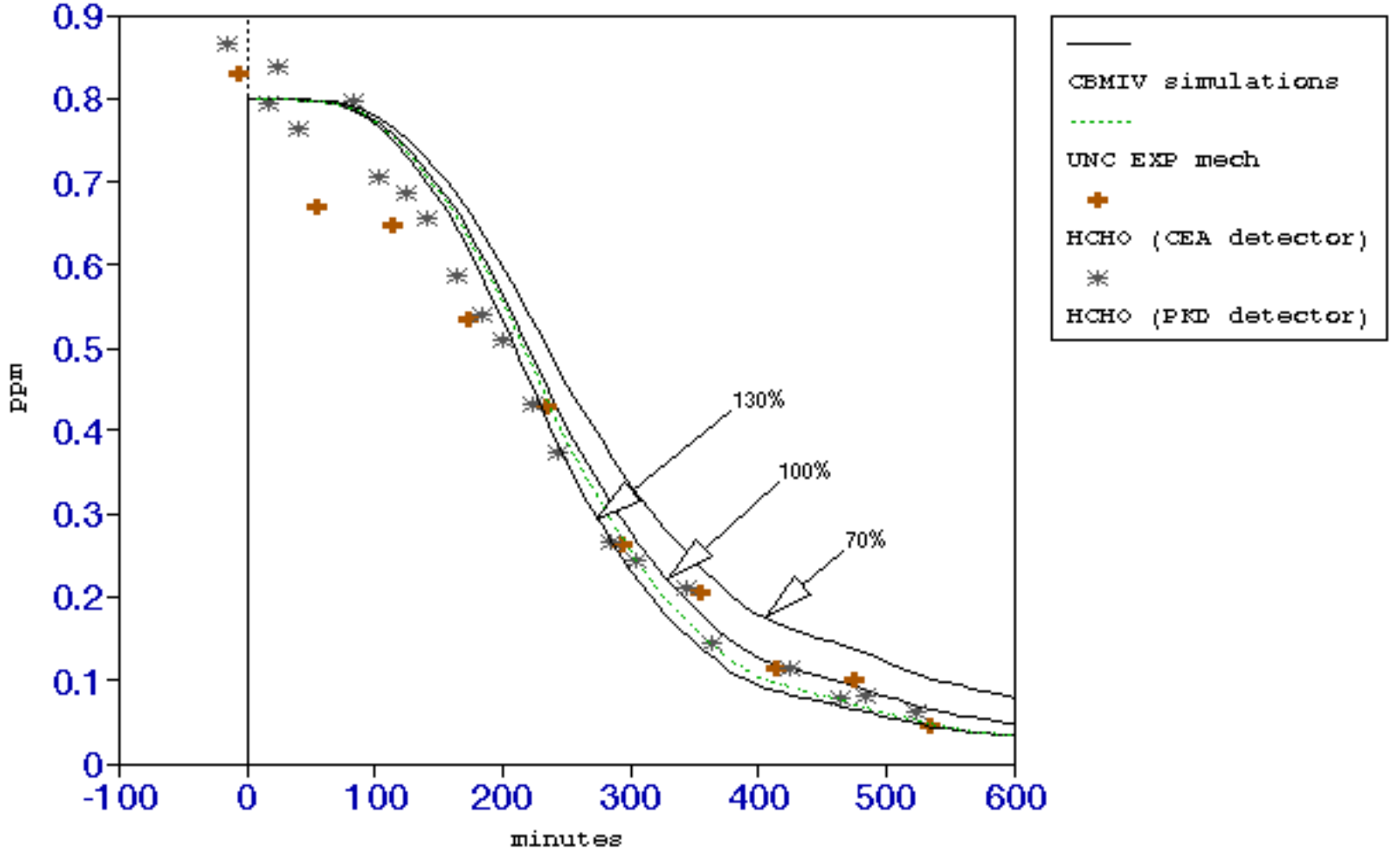

Figure 6: August 16, 1988 Red

HCHO-NOx (60 ppb vs 200 ppb BVOC)

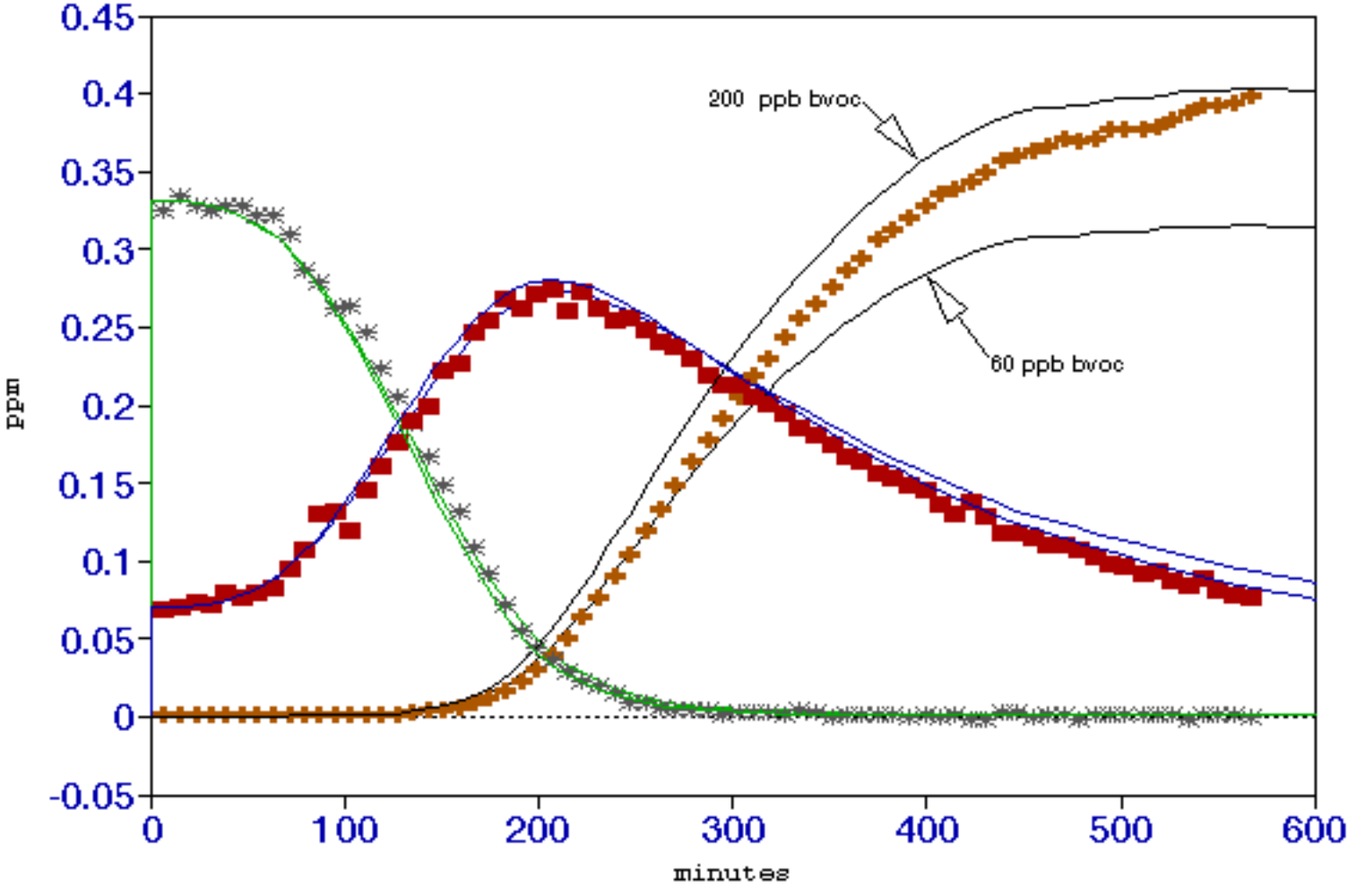

Figure 7: July 8, 1986 Blue

HCHO-NOx

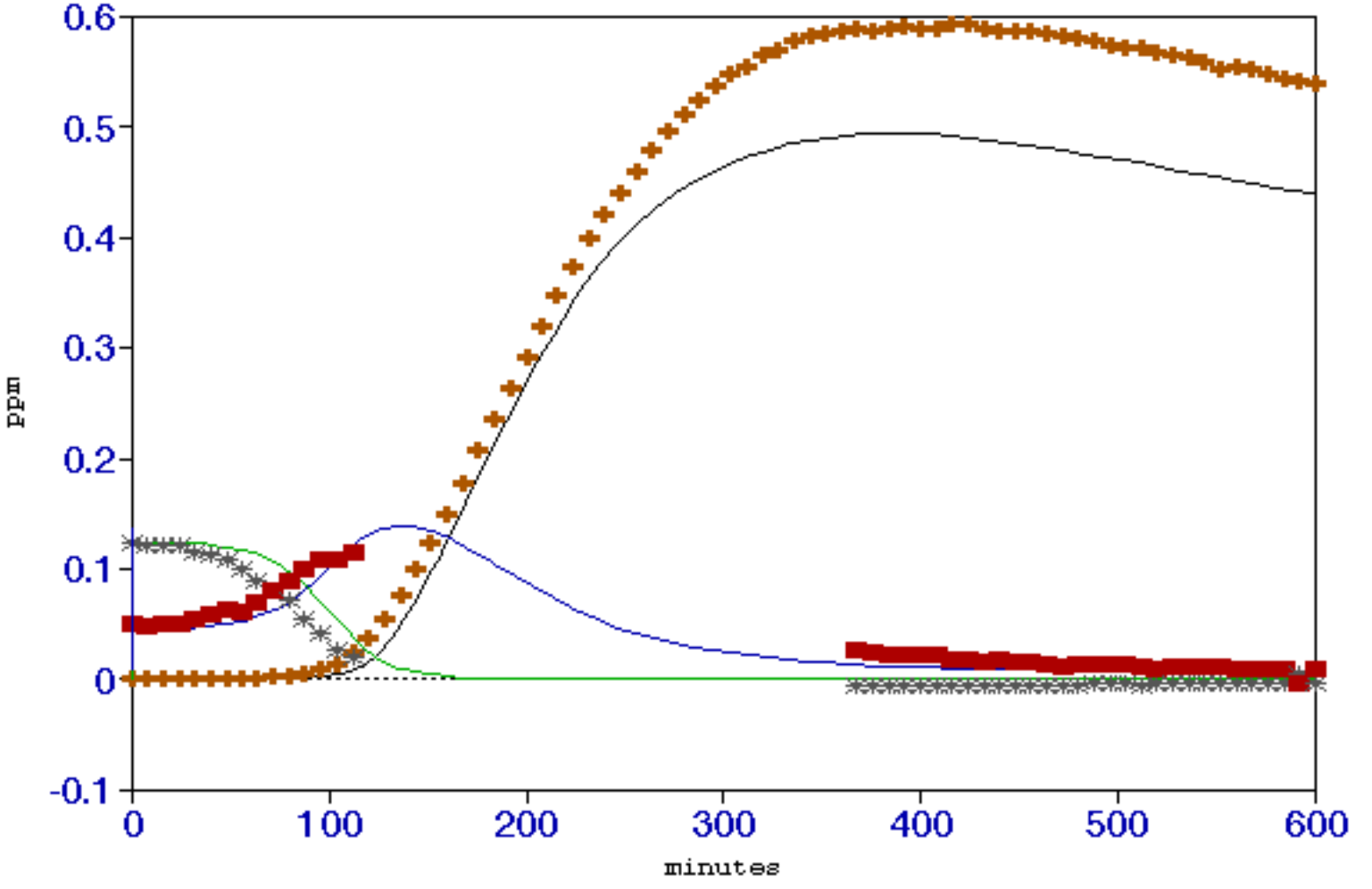

Figure 8: July 8, 1986 Red

HCHO-NOx (120% photolysis test)

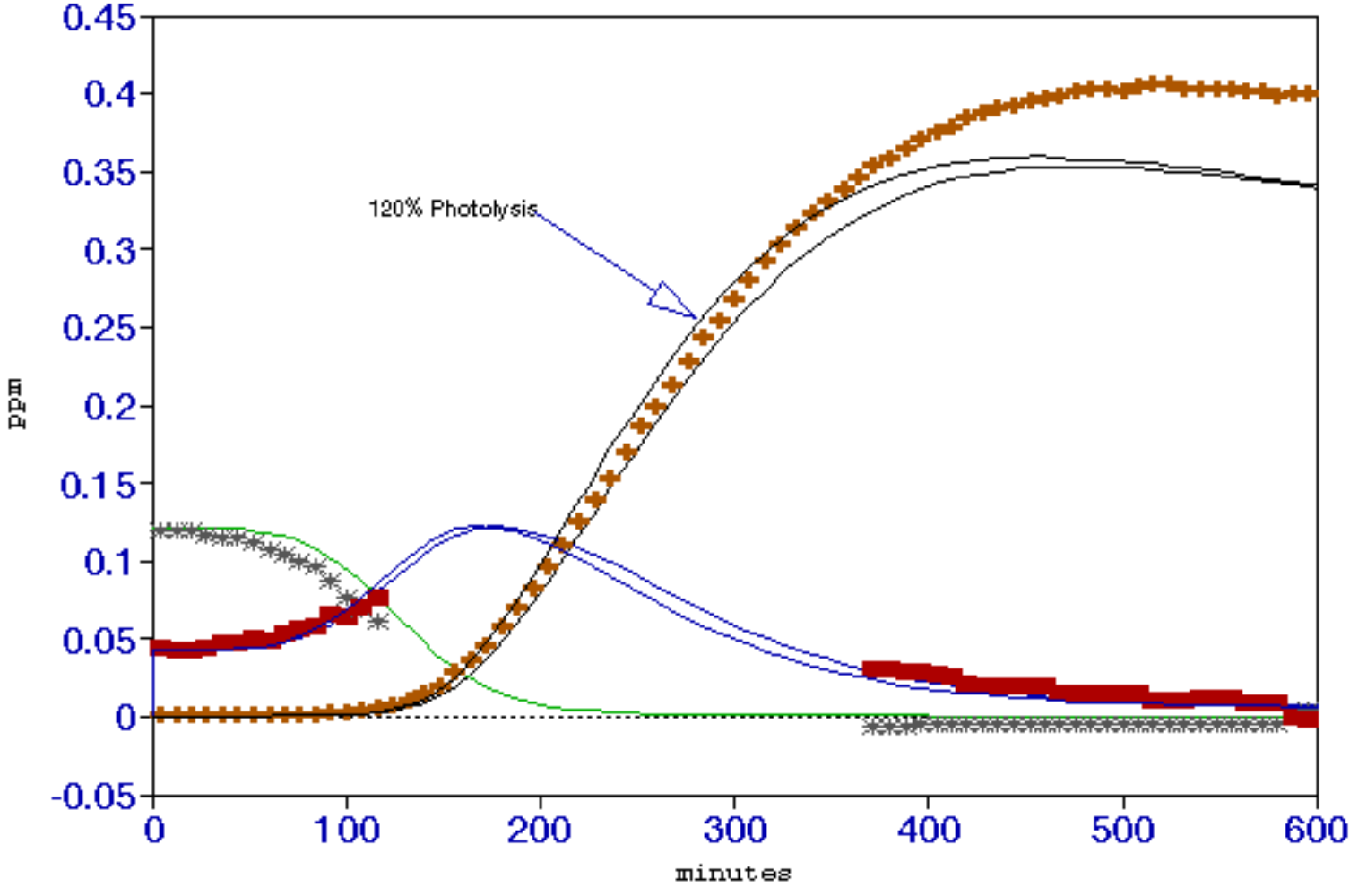

Figure 9: July 15, 1988 Blue

HCHO-NOx

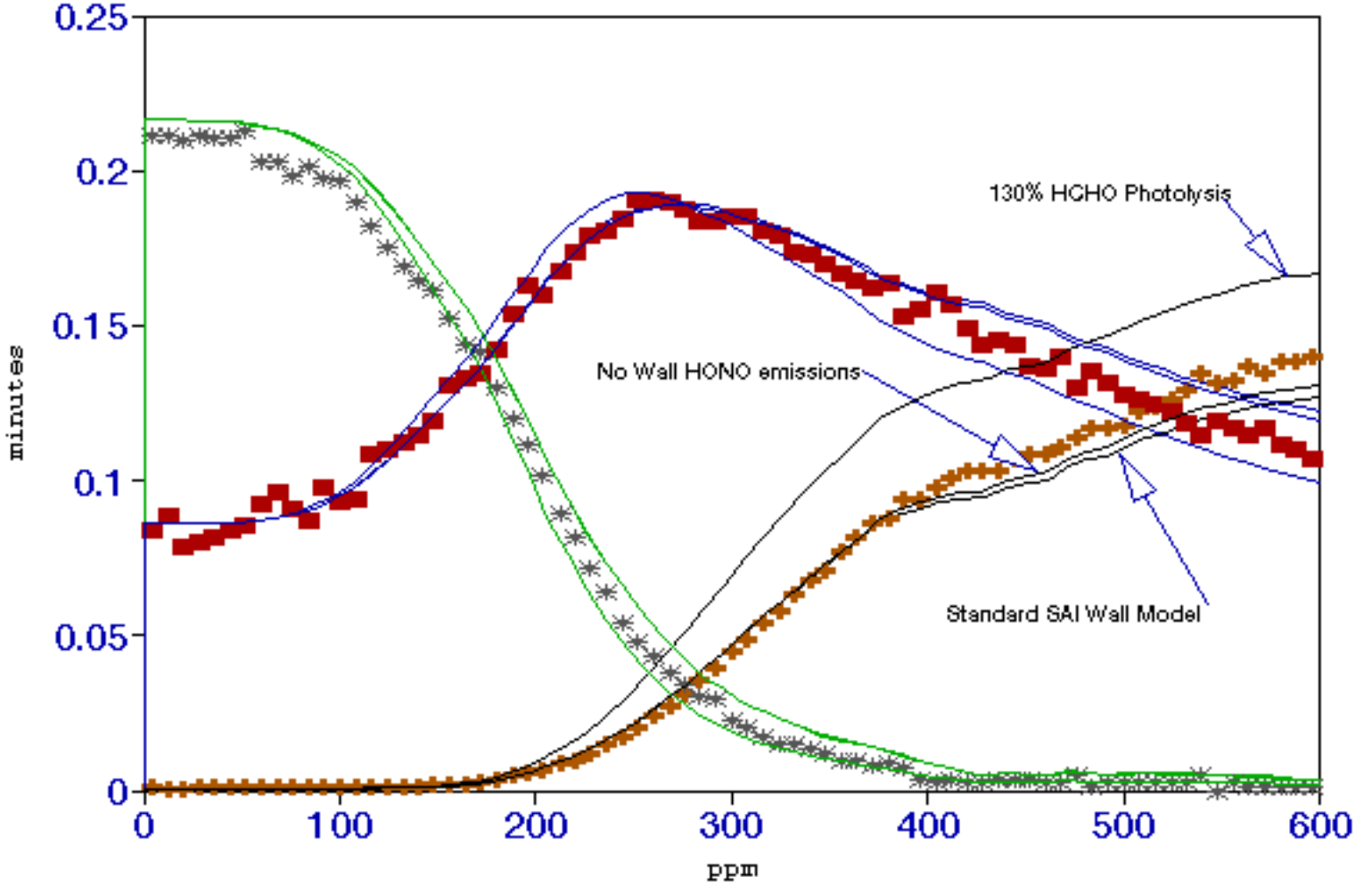

Figure 10a: September 23, 1996 Blue

HCHO-NOx (80%, 100%, 120% photolysis)

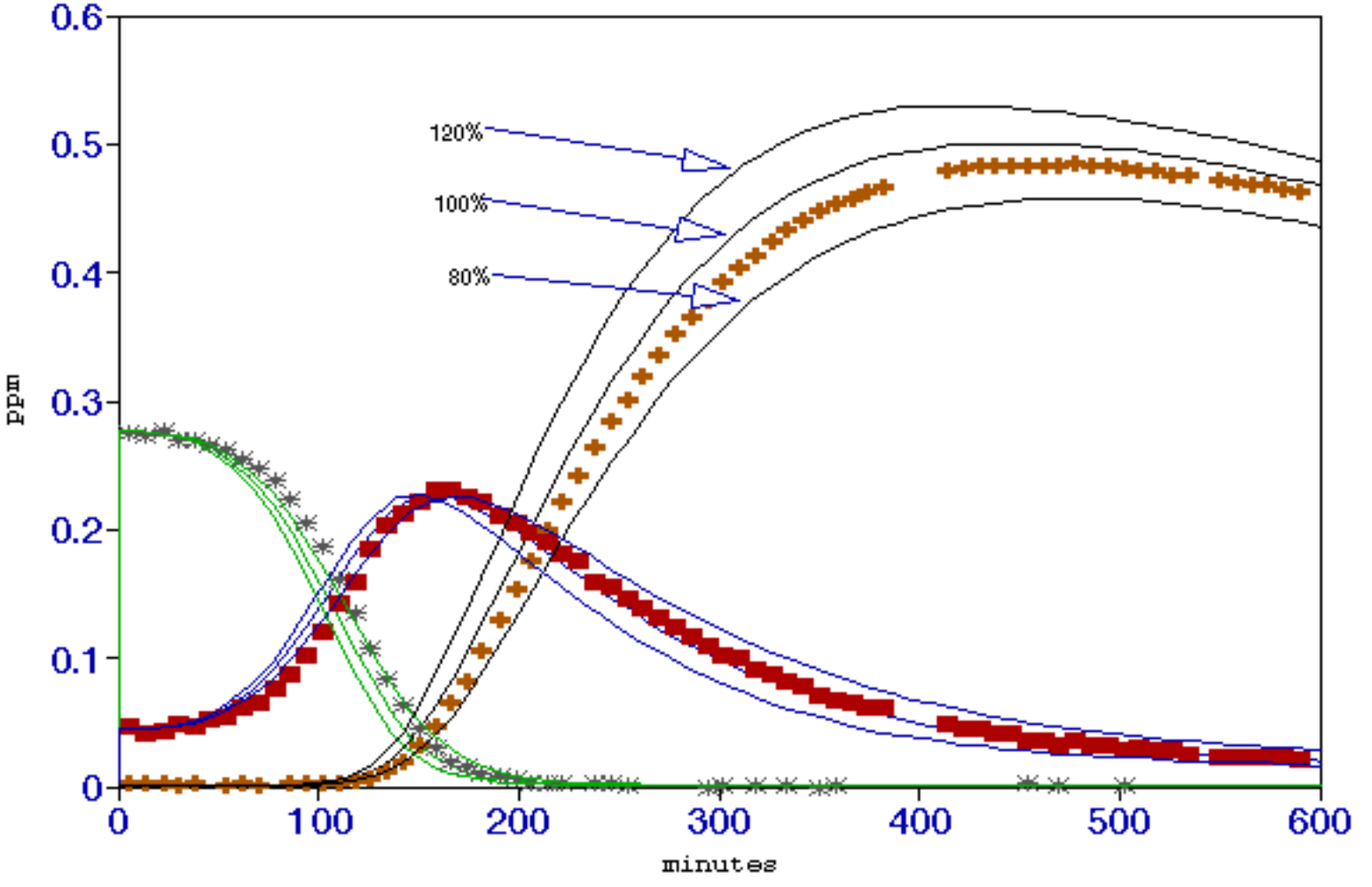

Figure 10b: September 23, 1996 Blue

HCHO-NOx (PKD HCHO instrument)

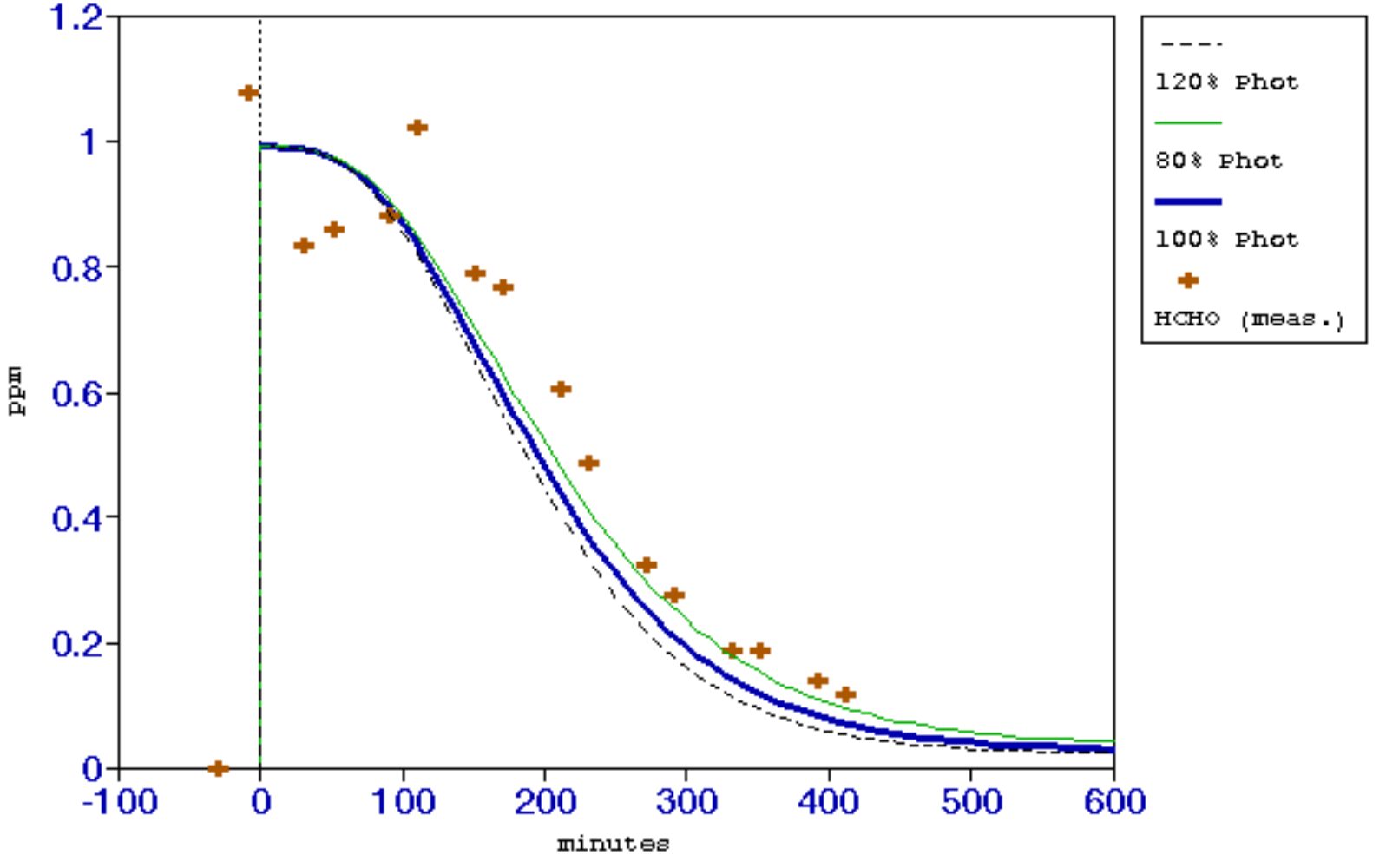

Figure 11a: September 23, 1996 Red
HCHO-NOx

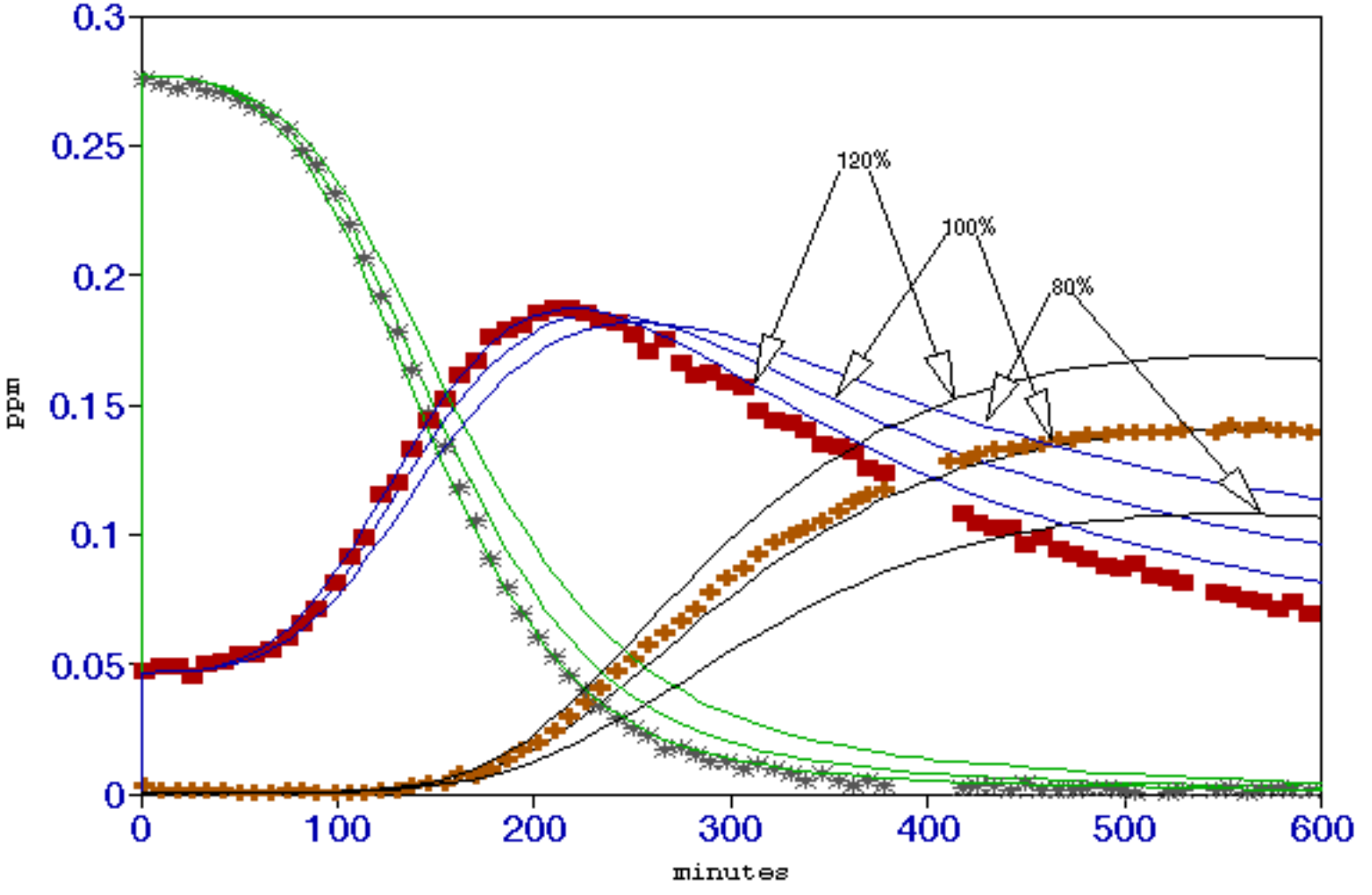

Figure 11b: September 23, 1996 Red

HCHO-NOx

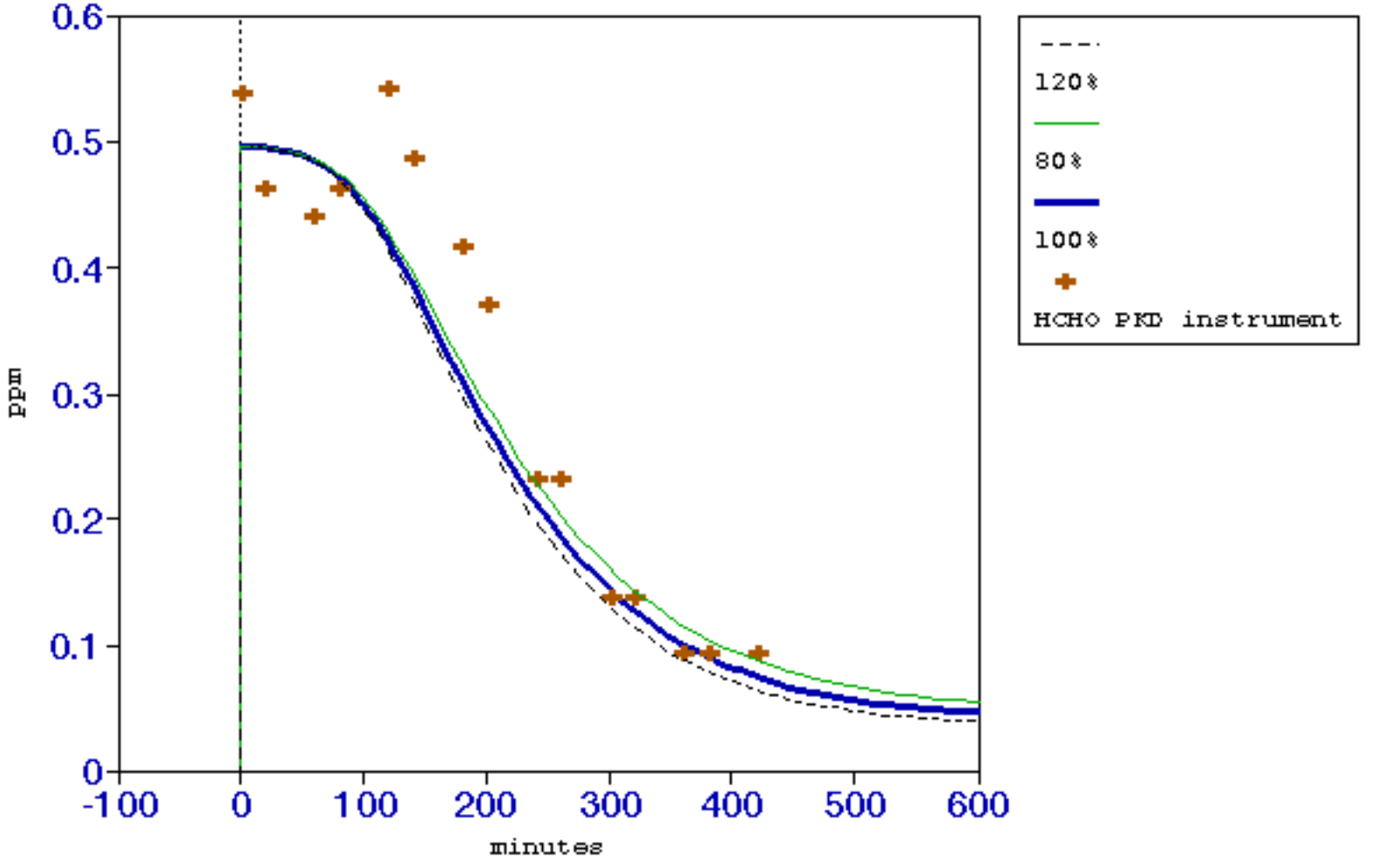

Figure 12a: August 24, 1982 Blue

Acetaldehyde-NOx

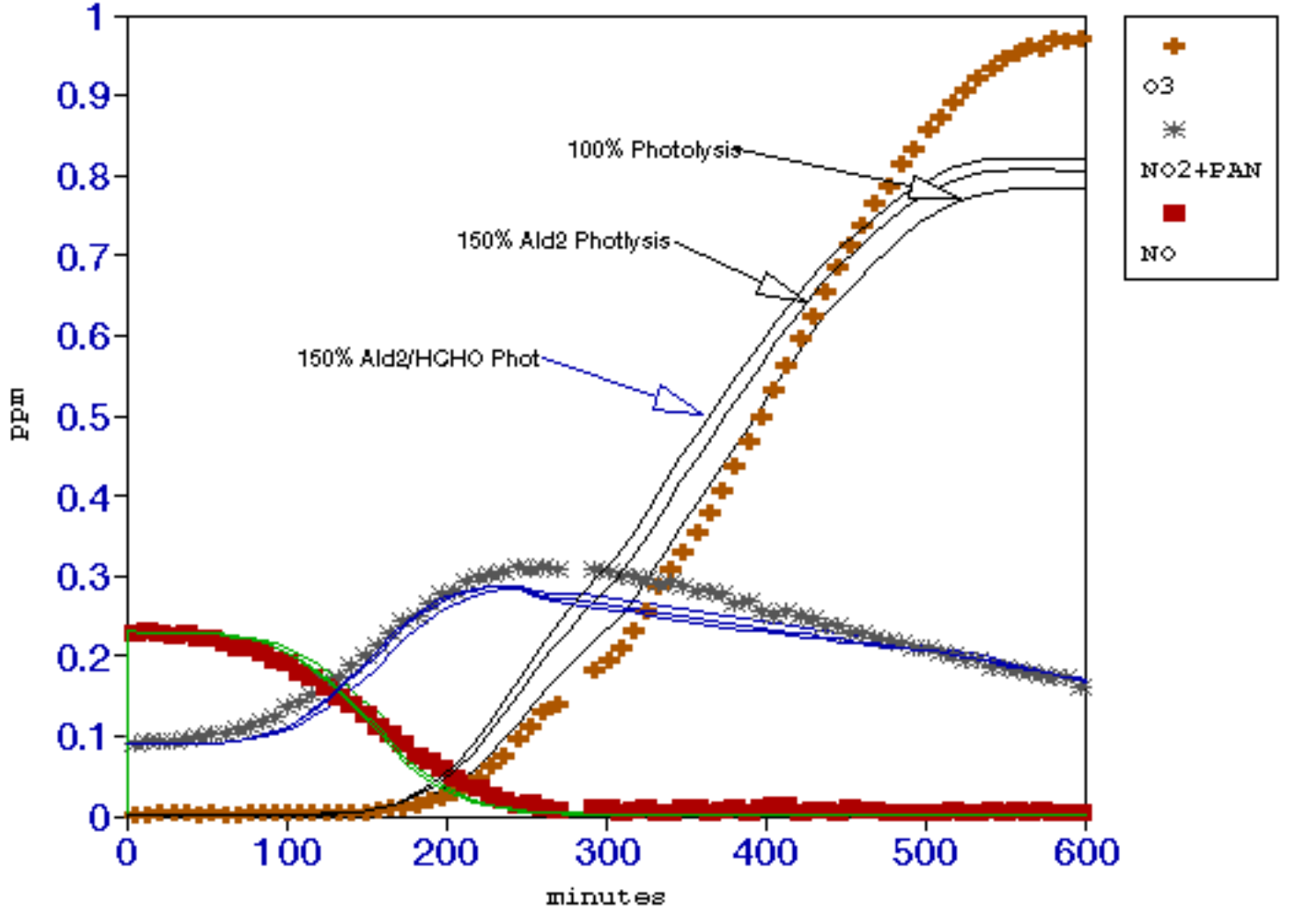

Figure 12b: August 24, 1982 Blue

Acetaldehyde-NOx (50%, 100% phot)

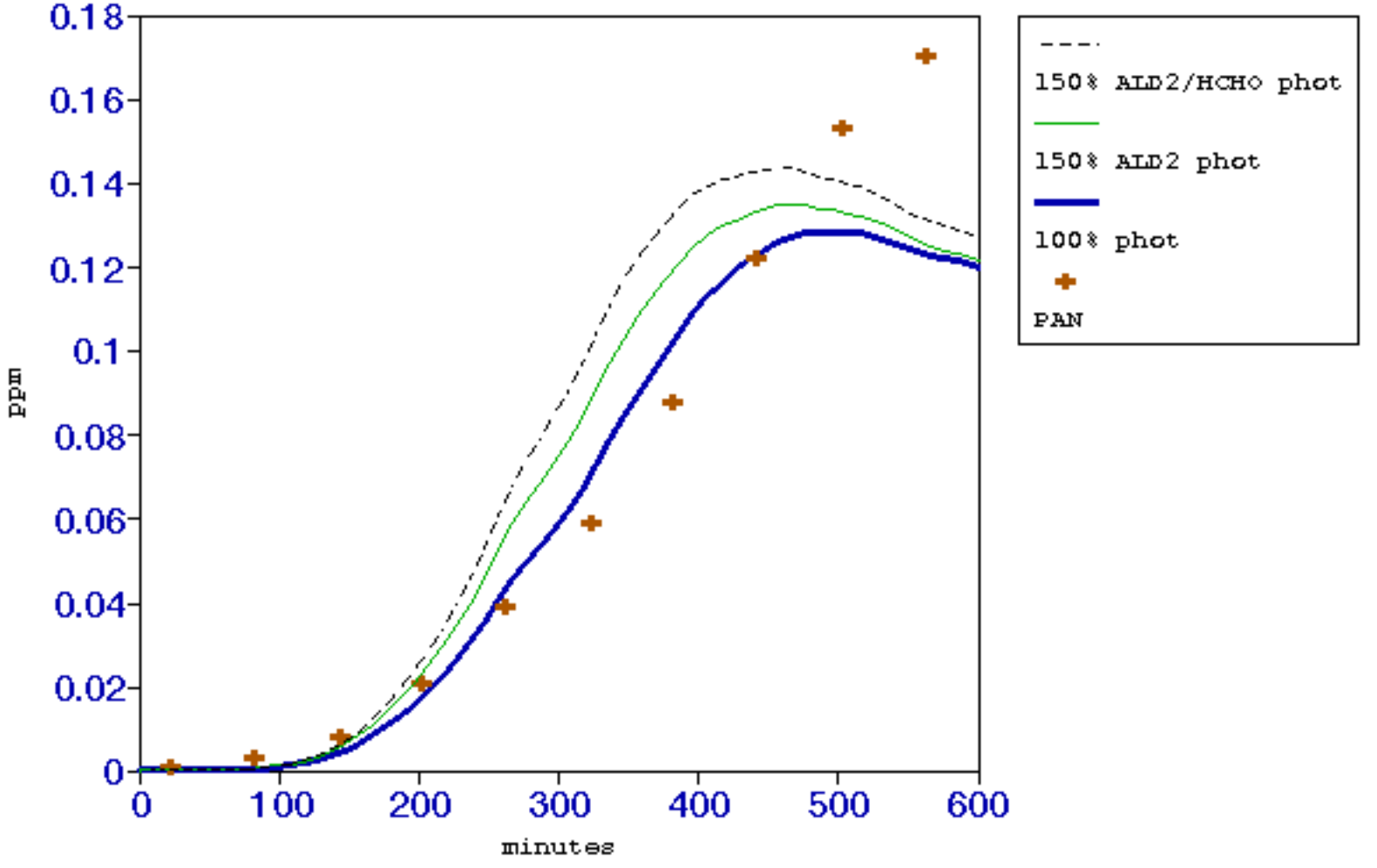

Figure 13a: August 24, 1982 Red

Propionald-NOx (70%, 100%, 150% phot)

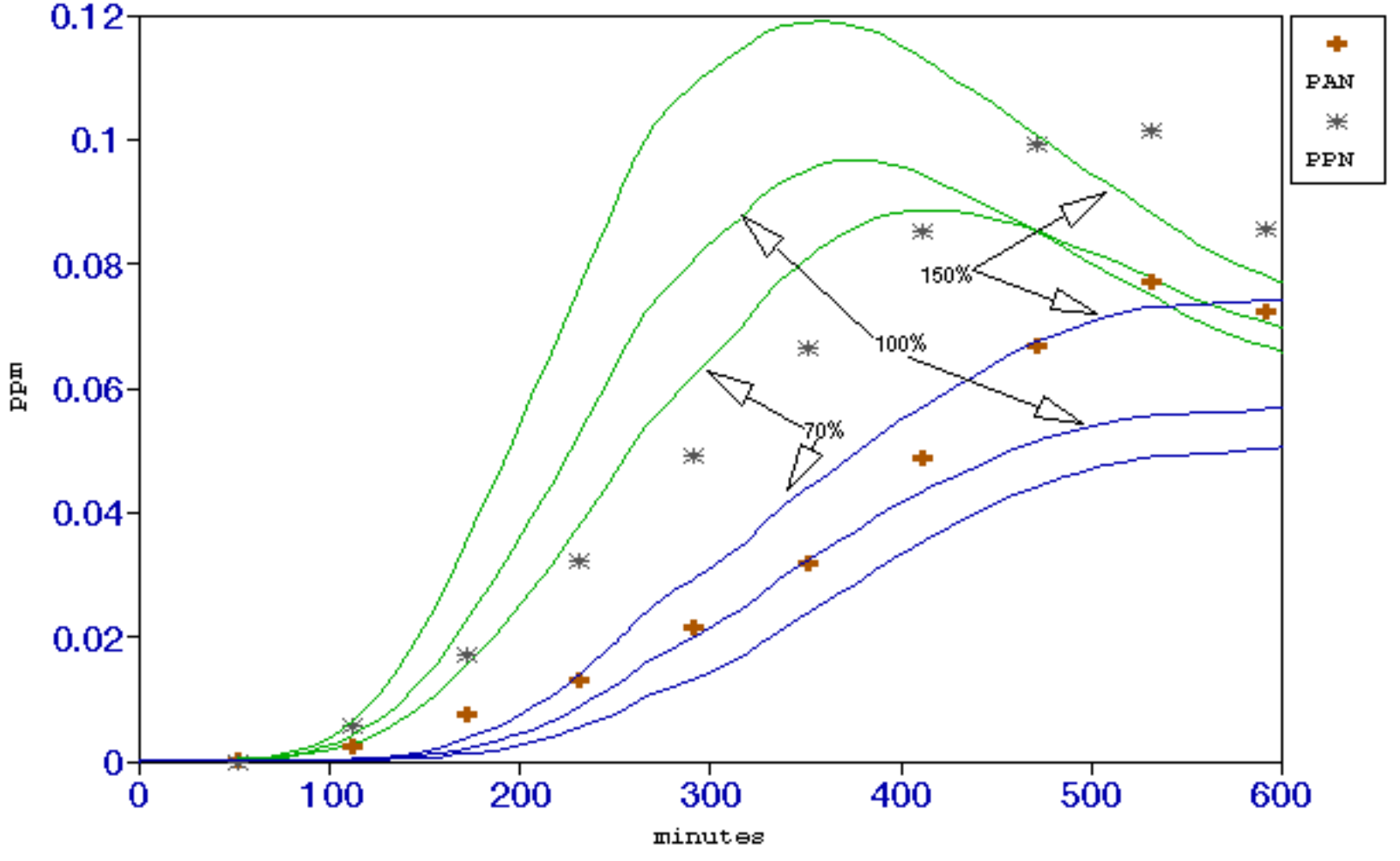

Figure 13b: August 24, 1982 Red

Propald-NOx (all ald photolysis varied)

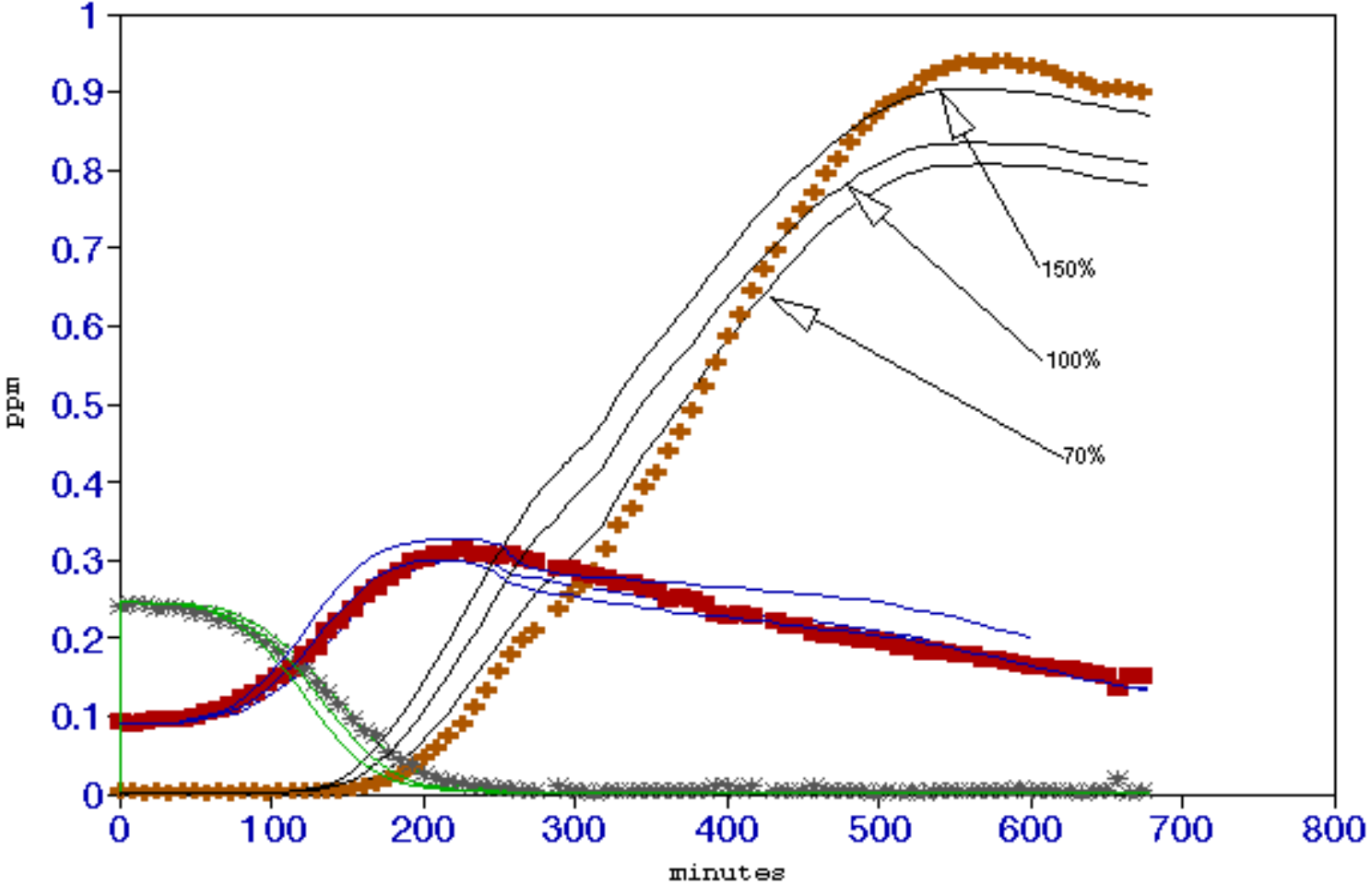

Figure 14a: June 14, 1982 Blue

Propionald-NOx

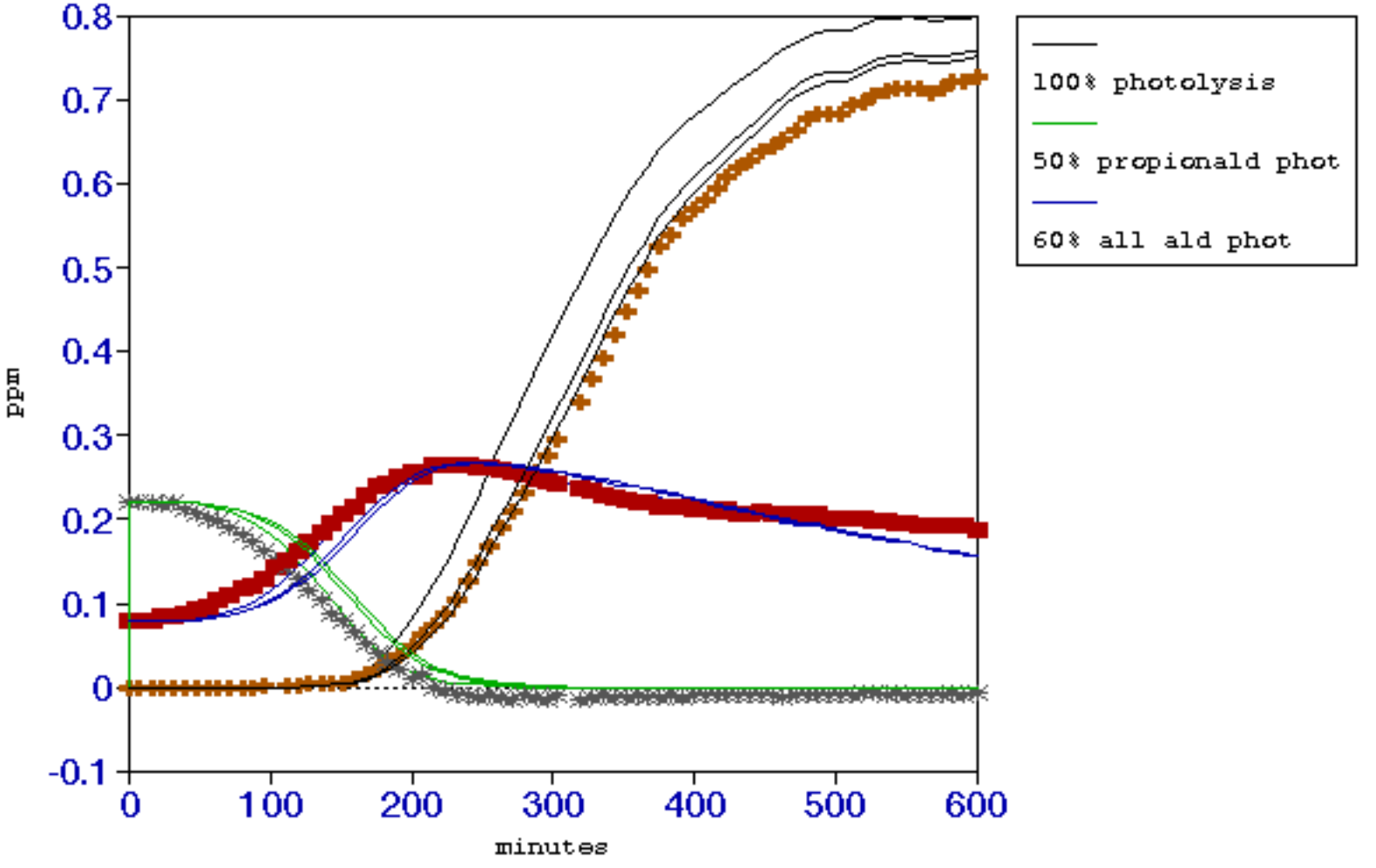

Figure 14b: June 14, 1982 Blue

Propionaldehyde-NOx

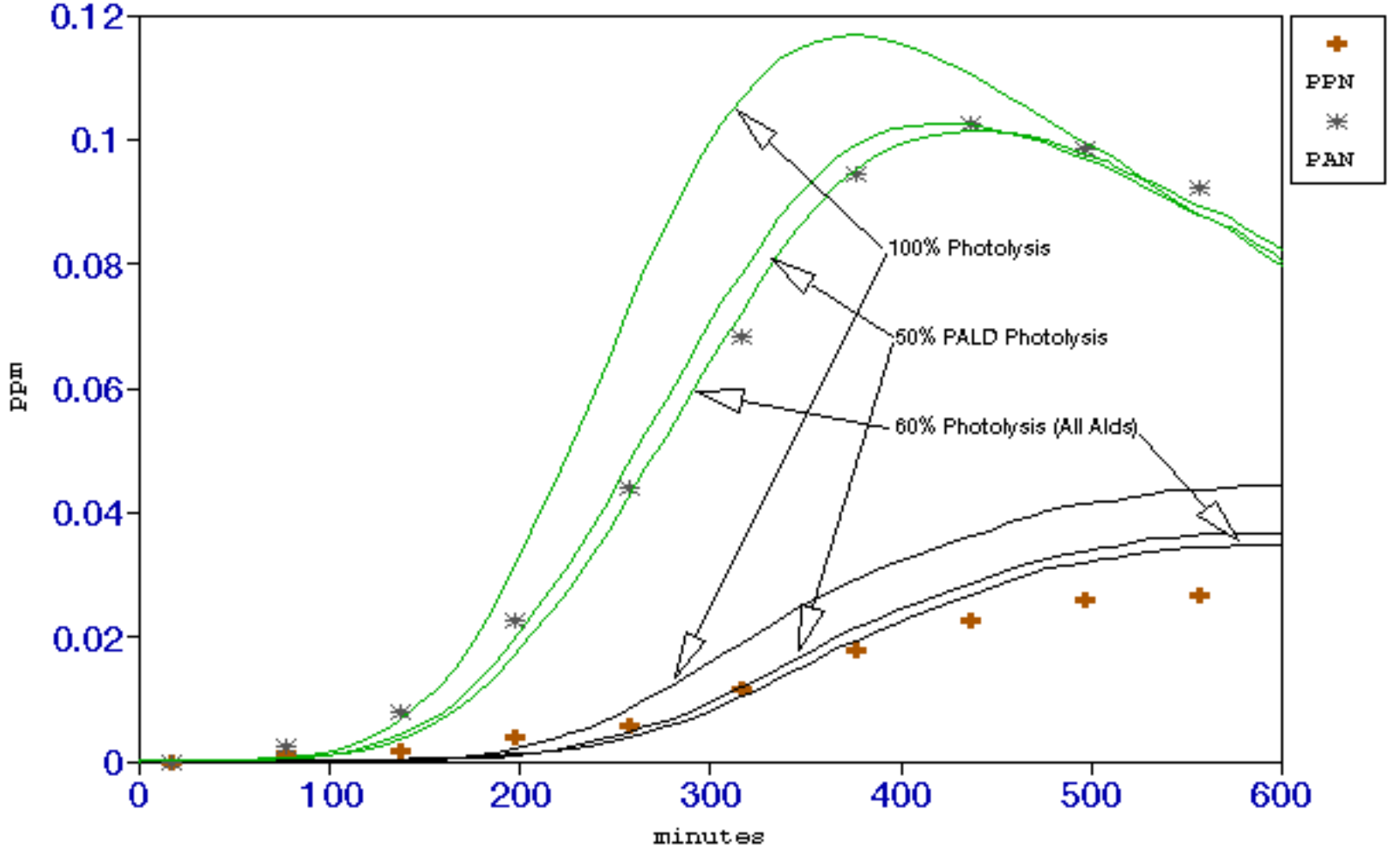

Figure 15a: June 14, 1982 Red Acetaldehyde-NOx

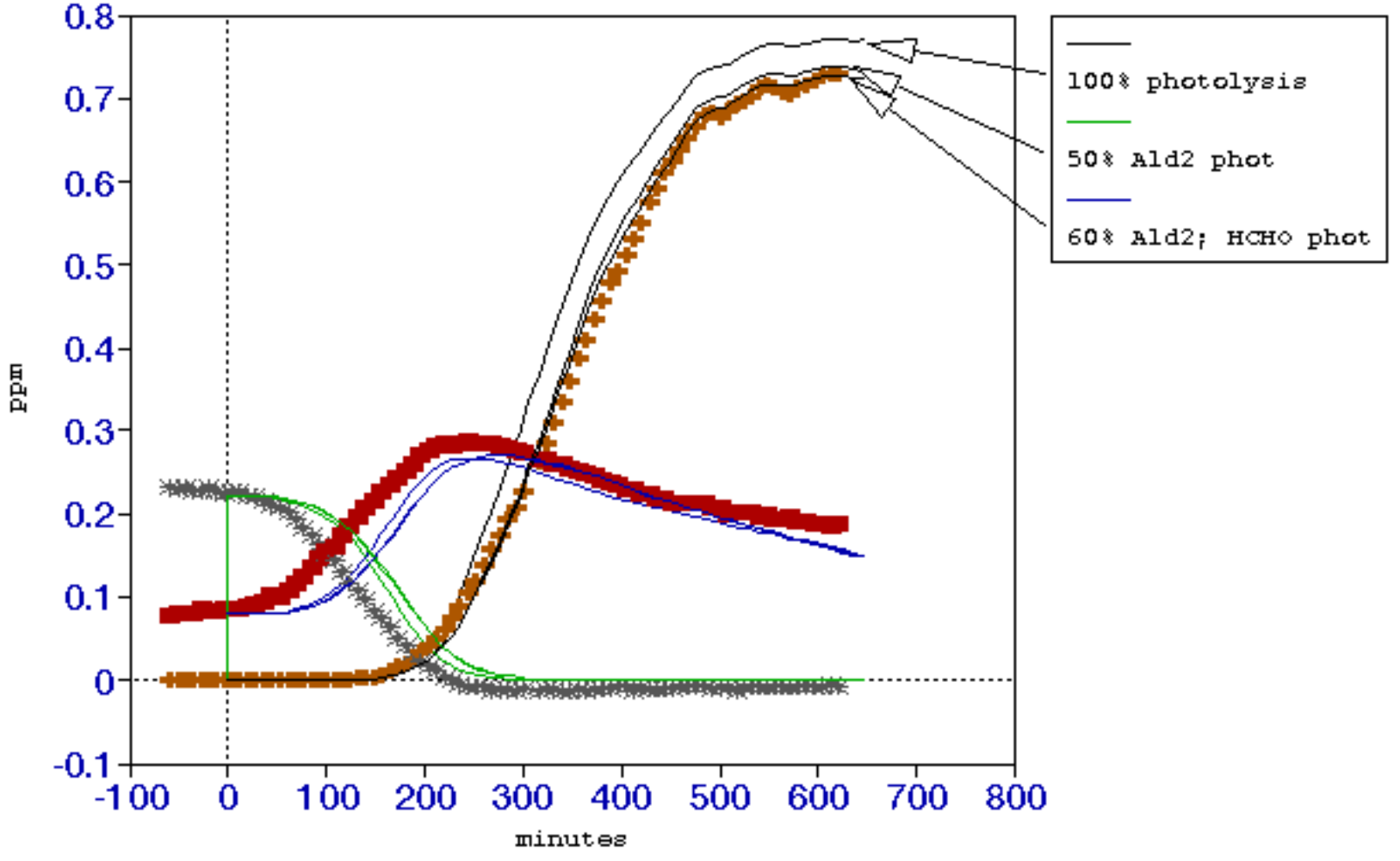

Figure 15b: June 14, 1982 Red

Acetaldehyde-NOx

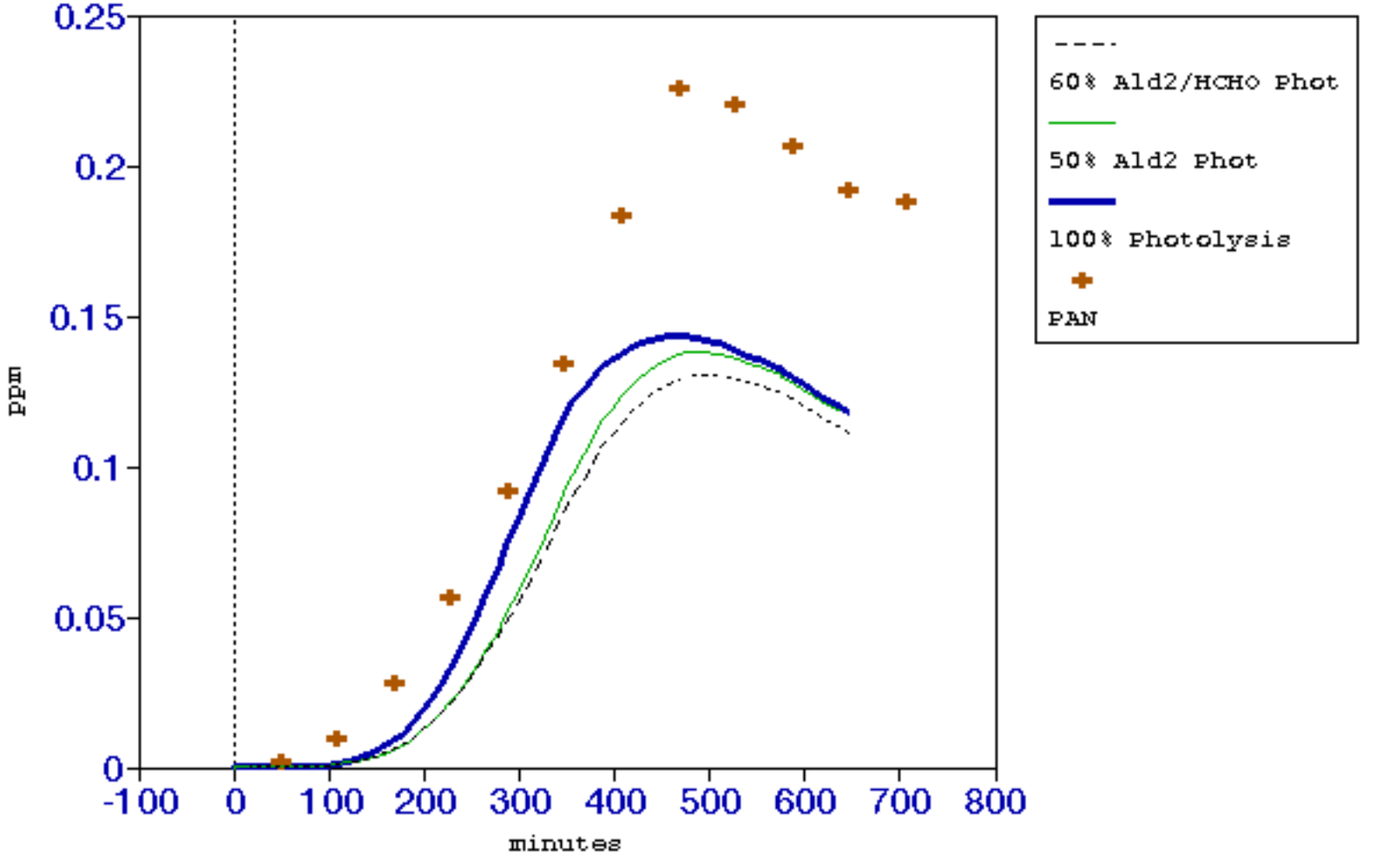

Figure 16a: October 4, 1996 Blue

Propionaldehyde/acetaldehyde-NOx

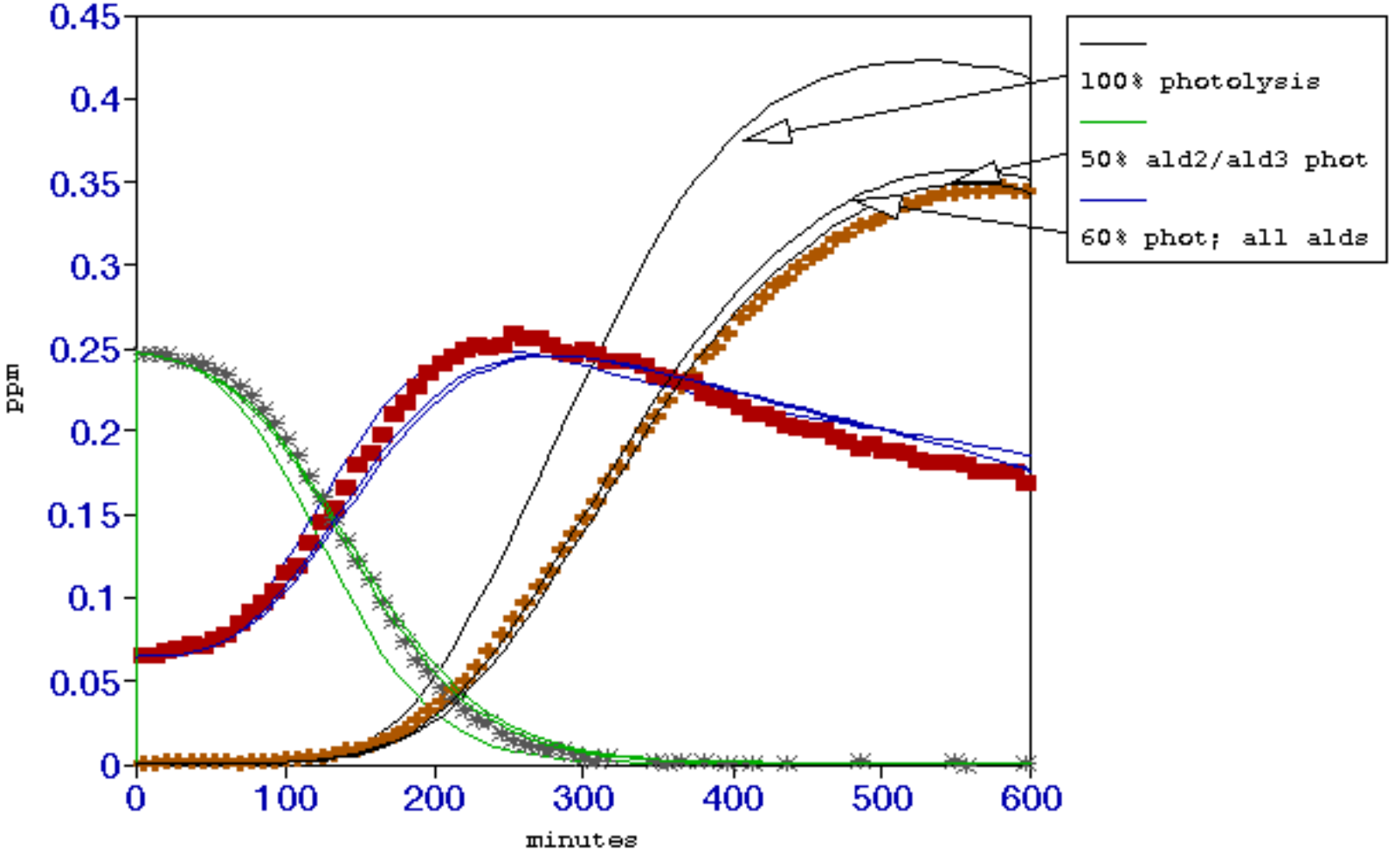

Figure 16b: October 4, 1996 Blue

Propionaldehyde/acetaldehyde-NOx

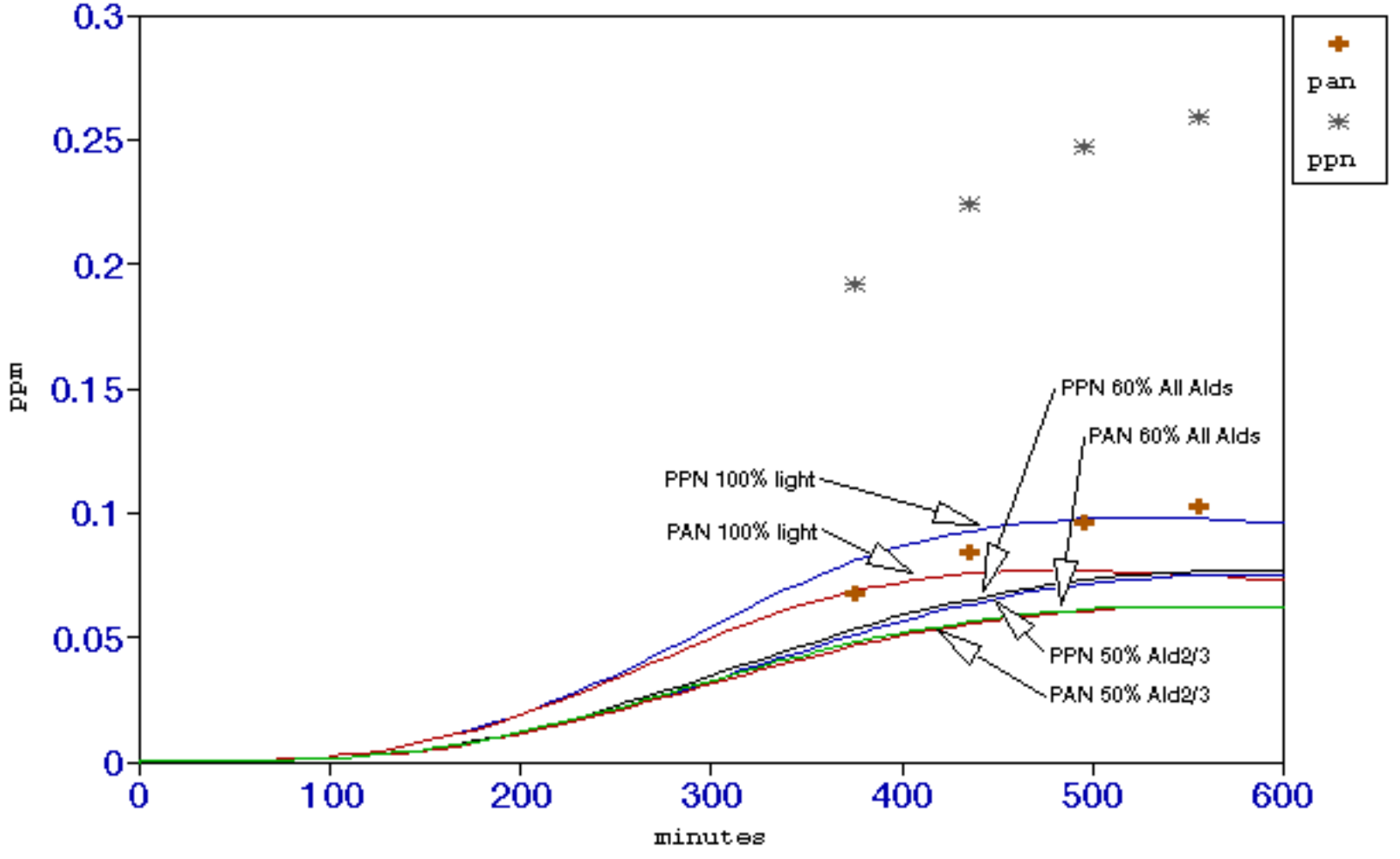

Figure 16c: October 4, 1996 Blue

Propionaldehyde/acetaldehyde-NOx

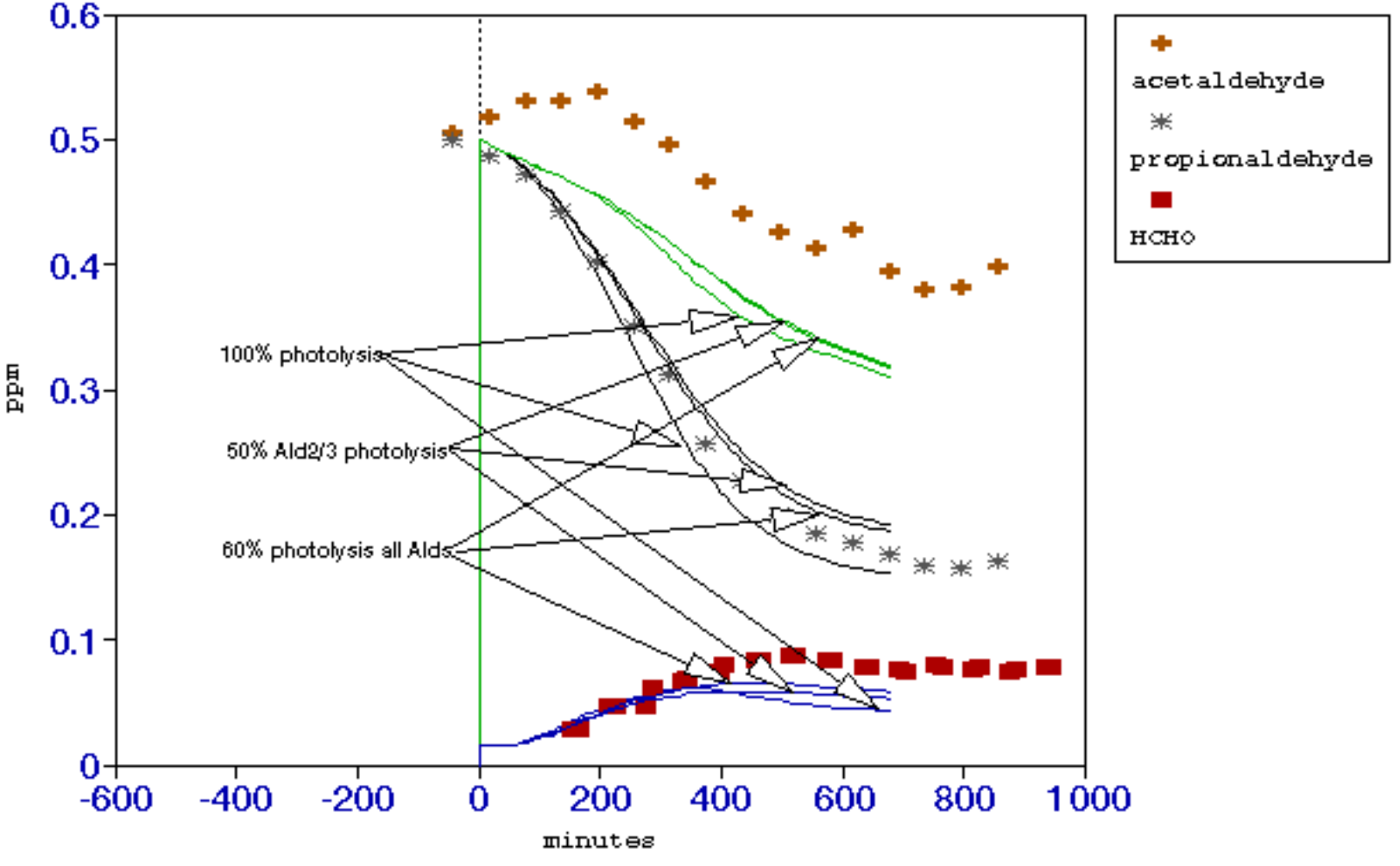

Figure 17a: October 4, 1996 Red

Acetaldehyde-NOx

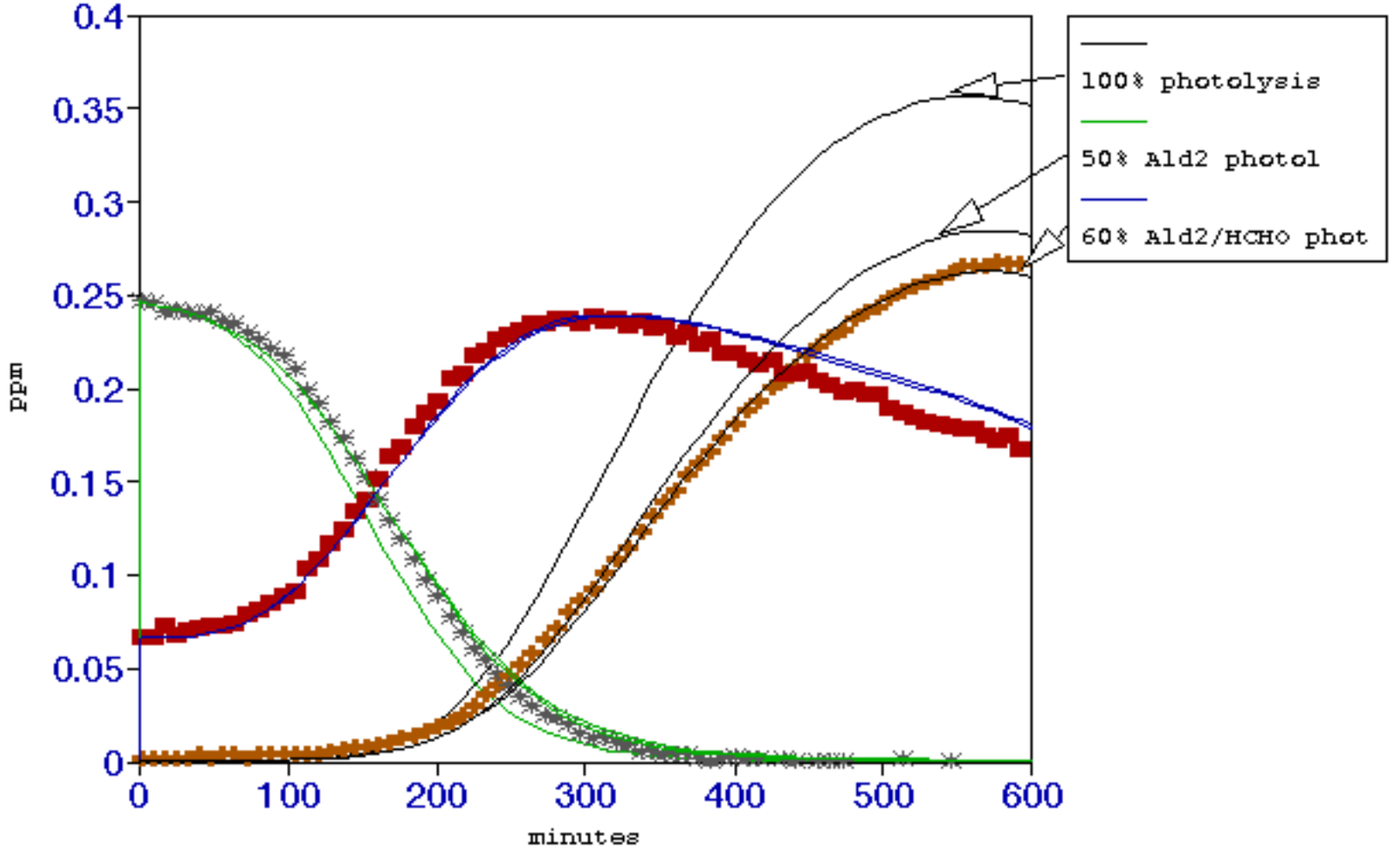

Figure 17b: October 4, 1996 Red

Acetaldehyde-NOx

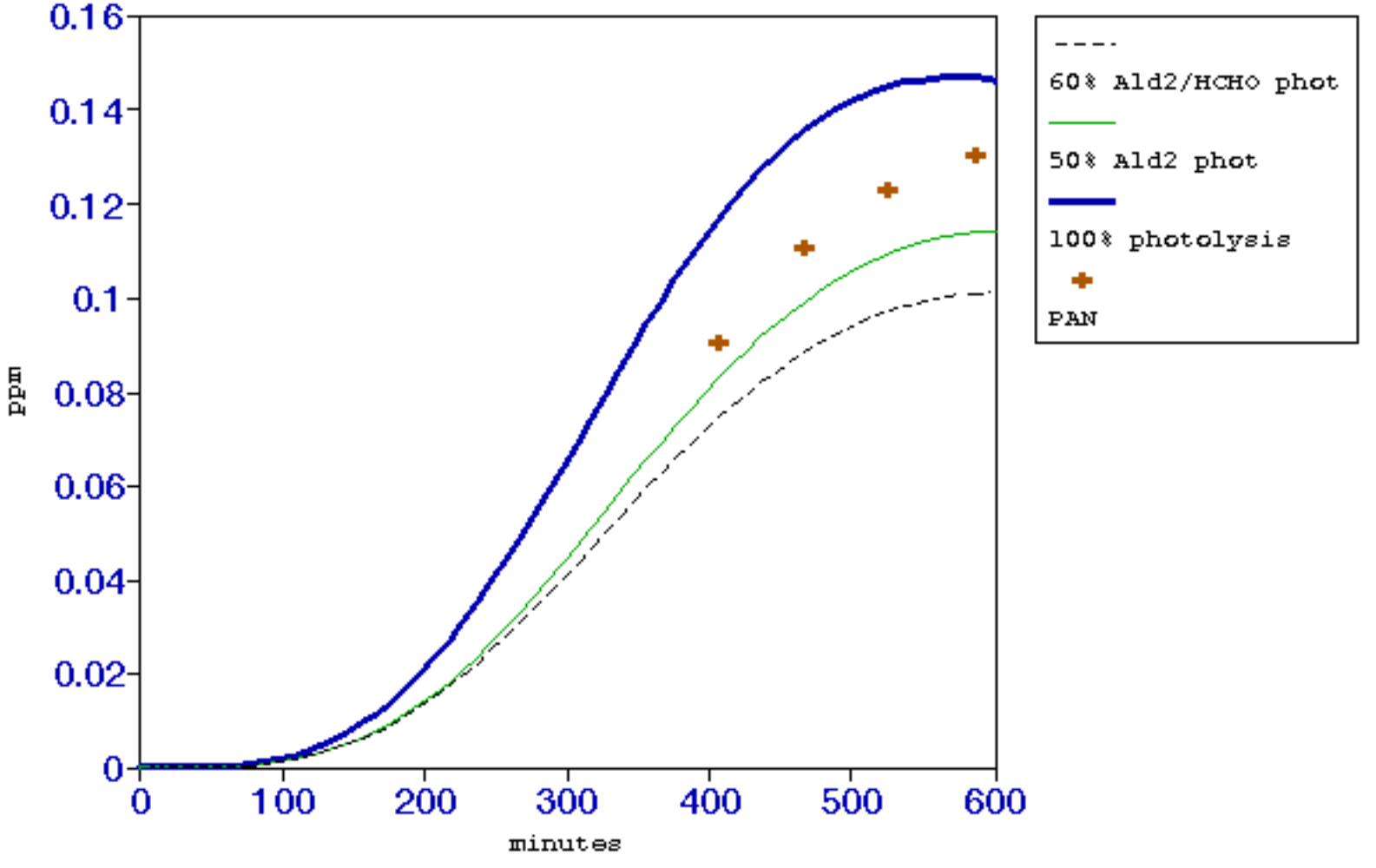

Figure 17c: October 4, 1996 Red

Acetaldehyde-NOx

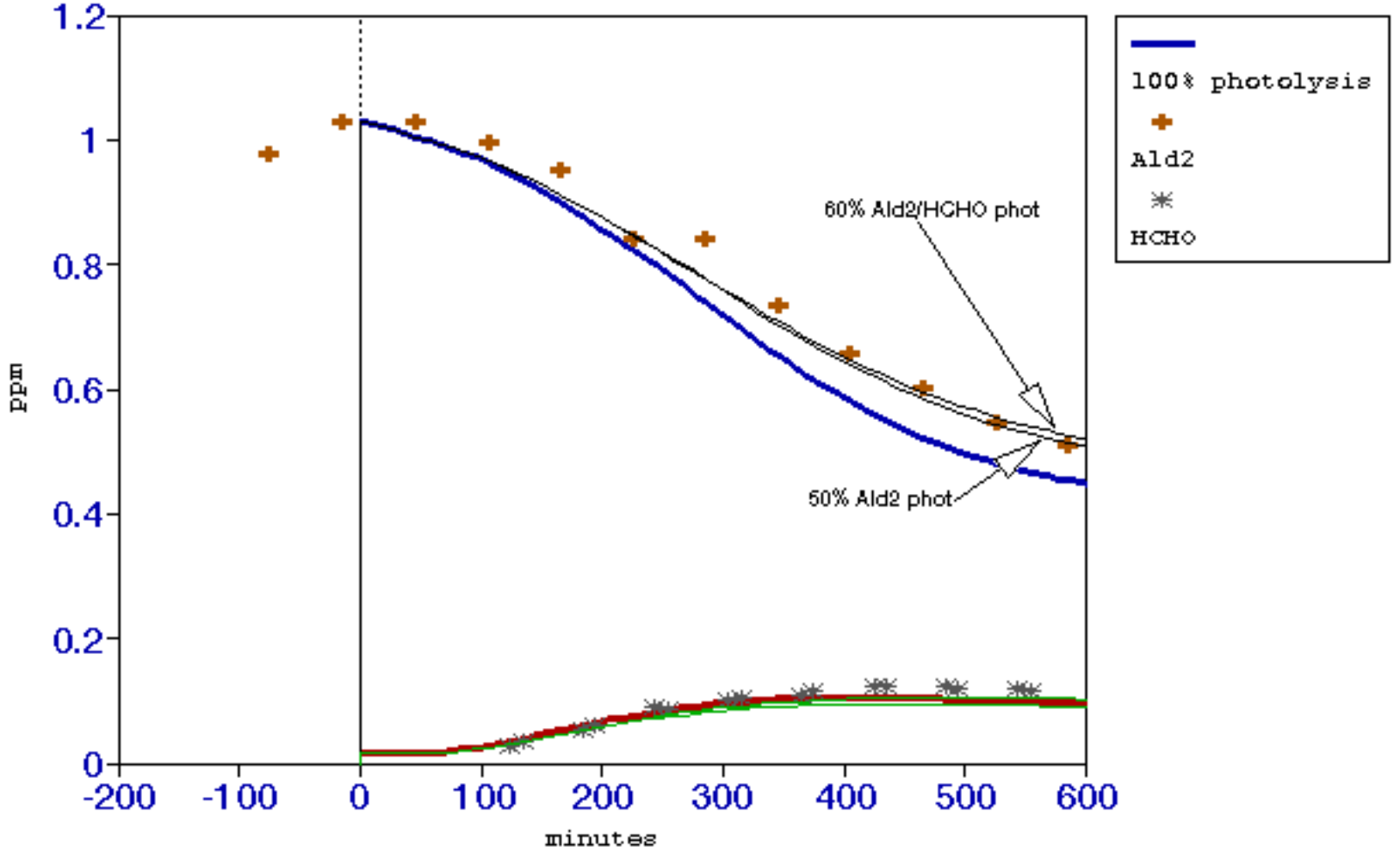

APPENDIX B

Task 2 Report

EFFECT OF CHEMICAL MECHANISM UNCERTAINTY ON AIRSHED MODEL RESULTS

January 17, 1997

Prepared for

California Air Resources Board
Technical Support Division
2020 L Street
Sacramento, California 95814

Prepared by

Gary Z. Whitten
Dongfen Gao

Systems Applications International, Inc.
101 Lucas Valley Road
San Rafael, California 94903
(415) 507-7100

and

James P. Killus
2305 Helena Court
Pinole, California 94903
(510) 222-8487

Task 2: Development of Alternative Chemical Mechanisms

The final phase of this task calls for a document proposing alternative mechanisms for further examination. This document is to be reviewed by ARB staff and a panel of independent reviewers. We have used an approach to developing alternative mechanisms that is based on high or low radical fluxes. In this report examples of the applications of this approach are presented for review.

The high and low radical approach was used to best meet the goals of this project. Simply stated these goals call for the development and testing of alternative versions of the Carbon Bond Mechanism version IV (CB-IV) that might generate different control strategy results in a grid model like the Urban Airshed Model (UAM). No new mechanism is to be developed in this project. These alternative versions of chemistry should simulate (within the limits of experimental uncertainty) a smog chamber database similar to that originally used for the CB-IV. Any changes proposed to critical parameters or condensation approaches should also fall within limits of experimental uncertainty. Thus, the overall purpose of this contract is not to develop a new chemical mechanism for use in the UAM, but merely to determine a range of uncertainty (due to uncertainties in the chemical mechanism) about control strategy estimates that might be based on the present CB-IV.

Prior to beginning this project two alternative versions of CB-IV were recently developed and implemented into special versions of the UAM. For one of these, known as UAM-Tox, the modified mechanism (CB-Tox) was never tested against a smog chamber database because the CB-Tox was considered only as a re-expansion for some of the condensation found in the CB-IV. The other, known as UAM-VO, was developed for use by the Ozone Transport Assessment Group (OTAG). The VO version is actually an update to the isoprene part of the standard CB-IV and this version was tested against 12 isoprene/NOx experiments from the University of North Carolina (UNC) outdoor smog chamber facility. The updated isoprene reaction set is a Carbon Bond translation of the condensed isoprene reaction set recently developed by W. Carter (1996). Surprisingly, this new reaction set provided simulations of the 12 UNC isoprene experiments that were virtually identical in quality to the original CB-IV isoprene reactions, but Maximum Incremental Reactivity (MIR) estimates for isoprene and UAM simulations involving isoprene were significantly different when the new isoprene chemistry was compared to the old isoprene chemistry. Changing UAM estimates while still fitting the isoprene smog chamber database is possible because a lower radical flux occurs in the updated isoprene chemistry than in the original CB-IV.

The Tox version of CB-IV chemistry was primarily intended to isolate the species acetaldehyde. In the standard CB-IV acetaldehyde is used as a surrogate for internal olefins and higher aldehydes. The CB-Tox version uses new CB species for internal olefins and aldehydes larger than acetaldehyde. When originally expanded the CB-Tox mechanism was tested in box model (OZIPM) simulations and provided virtually identical results compared to the standard CB-IV. However, it later came to our attention that one study of propionaldehyde photolysis quantum yields of Heicklin et al. (1986)

indicates that the photolysis of propionaldehyde may be as much as 5 times greater than acetaldehyde. In order for acetaldehyde to function as a suitable surrogate for all aldehydes heavier than formaldehyde, the photolysis rate of acetaldehyde used in the UAM should be a suitable average of these higher aldehydes. However, we believe that more evidence should be considered than a single quantum yield study of only one higher aldehyde, before concluding that an update to the CB-IV is appropriate. Nevertheless, these higher aldehyde photolysis rates offer an example of an uncertainty bound that will be included in this project.

It has been established that using higher aldehyde photolysis rates produce significant differences in control strategy estimates for both VOC and NOx control when VOC-to-NOx ratios are low or when control strategies involve changing the VOC-to-NOx ratio from a high ratio to a lower ratio. These effects can be attributed to higher radical fluxes. However, we do not yet know what impact these higher radical fluxes will have on the acceptability of simulations of the smog chamber database. We expect that using higher radical sink rates at the same time as using higher photolysis rates should improve the acceptability of the smog chamber simulations, but still maintain higher radical fluxes and, in turn, still provide different control strategy estimates. At any rate our opinion is that the best bet to produce changes in UAM control estimates, while still simulating a smog chamber database, will be alternative mechanisms based on higher or lower radical fluxes than the standard CB-IV. We know that higher fluxes definitely worked for the isoprene example and we feel confident that the CB-Tox example may also work even if some adjustment to radical sink rates may be necessary to simulate the smog chamber data. That is, we believe that our best bet to achieve acceptable smog chamber simulations will be to vary radical fluxes such that both radical sources and sinks are changed together.

Hierarchical Approach

As is the case with most model mechanisms, the original CB-IV was tested against a hierarchical series of smog chamber data. This hierarchy is based on the commonality of species and reactions. The inorganic reactions involving ozone and NOx are common to all smog-forming situations and these reactions form the lowest level in the hierarchy. However, smog chemistry requires radicals (HOx) based on water, and formaldehyde or some other source of these radicals must be present to run the smog system. This means that formaldehyde/NOx experiments generally form the lowest hierarchical level that can be tested directly. Other levels add species like PAN or aromatics. All higher levels would utilize the same formaldehyde/NOx reaction set. In order to preserve the ability of alternative mechanisms to simulate all levels of the hierarchy, we believe that alternative parts (i.e., high and low radical flux) are needed at each hierarchical level. Until the smog chamber simulation tests are undertaken in Task 3 we will not know how well the various high and low radical flux alternatives can be mixed between levels of the hierarchy. For example, can the high radical flux formaldehyde/NOx reactions be used with the low radical flux aromatics and still simulate the aromatics/NOx smog chamber experiments?

Important radical sources common to all levels of the hierarchy are formaldehyde photolysis and $O(^1D)$ formation and its subsequent reaction with water. We highlight the uncertainties in formaldehyde photolysis, especially for simulating smog chamber experiments, in Appendix A. The most important radical sink reaction common to all levels of the hierarchy is the hydroxyl radical reaction with nitrogen dioxide and we present next a special discussion leading to the upper and lower bounds of this reaction.

Rate constant for reaction $OH + NO_2 + M \rightarrow HNO_3 + M$

The combination of HNO3 is a Troe reaction. The formula for the Troe reactions is:

$$k(T, M) = \frac{k_o(T)[M]}{1 + \frac{k_o(T)[M]}{k_\infty(T)}} F\left\{1 + \left[\log_{10} \frac{k_o(T)[M]}{k_\infty(T)}\right]^2\right\}^{-1}$$

where

k_0 = the lower pressure limit rate constant
k_∞ = the upper pressure limit rate constant
[M] = the third body concentration
T = the temperature.

The upper and lower pressure rate constants are in the form:

$$k_o(T) = k_0^{300}\left[\frac{T}{300}\right]^{-n}$$

$$k_\infty(T) = k_\infty^{300}\left[\frac{T}{300}\right]^{-m}$$

where

k_o^{300} = the lower pressure limit rate constant at 300 ^{o}K
k_∞^{300} = the upper pressure limit rate constant at 300 ^{o}K
n, m = the respective temperature dependencies.

Table 1 lists the recommended values for k_o^{300}, k_∞^{300}, F, n and m from the IUPAC evaluation (1989; 1992; 1996). In the IUPAC evaluations, the third body is [N2].

Table 2 lists the recommended values for k_o^{300}, k_∞^{300}, F, n and m from the NASA evaluation (1994). In the NASA evaluations, the third body is [M]. The values are not changed from 1988 to 1994 for the NASA evaluations.

For the uncertainty factor IUPAC evaluations give uncertainty estimates at 298^{o}K as Dlogk. The term Dlogk is defined as Dlogk = $\log_{10}$f , where f is the same factor as given in the NASA evaluations (NASA, 1988; IUPAC, 1989).

The upper and lower bounds for the rate constants are calculated based on the uncertainty estimates given by NASA and IUPAC. Because of the complicated expression for the rate constants, monte carlo simulations are used to calculated the upper and lower bounds. In the monte carlo simulations, lognormal distributions were assumed for the random variable k_o^{300} and k_∞^{300}, and normal distributions were assumed for *n* and *m* (Gao et al., 1995). The standard deviations representing the uncertainties σ_o^{300} for k_o^{300}, σ_∞^{300} for k_∞^{300}, and s_n and s_m for *n* and *m* were obtained from NASA and IUPAC. The upper and lower bounds for the rate constants of HNO3 combination at atmospheric conditions (1 atm and 298 ^{o}K) are shown in Table 3. Table 4 lists the recommended rate constants and the value used in UAM modeling.

Table 1. Recommended values for k_o^{300}, k_∞^{300}, *F*, *n* and *m* from IUPAC evaluations

k_o^{300}	Dlogk	k_∞^{300}	Dlogk	*n*	D*n*	*m*	D*m*	*F*	Notes
2.6E-30	±0.1	5.2E-11	±0.1	2.9	±0.5	0.0	±0.5	0.43	IUPAC, 1989
2.6E-30	±0.1	6.0E-11	±0.1	2.9	±0.5	0.0	±0.3	0.43	IUPAC, 1992
2.6E-30	±0.1	6.7E-11	±0.1	2.9	±0.5	0.6	±0.5	0.43	IUPAC, 1996

Note: the unit for rate constants is cm^3 molecule^{-1} s^{-1}.

Table 2. Recommended values for k_o^{300}, k_∞^{300}, F, n and m from NSAS evaluations

k_o^{300}	D k_o^{300}	k_∞^{300}	D k_∞^{300}	*n*	D*n*	*m*	D*m*	*F*	Notes
2.6E-30	±3.0E-31	2.4E-11	±1.2E-11	3.2	±0.7	1.3	±1.3	0.6	NSAS, 1988-1994

Note: the unit for rate constants is cm^3 molecule^{-1} s^{-1}.

Table 3. Lower and upper bounds for the rate constant of HNO3 combinations at the atmospheric conditions (1 atm and 298 ^{o}K)

Rate Constant	Recommended Value	Lower Bound	Upper Bound	Sigma	Note
NASA:					
k_o^{300}	2.60E-30	2.30E-30	2.90E-30	3.00E-31	300 ^{o}K
k_∞^{300}	2.40E-11	1.20E-11	3.60E-11	1.20E-11	300 ^{o}K
k_0	2.66E-30	2.36E-30	2.95E-30	2.94E-31	298 ^{o}K
$k.$	2.42E-11	1.26E-11	3.58E-11	1.16E-11	298 ^{o}K
k	1.15E-11	8.41E-12	1.46E-11	3.08E-12	298 ^{o}K
IUPAC 1989:					
k_o^{300}	2.60E-30	2.07E-30	3.27E-30	6.04E-31	300 ^{o}K
k_∞^{300}	5.20E-11	3.28E-11	8.24E-11	2.48E-11	300 ^{o}K
k_0	2.65E-30	2.06E-30	3.24E-30	5.91E-31	298 ^{o}K
$k.$	5.20E-11	2.82E-11	7.58E-11	2.38E-11	298 ^{o}K
k	1.11E-11	7.38E-12	1.48E-11	3.69E-12	298 ^{o}K
IUPAC 1992:					
k_∞^{300}	6.00E-11	4.77E-11	7.55E-11	1.39E-11	300 ^{o}K
$k.$	6.00E-11	4.67E-11	7.33E-11	1.33E-11	298 ^{o}K
k	1.29E-11	9.32E-12	1.45E-11	2.58E-12	298 ^{o}K
IUPAC 1996:					
k_∞^{300}	6.70E-11	5.32E-11	8.43E-11	1.56E-11	300 ^{o}K
$k.$	6.73E-11	5.23E-11	8.23E-11	1.50E-11	298 ^{o}K
k	1.26E-11	9.88E-12	1.54E-11	2.74E-12	298 ^{o}K

Note: the unit is cm^3 $molecule^{-1}$ s^{-1}. The values for sigma are obtained from the Monte Carlo Simulations. The low pressure limit for IUPAC are same from 1989 to 1996 evaluations.

Table 4. Comparison of UAM modeling and recommended rate constants for $OH + NO_2 + M \rightarrow HNO_3 + M$ at atmospheric conditions (1 atm and 298 ^{o}K)

Source	Rate Constants $cm^3\ molecule^{-1}s^{-1}\ ppm^{-1}\ min^{-1}$		Lower Bound $ppm^{-1}\ min^{-1}$	Upper Bound	%change
NASA	1.15E-11	1.70E+04	1.24E+04	2.15E+04	±27
IUPAC 1989	1.11E-11	1.63E+04	1.09E+04	2.18E+04	±33
IUPAC 1992	1.19E-11	1.76E+04	1.38E+04	2.14E+04	±22
IUPAC 1996	1.26E-11	1.86E+04	1.46E+04	2.27E+04	±22
UAM (CB-IV)		1.68E+04			

From Table 4 we then see that the highest acceptable current value for this rate constant would be 2.27E+04 $ppm^{-1}\ min^{-1}$, from the most recent (1994) IUPAC recommendations. For the most recent lower bound we will use 1.24E+04 $ppm^{-1}\ min^{-1}$ from the most recent (1994) NASA recommendations. The 1989 IUPAC gives an even lower number, but it has been superseded by the more recent IUPAC evaluations. Thus, our high radical flux alternate formaldehyde mechanism can use values as high as 2.27E+04 $ppm^{-1}\ min^{-1}$, while the low radical flux alternative mechanism can use values as low as 1.24E+04 $ppm^{-1}\ min^{-1}$. Quality of the smog chamber simulations for the formaldehyde/NOx experiments will determine the final values that can be used in simulating experiments of species at higher levels of the hierarchy.

Ethene Chemistry

Ethene adds a species to the hierarchy without yet introducing PAN to any great extent. The CB-IV has only three reactions specific to ethene, but some glycolaldehyde (treated as acetaldehyde in the CB-IV) is introduced by the hydroxyl reaction with ethene. A key component to simulating the ethene/NOx experiments has been proper decay of the ethene primary species. An important part of the hierarchical approach that the CB-IV is based on means that good ozone formation performance with poor ethene decay will not be acceptable in the smog chamber simulation protocol. Using the high and low radical flux versions of the formaldehyde/NOx chemistry that provide adequate smog chamber performance, we will then attempt to simulate the ethene/NOx series of experiments. We expect to find high and low radical flux ethene reaction sets that adequately simulate the ethene/NOx experiments mainly by using the upper and lower bounds of the ethene reaction with hydroxyl. The Atkinson et al. (1989) review indicates that a factor of 2 uncertainty exists in this rate constant, which should give us adequate range to develop a high and low radical flux version of ethene chemistry.

Aldehydes

Primary olefinic (OLE) species used in the CB-IV bring not only PAR to account for the paraffinic "parts" of these higher olefins, but secondary aldehydes which are known to play a central role in the performance of olefin mechanisms. Therefore, the hierarchical approach requires that the aldehyde/NOx smog chamber experiments be adequately simulated before testing either paraffin/NOx experiments or the olefin/NOx experiments themselves. As for the formaldehyde reactions discussed above, we have reviewed (see Appendix A) the range of uncertainty in the photolysis rates for these species, especially as they are used in smog chambers. The high and low radical flux versions of these subsets of reactions will be based mainly on the photolysis uncertainties.

Aldehydes higher than formaldehyde bring peroxy acyl nitrates that are simulated in the CB-IV with PAN as a surrogate. PAN acts both as a sink and as a reservoir for radicals depending on the temperature (primarily for PAN decomposition back to NO2 and a radical) and on the ratio of NO and NO2. The original CB-IV utilized a significant temperature dependence for the competitive reaction rates between NO and NO2, but the recent versions of CB-IV no longer have such a strong temperature dependence. We believe that this is still somewhat uncertain, but we do not intend to address the impacts on control strategy estimates stemming from uncertain temperature dependent factors in this project. Therefore, the high and low radical flux versions of aldehyde (and carbonyl) chemistry will be tested against the aldehyde (and other carbonyls)/NOx smog chamber database (and adjusted as necessary) primarily within the range of aldehyde photolysis uncertainties and PAN reactions. The primary hydroxyl reactions may also need to be adjusted to ensure that aldehyde decay is properly simulated for both the high and low radical flux versions.

Paraffin Chemistry

Higher olefins than ethene all utilize some combination of paraffinic (PAR) and olefinic (OLE) bonded species to represent primary species. However, experience has shown that the OLE species is so much more reactive compared to PAR that simulations of olefin/NOx smog chamber experiments are not very sensitive to even wide variation in PAR chemistry. Nevertheless, a consistent application of the hierarchical approach more or less dictates that alkane chemistry be established before olefin chemistry.

The paraffin chemistry used in the CB-IV stems from a condensation of the reactions for primary, secondary and tertiary carbon atoms and assumption about the distribution of these three types of paraffinic bonds in urban atmospheres. The CB-IV uses only one primary reaction to represent the hydroxyl abstractions from paraffinic carbon atoms in general. This has been justified in the past by the striking consistency in the per carbon rate constants for the hydroxyl radical reactions with paraffin isomers between 4 and 10 carbons in size. The reason for this consistency is explained by the averaging coincidence that exists between the established rate constants for attack at primary, secondary and

tertiary carbons that combines with the ways in which the paraffinic isomers can be assembled. For example, the difference between all normal paraffins and all isoparaffins can be described as two secondary carbons and one primary carbon are found at the "end" of all normal paraffins, while all isoparaffins have two primary carbons and one tertiary carbon. Since at least one primary carbon exists in both these forms, the difference can be treated as substituting two secondary carbons for one tertiary and one primary. Since the work of Greiner (1970) the total rate constant for hydroxyl radical attack on most paraffins has been considered as the sum of the primary, secondary and tertiary carbon atom rate constants. Atkinson (1994) suggests values at 298 K of 273, 1830 (average if only one secondary carbon has a primary substituent) 3478 (if two substitutents are primary) ppm^{-1} min^{-1} for this example of primary, secondary and tertiary carbons, receptively. Thus, the average of two secondary carbons is 1830 ppm^{-1} min^{-1} and the average of one primary and one tertiary is 1876 ppm^{-1} min^{-1} , which is a difference of less than 3 percent.

Due to the low reactivity of alkanes to begin with, differences in smog chamber simulations have generally been minor when uncertainties in the alkane chemistry have been tested. One exception, which also appears to have significant uncertainty, has been the level of alkyl nitrate formation. Hence, we expect to adjust the level of nitrate formation (which is both a radical and a NOx sink) needed to accommodate the high and low radical flux versions of formaldehyde/NOx chemistry and still adequately simulate paraffin/NOx experiments. While many other uncertain elements exist in alkane chemistry, we believe that radical fluxes are the key to UAM control strategy uncertainties and nitrate formation in the paraffin reactions appears to have the strongest combined uncertainty and impact on radical fluxes.

Other adjustments in the paraffin reaction set may be explored and used, if necessary. One example is radical regeneration through the unimolecular decomposition of alkoxyl radicals. However, we suspect that similar final control strategy impacts may result between radical flux adjustments within the alkane-specific reactions that are focused on either nitrate formation or on radical recirculation.

Olefin Chemistry

Historically, the largest number of single hydrocarbon/NOx smog chamber experiments have been with propene. The CB-IV was mainly tested, therefore, with propene. However, we intend to use as many other olefins as might now be available. We expect that radical flux can be accommodated in the olefin chemistry by adjustments (within experimental uncertainties) in the ozone reactions with olefins. The yield of radicals from alkene reactions with ozone has a long history of uncertainty which continues, as is evidenced by the 20 December 1996 issue of the *Journal of Geophysical Research* where an article by Chew and Atkinson is presented on this subject.

Aromatics Chemistry

Aromatics chemistry in the CB-IV was originally developed by a much different procedure than all the other parts discussed above. *Van Nostrand's Scientific Encyclopedia* gives three definitions of "calibration." Two of these might be applied to the development of the CB-IV. The first, applicable to virtually all but the aromatics parts of the CB-IV refers to calibration as testing against a standard to determine the bias and range of agreement. The second definition of calibration implies that adjustments are made (i.e., tunning) to match a standard. For the aromatics chemistry a significant amount of adjustments were used in the set of reactions and photolysis constants in order to fit the aromatics/NOx subset of the smog chamber database. From the discussions above we also note that in this particular project high and low radical flux alternatives to the base CB-IV are being tuned to stay within reasonable bounds across several subsets of the smog chamber database. The aromatics parts of the CB-IV will be retuned to work with the high and low radical flux formaldehyde/NOx and other reactions needed to accompany the aromatics. Any adjustments made to the aromatics chemistry will be made within the bounds of experimental uncertainty developed in our recent literature review under Task 1 of this project (part of which follows).

The smog chemistry of aromatics remains highly uncertain mainly because large fractions of the organic products have not been identified. Glyoxal, methylglyoxal, and unsaturated dicarbonyls are known products of aromatic decomposition that can significantly influence radical fluxes. However, the yields and identity of many other photooxidation products have not identified in laboratory studies (Gao et al., 1996b).

Table 2-1 gives a listing of major product yields of toluene and xylene oxidations determined by several different laboratories (Atkinson, 1994). The average coefficients of variation for product yields of glyoxal are 19% in toluene oxidation and 20% in xylene oxidation. Those values for methylglyoxal are 14% in toluene and xylene oxidations. When aromatic reactions are incorporated into a mechanism, they are highly parameterized and adjusted to fit chamber observations, given a fixed formulation for the rest of the mechanism. Glyoxal and methylglyoxal are two major products in both toluene and xylene (Atkinson, 1990; 1994).

TABLE 2-1. Experimental product yield uncertainties for toluene and xylene (Atkinson, 1994).

Species	Mean Yield (m)	Standard Deviation(±s)	s/m (%)	Average s/m (%)
Toluene				
Benzaldehyde	0.073	0.022	30	20
	0.11	0.01	9	
	0.104	0.029	28	
	0.0645	0.008	12	
Cresol	0.131	0.072	55	29
	0.204	0.027	13	
	0.048	0.009	19	
Glyoxal	0.111	0.013	12	19
	0.15	0.04	27	
	0.105	0.019	18	
Methylglyoxal	0.146	0.014	10	14
	0.14	0.04	29	
	0.146	0.006	4	
Xylene				
Tolualdehyde	0.073	0.036	49	26
	0.05	0.01	20	
	0.172	0.07	41	
	0.0453	0.0059	13	
	0.04	0.01	25	
	0.122	0.059	48	
	0.0331	0.0041	13	
	0.08	0.01	13	
	0.0701	0.0103	15	
Dimethylphenol	0.097	0.024	25	31
	0.064	0.015	23	
	0.012	0.006	50	
	0.102	0.039	38	
	0.099	0.023	23	
	0.111	0.033	30	
	0.178	0.065	37	
	0.188	0.038	20	
Glyoxal	0.08	0.04	50	20
	0.087	0.012	14	
	0.104	0.02	19	

	0.13	0.03	23	
	0.086	0.011	13	
	0.12	0.02	17	
	0.24	0.02	8	
	0.225	0.039	17	
Methylglyoxal	0.265	0.035	13	14
	0.23	0.03	13	
	0.246	0.03	8	
	0.42	0.05	12	
	0.319	0.009	3	
	0.111	0.015	14	
	0.12	0.02	17	
	0.105	0.034	32	

In the mechanisms mentioned above, there are direct products of glyoxal and methylglyoxal from the toluene and xylene oxidations in SAPRC and RADM2 mechanisms. There is no direct glyoxal production from either toluene or xylene oxidation in CB-IV. No direct methylglyoxal product is formed in toluene oxidation, either. However, through radical TO2 reactions, methylglyoxal can be produced through OPEN + O3 reaction in CB-IV. Table 2-2 listed the product yields for cresol, glyoxal and methylglyoxal in the toluene and xylene oxidations for RADM2, SAPRC and CB-IV.

TABLE 2-2. Product yields for cresol, glyoxal and methylglyoxal in toluene and xylene oxidations for RADM2, SAPRC, and CB-IV.

	Cresol	Glyoxal	Methylglyoxal
Toluene + OH			
RADM2 [a]	0.25	0.12	0.13
SAPRC [b]	0.26	0.118	0.131
CB-IV [c]	0.45 - 0.92		0 - 0.0031
Xylene + OH			
RADM2 [a]	0.17		0.37
SAPRC [b]	0.18	0.108	0.37
CB-IV [c]	0.28 - 0.50		0.80 - 0.8015

Note: [a] Stockwell et al., 1990.
[b] Carter, 1990. See Gao, 1995.
[c] Gery et al., 1989.

It is apparent that the yields of dicarbonyls in CB-IV are different from those in the RADM2 and SAPRC mechanisms. In the RADM2 and SAPRC mechanisms, there are

four species, which includes glyoxal, methylglyoxal, CRES and AFG2/DCB for unknown aromatic fragmentation products, used to represent dicarbonyl products. In CB-IV, the dicarbonyls are represented by CRES, MGLY and OPEN. CRES represents cresol and higher molecular weight phenols, MGLY is an explicit species, and OPEN represents all other dicarbonyl products

References

Atkinson, R. 1986. Kinetics and mechanisms of the gas-phase reactions of the hydroxyl radical with organic compounds under atmospheric conditions. *Chem. Rev., 86*:69-201.

Atkinson, R. 1990. Gas-phase tropospheric chemistry of organic compounds: a review. *Atmos. Environ.,* 24A:1-41.

Atkinson, R. 1994. Gas-phase tropospheric chemistry of organic compounds. *J. Phys. Chem. Ref. Data*, Monograph No.2, 1-126.

Atkinson, R. and S.M. Aschmann. 1993. OH radical production from the gas-phase reactions of O_3 with a series of alkenes under atmospheric conditions. *Environ. Sci. Technol.,* 27:1357-1363.

Atkinson, R., D.L. Baulch, R.A. Cox, R.F. Hampson, Jr., J.A. Kerr, and J. Troe. 1989. Evaluated kinetic and photochemical data for atmospheric chemistry: supplement III. IUPAC Subcommittee on gas kinetic data evaluation for atmospheric chemistry. *J. Phys. Chem. Ref. Data*, 18:881-1097.

Atkinson, R., D.L. Baulch, R.A. Cox, R.F. Hampson, Jr., J.A. Kerr, and J. Troe. 1992. Evaluated kinetic and photochemical data for atmospheric chemistry: supplement IV. IUPAC Subcommittee on gas kinetic data evaluation for atmospheric chemistry. *J. Phys. Chem. Ref. Data*, 21:1125-1568.

Atkinson, R., D.L. Baulch, R.A. Cox, R.F. Hampson, Jr., J.A. Kerr, M.J. Rossi, and J. Troe. 1996. Evaluated kinetic and photochemical data for atmospheric chemistry: supplement V. IUPAC Subcommittee on gas kinetic data evaluation for atmospheric chemistry. *Atmos. Environ*., 30(22):3903-3904. (*J. Phys. Chem. Ref. Data*, 1996)

Atkinson, R., E.C. Tuazon, and S.M. Aschmann. 1995. Products of the gas-phase reactions of O_3 with alkenes. *Environ. Sci. Technol.*, 29:1860-1866.

Bridier, I., F. Caralp, H. Loirat, R. Lescalaux, B. Veyret, K.H. Becker, A. Reimer and F. Zabel. 1991. Kinetic and theoretical studies of the reactions CH3C(O)O2+NO2+M « CH3C(O)O2NO2+M between 248 and 393 K and between 30 and 760 Torr. *J. Phys. Chem.,* 95:3594-3600.

Cantrell, C.A., J.A. Davidson, A.H. McDaniel, R.E. Shetter and J.G. Calvert. 1990. Temperature-dependent formaldehyde cross sections in the near-ultraviolet spectral region. *J. Phys. Chem.,* 94(10):3902-3908.

Carter, W. P.L. 1990. A detailed mechanism for the gas-phase atmospheric reactions of organic compounds. *Atmos. Environ.*, 24A(3):481-518.

Carter, William P.L. 1995. Computer modeling of environmental chamber measurements of maximum incremental reactivities of volatile organic compounds. *Atmos. Environ.*, 29(18):2513-2527.

Carter, W.P.L. and R. Atkinson. 1996. Development and Evaluation of a Detailed Mechanism for the Atmospheric Reactions of Isoprene and NO_x. *International Journal of Chemical Kinetics*, 497-530.

Carter, W.P.L., J.A. Pierce, Dongmin Luo and I.L. Malkina. 1995. Environmental chamber study of maximum incremental reactivities of volatile organic compounds. *Atmos. Environ.*, 29(18):2499-2511.

DeMore, W.B., S.P. Sander, M.J. Molina, D.M. Golden, R.F. Hampson, M.J. Kurylo, C.J. Howard and A.R. Ravishankara, *Chemical Kinetics and Photochemical Data for Use in Stratospheric Modeling, Evaluation Number 8,* National Aeronautics and Space Administration (NASA), Jet Propulsion Laboratory, California Institute of Technology, Pasadena, CA, 1988.

DeMore, W.B., S.P. Sander, D.M. Golden, M.J. Molina, R.F. Hampson, M.J. Kurylo, C.J. Howard, and A.R. Ravishankara. 1990. *Chemical Kinetics for Use in Stratospheric Modeling, Evaluation Number 9.* National Aeronautics and Space Administration, Jet Propulsion Laboratory, California Institute of Technology, Pasadena, CA.

DeMore, W.B., S.P. Sander, D.M. Golden, R.F. Hampson, M.J. Kurylo, C.J. Howard, A.R. Ravishankara, C.E. Kolb, and M.J. Molina. 1992. *Chemical Kinetics and Photochemical Data for Use in Stratospheric Modeling, Evaluation Number 10.* National Aeronautics and Space Administration, Jet Propulsion Laboratory, California Institute of Technology, Pasadena, CA.

Gao, Dongfen. 1995. *Sensitivity and Uncertainty Analysis in Chemical Mechanisms for Air Quality Modeling*, Ph.D. Dissertation, Department of Civil and Environmental Engineering, The University of Connecticut, Storrs, Connecticut.

Gao, Dongfen, Jana B. Milford and William R. Stockwell. 1996b. *Analysis of Uncertainties in the Regional Acid Deposition Model, Version2 (RADM2), Gas-Phase Chemical Mechanism*, Final report prepared for Electric Power Research Institute. (EPRI TR-106433).

Gao, Dongfen, William R. Stockwell and Jana B. Milford. 1995. First order sensitivity and uncertainty analysis for a regional-scale gas-phase chemical mechanism. *J. Geophys. Res.*, 100(D11):23153-23166.

Gao, Dongfen, William R. Stockwell and Jana B. Milford. 1996a. Global uncertainty analysis of a regional scale gas-phase chemical mechanism. *J. Geophys. Res.*, 101(D4):9107-9119

Gery, M.W., G.Z. Whitten, J.P. Killus and M.C. Dodge. 1989. A photochemical mechanism kinetics for urban and regional scale computer modeling. *J. Geophys. Res.,* 94:12925-12956.

Grosjean, D., E. Grosjean and E.L. Williams II. 1994. Thermal decomposition of PAN, PPN and vinyl-PAN. *J. Air & Waste Manage. Assoc.,* 44:391-396.

Grosjean, Eric and Daniel Grosjean. 1996a. Carbonyl products of gas phase reaction of ozone with C5-C7 alkenes. *Environ. Sci. Technol*., 30(4):1321-1327.

Grosjean, Eric and Daniel Grosjean. 1996b. Carbonyl products of gas phase reaction of ozone with symmetrical alkenes. *Environ. Sci. Technol*., 30(6):2036-2044.

Grosjean, Eric, Jailson Bittencourt de Andrade and Daniel Grojean. 1996a. Carbonyl products of the gas-phase reaction of ozone with simple alkenes. *Environ. Sci. Technol.*, 30(3):975-983.

Grosjean, Eric, Daniel Grosjean and John H. Seinfeld. 1996b. Atmospheric chemistry of 1-Octene, 1-Decene, and Cyclohexene: Gas-phase carbonyl and peroxyacyl nitrate products. *Environ. Sci. Technol.*, 30(3):1038-1047.

Heicklen, J., J. Desai, A. Bahta, C. Harper, and R. Simonaitis. 1986. "The temperature and wavelength dependence of the photooxidation of propionaldehyde." *J. Photochem.*, 34:117-135.

Kirchner, F. and W.R. Stockwell. 1996. Effect of peroxy radical reactions on the predicted concentrations of ozone, nitrogenous compounds, and radicals. *J. Geophys. Res.*, 101(D15):21007-21022..

Kirchner, F., F. Zabel and K.H. Becker. 1990. Determination of the rate constant ratio for the reactions of the acetylperoxy radical with NO and NO_2. *Ber. Bunsenges. Physical. Chemistry*, 94:1379-1382.

Kwok, E.S.C., R. Atkinson and J. Arey. 1995. Observations of Hydroxycarbonyls from the OH Radical-Initiated Reaction of Isoprene. *Environ. Sci. Technol*., 29:2467-2469.

Ligocki, M.P., G.Z. Whitten, R.R. Schulhof, M.C. Causley, and G.M. Smylie. 1991a. Atmospheric Transformation of Air Toxics: Benzene, 1,3-Butadiene, and Formaldehyde. SYSAPP-91/106, Final report for U.S. EPA Contract No.

Ligocki, M.P., G.Z. Whitten, R.R. Schulhof, M.C. Causley, and G.M. Smylie. 1991b. Atmospheric Transformation of Air Toxics: Acetaldehyde and Polycyclic Organic Matter. SYSAPP-91/113, Final report for U.S. EPA Contract No.

Milford, J.B., Yang, Y-J, Stockwell, W.R. 1993. Uncertainties in chemical mechanisms for urban and regional scale oxidant modeling. *Proceedings of the International Conference on Regional Photochemical Measurement and Modeling Studies*, Air & Waste Manage. Assoc., San Diego, CA, November 1993.

Morgan, M.G., Henrion, M. 1990. *Uncertainty*. Cambridge University Press, Cambridge.

Rogers, J.D. 1990. Ultraviolet absorption cross sections and atmospheric photodissociation rate constants of formaldehyde. *J. Phys. Chem.*, 94(10):4011-4015.

Roumelis, N. and S. Glavas. 1992. Thermal decomposition of peroxyacetyl nitrate in the presence of O_2, NO_2 and NO, *Monatshefte für Chemie*, 123:63-72.

Stockwell, W.R. 1993. *Estimation of Parameter Uncertainties for the Regional Acid Deposition Model Mechanism*. interim report to Electric Power Research Institute, agreement RP3189-06, Woodward-Clyde Consultants, Santa Ana, California.

Stockwell, W.R., P. Middleton, J.S. Chang, and X. Tang. 1990. The second generation regional acid deposition model chemical mechanism for regional air quality modeling. *J. Geophys. Res.*, 95:16343-16367.

Stockwell, W.R., Milford, J.B. and D. Gao. 1994a. An assessment of the effect of the uncertainties in aromatic chemistry on predicted oxidant concentrations. *Proceedings of the Air & Waste Management Association 87th Annual Meeting & Exhibition, June 19-24, 1994, Cincinnati, Ohio,* Air & Waste Management Association, Pittsburgh, PA.

Stockwell, W.R., Y.-J. Yang and J.B. Milford. 1994b. *A Compilation of Estimated Uncertainty Factors for Rate Constants in W.P.L. Carter's Detailed Mechanism*. Final report prepared for Auto/Oil Air Quality Improvement Research Program.

Tuazon, E.C., W.P.L. Carter and R. Atkinson. 1991. Thermal decomposition of peroxyacetyl nitrate and reactions of acetyl peroxy radicals with NO and NO_2 over the temperature range 283-313 K. *J. Phys. Chem.*, 95:2434-2437.

Whitten, G.Z., Hogo, H. and J.P. Killus. 1980. The carbon-bond mechanism: a condensed kinetic mechanism for photochemical smog. *Environ. Sci. Technol.*, 18:280-287.

Yang, Yueh-Jiun. 1995. *Quantification of Uncertainty in Reactivities of VOC and Emissions from Reformulated Gasoline and Alternative Fuels*. Ph.D. Dissertation, Department of Civil and Environmental Engineering, The University of Connecticut, Storrs, Connecticut.

Yang, Yueh-Jiun, William R. Stockwell and Jana B. Milford. 1995. Uncertainties in incremental reactivities of volatile organic compounds. *Environ. Sci. Technol.*, 29(5):1336-11345.

Yang, Yueh-Jiun and Jana B. Milford. 1996a. Quantification of uncertainties in reactivity adjustment factors from reformalated gasolines and methanol fuels. *Environ. Sci. Technol.*, 30(1):196-203.

Yang, Yueh-Jiun, William R. Stockwell and Jana B. Milford. 1996b. Effect of chemical product yield uncertainties on reactivities of VOCs and emissions from reformulated gasolines and methanol fuels. *Environ. Sci. Technol.*, 30(4):1392-1397.

Yu, J., H.E. Jeffries, and R. M. Le Lacheur. 1995. Identifying Airborne Carbonyl Compounds in Isoprene Atmospheric Photooxidation Products by Their PFBHA Oximes Using Gas Chromatography/Ion Trap Mass Spectrometry, *Environmental Science and Technology*, Vol. 29, 1923-1932, 1995

Zimmermann, J. and D. Poppe. 1996. A supplement for the RADM2 chemical mechanism: The photooxidation of isoprene. *Atmos. Environ.*, 30(8):1255-1269.

Appendix A

An historical review of photolysis rates used in atmospheric simulation models

by

James P. Killus

Many photooxidation products of most VOC compounds contain oxygen in the form of carbonyl structures. Carbonyl containing compounds are of particular importance in smog chemistry because a substantial number of such compounds will photolyze in ordinary sunlight to form radical products that serve as a primary source of hydrogen centered radicals, (e.g. OH) that are chain initiating for the photooxidation process itself. Thus, VOC photooxidation is a feedback process, with the radical attack on the VOC compounds producing compounds that can then initiate further radical attack. The short form of the smog process can be written as:

1	NO2 + hν -> NO + O
2	O + O2 -> O3
3	NO + O3 -> NO2
4	OH + VOC -> RaO2
5	RaO2 + NO -> NO2 + CARB + HO2
6	HO2 + NO -> NO2 + OH
7	CARB + hν -> HO2 + RbO2

The short form ignores many details and complications, such as the fact that the VOC product need not be an alkyl chain (R), just as the VOC need not be an alkyl hydrocarbon, that the products must lose carbon mass as photooxidation proceeds (Rb must be of lower carbon number than Ra, hence an oxidized carbon -- either CO or CO2 -- must be formed in the reaction chain), or that the carbonyl containing compound is also subject to radical attack, not just photolysis. Expanding the mechanism to include such details and the complications that result from treating a wide variety of VOCs, can expand the reaction set to hundreds of reactions.

The short form of the smog reactions does emphasize the crucial framework of the smog formation system. Generally speaking, what we are interested in describing are

1) primary radical attack reactions

2) primary product yields

3) secondary product radical attack reactions and

4) secondary product photolysis rates

Of these four types of generic reactions, the most variable are photolysis rates. Radical reaction rates and product yields may change with temperature and pressure, and our estimates of those rates may be somewhat uncertain in any event, but photolysis rates are highly variable by their very nature, and even if those rates were perfectly known under one set of conditions (e.g. smog chambers) there could still be substantial uncertainty in their application to atmospheric simulations. In reality, of course, many photolysis rates are uncertain even under controlled experimental conditions.

For the purposes of this project, therefore, photolysis rates are in a special category, in that there is considerable uncertainty in atmospheric application of kinetic modeling irrespective of the goodness-of-fit for kinetic mechanisms to smog chamber modeling. Therefore, it is worth a particular effort to examine the range of uncertainty of photolytic rate constants. Since smog chambers present a limited example of the problem, let us first examine the estimation of photolysis rates in smog chambers.

Estimation of photolysis in smog chamber modeling

Generally, there are two methods of estimating photolysis rates that have been used for smog chamber modeling studies: chemical actinometry and *ab initio* estimation. In practice, both methods are often intertwined.

The estimation of photolysis *ab initio* involves specific characterization of the spectrally resolved actinic flux, the absorption cross-section spectrum of the compound in question, and determination of the quantum yield (also spectrally resolved) for the compound in question. It has been found that even such seemingly minor factors as the difference in spectral resolution between 1 and 5 nm bin sizes may have a significant effect on the photolysis rates derived by this method. Moreover, there is no assurance that errors in each of the steps (actinic flux, cross-section, quantum yield) is not additive with error in other steps. Finally, the estimation of actinic flux for atmospheric simulations is usually accomplished by use of a radiative transfer model. In short, there is sizable uncertainty in the *ab initio* calculation of photolytic rates.

Chemical actinometry has most often been used in the determination of the photolysis rate of NO2, a rate often referred to as K1, because of its prominence in the smog reaction set. Discussions of the use of the decay of NO2 to estimate K1 under controlled conditions may be found in Holmes et al. 1973, and Wu and Niki, (1975).

The estimation of other photolytic rates from smog chamber data is a more complex process, and may be termed "modeling actinometry." In this method, a series of smog chamber photooxidation experiments are performed, with the photolytic rates being set as a parameter, a constant in the case of artificial light smog chambers, a ratio to some other parameter in the case of natural light chambers. In early simulations of the UNC outdoor chamber, for example, formaldehyde (HCHO) photolysis to radical products (HCHOr) was first set to a constant ratio to NO2 photolysis, then later as a proportionality parameter to a ratio-to-

NO2-photolysis that varied with solar zenith angle, in accordance with estimates of how this ratio should change based on HCHO cross-section measurements and actinic flux. This may be viewed as an inclusion of *ab initio* computations, calibrated to the smog chamber via modeling.

For photolytic compounds less well studied than formaldehyde, the use of smog-chamber-actinometry is inevitable. However, such methods are still considerably more restrictive than mere "curve fitting," since the photolytic rates in one experiment or even one entire class of experiments, are still constrained to be consistent with the rates in other experiments. For example, both isoprene and certain aromatic experiments form the highly photolytic compound methyl glyoxal. The photolytic rates used in both types of experiments must be consistent; moreover, there are experiments involving the pure compound itself that further constrain the photolytic rates used.

Similarly, *ab initio* calculations constrain the freedom of the modeler to estimate photolytic rates, since quantum yields may not exceed 1, and absorption cross-sections give substantial information about the variation of photolytic rate ratios with actinic flux spectra.

The question then becomes, how much uncertainty exists in the estimation of important photolysis rates for kinetic mechanisms, both for smog chamber experiments and for atmospheric applications? I would suggest that one good method for estimating the uncertainty in smog chamber experiments is to examine the estimates of rates over a suitable period of time, in order to see what sort of variations have been accommodated via modeling. Differences of 20%, on a day-to-day basis do seem to exist in the historical record, and may even be explainable by real alterations in atmospheric conditions, even above such obvious variations as cloud cover.

Estimates of NO2 photolysis rates

Given that NO2 photolysis (K1) is simple, fundamental, and the best studied photolytic process in the smog reaction set, it seems likely that variations in NO2 photolysis estimates constitute a minimum degree of variability for photolytic rates in general. A review of prior estimates shows substantial variation.

Figure 1 gives a number of daily NO2 rates used for several smog chamber experiments in August at UNC. There are four main estimate protocols exemplified here, two ("lix" and "pri") being from a detailed light model applied to the UNC chamber by UNC investigators, followed by ab initio absorption and quantum yield calculations (the "pri" estimates are the most recent). The estimates labeled "lgx" are from a program called PKSSCVT which codified the methods developed over time by the Carbon Bond Mechanism development team; lgx estimates were used in the development and validation simulations leading to the CBM-IV. The two remaining estimates (from 8/11 and 8/15 1978; denoted by DTE) were made in the early 1980s by the CBM development team and come from simulation printouts from 1980 and 1984.

Obviously some of the variability is due to occasional clouds, as well as some inadvertent shading of the UV meter that is used to calibrate K1. However, apart from those deviations (which usually result in a temporary reduction in actinic flux and NO2 photolysis, but occasional increases may occur), the estimates are reasonably consistent, with two exceptions: the lix rate estimates and the development team estimate (DTE) for 8/11/78. The protocol for K1 estimation circa 1980-1984 (and later codified in the LGX estimates which were used until 1988) first used UV data, when available, then TSR data, and finally, if no light data were available for the day in question, a solar model was used. The values for the day in question were apparently derived from the solar function, which differed notably from the other methods of deriving K1, at least on the day in question.

Peak K1 for the lgx, pri, and 1980 development team estimates using UV data are within 10% of each other, and the range of lgx variation largely includes the variability of the other estimate. The peak lix estimate and the solar function DTE fall below the other estimates by about 20%.

Closer examination of the lgx file estimates (which are closely related to the earlier DTE methods) have shown that, in addition to a probable bias in the solar function estimates, there was a consistent bias when comparing days with K1 estimates derived from UV data versus K1 estimates for days lacking UV data but where TSR data was used instead. The TSR derived days tend toward the lower range of K1 estimates, and differ from UV derived estimates by about 10%. (See figure 2).

The discrepancy between UV and TSR derived estimates of K1 appears to result from the use of a constant conversion factor of 0.4 (see page 22 in Whitten, Killus, and Hogo, 1980) for TSR to UV. As may be seen from figure 3, the relationship between UV and TSR is variable with both intensity and season; however, the most typical value (as derived from a series of linear regressions) seems to be closer to 0.44, which probably accounts for the systematic discrepancy. The UV and TSR data also show that UV is less responsive to cloud attenuation (by about a factor of 2; see figure 4) than TSR readings, so any TSR derived estimates of K1 on days with cloud attenuation would also be lower than similar UV-derived estimates. It may be noted in passing, however, that clouds sometimes increase the light levels available (from cloud edge reflection), so that, under some circumstances, TSR-derived K1 may be over-estimated.

Conditions for the UNC chamber differ from a true atmospheric estimate of NO2 (and other) photolysis in a number of ways. The teflon film that forms the chamber reduces actinic flux by some degree, while the floor of the chamber is somewhat more reflective than the normal albedo of the ground. Moreover, the UNC chamber is at the surface, whereas the effective NO2 photolysis rate for smog formation conditions is more likely to represent some distance above the surface. We would generally expect the K1 for the UNC chamber to be greater than that used for an urban simulation (for the same atmospheric conditions). However, the degree of this difference is uncertain.

Different estimates of K1 have been made for atmospheric simulation purposes. Figure 5 shows several such estimates, along with near-equivalent estimates for (cloudless) K1 in the UNC chamber for comparison. As may be seen, the variations of these estimates in atmospheric simulations are similar to the differences in estimates for UNC chamber modeling, with a highest-to-lowest difference for low solar zenith angles of about 15% (the difference increases for higher zenith angles). Of particular interest is the fact that the UNC chamber estimates fall within the estimates used for atmospheric simulations, with the possible exception of high solar zenith angles.

Given the day-to-day variability of the UV measurements and related NO2 photolysis estimates at UNC, it is doubtful that atmospheric simulations can be more accurate than 15% without extensive, episode specific monitoring, and even then factors such as redistribution of light within the air column (e.g. due to haze scattering) make this problematic. This implies a fairly high baseline uncertainty in atmospheric simulation efforts.

Photolysis of carbonyl compounds

Central to the smog formation process is the slow oxidation of hydrocarbons via photolytically initiated radical chain reactions. This slow oxidation is a feedback process, because radical chain initiation occurs via photolysis of one subset of hydrocarbon oxidation products: carbonyl compounds. The major radical sink reactions involve nitrogen oxides (to either nitric acid or organic nitrates); NOx compounds also serve to convert peroxy radicals (intermediates in the hydrocarbon oxidation process) to ozone.

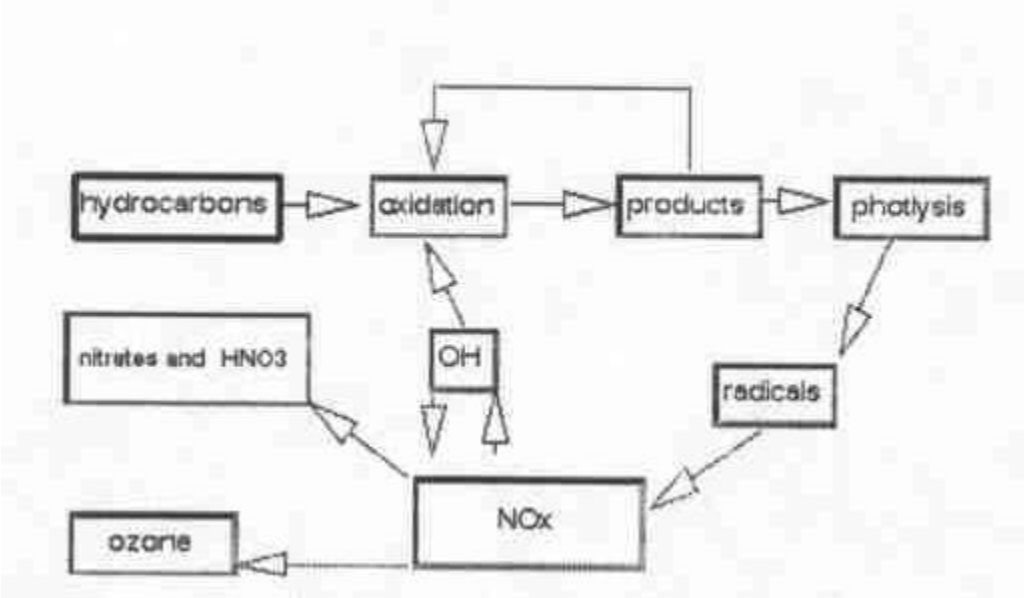

It is generally believed that the most important radical initiating carbonyl compound is formaldehyde (HCHO), which is a product of practically every hydrocarbon oxidation sequence. Formaldehyde photolysis is also the best studied carbonyl photolysis reaction. Therefore, variations in estimates for HCHO photolysis may be treated as a minimum uncertainty for radical chain initiating reactions via carbonyl photolysis.

The problems previously described for the ab initio calculations of NO2 photolysis are compounded for calculations of HCHO photolysis. In particular, HCHO photolysis to radicals (HCHOr) is more sensitive to actinic flux in the short wavelength region of the solar spectrum (290-340 nm), and this region is more variable than the longer wavelength UV which dominates NO2 photolysis. Moreover, in this region both the quantum yield and absorption cross section is changing rapidly and the cross section show substantial structure, which results in the calculations being sensitive to even such seemingly minor details as calculation bin size.

During the development of the CBM-IV, there were two competing measurements of the HCHO absorption cross-section, that of Bass et al. and that of Moortgat et al., which measurements differed by about 30% in the implied photolytic rate for HCHO to radicals. The CBM-IV used the cross-sections of Bass et al. in the HCHOr calculations, both because the measurements were more detailed (using 1 nm bin sizes), and because the calculated HCHOr photolysis seemed to better simulate HCHO-NOx experimental results.

Subsequent to the publication of the CBM-IV mechanism, the results of Bass et al. have been held to be in error, and the Moortgat results have generally been used by workers in the field. A fair amount has been made of what this change implies for the use and implementation of the CBM-IV mechanism, not just for HCHO photolysis per se, but also because some other photolysis rates are taken to be ratios of HCHOr, particularly methyl glyoxal. If the change in cross section calculations cause an increase in HCHOr photolysis, it would seem reasonable to reduce the photolysis of any compound tied to the HCHOr rate.

This reasoning, of course, presupposes that only the cross-section estimates have changed for UNC modeling work. However, the current estimates of all photolysis rates from UNC investigators use entirely different actinic flux estimates from earlier work. A review of the actual HCHOr rates used in UNC chamber modeling would seem to be in order.

Figure 6 shows the plot of HCHOr vs solar zenith angle for a set of UNC modeling days. It is fairly clear from figure 6 that the HCHOr photolysis rates currently recommended by UNC are, in fact, lower than those used in the CBM-IV development program, not greater (there is one single day examined so far -- August 17, 1978 -- for which the pri estimates are notably higher than the lgx estimates and those seem to be an error, since the light data on that day are no different from other days; we have notified UNC to this effect). This suggests that UNC estimates of actinic flux, especially in the short wavelength UV have decreased substantially relative to estimates in the mid-1980s.

Figure 7 shows the HCHOr photolysis rates that correspond to the NO2 photolysis rates shown in figure 5. As may be seen, the spread in the rates is similar to the K1 functions -- with the exception of the HCHOr photolysis currently used in the UAM 6.2 version that is recommended by the USEPA. The HCHOr rate used in that model is substantially greater than other estimates, including what one would extrapolate based upon the CBM-IV development program.

The origin of this increase in HCHOr photolysis in UAM simulations is uncertain. However, we suspect that it was incorporated into the UAM during atmospheric verification in the UAM, in order to correct a persistent underprediction. Such "atmospheric actinometry" is not unheard of, though it is suspect, since a variety of other factors (most notably, emissions inventory shortcomings) may cause persistent discrepancies between simulations and observations of urban oxidant formation.

However, we have also investigated another potential underestimation of carbonyl photolysis rates, that of higher aldehydes (e.g. propionaldehyde). The UAM version of the CBM-IV assumes that C3 and higher aldehydes photolyze at the same rate as acetaldehyde, whereas the more recent CBM-tox mechanism separates C3 and above aldehydes from acetaldehyde and uses a higher photolysis rate for these species. The result seems to mimic the (probably erroneous) higher values for HCHOr found in the UAM6.2. To that extent, therefore, it may be that the UAM6.2 is compensating for an underestimation of C3+ photolysis with an overestimation of HCHOr.

Acetaldehyde and higher aldehydes

The photolysis rates of acetaldehyde that were used in the CBM-IV development were somewhat higher (approximately 40%) than those currently recommended by UNC investigators (pri files; see figure 8). The development estimates (lgx files) also showed the bimodal distribution of curves due to differences in the UV and TSR data discussed above. The higher acetaldehyde photolysis rates used in the CBM-IV were chosen in part to match acetaldehyde-NOx experiments at UNC; however, the oxidation of acetaldehyde to yield formaldehyde, which has a much higher estimated photolysis, makes in-chamber actinometry for acetaldehyde photolysis more uncertain than for other compounds.

The UNC estimates for higher aldehydes is based on the absorption cross sections for propionaldehyde (which closely matched the measured cross sections for butyraldehyde and isobutylaldehyde) from Calvert and Pitts (1966) and the quantum yield measurements of Heiklin et al. (1986). There do exist C3 aldehyde runs at UNC, but these have not yet been modeled; we suggest that those runs be modeled as part of this project.

In the standard CBM-IV mechanism, there is a single lumped species to represent acetaldehyde, propionaldehyde and all higher aldehydes. It seems fairly clear that the photolysis of this lumped species would be highly uncertain even if we had precise estimates for the concentrations of those species. In practice, even the relative concentrations of the higher aldehydes are lacking, since few atmospheric measurements of those compounds exist, and their formation rates depend upon details of the primary hydrocarbon precursor mix that are often not available.

Recently, Grosjean et al. (1996) measured a series of carbonyl compounds in the ambient Los Angeles atmosphere. Of the aliphatic aldehydes measured, formaldehyde comprised 33% (volumetric equivalent), acetaldehyde 25%, and C3+ aldehydes 42% of the total. It seems clear, therefore, that the total fractional radical yield to the smog formation system from C3+ aldehydes is highly uncertain, and thus any sensitivity analysis should devote substantial attention to this potential radical source.

Methyl Glyoxal

Methyl glyoxal (MGLY) is a dicarbonyl compound that appears as an oxidation product in the photochemistry of both aromatic hydrocarbons and isoprene. Since its photolysis rate is substantially greater than that of formaldehyde, methyl glyoxal may serve as a major source of free radicals that drive the smog formation process.

Plum et al. measured the absorption cross section of methyl glyoxal and also estimated an overall radical yield such that methyl glyoxal was judged to photolyze at a rate of about 2% of NO2, with the absorption cross section measurements suggesting a wavelength dependence that also similar to NO2 photolysis. This estimate was in good agreement with estimates of methyl glyoxal photolysis made by the CBM development team in the early 1980s, based on several MGLY/NOx experiments at UNC.

In the Carbon Bond IV mechanism, however, MGLY photolysis is stipulated to be a multiple of formaldehyde photolysis, which has a different wavelength dependence and so varies differently with solar zenith angle. We have been unable to uncover any documentation giving the reasons for this change in estimated MGLY photolysis. Recent experiments at UCR (Carter, private communication, 1996) suggest that some aromatics compounds are less reactive in blacklight irradiated chamber experiments (blacklights are depleted in wavelengths at which formaldehyde photolyzes), and it is possible that similar observations affected the choice of MGLY spectral dependence in the CBM-IV development. However, the absorption cross section of MGLY is inconsistent with any similarity to formaldehyde, and we can only view the estimated MGLY photolysis variation with solar zenith angle as a mistake (see figure 9). However, in a recent modeling project for isoprene, we established that the overall photolysis of MGLY during UNC smog chamber experiments for that compound was similar for both estimates of MGLY photolysis, and the differing solar zenith angle dependence did not seem to greatly affect the simulation results.

We suggest, therefore, that both estimates be tested as sensitivity parameters in any chamber or atmospheric modeling studies performed in this project. We may also note that there is another photolytic compound in the CBM-IV aromatics mechanism, OPEN, which also is assumed to photolyze at a rate tied to formaldehyde photolysis. The OPEN species is a highly generalized species, representing probably ring opened compounds. Given the observation of Carter, mentioned above, it seems reasonable to leave this compound tied to formaldehyde photolysis and allow it to vary along with that compound. It is possible that we may wish to test greater variations for some reason that may become apparent as the project progresses.

Discussion

The day-to-day variability of any consistently applied photolysis algorithm using UNC data appears to be on the order of 10%. (There also appears to be a seasonal variability from summer to late fall of a similar amount, due in part to the fact that the earth is closer to the sun during winter in the northern hemisphere). Given that these estimates are tied to variations in solar UV and TSR measurements, it seems likely that this is a real variation that applies to atmospheric situations such as urban smog formation. Changes in

atmospheric turbidity and thin, high level clouds seem to be the major causes of such day-to-day variability.

The discovery that an entire development program failed to discern a 10% difference between UV and TSR derived data suggests that a difference of this magnitude cannot play a significant role in smog chamber validation; therefore we are confronted with an additional uncertainty on top of the (probably real) day-to-day variability of solar flux. For the purposes of our sensitivity studies, we suggest that these two uncertainties (each of which is at least 10%) may be additive.

Finally, there is a substantial uncertainty involved in the comparison of smog chamber actinic flux estimates and photolysis rates to the atmosphere. Carter (1991) has estimated the uncertainty of light flux for the UCR OTC as 15%, with a substantial fraction of this uncertainty being due to the uncertainty of inside/outside flux. We consider this to be a reasonably conservative estimate of this uncertainty factor.

If we were to simply add these uncertainties, we would arrive at a minimum uncertainty of photolysis estimates of roughly 25%, with some photolysis rates (e.g. higher aldehydes) being much higher, as much as the difference between acetaldehyde and propionaldehyde estimates i.e. a factor of four.

Thus for our general sensitivity analysis, we propose to vary the photolysis rate of each class of important compounds (NO2, formaldehyde, acetaldehyde, higher aldehydes, methyl glyoxal and OPEN) by a minimum of 25%, both individually and in tandem.

Figure 1

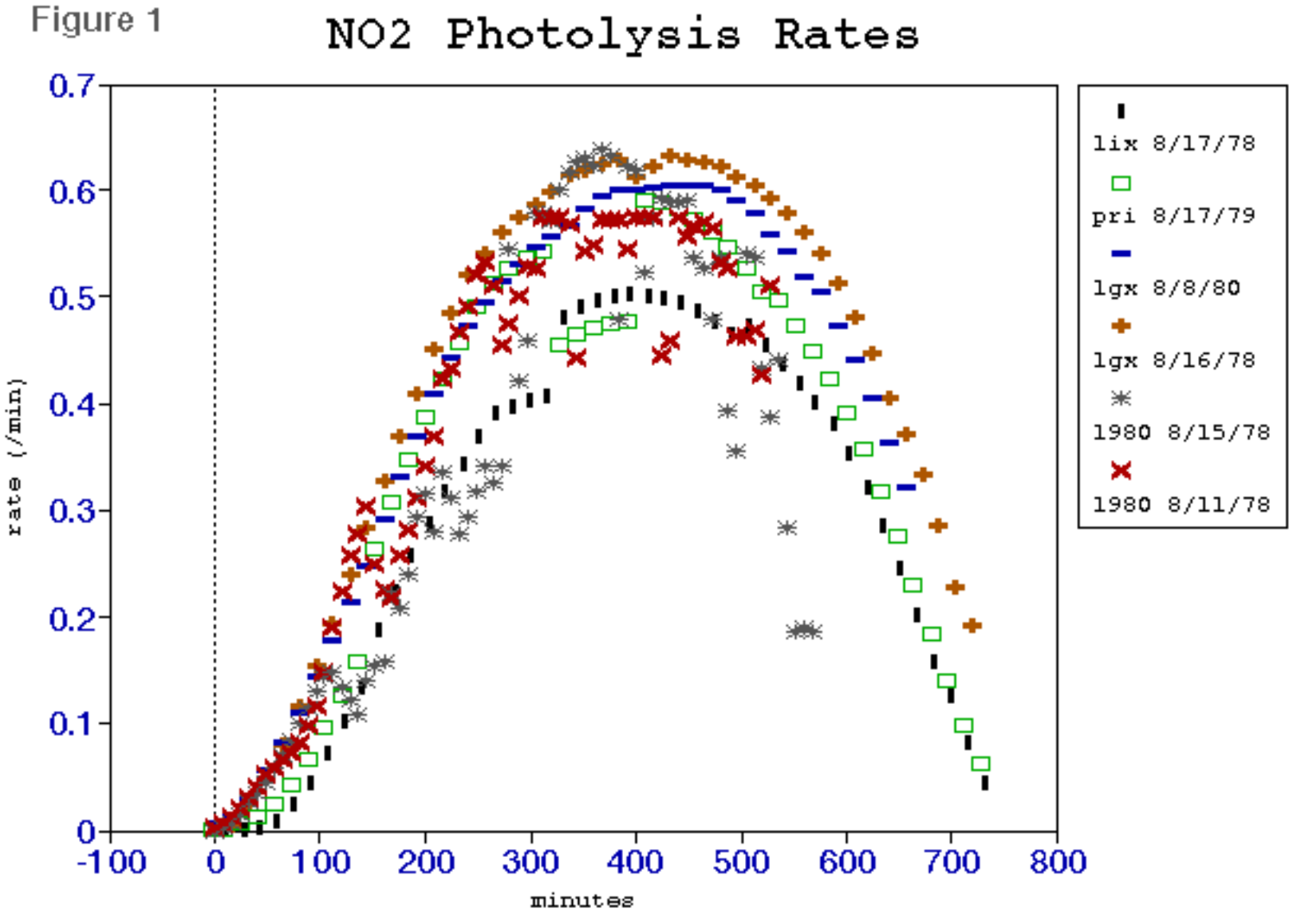
NO2 Photolysis Rates
0.7
0.6
0.5
0.4
0.3
0.2
0.1
0
rate (/min)
-100
0
100
200
300
400
500
600
700
800
minutes
lix 8/17/78
pri 8/17/79
lgx 8/8/80
lgx 8/16/78
1980 8/15/78
1980 8/11/78

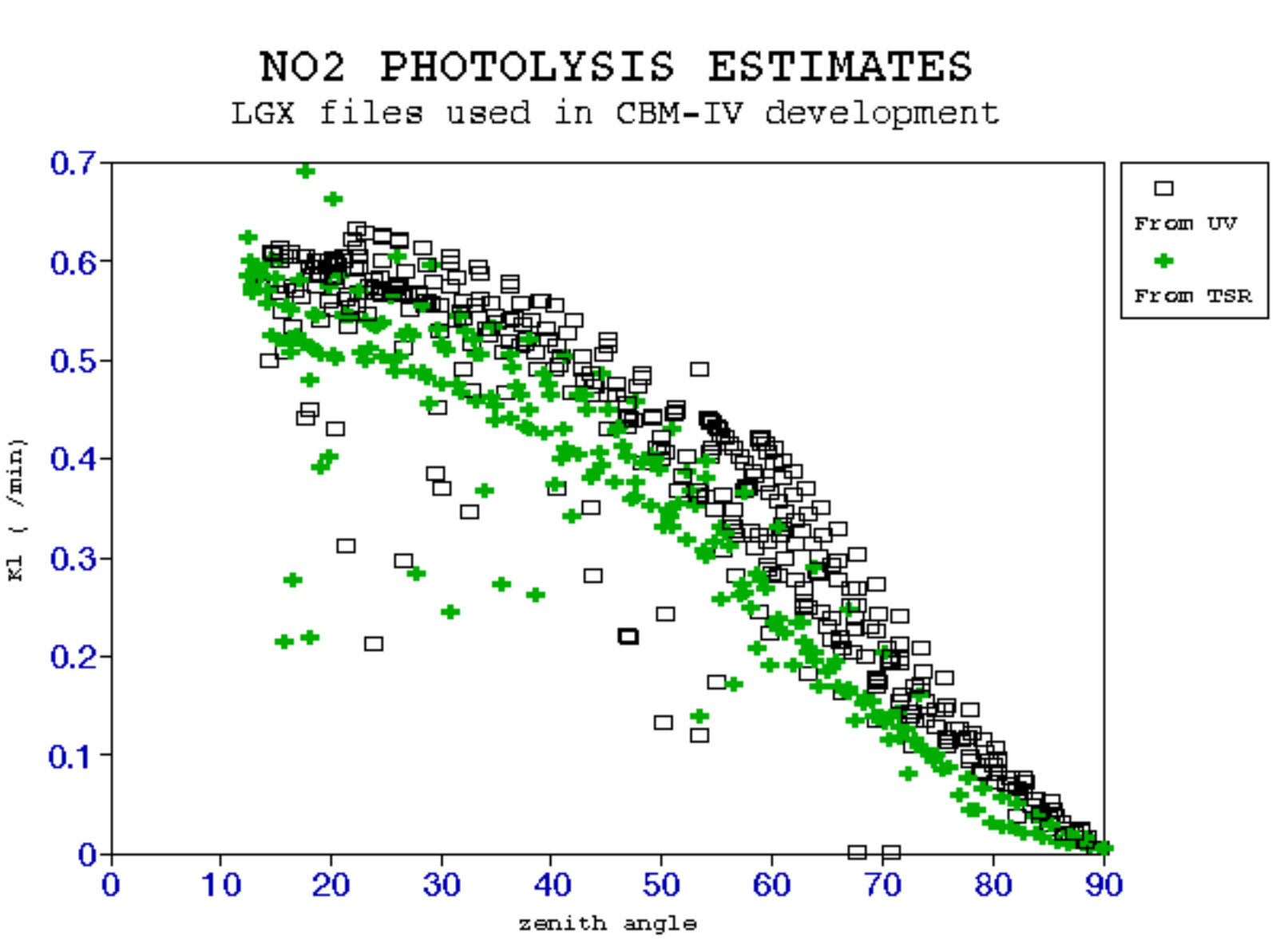
NO2 PHOTOLYSIS ESTIMATES
LGX files used in CBM-IV development
K1 (/min)
0.7
0.6
0.5
0.4
0.3
0.2
0.1
0
0
10
20
30
40
50
60
70
80
90
zenith angle
From UV
From TSR

UV VS TSR

UNC TOWER DATA

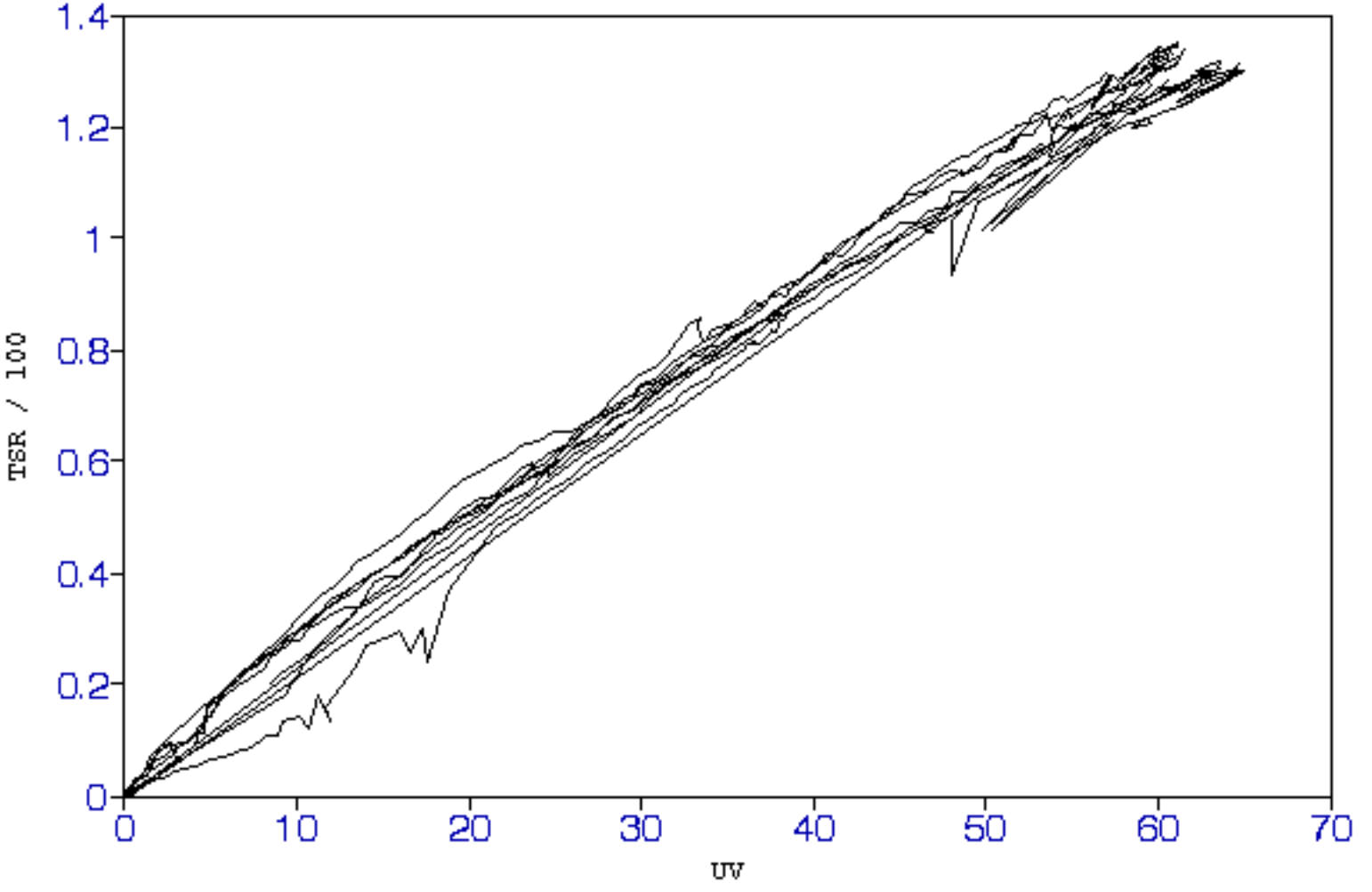

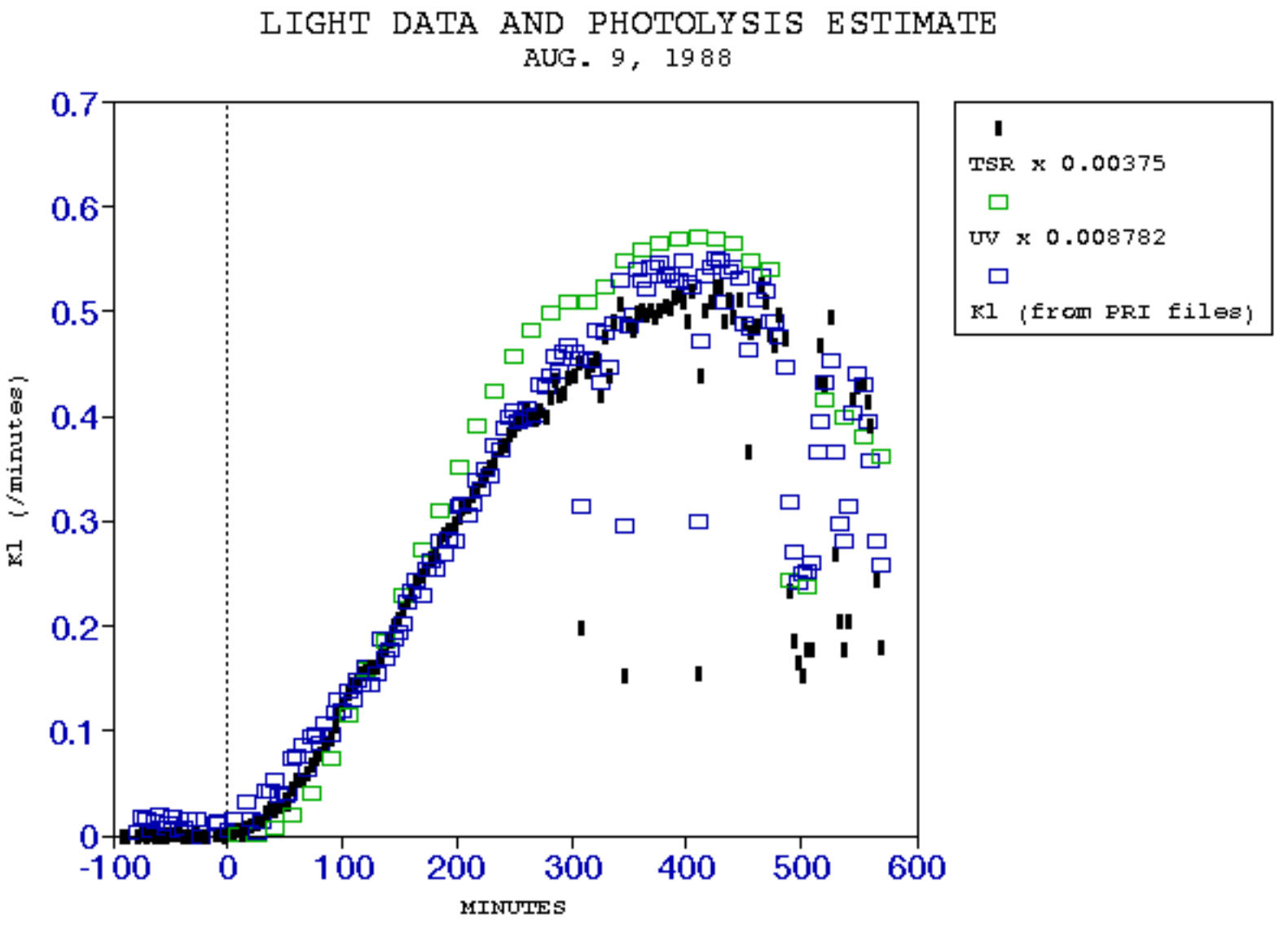
LIGHT DATA AND PHOTOLYSIS ESTIMATE
AUG. 9, 1988
0.7
0.6
0.5
0.4
0.3
0.2
0.1
0
Kl (/minutes)
-100
0
100
200
300
400
500
600
MINUTES
TSR x 0.00375
UV x 0.008782
Kl (from PRI files)

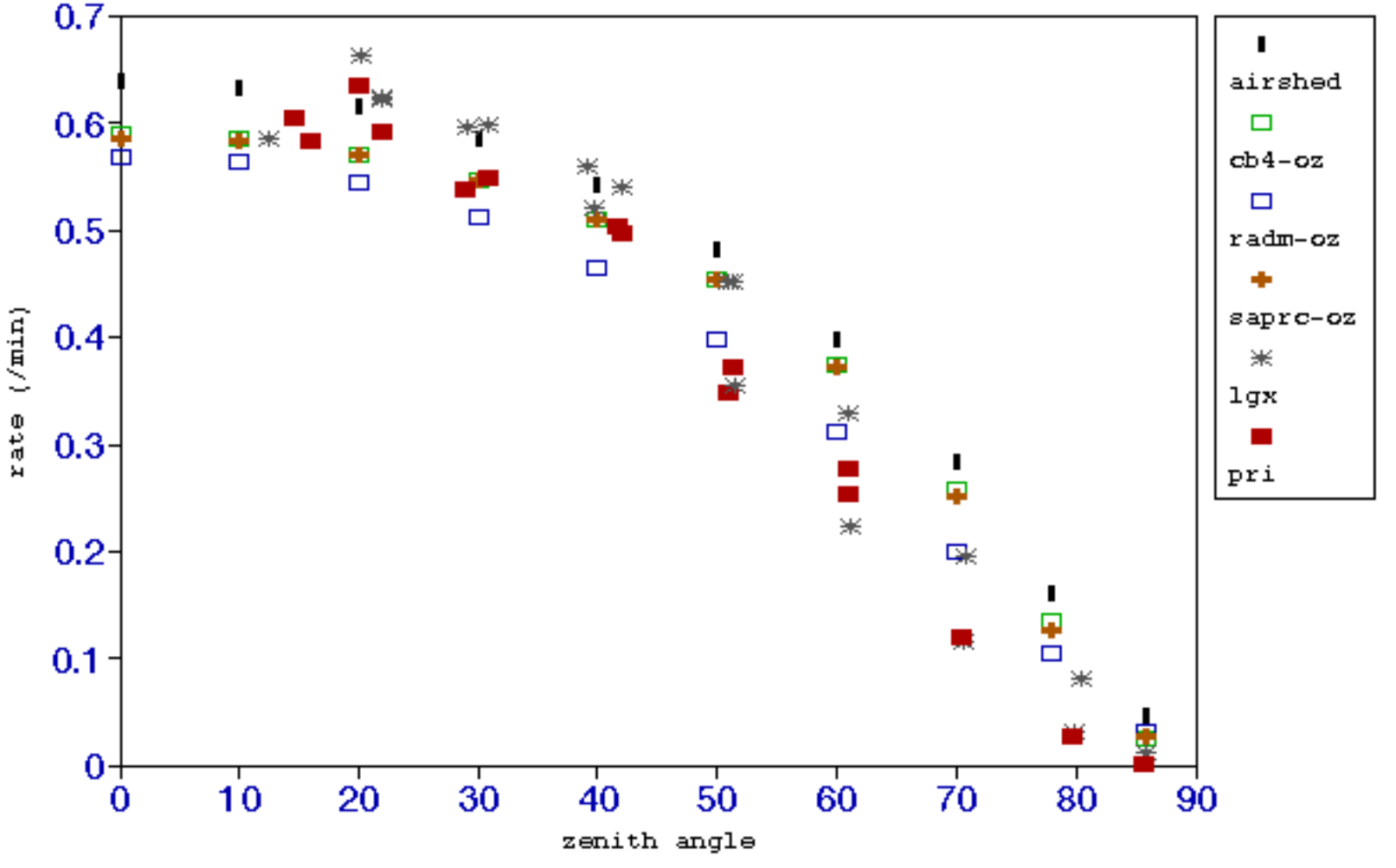
NO2 PHOTOLYSIS
(atmospheric and chamber modeling)
rate (/min)
0.7
0.6
0.5
0.4
0.3
0.2
0.1
0
0
10
20
30
40
50
60
70
80
90
zenith angle
airshed
cb4-oz
radm-oz
saprc-oz
lgx
pri

HCHO PHOTOLYSIS ESTIMATES

LGX files used in CBM-IV development

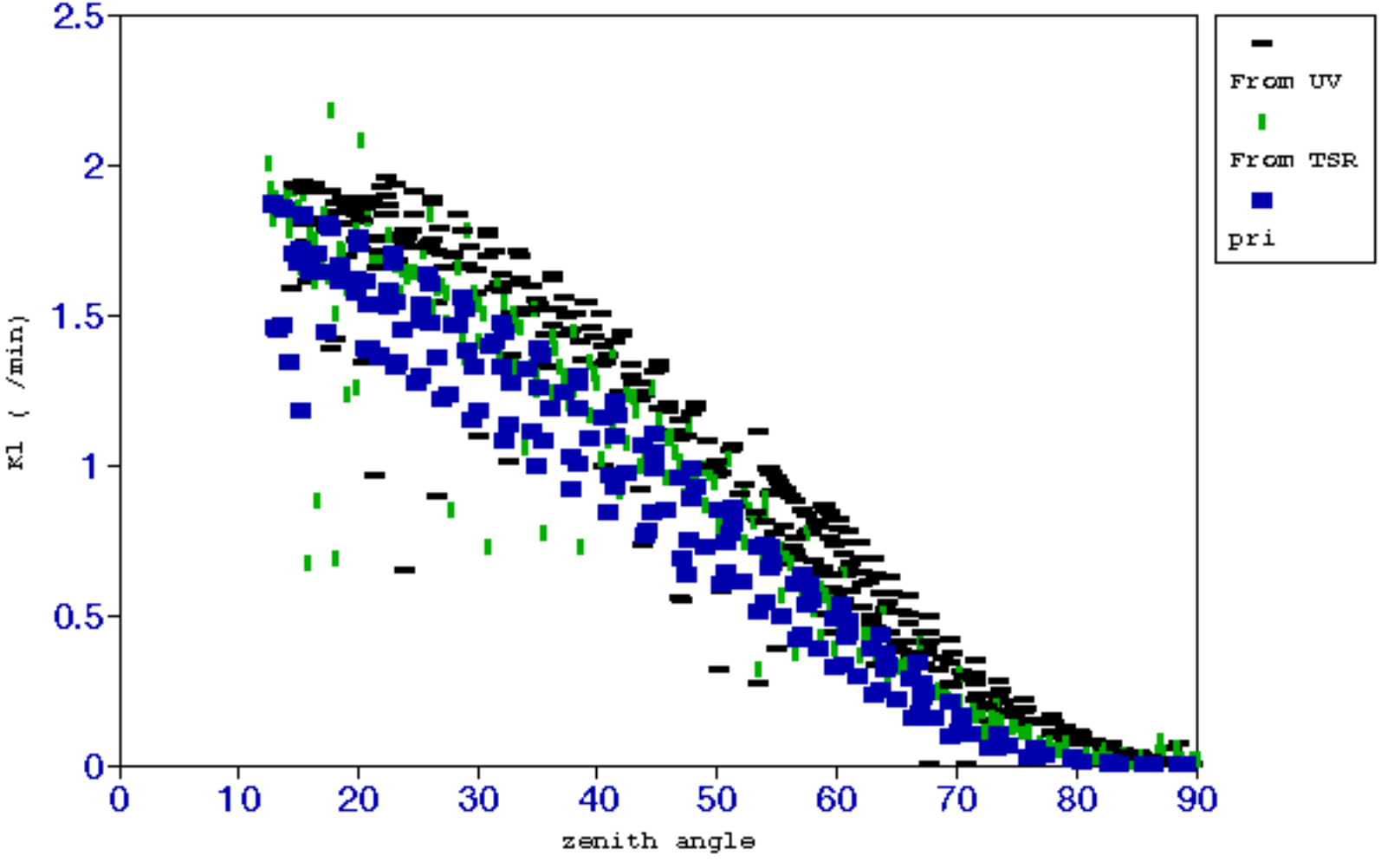

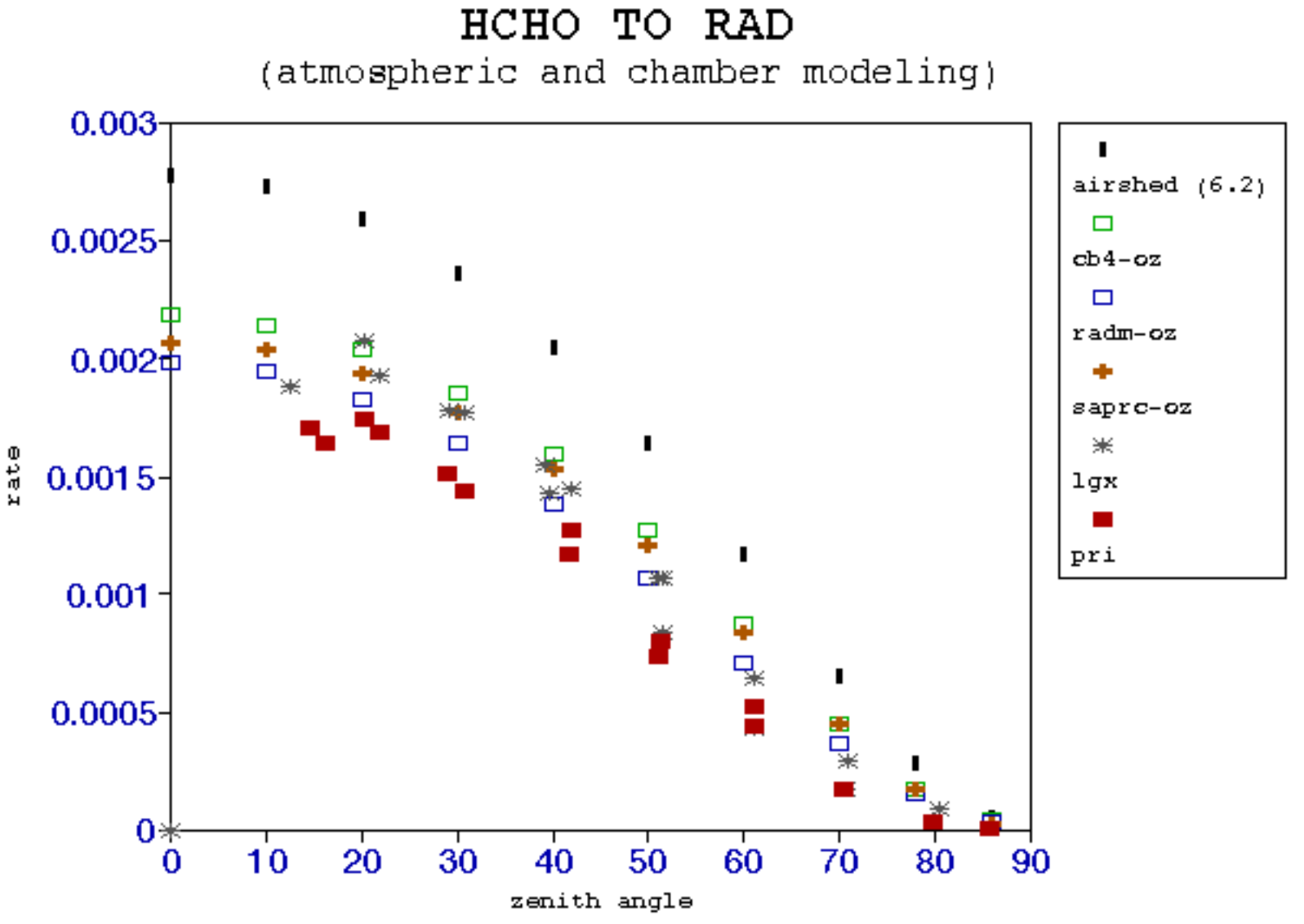
HCHO TO RAD
(atmospheric and chamber modeling)
0.003
0.0025
0.002
0.0015
0.001
0.0005
0
rate
0
10
20
30
40
50
60
70
80
90
zenith angle
airshed (6.2)
cb4-oz
radm-oz
saprc-oz
lgx
pri

HIGHER ALDEHYDE PHOTOLYSIS ESTIMATES

LGX files used in CBM-IV development

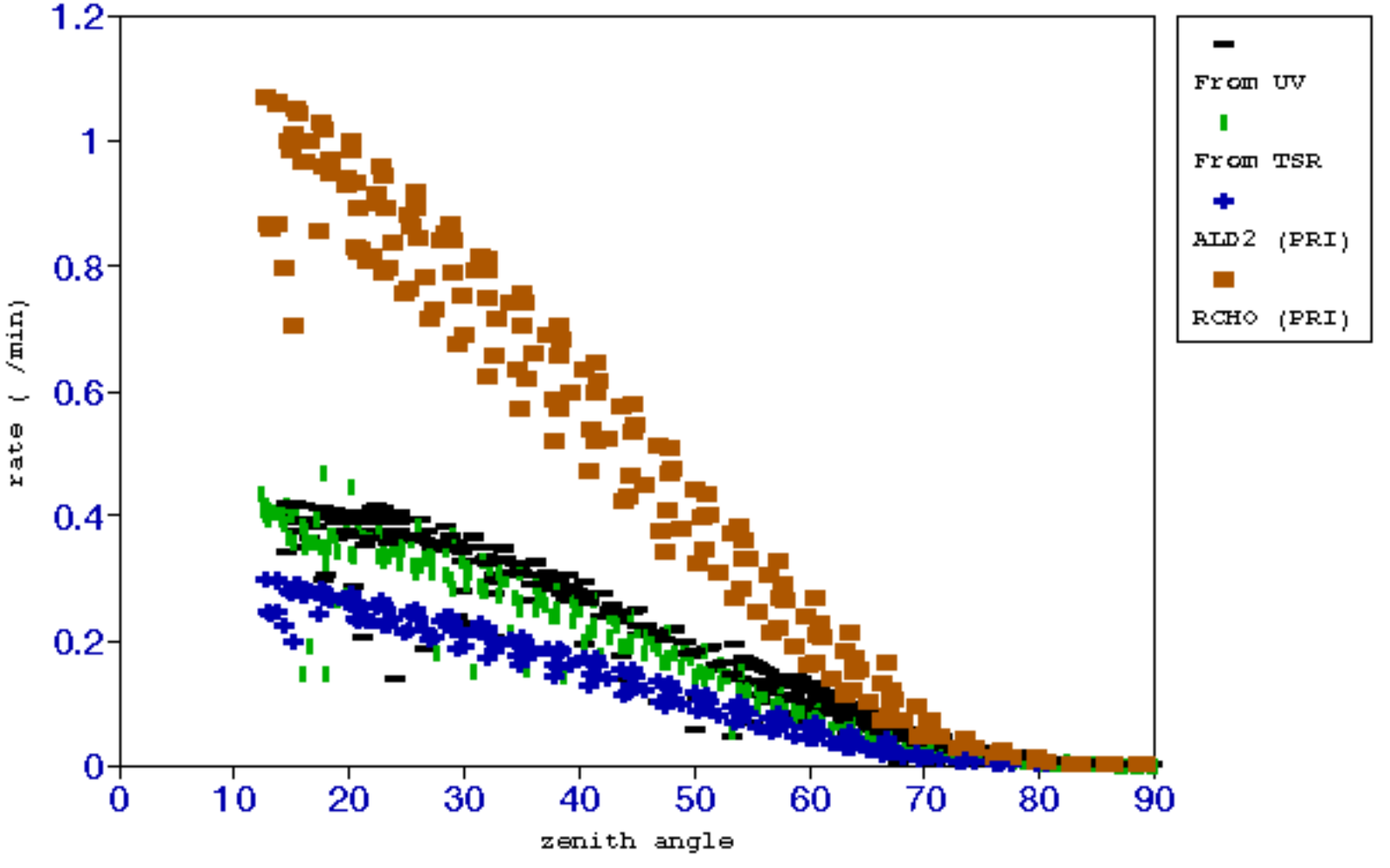

MGLY PHOTOLYSIS ESTIMATES

LGX files used in CBM-IV development

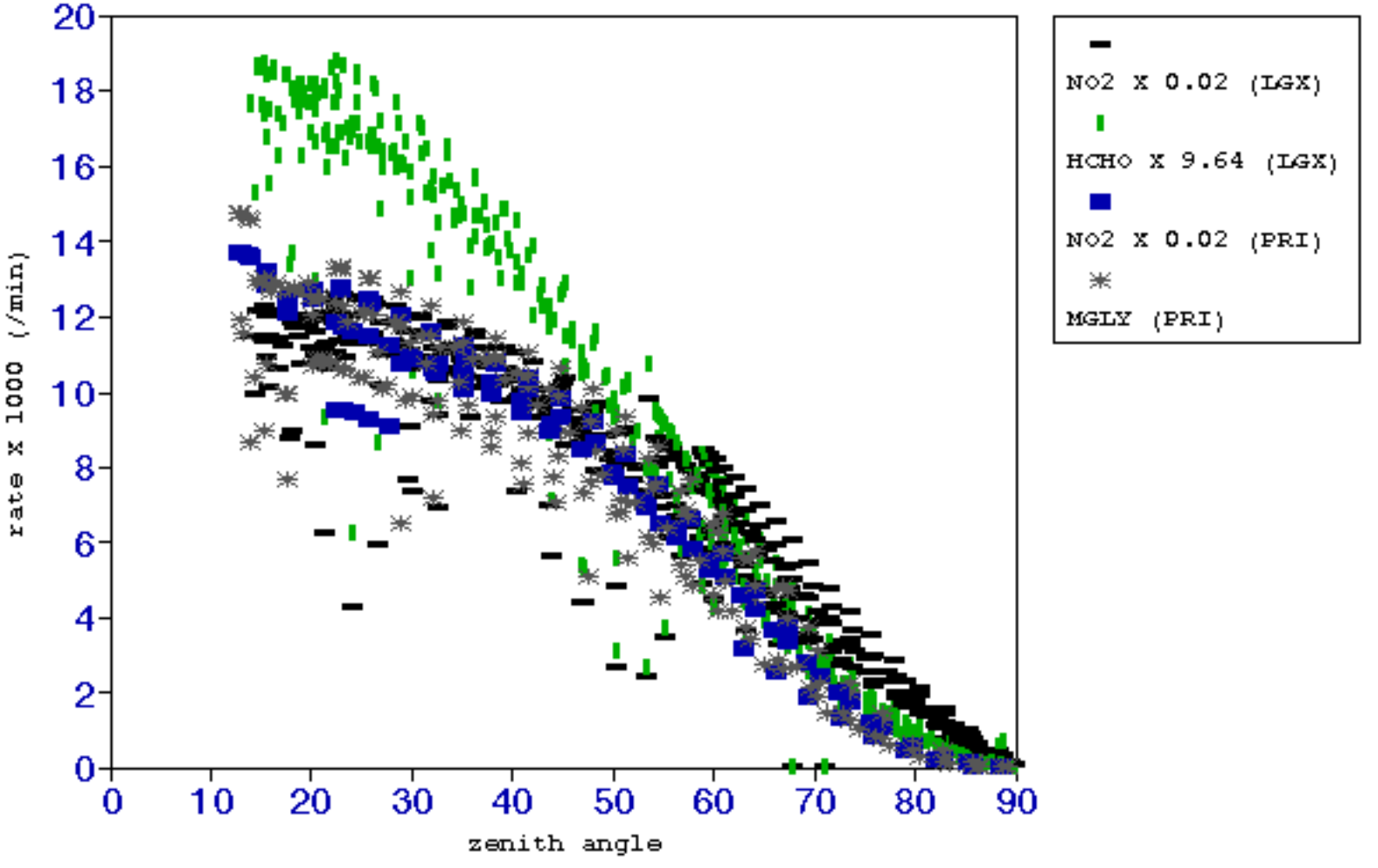

APPENDIX C

PROTOCOLS FOR MODELING SMOG CHAMBER EXPERIMENTS WITH KINETIC MECHANISMS

SUMMARY

From a database of nearly 2000 smog chamber experiments approximately 100 will be simulated by essentially three chemical mechanisms: the standard Carbon Bond-IV (CB-IV) as used in the Urban Airshed Model (UAM), plus high and low radical-flux alternative versions of this mechanism. The standard will be tested to provide a measure of how well the original mechanism performs on this particular database. The two alternative versions will be adjusted by increasing or decreasing radical fluxes within the bounds of uncertainty to maintain an acceptable range of performance. Radical fluxes will be maximized by using the highest known radical source and sink estimates, and the minimum flux will be similarly determined by using the lowest radical source and sink estimates available. The procedures to be used to account for chamber effects like light source inputs, background pollutants, and wall interactions are described below. Also some discussions are given about applying the hierarchical principles to adjust the sub-sets (e.g., aromatics reactions) used in the alternate versions of the chemistry.

INTRODUCTION

Kinetic mechanisms used for simulating photochemical smog formation in regulatory models such as the Urban Airshed Model (UAM) are evaluated using data from smog chamber experiments. Before being published in the *Journal of Geophysical Research* the Carbon Bond mechanism version four (CB-IV) was tested against 170 experiments involving three different smog chambers. The U.S. Environmental Protection Agency, who sponsored the development of the CB-IV, also carefully reviewed the protocols used to evaluate this mechanism before recommending its use in regulatory applications of the UAM.

The California Air Resources Board has designed the present study to develop alternative versions of the CB-IV that, on one hand, fall within the range of published mechanistic uncertainties and still meet some measure of acceptable performance for simulating a smog chamber database, but, on the other hand, provide different estimate of control strategy effectiveness when used in the UAM. These different control strategy estimates will then define a measure of the bounds of uncertainty that might exist in regulatory applications of the UAM, due solely to uncertainties in the CB-IV itself. Therefore, the protocols described in this document play a key role in this project; these protocols are intended to describe the smog chamber database to be used, to outline the procedures to be used to simulate that database, and to define the measures of acceptable simulation performance.

In a previous report (the Task 2 report of 17 January 1997) the development of the alternative mechanisms was described. These alternative versions of the CB-IV are called the high and low

radical flux versions. Since the original CB-IV was developed and tested against a smog chamber database using a hierarchical approach, the high and low radical flux alternates to the standard CB-IV are to follow a similar stepwise validation path. Thus, the database must have a sufficient number of experiments at each of these hierarchical steps. In addition to an adequate number of experiments at each step, a reasonable range of VOC-to-NOx precursor ratios also would appear to be important. Finally, a database involving several smog chamber facilities provides more confidence than using data from only one chamber.

THE DATABASE

Smog Chambers

There are two basic types of smog chambers, classified according to the nature of the light source used to drive the photochemical reactions: artificial or natural light. As a rule, the artificial light smog chambers (sometimes called "indoor" chambers since they are usually installed in indoor laboratories) induce a constant rate for each photolytic species of interest, and the temperature in such chambers tends to be more stable and reproducible than in natural light chambers. Natural light chambers are often called "outdoor" chambers, since the natural light source is sunlight. Outdoor chambers experience highly variable light and temperature profiles, offering conditions that more closely mimic the actual conditions of atmospheric modeling.

Both types of smog chambers offer distinct advantages to the process of kinetic mechanism development and evaluation. Experiments in constant light chambers yield kinetic systems that are simpler than natural light chambers, and for that reason are particularly well-suited for analyzing specific kinetic subsystems and even individual reactions. Indeed, an artificial light smog chamber may be viewed as a very large kinetic vessel, and such chambers are often used in experiments used to elucidate individual kinetic rate constants. The UCR evacuable chamber is regularly employed for the purpose of examining relative hydrocarbon decay rates, for example.

Outdoor chambers employ the sun as a light source and therefore experience photolysis rates that are, within the limits of the phototransmissivity of the material from which they are constructed, the same rates that would affect an atmospheric photochemical system. This makes outdoor chambers well-suited for the estimation of photolytic parameters, and also for the validation of kinetic mechanisms.

In general then, the CBM development team has used data from artificial light chambers for the design and development of kinetic mechanisms and data from outdoor chambers for the validation and verification of those mechanisms. This is only a generalization, of course, since data from artificial light chambers may serve verification purposes, and there are numerous circumstances where outdoor chambers may serve a kinetic design purpose. It is, for example, fairly easy to use outdoor chamber data to derive relative decay estimates for various hydrocarbons, which may be used to estimate reaction rate parameters in a fashion similar to artificial light chamber experiments.

Since this project is not a project to design or develop new kinetic mechanisms, but rather to estimate plausible uncertainties for use in atmospheric modeling sensitivity studies, we would anticipate a greater dependence upon outdoor chamber data than artificial light chamber data. Simply put, the greatest uncertainty in relating artificial light experiments to the atmosphere is in the relevant photolysis rates, and this uncertainty is not as great for outdoor chamber experiments. Use of artificial light chamber data, therefore, might well yield "translation" uncertainties that are unrealistically high.

There are some specific rate constant uncertainties, however, (e.g. the OH + NO2 reaction), which may be profitably examined using artificial light chamber data, and we will employ such experimental data when it seems relevant to the problem at hand. We currently have access to one set of artificial light chamber data (the UCR database, from several different chambers, employing several types of artificial light sources), and there may be another set of data forthcoming from the Tennessee Valley Authority smog chamber.

The data available from the smog chambers at UCR is summarized in Table A-1. There are over a thousand experiments available at this time. From the University of North Carolina (UNC) there are currently over 800 experiments available. These are summarized in Table A-2.

The majority of the chamber modeling on this project, however, will be using outdoor chamber data, primarily from the University of North Carolina outdoor smog chamber (there is another outdoor chamber at UCR, the OTC, but the nature of that chamber -- deformable teflon bags -- makes light characterization somewhat more uncertain than for the UNC chamber). We will now describe certain technical details important to the modeling of the UNC chamber, details which generally fall under the heading of "chamber effects."

Experiments to be modeled

We have three specific objectives to be accomplished in the chamber modeling phase of this contract. These are

1>Model photolytic species to estimate uncertainties in photolysis rate estimates

2>Verify that the CB-IV mechanism accurately simulates the original CB-IV validation set with the latest UNC photolysis rate estimates

3>Calibrate the high and low flux alternatives of the CB-IV at various hierarchical levels. There are two alternative definitions of “calibration” in this context: first, if a mechanism directly simulates the database within acceptable bounds, then the “calibration” is the measure of the agreement as indicated by the statistical mean error and standard deviation compared to observed ozone or other measured pollutants; second, if some adjustments must be made to bring an alternative form of the mechanism within acceptable bounds, then “calibration” is taken to mean the necessary adjustments.

We want to minimize the number of experiments to be analyzed so as to focus on those which define the uncertainty range. Many of the experiments used in the CB-IV validation study involved days where the light was less than ideal (e.g. cloudy) and need not be extensively analyzed. Also, testing to check that current implementations of CB-IV and its ancillary photolysis rates still give acceptable results can be accomplished with a subset of the original validation set. We anticipate that fewer than 20 experiments will be needed to accomplish the first task noted above and a similar number should suffice for the second, provided there has been no great alteration of CB-IV behavior, which appears to be the case at this time. Experiments from other chambers, such at TVA or UCR will be simulated whenever there is a specific question that may be answered using that data set. Generally, then, we expect the chamber modeling phase of this project to involve no more than 100 simulated experiments, although there may be more than one simulation for any given experiment in order to assess uncertainty limits.

SIMULATION PROCEDURES

Chamber effects in the UNC chamber

Chamber specific effects may be roughly divided into four categories:

>Wall related effects
>Background air effects
>Light effects
>Temperature and water effects

Let us consider each of these categories in turn.

Wall related effects

Chamber walls instigate three types of phenomena important to photochemical kinetics. The walls may act as a sink for various compounds; the walls may act as a source for various compounds; and the walls may serve as a catalyst for some kinds of chemical reactions. Needless to say, these three activities may act in concert, in that compounds which have been absorbed by the chamber walls (sink) may later return to the gas phase (source), often modified by the time on the chamber walls (catalysis).

Investigators at UNC recommend a standard set of wall-effects reactions for modeling UNC chamber data:

WallNO2a]	NO2	=	HONO			#K1*2.5E-3
WallNO2b]	NO2	=	0.50*HONO	+	0.50*WHNO3	#1.6E-4
WallNO2c]	WHNO3	=	NO2			#K1*2.0E-3,
WalN2O5a]	N2O5	=	2.0*WHNO3			#2.5E-3,

```
                        {Tuazon 83 "dry" Rate}
WalN2O5b]       N2O5 + WH2O  =   2.0*WHNO3          #2.3E-7@2000; {1.9E-4}

WallH2O2]       H2O2       =                        #4.0E-2, {UNC measured}
WallO3]         O3         =                       #1.4E-4, {UNC measured }
WallHNO3]       HNO3       =     WHNO3             #2.0E-4; {UNC estimate}
```

(reaction rates are in ppm-min units)

In this reaction scheme, the walls are a source of radical precursors only when NO_2 is present, although the walls are taken to emit NO_2 itself in small quantities in the presence of sunlight. There is ample evidence to suggest that the walls emit HONO directly under some circumstances, (See Killus and Whitten, *IJCK*, 22: 547, 1990)especially if liquid water condensate is seen prior to the loading of the chamber, and UNC investigators now take considerable care to dry the chamber prior to loading for this reason. The HONO emissions from this source take the form of a pulse of HONO early in the experiment, similar to the effects of an initial condition of HONO in the gas phase, but more drawn out, and a delayed pulse process was simulated in the original CB-IV development work, to model experiments where the "dry down" technique had not yet being used by UNC investigators. If a HONO release wall process takes place to a lesser degree even in a relatively dry chamber, it would be difficult to distinguish this effect from an initial HONO concentration. However, this confounding of effects has little impact on modeling practice or on the assessment of simulation results.

UNC investigators also recommend an assumed contamination level due to the background air with which the chamber is loaded and which constitutes the dilution mixture:

```
ENTRAINMENT
  = 0.50*CO + 0.07*O3 + 0.58*H2 + 1.79*CH4 + 0.002*HCHO +
0.045*BVOC                                              #DL*Dilution,
BACKGROUND
        OH + BVOC      = 0.667*XO2 + 0.667*HCHO + 0.667*HO2 +
                         0.167*C2O3 + 0.001*PAR          #4444.4
```

Assuming that the dilution air is similar to the air with which the chamber is loaded (there may well be differences in the initial ozone burden), there is a minimum initial loading of HCHO in the chamber of 3 ppb, which is similar to the amount needed to simulate background reactivity experiments that have been conducted in the UNC chamber. In typical high reactivity experiments, the background air reactivity burden is inconsequential; however, under low reactivity conditions (low HC to NOx ratio experiments), the background reactivity can be important, and thus may have implications for control strategy estimation, in the same way that background air reactivity can dominate control calculations in urban simulations. Thus, it is important to consider any uncertainty in background air estimates as one of our concerns in this project.

Temperature and water effects

The variability of temperature in the UNC chamber has demonstrated a phenomenon of potentially great importance to atmospheric smog chemistry: that of PAN decay. Since PAN and related compounds decompose to their radical and NO_2 constituents, it is possible under some circumstances for PAN decomposition to provide reactive precursors for ozone formation. Since this decomposition generally occurs under conditions of rising temperature (due to the strong temperature dependence of the PAN decomposition reaction), ozone formation from PAN decay generally occurs when temperatures increase. In some olefin systems such as isoprene, ozone may even show a double peak, with primary NOx being exhausted while unreacted isoprene still exits to deplete ozone, then when temperatures rise, PAN decay provides precursors for net ozone formation to resume (See Killus and Whitten, *ES&T*, 18: 142, 1984).

A recent communication from UNC (Sexton, private communication to James Killus), indicates that a significant change was observed in UNC chamber behavior with regards to temperature after the teflon film walls were replaced a couple of years ago. Specifically, the older chamber walls had significant IR absorption characteristics and experiments in that chamber ran very warm, 5-10 degrees above the later chamber temperatures using the replacement teflon film. There also appears to be a significant change in the ability of the CB-IV mechanism to simulate chamber experiments at the time of the replacement. We will examine this phenomenon to see if it leads to any significant uncertainties in atmospheric modeling.

Changes and variations in water vapor concentrations in smog chamber experiments seem more benign, except in cases (noted above) where liquid was present on the chamber walls, leading to HONO emissions from poorly understood processes (probably involving nitrate conversion in aqueous phase). To be sure, there are several water dependent processes affecting smog chamber experiments (e.g. O^1D reaction to OH and N_2O_5 hydrolysis), but these reactions do not seem to be of sufficient importance to create significant differences among smog chamber experiments having different water vapor levels.

Light effects

We have already described the photolysis rate calculation procedures at UNC in our previous report. We note here that as a result of our analysis of UNC photolysis estimates (PRI files obtained from UNC), UNC is now recalculating a number of those estimates in which the aerosol characteristics may have been erroneously assumed. We are in the process of learning to use the UNC chamber light model, and we will rerun the light model for any experiments which seem questionable to us, as a further QA on this critical set of parameters.

MECHANISM TESTING

The Hierarchical Scheme of Mechanism Design and Testing

As noted in our earlier reports, the CBM development team undertakes a specific protocol for both mechanism design and validation. This protocol is usually called the Hierarchical Method, since it places mechanism subsystems and smog chamber experiments in an explicit hierarchy of assessment, with a compound or mechanism subsystem having greater weight if it appears in other systems. For example, the inorganic chemical reactions (e.g. NOx, HOx) appear in every smog chamber experiment, so those reactions are at the top of the hierarchy and so must be fixed early in the development process. Certain hydrocarbon oxidation products (especially photolytic compounds such as HCHO, but also including compounds such as PAN, see above) are common to a number of different mechanism subsystems, so the chemistry of those products must be fixed before the parent compounds may be studied.

The uncertainty analysis in this project parallels the design process. The difference being that in mechanism design, the most probable values of each reaction are first selected, and then each mechanism subsystem is adjusted to give the best simulation on the selected design experiments. However, in an uncertainty analysis, the range of reaction values are considered, with the maximum allowed range being that which allows experimental simulation to be adequate rather than optimal. In practice, many reactions do not have a significant effect on the overall chemistry even when varied over the entire range of their uncertainty, and of those that do have an effect, only certain critical reactions appear worth considering in detail. We have elected to focus specifically on two types of reactions: radical sources and radical sinks, with photolysis reactions being the main example of the former, and the OH + NO2 reaction being the most important example of the latter. When both radical sources and sinks are increased, the overall radical flux through the smog system is expected to increase, with steady state radical levels remaining roughly the same as for lower flux conditions. We have prepared theoretically extreme "high flux" and "low flux" mechanisms to test the extent to which the radical flux may be varied and still retain reasonable fits to experiments. This will allow the application of these two extreme cases to atmospheric simulations to see the effects of radical flux on control strategies.

In addition to the radical flux concept, uncertainties in photolysis suggest that radical production per se is also uncertain, both in smog chambers and in the atmosphere. Variations in the photolysis rates of important compounds give overall smog chemistry that is of greater or lesser reactivity, and such variations in overall reactivity are known to cause variations in control strategy predictions. The effects of this uncertainty in reactivity could be examined now under Task 1.5 (Box Model Sensitivity Studies), without recourse to smog chamber experiments, since a significant source of uncertainty is the difference between chamber conditions and atmospheric conditions.

Analysis of experimental results

A substantial part of the analysis of smog chamber simulations is not specifically quantitative, since there is no good figure-of-merit for the goodness-of-fit in curves describing non-linear systems, especially systems with inconstant inputs (e.g. photolysis in sunlight driven systems). An ordinary least squares analysis, for example, may give a poor grade to curves whose only flaw is a time offset. The task of estimating the adequacy of a simulation fit is to a great extent a matter of

pattern matching, and human judgment is better at such pattern matching than algorithmic schemes. For that purpose, graphical display is the best method of assessment, and it has been our practice to rely heavily on ordinary time plots of smog chamber data and simulation results.

However, some aspects of the assessment process are amenable to quantitative assessment, especially those relating to peak observations. To that end, both scatter plots and ordinary linear regression of peak pollutant behavior have proved quite useful in mechanism assessment.

Of equal importance is the selection of species of interest. Ozone, of course, is the major air quality criteria pollutant in photochemical systems. However, we tend to give an almost equivalent weighting to PAN predictions and observations when analyzing data sets. This is because PAN may easily act as an ozone surrogate, in that ozone formation may be limited by competition from PAN formation (which may serve as a temporary sink for both NOx and radicals), and, as noted above, with rising temperatures PAN may decay to form ozone. From a mechanistic viewpoint, it is far too easy to improve ozone predictions by allowing greater errors in PAN formation. Yet in some circumstances involving the real atmosphere, PAN formation may dominate later behavior in the photochemical system. For example, PAN is often the main species of NOx transport into rural areas, and may be critical in regional transport scenarios.

Thus, we place primary importance to the ability of simulation models to adequately track the formation of both ozone and PAN in experimental systems. For a similar reason, we attempt to obtain as close a match to observations of hydrocarbon decay as possible, since hydrocarbon decay is an estimator of OH concentration, and OH levels dominate the system behavior. Moreover, hydrocarbon oxidation is what drives the photochemistry. Therefore, a good simulation fit to all other data is worthless if the hydrocarbon decay data is poorly described.

Of the remaining compounds of interest, we generally pay attention to important photolytic products, especially formaldehyde (HCHO), because it is central to radical initiation and also because it is a toxic compound of interest in itself. However, HCHO is difficult to measure and errors in HCHO concentration are not as critical to the overall photochemical process as the other compounds noted above. Therefore, we place less emphasis on HCHO concentrations than we do for ozone, PAN, and hydrocarbon decay in mechanism assessment.

Constant light chambers provide simulations that yield certain rates as fairly stable figures-of-merit, especially NOx oxidation behavior. Carter has suggested the rate of change of NO-O3 as one such figure-of-merit, especially in combination with the rate of hydrocarbon decay. In any simulations involving the UCR constant light chambers, or if the TVA chamber data becomes available, we anticipate adding this figure-of-merit to our analytical procedures.

Conclusion

For the modeling phase of this project, we anticipate concentrating primarily on data from UNC, specifically to address questions about photolysis rates, mechanism sub-units (e.g., aromatics chemistry), and the question of "low radical flux" vs "high radical flux" mechanisms. We

anticipate on the order of 50-100 modeled experiments, with the results presented both graphically and the ensemble compound peak results presented statistically. Results from the uncertainty analysis will then be used in atmospheric simulations of urban cases to assess the effects of uncertainty on control strategy scenarios.

				Initial NOx			Carbon			Run time	Max O3		(See below for codes)			
RunID	Classification		Data base status	ppm	unc		ppmC	unc		(min)	(ppm)	(min)	Cond-itions	Char. set	Model-able	Inp File
EC390	CHAR-0									360	0.063	345	d	11		
ITC940	CHAR-0			0.014	370%					360	0.073			10		
ITC973	CHAR-0									360				10		
ITC1008	CHAR-0									390	0.088			11		
ITC1552	CHAR-0		higher quality HCHO	0						360	0.054			12		
ETC045	CHAR-0			0.012	23%					465	0.083			1		
ETC057	CHAR-0			0.010	29%					360	0.051	345		1		
ETC151	CHAR-0									1110	0.077			2		
ETC320	CHAR-0									360	0.029			2		
ETC374	CHAR-0									405	0.002	345		3		
ETC458	CHAR-0									375	0.045			3		
ETC485	CHAR-0						0.01	15%		360	0.034	330		3		
DTC049A	CHAR-0									370	0.037			1		
DTC049B	CHAR-0									370	0.033			1		
EC353	CHAR-0		problems	2						240	0.099			1		
ETC141	CHAR-0		problems	2						1290	0.062	465		2		
ETC205	CHAR-0		problems	3						870	0.036			2		
ITC642	CHAR-0									360	0.044	345		5	3	no
EC442	CHAR-1			0.482	17%		0.03	6%						1		
EC464	CHAR-1			0.192	17%		0.04	6%						1		
EC597	CHAR-1			0.594	8%		0.04	6%		120	0.002	15		1		
EC599	CHAR-1			3.676	8%		0.03	6%		240			ri	1		
EC608	CHAR-1			0.302	14%		0.23			120	0.005	45		1		
EC612	CHAR-1			0.301	15%		0.38	15%		120				1		
EC613	CHAR-1			0.300	16%		0.04	6%						1		
EC654	CHAR-1			0.870	3%		0.08	4%						1		
EC674	CHAR-1			0.468	5%		0.07	4%						1		
EC680	CHAR-1			0.439	3%		0.07	4%		120	0.000			1		
EC683	CHAR-1			0.480	3%		0.08	7%		120	0.001	60	o	1		
EC686	CHAR-1			0.448	6%		0.08	6%		120	0.002	90	o	1		
EC690	CHAR-1			0.514	4%		0.08	7%					o	1		
EC864	CHAR-1			0.556	4%		0.07	5%		120	0.005	30		1		
EC869	CHAR-1			0.511	5%		0.07	4%		120	0.009	105	o	1		
EC902	CHAR-1			0.511	4%		0.07	4%		120	0.000	30		1		
ITC441	CHAR-1			0.073	20%		0.03	6%		120	0.001	45		2		
ITC443	CHAR-1			0.148	10%		0.07	6%		120	0.004	90		2		
ITC448	CHAR-1			0.077	19%		0.07	7%		120	0.004	105		2		
ITC453	CHAR-1			0.088	17%		0.07	6%		120	0.000			2		

				Initial NOx			Carbon			Run time	Max O3		(See below for codes)			
RunID	Classification		Data base status	ppm	unc		ppmC	unc		(min)	(ppm)	(min)	Cond-itions	Char. set	Model-able	Inp File
ITC463	CHAR-1			0.089	17%		0.07	6%		120	0.000	105		2		
ITC469	CHAR-1			0.086	17%		0.06	6%		120	0.004	30		2		
ITC480	CHAR-1			0.087	17%		0.07	6%						2		
ITC485	CHAR-1			0.083	18%		0.07	6%						2		
ITC490	CHAR-1			0.085	18%		0.07	6%		120	0.005	30		2		
ITC496	CHAR-1			0.090	17%		0.05	6%						2		
ITC504	CHAR-1			0.090	17%		0.07	6%		120	0.000			2		
ITC508	CHAR-1			0.559	3%		0.06	7%		120	0.000		hl	2		
ITC535	CHAR-1			0.552	3%		0.06	4%		120	0.000			3		
ITC539	CHAR-1			0.083			0.06	4%		120	0.008	105		3		
ITC550	CHAR-1			0.134	11%		0.06	4%		120	0.009	75		3		
ITC557	CHAR-1			0.119	23%		0.06	4%		120	0.011	75		3		
ITC563	CHAR-1			0.560	19%		0.05	5%		120	0.009	45		3		
ITC568	CHAR-1			0.132	20%		0.07	5%		120	0.001	15	nb	4		
ITC570	CHAR-1			0.109	22%		0.07	5%		180	0.002	165		4		
ITC577	CHAR-1			0.119	21%		0.07	5%		120	0.002	97		4		
ITC582	CHAR-1			0.085	18%		0.07	5%		120	0.008			4		
ITC588	CHAR-1			0.101	29%		0.07	5%		120	0.004			4		
ITC600	CHAR-1			0.089	17%		0.06	5%		120	0.003	105		4		
ITC605	CHAR-1			0.094	18%		0.08	5%		120	0.003	105		4		
ITC610	CHAR-1			0.089	19%		0.08	5%		120	0.009			4		
ITC614	CHAR-1			0.083	20%		0.08	5%		120	0.003	90		4		
ITC621	CHAR-1			0.282	9%		0.08	5%		120	0.001		nb	5		
ITC692	CHAR-1			0.505	3%		0.07	5%		120	0.000	90	nb	6		
ITC695	CHAR-1			0.487	4%		0.07	5%		120	0.000	60		6		
ITC700	CHAR-1			0.502	3%		0.08	5%		120	0.000			6		
ITC704	CHAR-1			0.504	3%		0.07	5%		120	0.000			6		
ITC707	CHAR-1			0.998	2%		0.08	5%		120	0.000			6		
ITC712	CHAR-1			0.486	5%		0.07	5%		120	0.000	30		6		
ITC714	CHAR-1			0.983	4%		0.07	5%		120	0.000	75		6		
ITC717	CHAR-1			0.520	4%		0.08	5%		120	0.008			6		
ITC731	CHAR-1			0.555	5%		0.07	5%		120	0.000	15		6		
ITC734	CHAR-1			0.279	6%		0.09	5%		120	0.000	30		6		
ITC737	CHAR-1			0.520	5%		0.07	5%		120	0.000			7		
ITC740	CHAR-1			0.554	5%		0.07	5%		120	0.000	15		7		
ITC745	CHAR-1			0.564	5%		0.07	5%		120	0.017	105		7		
ITC749	CHAR-1			0.250	7%		0.08	5%		120	0.007	90		7		
ITC752	CHAR-1			0.562	3%		0.08	5%		120	0.007			7		

				Initial NOx		Carbon		Run time	Max O3		(See below for codes)			
RunID	Classification		Data base status	ppm	unc	ppmC	unc	(min)	(ppm)	(min)	Cond-itions	Char. set	Model-able	Inp File
ITC757	CHAR-1			0.254	5%	0.08	5%	120	0.012	75		7		
ITC760	CHAR-1			0.565	3%	0.08	5%	120	0.003	30		7		
ITC772	CHAR-1			0.441	3%	0.08	5%	120	0.011			7		
ITC776	CHAR-1			0.557	3%	0.08	5%	120	0.001	90		7		
ITC787	CHAR-1			0.248	6%	0.07	5%	120	0.000			7		
ITC789	CHAR-1			0.560	4%	0.08	5%	120	0.000	45		7		
ITC793	CHAR-1			0.521	8%	0.08	5%	120	0.006	15		8		
ITC803	CHAR-1			0.320	8%	0.07	5%	120	0.003	90		8		
ITC808	CHAR-1			0.456	4%	0.07	5%	120	0.002	105		8		
ITC814	CHAR-1			0.529	3%	0.07	5%	120	0.000	75		8		
ITC824	CHAR-1			0.399	4%	0.07	5%	120	0.006	60		8		
ITC861	CHAR-1			0.553	3%	0.08	5%	120	0.000	90		9		
ITC870	CHAR-1			0.347	6%	0.07	5%	120	0.008	90		9		
ITC875	CHAR-1			0.396	6%	0.07	5%	120	0.002	105		9		
ITC878	CHAR-1			0.749	5%	0.11	4%	120	0.008	90		9		
ITC882	CHAR-1			0.689	4%	0.08	5%	120	0.000			9		
ITC884	CHAR-1			0.664	3%	0.08	5%	120	0.001	105		9		
ITC889	CHAR-1			0.351	5%	0.08	5%	120	0.000	30		9		
ITC893	CHAR-1			0.377	5%	0.09	5%	120	0.003	75		9		
ITC924	CHAR-1			0.664	9%	0.10	5%	120	0.011	60	nb	10		
ITC932	CHAR-1			0.532	11%	0.09	5%	120	0.003	105		10		
ITC958	CHAR-1			0.495	11%	0.08	10%	120	0.002	45		10		
ITC964	CHAR-1			0.520	10%	0.08		150	0.001	90		10		
ITC970	CHAR-1			0.446	12%	0.08		250	0.011	105		10		
ITC1004	CHAR-1			0.076	20%	0.08		210	0.012	180		11		
ITC1551	CHAR-1			0.452	7%	0.09		120	0.002	31		12		
ETC046	CHAR-1			0.500	2%	0.14		120	0.000			1		
ETC056	CHAR-1			0.501	2%	0.12		120	0.000			1		
ETC070	CHAR-1			0.541	3%	0.10	8%	120	0.010	60		1		
ETC076	CHAR-1			0.506	3%	0.12	8%	120	0.010	30		1		
ETC112	CHAR-1			0.503	2%	0.10	6%	120	0.005	60		2		
ETC211	CHAR-1			0.505	2%	0.13	5%	120	0.000			2		
ETC212	CHAR-1			0.500	2%	0.06	8%	180	0.001	165		2		
ETC317	CHAR-1			0.505	3%	0.11	7%	120	0.001			2		
ETC380	CHAR-1			0.493	2%			390	0.003	225		3		
ETC462	CHAR-1			0.540	2%	0.02		120	0.005	45		3		
DTC059A	CHAR-1			0.240	0%	0.06	5%	370	0.001	310		1		
DTC059B	CHAR-1			0.241	0%	0.06	5%	370	0.001	320		1		

					Initial NOx			Carbon			Run time	Max O3		(See below for codes)			
RunID	Classification		Data base status		ppm	unc		ppmC	unc		(min)	(ppm)	(min)	Cond-itions	Char. set	Model-able	Inp File
DTC062A	CHAR-1				0.270	1%		0.07	5%		375	0.006		rh	2		
DTC062B	CHAR-1				0.269	1%		0.07	5%		375	0.008		rh	2		
EC519	CHAR-1		minor problems	1	0.496	10%		0.03	6%		120	0.000			1		
EC521	CHAR-1		minor problems	1	0.994	10%		0.03	6%		120	0.000			1		
EC532	CHAR-1		minor problems	1	0.464	11%		0.03	6%		120	0.002	30		1		
EC534	CHAR-1		minor problems	1	0.520	10%		0.03	6%		120	0.000			1		
ITC514	CHAR-1		problems	2	0.590	3%		0.07	6%		120	0.000		hl	2		
ITC942	CHAR-1		problems	2	0.515	11%		0.07	5%		120	0.002	45		10		
ITC949	CHAR-1		NOx imprecise	2	0.269	19%		0.08	10%		120	0.008			10		
ETC213	CHAR-1		Do not model	9	0.494	2%		0.11	5%		120	0.001			2		
EC518	CHAR-1		don't model	9	0.519	11%		0.21			120	0.004	15	d,uv,lt	12	1	
EC436	CHAR-1		No Temp, SD	2	1.866	15%		0.04	6%						0	2	no
EC440	CHAR-1		No Temp	2	0.781	17%		0.07							0	2	no
EC457	CHAR-1		2-part run. No temp.	2	0.497	16%		0.03	6%						0	2	no
ITC782	CHAR-1				0.519	4%		0.03	7%		120	0.010	75		7	3	no
ITC436	CHAR-1		No Temp	2	0.079	19%		0.07	7%		60	0.000		nb	2	3	no
ITC449	CHAR-1		No Temp	2	0.829	2%		0.07	6%		120	0.001	75		2	3	no
EC898	CHAR-1		No k1	3	0.481	5%		0.08	4%		120	0.103			1	3	no
EC662	CHAR-1		Don't model	9	0.457	7%		0.06	4%					uv,o	1	3	no
ITC430	CHAR-1		don't model	9	1.303	4%		0.07	7%		120	0.023	15		1	3	no
ITC475	CHAR-1		reject	99	0.000										2	3	no
EC643	CHAR-1		Don't model	9	0.532	4%		0.07			120	0.008	60		1	9	
EC650	CHAR-1		do not model	9	0.468	5%		0.08	4%					ri	1	9	
EC664	CHAR-1		Don't model	9	0.458	7%		0.05	6%		120	0.995	15		1	9	
ITC428	CHAR-1		don't model	9	0.162	9%		0.08	7%		90	0.002			1	9	
ITC595	CHAR-1		Don't model	9	0.086	17%		0.07	5%		120	0.008	105	o	4	9	
ITC829	CHAR-1		Don't model	9	0.251	6%					120	0.000	15		8	9	
ITC976	CHAR-1		Don't model	9	0.045	113%		0.08			120	0.016	105		11	9	
EC526	CHAR-1		reject	99	0.529	11%		0.03	6%						1	9	
ITC641	CHAR-2				0.000						1090	0.491	205		5		
ITC624	CHAR-2				0.000										5	3	no
ITC697	CHAR-2				0.000						930	1.135			6	3	no
ITC822	CHAR-2				0.000										8	3	no
EC253	CHAR-3							1.16			360	0.134			1		
ITC627	CHAR-3							0.77	10%		360	0.060			5		
ITC892	CHAR-3							0.64	28%		240	0.038			9		
ITC957	CHAR-3							1.51	26%		360	0.076			10		
ITC1009	CHAR-3							1.41	26%		360	0.074			11		

					Initial NOx			Carbon			Run time	Max O3		(See below for codes)			
RunID	Classification		Data base status		ppm	unc		ppmC	unc		(min)	(ppm)	(min)	Cond-itions	Char. set	Model-able	Inp File
ETC319	CHAR-3							1.00	10%		360	0.025			2		
ETC382	CHAR-3							0.69	5%		360	0.039			3		
ITC616	CHAR-3		problems	2				0.75	10%		360	0.044	345		4		
ITC632	CHAR-3		problems	2				0.93	10%		360	0.051			5		
ITC636	CHAR-3		problems	2				0.75	10%		360	0.047	330		5		
ITC639	CHAR-3		problems	2				0.71	10%		300	0.036			5		
ITC825	CHAR-3		problems	2				0.82	10%		180	0.033			8		
ITC974	CHAR-3		problems	2				1.63	26%		360	0.086	345		10		
ITC1558	CHAR-3		problems	2				1.31			360	0.059			12		
ETC379	CHAR-4							0.24	2%		360	0.057			3		
ETC385	CHAR-4							0.28	2%		360	0.001	90		3		
EC250	CHAR-4		problems	2				0.40			360	0.211	345		1		
EC255	CHAR-4		problems	2				0.40			360	0.202	355		1		
ITC625	CHAR-5				0.270	9%		0.07	5%		240	0.005	225	ri	5		
ITC628	CHAR-5				0.323	8%		0.08	5%		240	0.010		ri	5		
ITC634	CHAR-5				0.565	8%		0.08	5%		250	0.000		ri	5		
EC624	CHAR-5		Don't model	9	0.559	15%					330	0.014	315	d,ht	13	1	no
ITC638	CHAR-5	A	minor dataset problems	1	0.303	9%		0.08	5%		240	0.000		ri	5		
EC895	CHAR-6		don't model	9	0.000										0	2	no
EC896	CHAR-6		don't model	9	0.000										0	2	no
EC972	CHAR-6		don't model.	9											0	2	no
EC726	CHAR-6		Don't model	9	0.923										1	3	no
ITC821	CHAR-6		Don't model	9	0.000										8	3	no
EC670	CHAR-7				0.000						280	0.448			0	2	no
ETC483	CO	MRE			0.424	2%		158.39			360	1.164			3		
ETC487	CO	MRE			0.457	2%		110.59			360	1.098			3		
ETC414	CO	MR3			0.547	3%		141.25			360	0.959			3		
ETC416	CO	MR3			0.619	3%		151.89			360	0.668			3		
ETC418	CO	MR3			0.519	2%		106.61			360	0.717			3		
DTC014A	CO	MR8			0.477	1%		159.18			375	1.094			1		
DTC016A	CO	MR8			0.479	1%		78.90			380	0.862			1		
DTC015B	CO	MR8	problems	1	0.505	1%		165.47			360	1.141			1		
DTC020B	CO	MR8	problems	2	0.502	1%		107.39			375	0.879			1		
DTC029A	CO	R8			0.175	0%		90.00			370	0.701	290		1		
ETC049	ETHANE				0.508	2%		124.00	5%		360	0.015	315		1		
ITC999	ETHANE	A			0.081	19%		0.08			360	0.260		ri	11		
ETC506	ETHANE	MRE			0.412	2%		102.53	5%		360	0.918			3		
ETC062	ETHANE	MR3			0.508	3%		39.14	5%		360	0.499			1		

					Initial NOx			Carbon			Run time	Max O3		(See below for codes)			
RunID	Classification		Data base status		ppm	unc		ppmC	unc		(min)	(ppm)	(min)	Cond-itions	Char. set	Model-able	Inp File
ETC068	ETHANE	MR3			0.503	3%		23.80	4%		360	0.313			1		
ETC073	ETHANE	MR3			0.505	3%		39.83	5%		360	0.325			1		
ETC079	ETHANE	MR3			0.508	3%		39.40	5%		360	0.351			1		
ETC088	ETHANE	MR3			0.526	3%		52.32	5%		360	0.494			1		
ETC092	ETHANE	MR3			0.512	2%		38.66	5%		360	0.217			2		
ETC099	ETHANE	MR3			0.503	2%		38.75	5%		360	0.204			2		
ETC235	ETHANE	MR3			0.491	2%		91.34	5%		360	0.606			2		
ETC332	ETHANE	MR3			0.504	2%		43.15			360	0.696			2		
ETC333	ETHANE	MR3			0.491	2%					360	0.880			2		
ITC979	ETHANE	R4	Don't model	9	0.089	57%		32.00	9%		360	0.459			11	9	
ITC992	ETHANE	R4	Don't model	9	0.081	63%		44.40	9%		360	0.405			11	9	
ETC226	PROPANE	MR3			0.477	2%		38.50	5%		360	0.355			2		
ETC230	PROPANE	MR3			0.513	2%		88.68	5%		360	0.738			2		
ETC305	PROPANE	MR3			0.544	3%		64.96			360	0.612			2		
EC134	N-C4				0.414			8.27	5%		360	0.034		d	11		
EC137	N-C4				0.386			8.65	5%		360	0.042		d	11		
EC162	N-C4				0.540	4%		8.20			360	0.112			1		
EC178	N-C4				0.099	11%		7.84			490	0.380	450		1		
EC304	N-C4				0.507	8%		17.11	11%		430	0.353			1		
EC305	N-C4				0.108	9%		17.19	11%		360	0.397	345		1		
EC307	N-C4				0.114	9%		25.74	11%		390	0.418	345		1		
EC355	N-C4				0.502	11%		16.80			360	0.188		vn	1		
EC356	N-C4				0.496	11%		17.30			360	0.178		vn	1		
ITC533	N-C4				0.102	15%		11.80	5%		420	0.164			3		
ITC939	N-C4				0.532	11%		19.43	5%		360	0.010	285		10		
ETC054	N-C4				0.509	2%		17.94	14%		360	0.003	330		1		
ETC214	N-C4				0.485	2%		15.71	8%		360	0.002	345		2		
ETC318	N-C4				0.522	4%		16.89	10%		360	0.001	45		2		
DTC058A	N-C4				0.241	0%		14.73	5%		370	0.021			1		
DTC058B	N-C4				0.240	0%		15.13	5%		370	0.015			1		
XTC085	N-C4				0.548	3%		15.18	6%		360	0.001	230		1		
XTC098	N-C4				0.567	3%		16.23	6%		360	0.005	345		1		
EC133	N-C4		Minor data problems	2	0.396			8.60	5%		360	0.249			1		
ITC507	N-C4		No Temp	2	0.094	16%		14.99			360	0.148			2		
ITC948	N-C4		NOx imprecise	2	0.256	20%		18.72			360	0.045			10		
EC354	N-C4				0.047	42%		17.07			360	0.236			1	3	no
EC130	N-C4		Reject	99	0.052			17.44	5%		600	0.458	240		1	9	
ITC770	N-C4	A			0.549	3%		0.03	7%		360	0.023		ri	7		

					Initial NOx			Carbon			Run time	Max O3		(See below for codes)			
RunID	Classification		Data base status		ppm	unc		ppmC	unc		(min)	(ppm)	(min)	Cond-itions	Char. set	Model-able	Inp File
ETC484	N-C4	MRE			0.456	2%		64.09	6%		360	1.063	330		3		
ETC488	N-C4	MRE			0.419	2%		44.44	5%		360	1.013			3		
ETC051	N-C4	MR3			0.497	2%		13.55	10%		360	0.461			1		
ETC053	N-C4	MR3			0.511	2%		24.68	12%		360	0.433			1		
ETC059	N-C4	MR3			0.503	3%		10.91	9%		360	0.378			1		
ETC082	N-C4	MR3			0.516	3%		30.58	12%		360	0.342			1		
ETC086	N-C4	MR3			0.514	3%		31.61	12%		360	0.438			1		
ETC094	N-C4	MR3			0.481	2%		31.86			360	0.234			2		
ETC097	N-C4	MR3			0.502	2%		28.18			360	0.259			2		
ETC135	N-C4	MR3			0.515	5%		27.50			360	0.182			2		
ETC224	N-C4	MR3			0.498	2%		44.77	7%		360	0.542			2		
ETC389	N-C4	R3	problems	1	0.155	4%		19.01	5%		360	0.599			3		
ETC393	N-C4	R3	problems	1	0.158	4%		18.34	5%		360	0.615			3		
ITC482	N-C4	R4			0.083	14%		1.13	6%		360	0.279			2		
ITC492	N-C4	R4	No Temp	2	0.083	14%		7.21	9%		360	0.325			2	3	no
ITC494	N-C4	R4	No Temp	2	0.088	14%		7.61	9%		360	0.318	300		2	3	no
DTC019B	N-C4	MR8			0.460	1%		28.49			375	0.936			1		
DTC031A	N-C4	R8			0.171	1%		24.59			370	0.662	250		1		
EC135	N-C5		No Temp	2	0.096	6%		20.42	19%		390	0.434	300		0	2	no
EC606	N-C6				0.560	13%		27.41			360	0.229			1		
EC607	N-C6				0.625	13%		56.84			360	0.293			1		
EC615	N-C6				0.241	15%		59.13			480	0.396	405		1		
EC677	N-C6				0.172	6%		55.96	5%		360	0.167			1		
EC610	N-C6		problems	2	0.298	14%		29.74			360	0.273			1		
EC611	N-C6		problems	2	0.296	14%		56.37			360	0.320			1		
ITC559	N-C6		problems	2	0.081	31%		290.09	5%		360	0.350			3		
EC131	N-C6		No Temp	2	0.098	6%		24.61			600	0.392	330		0	2	no
DTC072A	N-C6	MRE			0.468	1%		21.46	4%		375	0.566			1		
ETC209	N-C6	MR3			0.507	3%		14.12	10%		360	0.109			2		
ETC201	N-C6	MR3	problems	3	0.504	3%					360	0.185			2		
ITC538	N-C7				0.102	15%		61.67	5%		360	0.149			3		
ITC540	N-C7				0.108	13%		281.01	5%		360	0.350			3		
ITC552	N-C8				0.117	10%		445.57	5%		360	0.313			3		
ITC762	N-C8	A			0.281	4%		0.08	5%		420	0.101		ri	7		
ITC763	N-C8	A			0.288	5%					420	0.034		ri	7		
ITC797	N-C8	A			0.541	4%		0.07	5%		390	0.003	375	ri	8		
ITC761	N-C8	A	Don't model	9							420	0.018		ri	7	9	
ETC472	N-C8	MRE			0.421	2%		16.43	4%		360	0.650			3		

					Initial NOx			Carbon			Run time	Max O3		(See below for codes)			
RunID	Classification		Data base status		ppm	unc		ppmC	unc		(min)	(ppm)	(min)	Cond-itions	Char. set	Model-able	Inp File
ETC474	N-C8	MRE			0.455	3%		21.76	4%		360	0.604			3		
ETC237	N-C8	MR3			0.476	2%		17.79	8%		360	0.037			2		
ETC239	N-C8	MR3			0.525	2%		16.90	8%		360	0.019			2		
DTC024B	N-C8	MR8			0.503	1%		12.19			380	0.620			1		
DTC070A	N-C8	MR8			0.488	1%		9.32	3%		375	0.492			1		
DTC037B	N-C8	R8			0.175	0%		12.44			380	0.529	280		1		
DTC071B	N-C8	R8			0.177	0%		8.32	3%		375	0.511	335		1		
EC155	N-C9		Don't model	9	0.046	68%		37.35			540	0.263	345		0	2	no
ITC1001	N-C15				0.070	21%		2.51			360	0.042			11		
ITC981	N-C15	R4	Don't model	9	0.100	51%		6.48			360	0.361	300		11	9	
ITC993	N-C15	R4	Don't model	9	0.067	76%		7.23			360	0.259	345		11	9	
ETC228	2-ME-C3	MR3			0.507	2%		15.49	5%		360	0.332			2		
ETC232	2-ME-C3	MR3			0.512	2%		88.07	6%		360	0.929			2		
ETC241	2-ME-C3	MR3			0.481	2%		45.69	6%		360	0.816			2		
ETC303	2-ME-C3	MR3			0.453	3%		30.83			360	0.540			2		
EC171	23-DMB				0.100	6%		3.52			630	0.402			1		
EC169	23-DMB		problems	2	0.203	7%		4.44			690	0.490			1		
EC165	23-DMB		dataset problems	7	0.107	5%		11.31			540	0.487	510		1		
ETC291	224TM-C5	MR3			0.503	3%		84.67	10%		360	0.640			2		
ETC293	224TM-C5	MR3			0.486	3%		90.09	10%		360	0.617			2		
ITC766	ME-CYCC6	A			0.268	5%		0.08	5%		420	0.109		ri	7		
ITC767	ME-CYCC6	A			0.565	3%		0.08	5%		420	0.023		ri	7		
ITC800	ME-CYCC6	A			0.608	7%		0.07	5%		360	0.015	285	ri	8		
ITC765	ME-CYCC6	A	minor problems	1	0.571	3%		0.07	5%		420	0.016	375	ri	7		
EC142	ETHENE				0.489	3%		1.90	6%		360	0.780	355		1		
EC143	ETHENE				0.502	2%		4.05	6%		360	1.085	210		1		
EC156	ETHENE				0.472	6%		3.99	6%		360	1.103	200		1		
EC285	ETHENE				1.014	8%		3.90	6%		360	0.837			1		
EC286	ETHENE				0.973	8%		7.52			360	1.076	175		1		
EC287	ETHENE				0.545	8%		7.99	6%		360	0.961	130		1		
ITC926	ETHENE				0.530	11%		7.88	6%		360	0.992	195		10		
ITC936	ETHENE				0.518	11%		3.88	6%		420	0.949			10		
ITC1555	ETHENE		higher quality HCHO	0	0.450	8%		4.19	10%		420	1.117	390		12		
ETC220	ETHENE				0.507	2%		1.22	13%		360	0.005			2		
ETC221	ETHENE				0.515	2%		8.09	5%		360	1.121	255		2		
ETC377	ETHENE				0.268	2%					360	0.845			3	no	no
ETC381	ETHENE				0.519	2%		4.12	5%		360	1.105			3		
ETC439	ETHENE				0.664	2%		3.91	6%		360	0.859			3		

					Initial NOx			Carbon			Run time	Max O3		(See below for codes)			
RunID	Classification		Data base status		ppm	unc		ppmC	unc		(min)	(ppm)	(min)	Cond-itions	Char. set	Model-able	Inp File
ETC464	ETHENE				0.375	2%		3.01	6%		360	0.874			3		
ETC466	ETHENE				0.412	2%		3.00	6%		360	0.766			3		
ETC467	ETHENE				0.525	2%		2.98	6%		360	0.337			3		
ETC469	ETHENE				0.455	2%		3.60	6%		360	0.794			3		
ETC471	ETHENE				0.452	2%		3.61	6%		360	0.925			3		
ETC473	ETHENE				0.459	2%		3.79	6%		360	0.889			3		
ETC476	ETHENE				0.432	3%		3.42	6%		360	0.745			3		
ETC479	ETHENE				0.418	2%		3.57	6%		360	0.828			3		
ETC482	ETHENE				0.410	2%		3.20	6%		360	0.820			3		
ETC486	ETHENE				0.440	2%		3.18	6%		360	0.737			3		
ETC497	ETHENE				0.454	3%		3.54	6%		360	0.868			3		
ETC502	ETHENE				0.429	2%		3.45	6%		360	0.752			3		
ETC505	ETHENE				0.398	2%		3.29			360	0.798			3		
DTC041B	ETHENE				0.167	0%		4.08	5%		375	0.742	355		1		
DTC043A	ETHENE				0.467	1%		3.95	5%		375	0.671			1		
DTC044B	ETHENE				0.165	0%		4.19	5%		380	0.757	360		1		
DTC045A	ETHENE				0.476	1%		4.06	5%		375	0.776			1		
DTC046B	ETHENE				0.170	0%		4.44	5%		370	0.440			1		
DTC047A	ETHENE				0.480	1%		4.53	5%		370	0.799			1		
DTC048B	ETHENE				0.169	0%		4.55	5%		375	0.751	335		1		
DTC050A	ETHENE				0.162	0%		4.57	5%		370	0.731	330		1		
DTC051A	ETHENE				0.484	1%		4.55	5%		375	0.814			1		
DTC072B	ETHENE				0.467	1%		4.33	4%		375	0.722			1		
XTC105	ETHENE				0.241	3%		4.54	5%		360	0.781			1		
XTC112	ETHENE				0.518	3%		6.24	4%		375	0.934			1		
ETC199	ETHENE	MR3	problems	3				5.28	6%		360	0.845			2		
ETC203	ETHENE	MR3	problems	3	0.516	3%		4.79	3%		360	0.573			2		
DTC017A	ETHENE	MR8			0.479	1%		5.02	3%		380	0.821			1		
DTC038A	ETHENE	R8			0.169	0%		5.03			370	0.526	190		1		
EC121	PROPENE				0.514	2%		1.45	5%		390	0.505	310		1		
EC177	PROPENE				0.501	10%		1.48			460	0.539	435		1		
EC216	PROPENE				0.524	2%		1.51			490	0.563	465		1		
EC230	PROPENE				0.504	2%		1.64			420	0.341			1		
EC256	PROPENE				0.532	3%		0.39			360	0.002	315		1		
EC276	PROPENE				0.520	8%		1.62			360	0.372			1		
EC277	PROPENE				0.114	10%		1.69			360	0.311	130		1		
EC278	PROPENE				0.498	9%		3.05	6%		360	0.623	185		1		
EC279	PROPENE				0.984	8%		3.43			360	0.674	350		1		

					Initial NOx			Carbon			Run time	Max O3		(See below for codes)			
RunID	Classification		Data base status		ppm	unc		ppmC	unc		(min)	(ppm)	(min)	Cond-itions	Char. set	Model-able	Inp File
EC314	PROPENE				0.980	2%		3.19	6%		360	0.725			1		
EC317	PROPENE				0.566	2%		1.48	6%		390	0.613	385		1		
EC665	PROPENE				0.443	8%		1.43	5%		360	0.191			1		
EC684	PROPENE				0.438	7%		3.38	6%		360	0.400	210	o	1		
EC687	PROPENE				0.470	5%		3.12	6%		360	0.547	270	o	1		
EC691	PROPENE				0.490	12%		3.25	6%		360	0.466	255		1		
EC863	PROPENE				0.565	4%		1.55	7%		360	0.114			1		
EC870	PROPENE				0.538	4%		3.13	5%		360	0.490	210		1		
EC885	PROPENE				0.522	3%		2.78	5%		360	0.490	300		1		
EC899	PROPENE				0.485	3%		3.18	5%		360	0.439	240		1		
ITC484	PROPENE				0.453	4%		1.38	6%		1545	0.400		o	2		
ITC510	PROPENE				0.594	3%		2.85	6%		360	0.769		hl	2		
ITC532	PROPENE				0.555	3%		2.72	5%		360	0.581		nb	3		
ITC569	PROPENE				0.478	22%		2.81	7%		360	0.691			4		
ITC693	PROPENE				0.478	3%		3.20	7%		360	0.774			6		
ITC716	PROPENE				0.530	10%		3.03	7%		360	0.707			6		
ITC728	PROPENE				0.490	5%		3.05	7%		400	0.626	360		6		
ITC736	PROPENE				0.490	5%		1.49	7%		420	0.271		nb	7		
ITC754	PROPENE				0.571	3%		2.84	7%		360	0.811			7		
ITC791	PROPENE				0.528	3%		2.77	7%		420	0.772			7		
ITC792	PROPENE				0.499	7%		2.85	7%		360	0.739			8		
ITC810	PROPENE				0.521	3%		2.70	7%		360	0.816			8		
ITC860	PROPENE				0.523	3%		2.93	7%		360	0.586		nb	9		
ITC925	PROPENE				0.558	10%		3.17	7%		420	0.782			10		
ITC938	PROPENE				0.535	11%		2.42	7%		420	0.733	405		10		
ITC947	PROPENE				0.541	10%		1.80			450	0.717			10		
ITC972	PROPENE				0.507	10%		2.37							10		
ITC1550	PROPENE		higher quality HCHO	0	0.486	7%		2.95	5%		330	0.851	300		12		
ITC1556	PROPENE		higher quality HCHO	0	0.488	6%		2.98	5%		390	0.850			12		
ETC044	PROPENE				0.529	2%		3.72	5%		360	1.080	174		1		
ETC321	PROPENE				0.443	3%		3.05	5%		360	0.800	315		2		
ETC440	PROPENE				0.595	2%		3.51			360	0.843			3		
ETC449	PROPENE				0.252	2%		2.78			360	0.580	165		3		
ETC475	PROPENE				0.264	4%		2.72			360	0.589	135		3		
DTC026A	PROPENE				0.488	1%		3.50			370	0.863	240		1		
DTC026B	PROPENE				0.493	1%		3.53			370	0.871	210		1		
DTC052A	PROPENE				0.302	1%		2.83	5%		370	0.655	150		1		
DTC054A	PROPENE				0.287	1%		3.60	4%		375	0.645	145		1		

					Initial NOx			Carbon			Run time	Max O3		(See below for codes)			
RunID	Classification		Data base status		ppm	unc		ppmC	unc		(min)	(ppm)	(min)	Cond-itions	Char. set	Model-able	Inp File
DTC060A	PROPENE				0.245	1%		3.47	4%		300	0.577	160		1		
DTC060B	PROPENE				0.514	1%		3.60	4%		300	0.809			1		
DTC061A	PROPENE				0.502	1%		3.36	4%		370	0.792	320	rh	2		
DTC061B	PROPENE				0.502	1%		3.54	4%		370	0.803	310	rh	2		
XTC081	PROPENE				0.557	2%		4.21	4%		360	0.866			1		
XTC082	PROPENE				0.540	2%		4.09	4%		360	0.873			1		
XTC097	PROPENE				0.561	3%		4.63	4%		360	0.857	350		1		
XTC113	PROPENE				0.533	3%		4.57	4%		370	0.775	325		1		
DTC063A	PROPENE		problems	1	0.477	1%		3.53	4%		375	0.819	305		1		
DTC063B	PROPENE		problems	1	0.476	1%		3.57	4%		375	0.828	295		1		
EC673	PROPENE		sparse data	2	0.471	4%		1.42	5%		360	0.163			1		
EC682	PROPENE		sparse data	2	0.452	5%		2.85	5%		360	0.596	270	o	1		
EC689	PROPENE		sparse data	2	0.563	5%		3.22	6%		360	0.394	240	o	1		
ITC759	PROPENE		data sparse	2	0.568	3%		2.97	7%		360	0.797			7		
ITC1005	PROPENE		data sparse	2	0.399	4%		1.67			360	0.833	329		11		
ETC216	PROPENE		problems	2	0.510	2%		3.05	33%		420	0.809	285		2		
EC678	PROPENE		major problems	3	0.443	4%		1.41	5%		360	0.129	345		1		
ETC375	PROPENE		Do not model	9	0.516	2%		3.69			360	0.833	315		3		
EC685	PROPENE		No temp.	2	0.464	4%		3.22	6%		300	0.470	225	o	0	2	no
EC921	PROPENE		No k1	3	0.515	4%		2.39	7%		360	0.332		o	0	2	no
EC930	PROPENE		No k1	3	0.449	5%		2.69	7%		360	0.613		o	1	3	no
ITC623	PROPENE		don't model	9	0.445	7%					220	0.679		ri	5	3	no
EC095	PROPENE		Don't model	9	0.463	2%		1.51	5%		360	0.434	265		1	9	
EC096	PROPENE		Don't model	9	0.464	6%		1.52			360	0.424	295		1	9	
EC318	PROPENE		don't model	9	0.635	3%		1.53	6%		380	0.689	280		1	9	
EC319	PROPENE		don't model	9	0.788	3%		1.51	6%		360	0.752	255		1	9	
EC320	PROPENE		don't model	9	0.601	3%		1.61	6%		360	0.640	330		1	9	
EC663	PROPENE		Don't model	9	0.461	7%		1.38	5%		300	0.117			1	9	
EC681	PROPENE		don't model	9	0.439	5%		2.82	5%		360	0.327	285		1	9	
ITC960	PROPENE		do not model	9	0.493	11%		2.59	5%		360	0.728	330	ht	10	9	
ITC975	PROPENE		Don't model	9	0.412	13%		1.27			360	0.461		nb	11	9	
ITC990	PROPENE		Don't model	9	0.418	12%		1.02			360	0.479			11	9	
ITC1547	PROPENE		Don't model	9				2.86	5%		345	0.787	300	nb	12	9	
ETC496	PROPENE	MRE			0.375	2%		4.13	6%		360	0.947			3		
ETC500	PROPENE	MRE			0.420	2%		4.03	6%		360	0.966			3		
ETC065	PROPENE	MR3			0.510	3%		4.16	6%		360	0.390			1		
ETC072	PROPENE	MR3			0.499	3%		4.04	6%		360	0.333			1		
ETC106	PROPENE	MR3			0.515	2%		3.98	6%		360	0.283			2		

					Initial NOx			Carbon			Run time	Max O3		(See below for codes)			
RunID	Classification		Data base status		ppm	unc		ppmC	unc		(min)	(ppm)	(min)	Cond-itions	Char. set	Model-able	Inp File
ETC108	PROPENE	MR3			0.523	2%		4.01	6%		360	0.196			2		
ETC110	PROPENE	MR3			0.522	2%		3.69	6%		360	0.202			2		
ETC118	PROPENE	MR3	problems	1	0.500	2%		4.06	6%		360	0.336			2		
ITC474	PROPENE	R4			0.085	14%		3.76	7%		360	0.294	345		2		
ITC478	PROPENE	R4			0.086	13%		4.53	6%		360	0.322	345		2		
ITC575	PROPENE	R4			0.099	21%		2.89	6%		360	0.320	345		4		
ITC579	PROPENE	R4			0.095	16%		3.13	6%		360	0.354			4		
ITC585	PROPENE	R4			0.078	16%		4.59	5%		360	0.312			4		
ITC472	PROPENE	R4	No Temp	2	0.093	12%		3.26	9%		360	0.258			2		
DTC018A	PROPENE	MR8			0.482	1%		5.16			375	0.787	340		1		
DTC032B	PROPENE	R8			0.175	0%		4.86			380	0.469	120		1		
EC122	1-BUTENE				0.505	3%		0.87	7%		420	0.219	415		1		
EC123	1-BUTENE				0.510	2%		1.62	7%		450	0.505	430		1		
EC124	1-BUTENE				1.004	2%		1.70	7%		630	0.246			1		
ITC927	1-BUTENE				0.538	10%		4.25	6%		360	0.651			10		
ITC930	1-BUTENE				0.526	11%		11.17	10%		360	0.725	135		10		
ITC935	1-BUTENE				1.088	7%		11.45	10%		360	0.879	330		10		
ITC928	1-BUTENE	A			1.050	7%		0.04	7%		360	0.019		ri	10		
ITC929	1-HEXENE				0.519	11%		5.07			360	0.299			10		
ITC931	1-HEXENE				0.512	11%		10.23			360	0.610	255		10		
ITC934	1-HEXENE				1.069	7%		9.68			420	0.382			10		
ITC937	1-HEXENE	A			1.078	7%		0.08			360	0.006	180	ri	10		
ITC694	ISOBUTEN				0.500	3%		4.05	8%		360	0.893	315		6		
DTC052B	ISOBUTEN				0.297	1%		2.17	5%		370	0.723			1		
ETC253	ISOBUTEN	MR3			0.476	2%		5.41			360	0.855			2		
ETC255	ISOBUTEN	MR3			0.477	2%		5.34	5%		360	0.830			2		
ETC257	ISOBUTEN	MR3			0.482	2%		4.98	5%		360	0.604			2		
EC146	T-2-BUTE				0.512	3%		0.92	6%		360	0.239	355		1		
EC147	T-2-BUTE				0.962	2%		1.67	6%		360	0.154			1		
EC157	T-2-BUTE				0.557	3%		0.86			360	0.205	355		1		
ETC493	T-2-BUTE	MRE			0.425	2%		4.20	5%		360	0.931	315		3		
ETC501	T-2-BUTE	MRE			0.424	2%		3.72	6%		360	0.969			3		
DTC043B	T-2-BUTE	MRE			0.466	1%		4.37	5%		375	1.052			1		
DTC041A	T-2-BUTE	RE			0.167	0%		4.43	5%		375	0.629	185		1		
ETC307	T-2-BUTE	MR3			0.543	3%		4.65	6%		360	0.703			2		
ETC309	T-2-BUTE	MR3			0.524	3%		4.35	6%		360	0.660			2		
ITC498	T-2-BUTE	R4			0.090	13%		3.56	8%		360	0.280	330	o	2		
ITC500	T-2-BUTE	R4			0.091	13%		3.74	7%		360	0.285			2		

					Initial NOx			Carbon			Run time	Max O3		(See below for codes)			
RunID	Classification		Data base status		ppm	unc		ppmC	unc		(min)	(ppm)	(min)	Cond-itions	Char. set	Model-able	Inp File
ITC502	T-2-BUTE	R4			0.092	12%		4.21	7%		360	0.269			2		
DTC021B	T-2-BUTE	MR8			0.492	1%		5.22			380	0.730	350		1		
DTC069A	T-2-BUTE	MR8			0.478	1%		4.35	2%		375	0.682			1		
DTC033A	T-2-BUTE	R8			0.168	0%		4.52			370	0.456			1		
EC669	ISOPRENE				0.471	4%		2.38	9%		360	0.293			1		
ITC511	ISOPRENE				0.599	3%		5.01	9%		300	0.892	120	hl	2		
ITC811	ISOPRENE				0.464	8%		3.17	7%		240	0.917	195		8		
ITC812	ISOPRENE				0.534	3%		1.67	7%		390	0.760			8		
DTC053A	ISOPRENE				0.146	0%		1.52	5%		370	0.461			1		
DTC053B	ISOPRENE				0.243	1%		1.53	5%		370	0.595			1		
DTC056A	ISOPRENE				0.473	1%		4.29	4%		375	0.880	265		1		
DTC056B	ISOPRENE				0.472	1%		2.67	4%		375	0.626			1		
XTC093	ISOPRENE				0.165	3%		2.41	7%		360	0.387			1		
XTC101	ISOPRENE				0.527	3%		3.10	7%		360	0.453			1		
EC520	ISOPRENE		minor problems	1	0.492	11%		2.21			360	0.503	300		1		
EC522	ISOPRENE		minor problems	1	0.958	10%		2.25			360	0.273			1		
EC524	ISOPRENE		minor problems	1	1.003	10%		4.36	10%		360	0.757	240		1		
EC527	ISOPRENE		minor problems	1	0.527	10%		2.10	10%		360	0.508	300		1		
EC525	ISOPRENE		reject	99	0.562	10%		4.21			300	0.686	120	o	1	9	
ETC495	ISOPRENE	MRE			0.417	2%		4.45	5%		360	1.007			3		
ETC503	ISOPRENE	MRE			0.420	2%		4.78	5%		360	0.974	315		3		
ETC510	ISOPRENE	MRE			0.408	2%		4.57	5%		360	0.977			3		
DTC047B	ISOPRENE	MRE			0.478	1%		5.05	4%		370	1.072			1		
DTC046A	ISOPRENE	RE			0.171	0%		5.11	4%		370	0.416			1		
DTC050B	ISOPRENE	RE			0.162	0%		4.99	4%		370	0.653	280		1		
ETC271	ISOPRENE	MR3			0.495	2%		5.25	5%		360	0.800			2		
ETC273	ISOPRENE	MR3			0.486	3%		5.09	5%		360	0.837			2		
ETC275	ISOPRENE	MR3			0.489	3%		4.81	5%		360	0.794			2		
ETC277	ISOPRENE	MR3			0.496	3%		4.65	5%		360	0.748			2		
ETC420	A-PINENE				0.291	2%		2.63	5%		360	0.333			3		
ETC443	A-PINENE				0.257	2%		2.81	5%		360	0.401			3		
ETC444	A-PINENE				0.299	2%		2.77	5%		360	0.379			3		
ETC446	A-PINENE				0.534	2%		2.77	5%		360	0.134			3		
ETC447	A-PINENE				0.132	3%		2.79	5%		360	0.300			3		
XTC095	A-PINENE				0.242	3%		3.77	7%		360	0.280	345		1		
ETC426	A-PINENE		Can't model	9	0.266	2%									3	no	no
ETC492	A-PINENE	MRE			0.384	2%		4.45	5%		360	0.921			3		
ETC508	A-PINENE	MRE			0.409	2%		4.71			360	0.924			3		

					Initial NOx			Carbon			Run time	Max O3		(See below for codes)			
RunID	Classification		Data base status		ppm	unc		ppmC	unc		(min)	(ppm)	(min)	Cond-itions	Char. set	Model-able	Inp File
DTC045B	A-PINENE	MRE			0.476	1%		5.16	5%		375	1.039			1		
DTC044A	A-PINENE	RE			0.165	0%		5.19	5%		380	0.592	270		1		
DTC034B	A-PINENE	R8			0.165	0%		6.57			370	0.358	80		1		
ETC433	B-PINENE				0.269	2%		2.66	5%		360	0.035			3		
ETC434	B-PINENE				0.293	2%		9.69	5%		360	0.295	225		3		
ETC435	B-PINENE				0.137	3%		2.78	5%		360	0.246			3		
ETC442	B-PINENE				0.288	2%		2.72	5%		360	0.032			3		
XTC099	B-PINENE				0.233	3%		6.25	9%		375	0.283	345		1		
ETC421	B-PINENE		Problems	3	0.252	2%		2.73	5%		360	0.067			3		
ETC494	B-PINENE	MRE			0.446	2%		5.02			360	0.849			3		
DTC051B	B-PINENE	MRE			0.484	1%		5.59	4%		375	0.868			1		
ETC507	B-PINENE	MRE	Can't model	9	0.410	2%					360	0.774			3	no	no
DTC048A	B-PINENE	RE			0.170	0%		5.64	4%		375	0.563	345		1		
ETC422	TERPINEN		Can't model	9	0.239	2%					360	0.504			3	no	no
ETC425	D-LIMONE				0.251	2%		3.00	7%		360	0.411			3		
ETC450	D-LIMONE				0.242	2%		2.74	7%		360	0.438			3		
ETC451	D-LIMONE				0.566	2%		2.63	7%		360	0.137			3		
ETC452	D-LIMONE				0.160	2%		2.73	7%		360	0.378			3		
ETC424	3-CARENE				0.254	2%		2.94	5%		360	0.365			3		
ETC456	3-CARENE				0.234	2%		2.48	5%		360	0.354			3		
ETC457	3-CARENE				0.158	3%		2.66	5%		360	0.283			3		
ETC459	3-CARENE				0.498	2%		2.30	5%		360	0.124			3		
ETC423	SABINENE				0.253	2%		2.56	9%		360	0.327			3		
ETC436	SABINENE				0.288	2%		2.58	9%		360	0.268			3		
ETC437	SABINENE				0.576	2%		2.59	9%		360	0.059			3		
ETC438	SABINENE				0.136	3%		1.37	9%		360	0.187			3		
ITC560	BENZENE				0.108	22%		344.90	10%		180	0.321	90		3		
ITC561	BENZENE				0.114	22%		41.06	10%		150	0.271	105		3		
ITC562	BENZENE				0.569	20%		43.46	10%		360	0.409	285		3		
ITC698	BENZENE				0.485	3%		84.27			300	0.370	240		6		
ITC710	BENZENE				0.534	3%		84.48			360	0.363	270		6		
ITC831	BENZENE	A			1.008	2%		0.07			360	0.009	345	ri	8		
ETC263	BENZENE	MR3			0.476	2%		44.99	9%		360	0.595	300		2		
ETC265	BENZENE	MR3			0.485	2%		39.18	9%		360	0.601	345		2		
DTC039B	BENZENE	R8	problems	2	0.178	0%		48.38			380	0.387	100		1		
EC264	TOLUENE				0.440	2%		8.09			240	0.417	210		1		
EC266	TOLUENE				0.440	3%		8.37			360	0.404	215		1		
EC269	TOLUENE				0.485	9%		3.96			360	0.297			1		

					Initial NOx			Carbon			Run time	Max O3		(See below for codes)			
RunID	Classification		Data base status		ppm	unc		ppmC	unc		(min)	(ppm)	(min)	Cond-itions	Char. set	Model-able	Inp File
EC270	TOLUENE				0.466	9%		4.20			360	0.367	325		1		
EC271	TOLUENE				0.215	9%		8.02			360	0.294	90		1		
EC273	TOLUENE				0.112	9%		4.11			380	0.214	75	o	1		
EC293	TOLUENE				0.487	8%		7.49	10%		360	0.416	155		1		
EC327	TOLUENE				0.492	2%		4.01	10%		360	0.375			1		
ITC534	TOLUENE				0.526	3%		15.02	10%		330	0.490	195		3		
ITC699	TOLUENE				0.493	3%		11.31	13%		250	0.480	195		6		
DTC042A	TOLUENE				0.986	2%		7.47	5%		375	0.030			1		
DTC042B	TOLUENE				0.099	0%		3.94	5%		375	0.256	215		1		
XTC106	TOLUENE				0.245	3%		14.49	5%		360	0.395	145		1		
EC340	TOLUENE		problems	2	0.493	4%		3.76	10%		330	0.343	325		1		
EC292	TOLUENE		Low Temp.	6	0.505	8%		6.61	10%		360	0.124		lt	12	1	
EC265	TOLUENE		Don't model	9	0.437	2%		7.49			260	0.391	205		1	9	
EC671	TOLUENE		Don't model	9	0.434	4%		8.16	10%		360	0.189			1	9	
ITC828	TOLUENE	A			1.008	2%		0.07	5%		360	0.011		ri	8		
ETC061	TOLUENE	MR3			0.509	3%		5.06	6%		360	0.652			1		
ETC064	TOLUENE	MR3			0.552	3%		4.46	6%		360	0.297			1		
ETC069	TOLUENE	MR3			0.498	3%		4.43	6%		360	0.406			1		
ETC101	TOLUENE	MR3			0.503	2%		4.71	6%		360	0.284			2		
ETC103	TOLUENE	MR3			0.516	2%		4.78	6%		360	0.308			2		
ITC451	TOLUENE	R4			0.090	13%		4.73	6%		360	0.312			2		
ITC455	TOLUENE	R4			0.083	14%		4.01	7%		360	0.304			2		
DTC023A	TOLUENE	MR8			0.469	1%		7.51			375	0.721	305		1		
DTC030B	TOLUENE	R8			0.166	0%		11.34			375	0.369	85		1		
ETC311	C2-BENZ	MR3			0.522	3%		5.29	6%		360	0.230			2		
ETC313	C2-BENZ	MR3			0.528	3%		5.03	6%		360	0.273			2		
ETC315	C2-BENZ	MR3			0.526	3%		6.14	6%		360	0.399			2		
EC288	O-XYLENE				0.502	8%		1.44	10%		360	0.253			1		
EC291	O-XYLENE				0.495	9%		4.83	10%		360	0.462	165		1		
ETC259	O-XYLENE	MR3			0.490	2%		5.01	5%		360	0.573			2		
ETC261	O-XYLENE	MR3			0.476	2%		5.01	5%		360	0.644			2		
ETC346	P-XYLENE	MR3			0.467	2%					360	0.772			2	no	no
ETC348	P-XYLENE	MR3			0.519	2%		5.73	3%		360	0.658			2		
EC344	M-XYLENE				0.776	2%		3.89	25%		360	0.587	170		1		
EC345	M-XYLENE				0.315	6%		3.84	25%		360	0.394	65		1		
ITC702	M-XYLENE				0.503	3%		4.42	10%		270	0.622	195		6		
ETC222	M-XYLENE				0.482	2%		4.11	10%		360	0.674	240		2		
DTC073A	M-XYLENE				0.485	1%		1.28	4%		360	0.075			1		

					Initial NOx			Carbon			Run time	Max O3		(See below for codes)			
RunID	Classification		Data base status		ppm	unc		ppmC	unc		(min)	(ppm)	(min)	Cond-itions	Char. set	Model-able	Inp File
DTC076B	M-XYLENE				0.484	1%		1.41	4%		370	0.082			1		
XTC107	M-XYLENE		Problems	1	0.249	3%		3.45	6%		360	0.447	195		1		
EC346	M-XYLENE		incomplete results	2	0.297	3%		3.89	25%		120	0.382	55		1		
ETC150	M-XYLENE		can't model	9							360	0.010	330		2		
EC343	M-XYLENE		reject	99	0.326	5%		3.98	25%		360	0.282	75		1	9	
ITC827	M-XYLENE	A			1.051	2%		0.07	5%		360	0.016	270	ri	8		
ETC477	M-XYLENE	MRE			0.461	3%		4.94	5%		360	0.981	285		3		
ETC478	M-XYLENE	MRE			0.429	3%		4.21	5%		360	1.002			3		
ETC499	M-XYLENE	MRE			0.429	2%		4.69	5%		360	0.962	315		3		
ETC301	M-XYLENE	MR3			0.462	3%		4.87	6%		360	0.617			2		
ETC344	M-XYLENE	MR3			0.525	2%		5.11			360	0.912			2		
ETC196	M-XYLENE	MR3	problems	3	0.477	7%					360	0.560			2		
ETC207	M-XYLENE	MR3	problems	3	0.508	3%					360	0.586			2		
DTC025A	M-XYLENE	MR8			0.467	1%		4.87			375	0.781			1		
DTC068B	M-XYLENE	MR8			0.484	1%		4.25	2%		375	0.640			1		
DTC035A	M-XYLENE	R8			0.166	0%		4.82			370	0.423			1		
DTC067B	M-XYLENE	R8			0.171	0%		5.12	3%		375	0.398	175		1		
EC901	135-TMB				0.490	5%		2.78	10%		360	0.382	180		1		
EC903	135-TMB				1.011	3%		4.91	10%		360	0.500	226		1		
ITC703	135-TMB				0.495	4%		5.02	10%		240	0.702	150		6		
ITC706	135-TMB				0.466	4%		2.49	10%		360	0.635			6		
ITC709	135-TMB				0.973	2%		4.47	10%		360	0.773			6		
ITC742	135-TMB				0.522	5%		4.44	10%		270	0.775			7		
XTC103	135-TMB				0.496	3%		3.02	9%		360	0.671			1		
EC900	135-TMB		don't model	9	0.521	3%		5.59	10%		240	0.380	90		1	3	no
ITC826	135-TMB	A			0.903	2%		0.07	5%		360	0.013	300	ri	8		
ETC249	135-TMB	MR3			0.494	2%		5.43	5%		360	0.885			2		
ETC251	135-TMB	MR3	problems	1	0.500	2%		5.05	5%		300	0.511			2		
ETC297	123-TMB	MR3			0.462	3%		4.83	5%		360	0.861			2		
ETC299	123-TMB	MR3			0.481	3%		4.71	5%		360	0.801			2		
ETC267	124-TMB	MR3			0.486	2%		4.93	6%		360	0.563			2		
ETC269	124-TMB	MR3			0.484	2%		4.85	6%		360	0.653			2		
ITC739	TETRALIN				0.545	5%		2.74	27%		360	0.001			7		
ITC747	TETRALIN				0.540	5%		114.69	27%		390	0.479	360		7		
ITC748	TETRALIN				0.234	7%		103.34	27%		330	0.337	255		7		
ITC750	TETRALIN				0.536	3%		54.02	27%		360	0.452			7		
ITC832	TETRALIN	A			0.993	2%		0.07			360	0.023		ri	8		
ITC751	NAPHTHAL				0.538	3%		7.49	10%		390	0.083			7		

					Initial NOx			Carbon			Run time	Max O3		(See below for codes)			
RunID	Classification		Data base status		ppm	unc		ppmC	unc		(min)	(ppm)	(min)	Cond-itions	Char. set	Model-able	Inp File
ITC755	NAPHTHAL				0.272	11%		14.08	10%		360	0.248	300		7		
ITC756	NAPHTHAL				0.252	3%		27.43	10%		300	0.242	240		7		
ITC798	NAPHTHAL				0.599	8%		19.41	10%		360	0.186			8		
ITC802	NAPHTHAL				0.595	8%		8.46	10%		360	0.105			8		
ITC771	23-DMN				0.246	5%		4.77	10%		300	0.293	240		7		
ITC774	23-DMN				0.557	3%		4.04	10%		360	0.341			7		
ITC775	23-DMN				0.256	5%		1.74	10%		360	0.273			7		
ITC806	23-DMN				0.380	8%		5.87	10%		360	0.360			8		
ITC1006	ACETYLEN				0.269	10%		119.07	11%		240	0.942	165	o	11		
ITC1007	ACETYLEN				0.227	6%		127.53	11%		240	0.878	135		11		
ITC1000	ACETYLEN	A			0.095	15%		0.07			360	0.490		ri	11		
ITC866	MEOH	A	2-part run	0	0.512	3%		0.07			255	0.003		ri	9		
ITC887	MEOH	A			0.326	5%		0.07			240	0.050		ri	9		
ETC285	MEOH	MR3			0.517	2%		11.97	4%		360	0.873			2		
ETC287	MEOH	MR3			0.512	3%		5.06	5%		360	0.477			2		
ETC289	MEOH	MR3			0.505	3%		6.68	4%		360	0.683			2		
ITC612	MEOH	R4	Don't model	9	0.051	83%		4.85			360	0.359			4	9	
ETC131	ETOH	MR3			0.538	5%		9.64	4%		360	0.216			2		
ETC133	ETOH	MR3			0.534	5%		9.10	4%		360	0.222			2		
ETC138	ETOH	MR3			0.536	5%		9.70	4%		360	0.181			2		
ITC587	ETOH	R4			0.089	29%		5.30			360	0.370			4		
ITC593	ETOH	R4	data sparse	2	0.084	34%		7.74			360	0.353		o	4		
ITC591	ETOH	R4	Don't model	9	0.053	114%		5.55			360	0.400	345		4	9	
ETC148	I-C3-OH	MR3			0.515	2%		16.67	19%		360	0.394			2		
ETC155	I-C3-OH	MR3			0.503	3%		8.58	12%		360	0.540			2		
ETC157	I-C3-OH	MR3			0.512	3%		7.27	10%		360	0.385			2		
ETC159	I-C3-OH	MR3			0.503	3%		8.23	11%		360	0.428			2		
ETC279	ME-O-ME	MR3			0.505	3%		12.38	4%		360	0.929			2		
ETC281	ME-O-ME	MR3			0.509	3%		11.06	4%		360	0.825			2		
ETC283	ME-O-ME	MR3			0.508	2%		8.60	4%		360	0.776			2		
ETC295	ME-O-ME	MR3			0.477	3%		8.47	4%		360	0.659			2		
ETC120	MTBE	MR3			0.529	2%					360	0.149			2		
ETC123	MTBE	MR3			0.515	2%					360	0.375			2		
ETC125	MTBE	MR3			0.515	2%					360	0.153			2		
ETC127	MTBE	MR3			0.532	2%					360	0.168			2		
ITC602	MTBE	R4			0.094	12%		8.48	6%		360	0.370			4		
ITC606	MTBE	R4			0.092	14%		13.14	7%		360	0.430	345		4		
ITC608	MTBE	R4			0.088	15%		17.18	8%		360	0.430	270		4		

					Initial NOx			Carbon			Run time	Max O3		(See below for codes)			
RunID	Classification		Data base status		ppm	unc		ppmC	unc		(min)	(ppm)	(min)	Cond-itions	Char. set	Model-able	Inp File
ETC171	ETO-ETOH	MR3			0.492	4%		7.10	3%		360	0.842			2		
ETC163	ETO-ETOH	MR3	problems	1	0.492	2%					360	1.054			2		
ETC175	ETO-ETOH	MR3	problems	3	0.503	4%					360	0.525			2		
ETC166	CARBITOL	MR3			0.507	2%		7.66	4%		360	0.734			2		
ETC169	CARBITOL	MR3			0.513	2%		6.83	5%		360	0.424			2		
ETC173	CARBITOL	MR3			0.511	4%		10.33	4%		360	0.489			2		
ITC711	FURAN				0.511	3%		1.69	8%		300	0.467	165		6		
ITC713	FURAN				0.975	4%		1.62	8%		360	0.039	255		6		
ITC715	FURAN				0.490	5%		0.90	8%		360	0.057			6		
ITC743	FURAN				0.540	5%		1.56	8%		360	0.585			7		
EC389	FORMALD				4.747	12%		9.53			260	0.002	145	vn,d	11		
EC391	FORMALD				5.395	4%		18.06			300	2.363	235	vn,d	11		
EC392	FORMALD				11.366	4%		9.95			240	0.000		d	11		
EC407	FORMALD				5.069	5%		9.71			360	0.002	225	d	11		
ITC1549	FORMALD		higher quality HCHO	0	0.368	7%		0.08			390	0.042		ri	12		
ITC1554	FORMALD		higher quality HCHO	0	0.436	7%		1.01			330	0.181			12		
ETC378	FORMALD				0.240	2%		0.22	2%		360	0.012			3		
ETC441	FORMALD				0.274	2%		0.50	2%		360	0.064			3		
XTC086	FORMALD				0.161	3%		1.68	3%		360	0.322			1		
XTC091	FORMALD		problems	1	0.153	3%		1.73	3%		360	0.308			1		
EC251	FORMALD		problems	2	0.108	7%		0.25			360	0.270	320		1		
EC252	FORMALD		problems	2	0.467	3%		0.42			360	0.024			1		
XTC096	FORMALD		Problems	2	0.170	3%		1.65	3%		360	0.236			1		
EC406	FORMALD		problems	2	4.983	5%		9.29			360	0.002	170	d,lt	12	1	
EC403	FORMALD		High T. Don't model	6				9.64			360	0.007	335	d,ht	13	1	
EC404	FORMALD		Low T. Don't model	6				1.17			360	0.000		d,lt	12	1	
EC393	FORMALD				5.442	4%		9.94			260	0.798		d,uv	11	4	
ITC864	FORMALD	A			0.544	3%		0.08			300	0.000			9		
ETC468	FORMALD	MRE			0.428	2%		3.51	6%		360	0.949			3		
ETC470	FORMALD	MRE			0.390	2%		3.57	6%		360	1.078			3		
ETC489	FORMALD	MRE	Problems	3	0.419	2%		3.61	6%		360	1.062			3		
ETC352	FORMALD	MR3			0.525	2%		4.89	3%		360	0.701			2		
ETC357	FORMALD	MR3			0.527	2%		4.97	3%		360	0.793			2		
DTC022B	FORMALD	MR8			0.505	1%		4.48			380	0.692			1		
DTC036A	FORMALD	R8			0.182	0%		4.64			375	0.492	225		1		
EC254	ACETALD				0.107	5%		0.98			360	0.263			1		
EC400	ACETALD				5.535	11%		22.03			360	0.019	5	d	11		
DTC055B	ACETALD				0.145	0%		3.30	6%		370	0.336			1		

					Initial NOx			Carbon			Run time	Max O3		(See below for codes)			
RunID	Classification		Data base status		ppm	unc		ppmC	unc		(min)	(ppm)	(min)	Cond-itions	Char. set	Model-able	Inp File
XTC083	ACETALD				0.246	3%		2.63	5%		360	0.286			1		
XTC092	ACETALD				0.248	3%		3.32	4%		360	0.225			1		
EC164	ACETALD		problems	2	0.542	4%		0.68	10%		360	0.085			1		
EC397	ACETALD							32.37			270	1.663	180	d,uv	11	4	
EC399	ACETALD		Don't model	9				24.23			360	1.685	285	d,uv	11	4	
EC405	ACETALD		Low T. reject	99				16.16			360	0.407		d,lt	11	9	
ETC335	ACETALD	MR3			0.536	2%		5.90	4%		360	0.608			2		
ETC338	ACETALD	MR3			0.521	2%		7.02	5%		360	0.625			2		
DTC065A	ACETALD	MR8			0.455	1%		6.96	3%		375	0.629			1		
DTC066B	ACETALD	R8			0.175	0%		7.15	3%		375	0.406			1		
ITC941	ACROLEIN				0.546	10%		2.02			360	0.092			10		
ITC943	ACROLEIN				0.534	11%		0.32			420	0.725	405		10		
ITC944	ACROLEIN				0.267	20%		4.93			360	0.489			10		
ITC945	ACROLEIN	A			0.523	10%		0.07			300	0.032	285	ri	10		
ITC946	ACROLEIN	M			0.538	10%		4.11			360	0.786	255		10		
EC651	METHACRO				0.445	5%		5.78	10%		360	0.247	315		1		
EC652	METHACRO				0.449	5%		3.17	10%		360	0.229			1		
EC655	METHACRO				0.796	6%		5.86	10%		390	0.350			1		
ITC513	METHACRO				0.571	3%		10.05	10%		390	0.672	255	hl	2		
ITC819	METHACRO				0.482	4%		6.89			360	0.747			8		
ITC823	METHACRO				0.511	3%		129.34			360	0.674	240		8		
ETC386	METHACRO				0.564	3%		8.83	5%		360	0.664	270		3		
DTC075A	METHACRO				0.497	1%		18.49	16%		370	0.600	210		1		
DTC075B	METHACRO				0.259	1%		10.37	15%		370	0.450	260		1		
XTC094	METHACRO				0.492	3%		16.77	5%		360	0.457	245		1		
XTC102	METHACRO				0.236	3%		7.17	4%		360	0.405	305		1		
EC530	METHACRO		minor problems	1	0.427	11%		3.01	10%		360	0.300			1		
DTC057A	METHACRO		do not model	9	0.449	1%		13.81	16%		380	0.464	60		1	no	
DTC057B	METHACRO		do not model	9	0.243	1%		7.30	15%		380	0.383			1	no	
DTC074A	BIACET		can't model	9	0.000										1	no	no
DTC074B	BIACET		can't model	9	0.000										1	no	no
EC401	ACETONE				6.410	9%		1.64			360	0.056	5	d	11		
ETC445	ACETONE				0.137	3%		25.44	10%		360	0.231			3		
DTC054B	ACETONE				0.286	1%		33.68	7%		375	0.220			1		
DTC055A	ACETONE				0.146	0%		45.79	7%		370	0.416			1		
XTC084	ACETONE				0.241	3%		27.94	5%		360	0.377			1		
XTC090	ACETONE		problems	1	0.195	3%		30.07	6%		360	0.357			1		
ETC480	ACETONE	MRE			0.417	2%		13.91	8%		360	0.890			3		

					Initial NOx			Carbon			Run time	Max O3		(See below for codes)			
RunID	Classification		Data base status		ppm	unc		ppmC	unc		(min)	(ppm)	(min)	Cond-itions	Char. set	Model-able	Inp File
ETC481	ACETONE	MRE			0.417	2%		20.59	9%		360	0.878			3		
ETC490	ACETONE	MRE			0.422	2%		27.74	9%		360	0.953			3		
ETC243	ACETONE	MR3			0.494	2%		6.37	10%		360	0.398			2		
ETC245	ACETONE	MR3			0.496	2%		9.14	13%		360	0.478			2		
ETC247	ACETONE	MR3			0.491	2%		13.01	17%		360	0.551			2		
DTC028A	ACETONE	MR8			0.483	1%		30.24			375	0.672			1		
DTC064B	ACETONE	MR8			0.487	1%		52.61	7%		375	0.788			1		
EC648	MVK				0.835	6%		3.60	25%		360	0.375	300		1		
ITC512	MVK				0.605	3%		8.01	25%		360	0.570	210	hl	2		
ITC815	MVK				0.520	3%		7.39	25%		330	0.592	254		8		
ITC816	MVK				0.506	3%		3.49	25%		450	0.731			8		
XTC120	MVK				0.529	3%		8.98	4%		365	0.471	240		1		
XTC121	MVK				0.517	3%		4.72	4%		375	0.456			1		
EC529	MVK		minor problems	1	0.484	11%		3.91	25%		360	0.469	330		1		
EC644	MVK			1	0.491	7%		2.34	25%		330	0.312	255		1		
EC649	MVK	A			0.465	5%		0.07			360	0.235	345	ri	1		
EC647	BENZALD	A			0.873	3%		0.07						ri	1		
ITC460	BENZALD	A			0.085	18%		0.07	6%		360	0.013	105	ri	2		
EC646	BENZALD	A		1	0.486	5%		0.07			390	0.992	270	ri	1		
ITC457	BENZALD	R4			0.085	13%		8.12	17%		330	0.187	255		2		
ITC462	BENZALD	R4			0.094	12%		6.92	7%		345	0.099	225		2		
ITC466	BENZALD	R4			0.097	13%		5.93	6%		360	0.131	240		2		
ITC468	BENZALD	R4			0.086	13%		4.20	7%		360	0.176	240		2		
EC281	CRESOL				0.488	10%		2.76			390	0.075	385		1		
EC289	CRESOL				0.468	10%		2.08			360	0.136	175		1		
EC290	CRESOL				0.500	9%		2.55			360	0.071	350		1		
EC280	CRESOL		reject	99							360	0.073			1	9	
ITC778	PYRROLE				0.491	8%		3.87	5%		60	0.511			7		
ITC779	PYRROLE				0.566	17%		1.07	5%		90	0.057			7		
ITC735	PYRROLE		VOC/NOx too high	1	0.513	5%		2.11			270	0.319	30		6		
ITC780	PYRROLE	A			0.537	4%		0.08	5%		300	0.030	285	ri	7		
ITC729	THIOPHEN				0.526	5%		1.72			360	0.068			6		
ITC730	THIOPHEN				0.492	5%		7.11			300	0.405	195		6		
ITC733	THIOPHEN				0.262	5%		1.73			450	0.248			6		
ITC744	THIOPHEN				0.572	5%		6.55			270	0.479	195		7		
ETC342	CL2IBUTE	MR3			0.549	2%		4.51			360	0.899			2		
ETC343	CL2IBUTE	MR3			0.543	2%		4.87			360	0.887			2		
ETC350	CL2IBUTE	MR3			0.532	2%		5.29			360	0.959			2		

					Initial NOx			Carbon			Run time	Max O3		(See below for codes)			
RunID	Classification		Data base status		ppm	unc		ppmC	unc		(min)	(ppm)	(min)	Cond-itions	Char. set	Model-able	Inp File
ETC179	SI2OME6	MR3	problems	3	0.387						360	0.012			2		
ETC183	SI2OME6	MR3	problems	3	0.369						360	0.022			2		
ETC391	SI2OME6	R3			0.145	4%		28.28	4%		360	0.192			3		
ETC396	SI2OME6	R3			0.150	4%		21.29	4%		360	0.296			3		
ETC406	(SIOME)4	MR3			0.165	4%		14.74	5%		360	0.304			3		
ETC181	(SIOME)4	MR3	problems	3	0.389						360	0.010	315		2		
ETC185	(SIOME)4	MR3	problems	3	0.382						360	0.021	315		2		
ETC194	(SIOME)4	MR3	problems	3							360	0.082			2		
ETC398	(SIOME)4	R3			0.136	4%		25.50	5%		360	0.212			3		
ETC402	(SIOME)4	R3			0.116	4%		18.44	5%		360	0.260			3		
ETC187	(SIOME)5	MR3	problems	3	0.388						360	0.014			2	no	no
ETC190	(SIOME)5	MR3	problems	3							360	0.031			2	no	no
ETC192	(SIOME)5	MR3	problems	3							360	0.032			2		
ETC404	SI2OMEOH	MR3			0.195	4%		9.64	35%		360	0.219			3	no	
ETC412	SI2OMEOH	MR3			0.523	3%		8.47	24%		360	0.149			3	no	
ETC409	SI2OMEOH	MR3	poroblems	3	0.561	3%		16.41	38%		360	0.040			3	no	
ETC400	SI2OMEOH	R3			0.130	4%		18.45	41%		360	0.119			3	no	
EC166	MIX-A				0.106	12%		9.18			480	0.461	410		1		
EC172	MIX-A				0.102	12%		2.78			690	0.368			1		
EC144	MIX-E				0.510	2%		4.72	5%		360	1.063	170		1		
EC145	MIX-E				1.004	2%		3.38	4%		360	0.775			1		
EC149	MIX-E				0.999	2%		1.99	4%		360	0.275			1		
EC150	MIX-E				1.015	2%		3.46	4%		360	0.797			1		
EC151	MIX-E				2.065	2%		4.87	3%		360	0.146			1		
EC152	MIX-E				0.512	3%		3.67	4%		380	0.790	215		1		
EC160	MIX-E				1.013	2%		3.23			360	0.873			1		
EC161	MIX-E				0.542	5%		3.23			345	0.855	210		1		
EC153	MIX-E		problems	2	0.987	2%		6.61	4%		360	1.048	180		1		
XTC111	MIX-AE				0.224	3%		15.91	4%		375	0.488			1		
EC114	MIX-AE		Don't model	9	1.155	2%		16.94	4%		360	0.744	330		1	3	no
EC115	MIX-AE		Don't model	9	0.589	3%		12.69	5%		450	0.590	420		1	3	no
EC116	MIX-AE		Don't model	9	0.574	3%		18.47	4%		450	0.743	170		1	3	no
EC097	MIX-AE		Don't model	9	0.484	2%		9.74			360	0.578	240		1	9	
EC099	MIX-AE		Don't model	9	0.500	3%		9.20			360	0.557	300		1	9	
EC106	MIX-AE		Don't model	9	0.509	3%		9.21			440	0.592	380		1	9	
EC113	MIX-AE		Don't model	9	0.134	7%		9.43	4%		360	0.352	130		1	9	
EC163	MIX-AO		problems	2	0.508	3%		8.81			360	0.429			1		
EC168	MIX-AO		reject	99	0.488	4%		7.95			690	0.653	640		1	9	

					Initial NOx			Carbon			Run time	Max O3		(See below for codes)			
RunID	Classification		Data base status		ppm	unc		ppmC	unc		(min)	(ppm)	(min)	Cond-itions	Char. set	Model-able	Inp File
EC217	MIX-EO				0.479	4%		0.59			720	0.149			1		
EC257	MIX-EO		problems	2	0.524	3%		0.77			360	0.066			1		
EC272	MIX-RO		problems		0.479	8%		4.78			360	0.409	355		1		
EC335	MIX-RO				0.499	4%		7.64	9%		360	0.397	220		1		
EC336	MIX-RO				0.495	4%		7.36			360	0.394	160		1		
EC337	MIX-RO				0.507	4%		7.92	9%		360	0.324	255		1		
EC338	MIX-RO				0.502	3%		14.79	8%		360	0.482	230		1		
EC339	MIX-RO				0.503	3%		5.07	8%		360	0.224			1		
EC328	MIX-AR				0.496	3%		12.13	8%		360	0.521	350		1		
EC331	MIX-AR				0.520	3%		22.11	8%		360	0.523	125		1		
DTC073B	MIX-AR				0.487	1%		9.11	4%		360	0.014			1		
DTC076A	MIX-AR				0.483	1%		5.75	4%		370	0.033			1		
EC329	MIX-ER				0.498	3%		4.18	9%		360	0.402	300		1		
EC330	MIX-ER				0.316	2%		4.25	9%		360	0.343	180		1		
EC334	MIX-ER				0.499	3%		7.24	10%		360	0.407	175		1		
ETC218	MIX-ER				0.469	2%		4.83	8%		360	0.788	225		2		
EC231	SURG-7				0.681	3%		13.17			360	0.621	240	o	1		
EC232	SURG-7				0.482	4%		9.31			390	0.339			1		
EC233	SURG-7				0.094	20%		9.50			360	0.326	240		1		
EC238	SURG-7				0.906	2%		10.10			490	0.688	430		1		
EC241	SURG-7				0.465	2%		4.97			360	0.406			1		
EC242	SURG-7				0.462	5%		12.83			360	0.678	100		1		
EC243	SURG-7				0.469	3%		9.74			150	0.712	125		1		
EC245	SURG-7				0.937	2%		12.86			360	0.890	175		1		
EC246	SURG-7				0.478	2%		8.56			570	0.571	560		1		
EC247	SURG-7				0.481	2%		6.17			300	0.654	220		1		
EC237	SURG-7		problems	2	0.465	2%		10.66			360	0.649	240		1		
ITC438	SURG-4				0.080	17%		3.93	8%		360	0.298			2		
ITC440	SURG-4				0.079	16%		1.84	8%		360	0.313			2		
ITC442	SURG-4				0.139	9%		3.67	8%		360	0.481			2		
ITC444	SURG-4				0.138	10%		1.78	8%		630	0.446			2		
ITC446	SURG-4				0.075	16%		5.49	6%		360	0.246	165		2		
ITC450	SURG-4				0.082	14%		3.62	8%		360	0.343	345		2		
ITC452	SURG-4				0.084	13%		3.51	8%		360	0.342			2		
ITC456	SURG-4				0.083	14%		17.47			360	0.337			2		
ITC459	SURG-4				0.080	14%		3.68	8%		360	0.330	345		2		
ITC461	SURG-4				0.086	13%		3.74	8%		360	0.327			2		
ITC465	SURG-4				0.091	12%		3.55	8%		360	0.331	345		2		

					Initial NOx			Carbon			Run time	Max O3		(See below for codes)			
RunID	Classification		Data base status		ppm	unc		ppmC	unc		(min)	(ppm)	(min)	Cond-itions	Char. set	Model-able	Inp File
ITC467	SURG-4				0.094	13%		3.61	8%		360	0.305			2		
ITC471	SURG-4				0.088	14%		3.46	8%		360	0.297			2		
ITC483	SURG-4				0.083	15%		3.61	8%		360	0.337			2		
ITC488	SURG-4				0.081	14%		5.35	9%		360	0.292			2		
ITC489	SURG-4				0.085	13%		3.69	8%		360	0.293			2		
ITC497	SURG-4				0.086	13%		3.60	8%		360	0.292			2		
ITC501	SURG-4				0.088	13%		3.58	8%		360	0.316	345		2		
ITC503	SURG-4				0.094	15%		3.64	8%		360	0.284			2		
ITC571	SURG-4				0.110	21%		3.57	5%		360	0.313	331		4		
ITC572	SURG-4				0.120	19%		3.66	5%		360	0.361			4		
ITC574	SURG-4				0.095	21%		3.47	5%		360	0.329	345		4		
ITC578	SURG-4				0.088	18%		3.39	5%		360	0.349			4		
ITC580	SURG-4				0.093	13%		3.52	5%		360	0.352			4		
ITC581	SURG-4				0.092	13%		3.99	5%		360	0.350	345		4		
ITC584	SURG-4				0.093	12%		3.73	5%		360	0.375			4		
ITC586	SURG-4				0.080	19%		3.58	5%		360	0.352			4		
ITC590	SURG-4				0.086	34%		3.54	5%		360	0.369			4		
ITC598	SURG-4				0.096	12%		3.69	5%		360	0.363			4		
ITC603	SURG-4				0.088	13%		3.47	5%		360	0.330			4		
ITC607	SURG-4				0.096	14%		3.81	5%		360	0.380			4		
ITC609	SURG-4				0.090	15%		3.82	5%		360	0.363			4		
ITC613	SURG-4				0.083	16%		3.81	5%		360	0.334	345		4		
EC676	SURG-4		problems	3	0.090	18%		4.22	8%		360	0.171	150		1		
ITC437	SURG-4		problems	3	0.080	16%		3.79	8%		360	0.396			2		
ITC473	SURG-4		No Temp	2	0.086	15%		3.54	8%		360	0.296	285		2	3	no
ITC493	SURG-4		No Temp	2	0.083	14%		3.70	8%		360	0.296			2	3	no
ITC499	SURG-4		No Temp	2	0.086	13%		3.63	8%		360	0.287			2	3	no
ITC439	SURG-4		Reject	99	0.075	15%					360	0.345	345		2	3	no
EC675	SURG-4		Don't model	9	0.121	16%		4.10	8%		300	0.174	165		1	9	
ITC445	SURG-4		don't model	9	0.038	92%		3.41	8%		400	0.332			2	9	
ITC479	SURG-4		Don't model	9	0.083	14%		3.61	8%		360	0.332			2	9	
ITC592	SURG-4		Don't model	9	0.053	98%		3.19	5%		360	0.359	345		4	9	
ITC597	SURG-4		Don't model	9	0.087	13%		3.43	5%		360	0.339		o	4	9	
ITC977	SURG-4		Don't model	9	0.097	53%		3.17	2%		360	0.365	345		11	9	
ITC978	SURG-4		Don't model	9	0.074	69%		3.28	2%		360	0.351	345		11	9	
ITC980	SURG-4		Don't model	9	0.100	51%		2.64	2%		360	0.400			11	9	
ITC982	SURG-4		Don't model	9	0.084	60%		2.95	2%		360	0.364			11	9	
ITC985	SURG-4		Don't model	9	0.088	58%		2.70	2%		360	0.355			11	9	

					Initial NOx			Carbon			Run time	Max O3		(See below for codes)			
RunID	Classification		Data base status		ppm	unc		ppmC	unc		(min)	(ppm)	(min)	Cond-itions	Char. set	Model-able	Inp File
ITC991	SURG-4		Don't model	9	0.106	48%		2.56	2%		360	0.387	345		11	9	
ITC994	SURG-4		Don't model	9	0.075	68%		2.47	2%		360	0.333			11	9	
ITC997	SURG-4		Don't model	9	0.105	49%		2.69	2%		360	0.322			11	9	
ITC477	SURG-4		reject	99	0.089	13%		3.46	8%		360	0.359	165		2	9	
ITC487	SURG-4		reject	99	0.084	14%		3.58	8%		360	0.278	345		2	9	
ITC573	SURG-4R				0.111	20%		3.10	6%		360	0.339			4		
ETC455	SURG-8				0.550	2%		4.07			360	0.234			3		
ETC460	SURG-8				0.500	2%		3.83			360	0.286			3		
ETC463	SURG-8				0.515	2%		0.06			360	0.235			3		
DTC029B	SURG-8				0.174	0%		4.27			370	0.495			1		
DTC030A	SURG-8				0.167	0%		4.00			375	0.459			1		
DTC031B	SURG-8				0.171	1%		4.27			370	0.480			1		
DTC032A	SURG-8				0.174	0%		4.21			380	0.468			1		
DTC033B	SURG-8				0.168	0%		4.15			370	0.476	340		1		
DTC034A	SURG-8				0.165	0%		3.96			370	0.465	350		1		
DTC035B	SURG-8				0.167	0%		3.98			370	0.474	340		1		
DTC036B	SURG-8				0.181	0%		4.35			375	0.481	315		1		
DTC037A	SURG-8				0.174	0%		4.25			380	0.471	350		1		
DTC038B	SURG-8				0.169	0%		3.91			370	0.468	340		1		
DTC066A	SURG-8				0.173	0%		3.80	2%		375	0.459	325		1		
DTC067A	SURG-8				0.171	0%		3.84	2%		375	0.457			1		
DTC071A	SURG-8				0.178	0%		3.97	2%		375	0.464	345		1		
XTC109	SURG-8				0.243	3%		3.75	3%		360	0.517			1		
XTC116	SURG-8				0.222	3%		4.07	3%		365	0.491			1		
DTC027A	SURG-8		minor problems	1	0.153	0%		3.98			385	0.493	345		1		
DTC027B	SURG-8		minor problems	1	0.153	0%		4.03			385	0.498			1		
ETC454	SURG-8		problems	2	0.517	2%		4.17			360	0.292			3		
DTC039A	SURG-8		problems	2	0.178	0%		4.09			380	0.469			1		
ETC504	SURG-8		Can't model	9	0.402	2%					360	0.382			3		
ITC626	SURG-8	MD			0.293	8%		4.07	3%		1800	0.615	660	md,ri	5		
ITC630	SURG-8	MD			0.312	8%		1.93	4%		3600	0.282	720	md,ri	5		
ITC631	SURG-8	MD			0.319	11%		1.05	3%		4170	0.042	705	md,ri	5		
ITC633	SURG-8	MD			0.613	8%		3.94	4%		3300	0.230	720	md	5		
ITC635	SURG-8	MD			1.188	7%		4.01	4%		2850	0.006	660	md	5		
ITC637	SURG-8	MD			0.298	9%		3.93	4%		5190	0.614	570	md,ri	5		
ITC865	SURG-8	MD			0.310	10%		4.51	4%		4680	0.635	510	md,ri	9		
ITC867	SURG-8	MD	4-day run, inj. days 3,4	0	0.280	6%		5.02			4680	0.634	675	md,ri	9		
ITC868	SURG-8	MD			0.366	4%		2.49	4%		2805	0.520	675	md	9		

					Initial NOx			Carbon			Run time	Max O3		(See below for codes)			
RunID	Classification		Data base status		ppm	unc		ppmC	unc		(min)	(ppm)	(min)	Cond-itions	Char. set	Model-able	Inp File
ITC871	SURG-8	MD			0.366	5%		1.97	4%		2760	0.377	735	md	9		
ITC872	SURG-8	MD			0.361	5%		2.12			1800	0.214	705	md	9		
ITC873	SURG-8	MD			0.375	5%		1.20	4%		2775	0.161	735	md	9		
ITC874	SURG-8	MD			0.359	5%		2.05	9%		2865	0.192	750	md	9		
ITC877	SURG-8	MD			0.376	7%		2.53			2160	0.251	735	md	9		
ITC880	SURG-8	MD			0.664	5%		2.34	5%		4590	0.031	735	md	9		
ITC881	SURG-8	MD			0.665	5%		2.27			4200	0.012	450	md	9		
ITC885	SURG-8	MD			0.638	2%		1.39	4%		4215	0.012	720	md	9		
ITC888	SURG-8	MD			0.317	4%		3.61	11%		2760	0.583	720	md	9		
ITC891	SURG-8	MD			0.321	4%		4.18	4%		2760	0.606	495	md	9		
ITC886	SURG-8	MD	Don't model	9	0.708	2%		2.33			4200	0.012	600	md	9	9	
ETC047	SURG-3M				0.530	2%		4.24	8%		360	0.355			1		
ETC050	SURG-3M				0.511	2%		3.87	8%		360	0.310			1		
ETC052	SURG-3M				0.514	2%		3.85	8%		360	0.243			1		
ETC058	SURG-3M				0.500	3%		3.83	7%		360	0.231			1		
ETC060	SURG-3M				0.505	3%		3.88	7%		360	0.285			1		
ETC063	SURG-3M				0.507	3%		3.78	7%		360	0.243			1		
ETC067	SURG-3M				0.504	3%		3.76	7%		360	0.246			1		
ETC071	SURG-3M				0.498	3%		3.57	7%		360	0.291			1		
ETC075	SURG-3M				0.509	3%		3.68	7%		360	0.182			1		
ETC077	SURG-3M				0.508	3%		3.60	7%		360	0.213			1		
ETC080	SURG-3M				0.505	3%		3.65	7%		360	0.290			1		
ETC081	SURG-3M				0.513	3%		3.67	7%		360	0.195			1		
ETC083	SURG-3M				0.503	3%		3.64	7%		360	0.235			1		
ETC087	SURG-3M				0.512	3%		3.65	7%		360	0.187			1		
ETC089	SURG-3M				0.520	3%		3.63	7%		360	0.182			1		
ETC090	SURG-3M				0.546	3%		3.80	7%		360	0.109			2		
ETC091	SURG-3M				0.508	2%		3.55	7%		360	0.090			2		
ETC093	SURG-3M				0.515	2%		3.63	7%		360	0.122			2		
ETC095	SURG-3M				0.509	2%		3.67	7%		360	0.105			2		
ETC098	SURG-3M				0.511	2%		3.52	7%		360	0.088			2		
ETC100	SURG-3M				0.510	2%		3.56	7%		360	0.109			2		
ETC102	SURG-3M				0.507	2%		3.59	7%		360	0.138			2		
ETC104	SURG-3M				0.498	2%		3.51	7%		360	0.110			2		
ETC107	SURG-3M				0.501	2%		3.71	7%		360	0.130			2		
ETC109	SURG-3M				0.518	2%		3.60	7%		360	0.075			2		
ETC113	SURG-3M				0.508	2%		3.62	7%		360	0.085			2		
ETC114	SURG-3M				0.486	2%		3.59	7%		360	0.089			2		

			Initial NOx		Carbon		Run time	Max O3		(See below for codes)			
RunID	Classification	Data base status	ppm	unc	ppmC	unc	(min)	(ppm)	(min)	Cond-itions	Char. set	Model-able	Inp File
ETC115	SURG-3M		0.533	2%	3.54	7%	360	0.066			2		
ETC116	SURG-3M		0.514	2%	3.79	7%	360	0.194			2		
ETC117	SURG-3M		0.521	2%	3.64	7%	360	0.088			2		
ETC119	SURG-3M		0.523	2%	3.77	7%	360	0.111			2		
ETC122	SURG-3M		0.527	2%	3.46	7%	360	0.121			2		
ETC124	SURG-3M		0.502	2%	3.42	7%	360	0.111			2		
ETC126	SURG-3M		0.524	2%	3.50	7%	360	0.083			2		
ETC128	SURG-3M		0.531	2%	3.53	7%	360	0.066			2		
ETC129	SURG-3M		0.527	2%	3.50	7%	360	0.071			2		
ETC130	SURG-3M		0.523	5%	3.39	7%	360	0.077			2		
ETC132	SURG-3M		0.540	5%	3.50	7%	360	0.082			2		
ETC134	SURG-3M		0.531	5%	3.46	7%	360	0.085			2		
ETC137	SURG-3M		0.523	5%	3.29	7%	360	0.064			2		
ETC139	SURG-3M		0.530	5%	3.43	7%	360	0.074			2		
ETC143	SURG-3M				3.16	7%	360	0.097			2		
ETC145	SURG-3M		0.513	2%	3.06	8%	360	0.051			2		
ETC147	SURG-3M		0.503	2%	3.06	8%	360	0.055			2		
ETC149	SURG-3M		0.514	2%	3.06	7%	360	0.064			2		
ETC153	SURG-3M		0.527	3%			360	0.316			2	no	no
ETC154	SURG-3M		0.505	3%			360	0.249			2	no	no
ETC156	SURG-3M		0.508	3%	4.35	7%	360	0.301			2		
ETC158	SURG-3M		0.495	3%	4.33	7%	360	0.236			2		
ETC160	SURG-3M		0.500	3%	4.87	8%	360	0.297			2		
ETC161	SURG-3M		0.518	2%	4.69	8%	360	0.300			2		
ETC162	SURG-3M		0.496	2%	4.71	8%	360	0.316			2		
ETC165	SURG-3M		0.503	2%	4.89		360	0.411			2		
ETC168	SURG-3M		0.518	2%	4.51	7%	360	0.336			2		
ETC170	SURG-3M		0.511	2%	4.54	9%	360	0.337			2		
ETC172	SURG-3M		0.501	4%	4.54	7%	360	0.307			2		
ETC174	SURG-3M		0.496	4%	4.80	6%	360	0.297			2		
ETC210	SURG-3M		0.502	3%	4.78	7%	360	0.280			2		
ETC215	SURG-3M		0.481	2%	4.59	8%	360	0.265			2		
ETC223	SURG-3M		0.500	2%	4.39	8%	360	0.324			2		
ETC225	SURG-3M		0.502	2%	4.40	8%	360	0.169			2		
ETC227	SURG-3M		0.501	2%	4.86	8%	360	0.242			2		
ETC229	SURG-3M		0.514	2%	4.70	8%	360	0.236			2		
ETC231	SURG-3M		0.504	2%	4.72	8%	360	0.255			2		
ETC236	SURG-3M		0.499	2%	4.31	8%	360	0.314			2		

			Initial NOx		Carbon		Run time	Max O3		(See below for codes)			
RunID	Classification	Data base status	ppm	unc	ppmC	unc	(min)	(ppm)	(min)	Cond-itions	Char. set	Model-able	Inp File
ETC238	SURG-3M		0.474	2%	4.10	8%	360	0.313			2		
ETC240	SURG-3M		0.479	2%	4.18	8%	360	0.263			2		
ETC242	SURG-3M		0.480	2%	4.35	8%	360	0.362			2		
ETC244	SURG-3M		0.475	2%	4.20	8%	360	0.320			2		
ETC246	SURG-3M		0.490	2%	4.33	8%	360	0.341			2		
ETC248	SURG-3M		0.490	2%	4.61	8%	360	0.452			2		
ETC250	SURG-3M		0.498	2%	4.84	5%	360	0.347			2		
ETC252	SURG-3M		0.495	2%	4.36		360	0.295			2		
ETC254	SURG-3M		0.423	2%	4.14	6%	360	0.258			2		
ETC256	SURG-3M		0.489	2%	4.50	6%	360	0.399			2		
ETC258	SURG-3M		0.483	2%	4.57	6%	360	0.391			2		
ETC260	SURG-3M		0.493	2%	4.60	6%	360	0.331			2		
ETC262	SURG-3M		0.474	2%	4.47	6%	360	0.391			2		
ETC264	SURG-3M		0.488	2%	4.55	6%	360	0.386			2		
ETC266	SURG-3M		0.475	2%	4.54	6%	360	0.375			2		
ETC268	SURG-3M		0.484	2%	4.44	6%	360	0.460			2		
ETC270	SURG-3M		0.491	2%	4.45	6%	360	0.368			2		
ETC272	SURG-3M		0.483	3%	4.53	6%	360	0.395			2		
ETC274	SURG-3M		0.518	4%	4.44	6%	360	0.438			2		
ETC276	SURG-3M		0.490	3%	4.29	6%	360	0.424			2		
ETC278	SURG-3M		0.509	3%	4.25	6%	360	0.419			2		
ETC280	SURG-3M		0.503	3%	4.31	6%	360	0.459			2		
ETC282	SURG-3M		0.503	3%	4.21	6%	360	0.433			2		
ETC284	SURG-3M		0.494	2%	4.32	6%	360	0.456			2		
ETC286	SURG-3M		0.482	2%	4.28	6%	360	0.473			2		
ETC288	SURG-3M		0.491	3%	4.09	6%	360	0.505			2		
ETC290	SURG-3M		0.493	3%	4.46	3%	360	0.527			2		
ETC292	SURG-3M		0.491	3%	4.29	6%	360	0.410			2		
ETC294	SURG-3M		0.476	3%	4.27	3%	360	0.425			2		
ETC296	SURG-3M		0.472	3%	4.15	6%	360	0.465			2		
ETC298	SURG-3M		0.486	3%	4.46	6%	360	0.517			2		
ETC300	SURG-3M		0.476	3%	4.42	6%	360	0.436			2		
ETC302	SURG-3M		0.458	3%	4.40	6%	360	0.222			2		
ETC304	SURG-3M		0.486	3%	4.29	6%	360	0.222			2		
ETC306	SURG-3M		0.541	3%	4.22	6%	360	0.241			2		
ETC308	SURG-3M		0.526	3%	4.30	6%	360	0.272			2		
ETC310	SURG-3M		0.528	3%	4.34	6%	360	0.196			2		
ETC312	SURG-3M		0.524	3%	4.35	6%	360	0.176			2		

					Initial NOx			Carbon			Run time	Max O3		(See below for codes)			
RunID	Classification		Data base status		ppm	unc		ppmC	unc		(min)	(ppm)	(min)	Cond-itions	Char. set	Model-able	Inp File
ETC314	SURG-3M				0.535	3%		4.26	6%		360	0.208			2		
ETC316	SURG-3M				0.499	3%		4.15	6%		360	0.234			2		
ETC323	SURG-3M				0.544	2%		4.71	6%		360	0.606			2		
ETC324	SURG-3M				0.619	2%		4.78	6%		360	0.201			2		
ETC325	SURG-3M				0.528	2%		4.73	4%		360	0.392			2		
ETC326	SURG-3M				0.530	2%		4.66	4%		360	0.440			2		
ETC327	SURG-3M				0.491	2%		4.62			360	0.492			2		
ETC328	SURG-3M				0.520	2%		4.56			360	0.380			2		
ETC329	SURG-3M				0.525	2%		4.65	4%		360	0.416			2		
ETC330	SURG-3M				0.498	2%		4.59			360	0.480			2		
ETC331	SURG-3M				0.509	2%		4.58	4%		360	0.413			2		
ETC334	SURG-3M				0.523	2%		4.62	4%		360	0.423			2		
ETC336	SURG-3M				0.529	2%		4.72	3%		360	0.439			2		
ETC339	SURG-3M				0.520	2%		4.95	3%		360	0.522			2		
ETC345	SURG-3M				0.520	2%		4.85	4%		360	0.502			2		
ETC347	SURG-3M				0.518	2%		4.84	4%		360	0.457			2		
ETC349	SURG-3M				0.509	2%		4.77	3%		360	0.509			2		
ETC351	SURG-3M				0.572	2%		4.66	3%		360	0.331			2		
ETC353	SURG-3M				0.507	2%		4.70	3%		360	0.437			2		
ETC356	SURG-3M				0.512	2%		4.31	3%		360	0.375			2		
ETC373	SURG-3M				0.561	2%		4.71	3%		360	0.757			3		
ETC376	SURG-3M				0.499	2%		4.70	3%		360	0.388			3		
ETC408	SURG-3M				0.532	3%		4.60	4%		360	0.255			3		
ETC411	SURG-3M				0.519	3%		4.80	4%		360	0.289			3		
ETC413	SURG-3M				0.537	3%		4.68	4%		360	0.251			3		
ETC415	SURG-3M				0.535	3%		4.71	4%		360	0.182			3		
ETC417	SURG-3M				0.583	2%		5.02	3%		360	0.209			3	no	no
ETC419	SURG-3M				0.541	2%		4.97	4%		360	0.231			3		
XTC104	SURG-3M				0.509	3%		3.83	4%		360	0.166			1		
ETC164	SURG-3M		problems	1	0.501	2%					360	0.280			2	no	no
ETC234	SURG-3M		problems	1	0.496	2%		4.35	8%		360	0.342			2		
ETC176	SURG-3M		problems	3							360	0.261			2	no	no
ETC177	SURG-3M		problems	3							360	0.259			2	no	no
ETC178	SURG-3M		problems	3							360	0.282			2	no	no
ETC180	SURG-3M		problems	3	0.381			3.83	9%		360	0.430			2		
ETC182	SURG-3M		problems	3	0.378						360	0.328			2		no
ETC184	SURG-3M		problems	3	0.377						360	0.242			2		no
ETC186	SURG-3M		problems	3	0.405			2.19	5%		360	0.283			2		

					Initial NOx			Carbon			Run time	Max O3		(See below for codes)			
RunID	Classification		Data base status		ppm	unc		ppmC	unc		(min)	(ppm)	(min)	Cond-itions	Char. set	Model-able	Inp File
ETC188	SURG-3M		problems	3				3.04	5%		360	0.383			2		
ETC189	SURG-3M		problems	3	0.533	9%					360	0.332			2	no	no
ETC191	SURG-3M		problems	3	0.457	8%					360	0.351			2	no	no
ETC193	SURG-3M		problems	3	0.444	8%					360	0.305			2	no	no
ETC195	SURG-3M		problems	3	0.475	7%					360	0.340			2	no	no
ETC197	SURG-3M		problems	3				2.93	4%		360	0.454			2		
ETC198	SURG-3M		problems	3	0.507	3%					360	0.282			2	no	no
ETC200	SURG-3M		problems	3	0.495	3%					360	0.307			2	no	no
ETC202	SURG-3M		problems	3	0.504	3%					360	0.297			2	no	no
ETC204	SURG-3M		problems	3	0.518	3%					360	0.353			2	no	no
ETC208	SURG-3M		problems	3	0.489	3%		4.48	3%		360	0.196			2		
ETC233	SURG-3M		problems	9	0.518	2%					360	0.268			2		no
ETC372	SURG-3M		Do not model	9	0.483	2%		4.72	3%		360	0.758			3		
ETC217	SURG-3				0.257	2%		4.49	8%		360	0.644			2		
ETC219	SURG-3				0.250	2%		4.39	8%		420	0.706			2		
ETC387	SURG-3				0.147	4%		3.16	4%		360	0.504			3		
ETC388	SURG-3				0.149	4%		3.78	3%		360	0.536			3		
ETC390	SURG-3				0.144	4%		3.92	4%		360	0.543			3		
ETC392	SURG-3				0.154	4%		3.65	3%		360	0.557			3		
ETC395	SURG-3				0.143	4%		3.91	4%		360	0.547			3		
ETC399	SURG-3				0.155	4%		3.90	4%		360	0.480			3		
ETC401	SURG-3				0.148	4%		3.93	4%		360	0.486	330		3		
ETC403	SURG-3				0.151	4%		3.41	4%		360	0.510			3		
ETC405	SURG-3				0.134	4%		3.68	4%		360	0.506			3		
ETC407	SURG-3				0.158	4%		3.73	3%		360	0.539			3		
ETC397	SURG-3		probmems	2	0.135			3.86	3%		360	0.531			3	no	no
DTC011A	SURG-8M				0.522	2%		3.91			360	0.343			1		
DTC011B	SURG-8M				0.521	2%		3.78			360	0.368			1		
DTC013A	SURG-8M				0.452	1%		4.11			365	0.440			1		
DTC013B	SURG-8M				0.454	1%		4.00			365	0.437			1		
DTC014B	SURG-8M				0.477	1%		3.99			375	0.449			1		
DTC016B	SURG-8M				0.475	1%		3.92	3%		380	0.440			1		
DTC017B	SURG-8M				0.479	1%		3.94	3%		380	0.428			1		
DTC018B	SURG-8M				0.484	1%		4.23			375	0.469			1		
DTC019A	SURG-8M				0.459	1%		4.13			375	0.428			1		
DTC021A	SURG-8M				0.492	1%		4.15			380	0.411			1		
DTC022A	SURG-8M				0.503	1%		4.01			380	0.400			1		
DTC023B	SURG-8M				0.471	1%		4.08			375	0.462			1		

					Initial NOx			Carbon			Run time	Max O3		(See below for codes)			
RunID	Classification		Data base status		ppm	unc		ppmC	unc		(min)	(ppm)	(min)	Cond-itions	Char. set	Model-able	Inp File
DTC024A	SURG-8M				0.502	1%		4.09			380	0.450			1		
DTC025B	SURG-8M				0.466	1%		4.19			375	0.482			1		
DTC028B	SURG-8M				0.485	1%		4.11			375	0.418			1		
DTC064A	SURG-8M				0.486	1%		3.97	2%		375	0.384			1		
DTC065B	SURG-8M				0.477	1%		3.95	2%		375	0.393			1		
DTC068A	SURG-8M				0.484	1%		3.80	2%		375	0.345			1		
DTC069B	SURG-8M				0.478	1%		3.65	2%		375	0.389			1		
DTC070B	SURG-8M				0.487	1%		4.01	2%		375	0.368			1		
XTC114	SURG-8M				0.478	3%		4.70	3%		365	0.366			1		
DTC012A	SURG-8M		problems	1	0.517	2%		4.07			360	0.403			1		
DTC012B	SURG-8M		problems	1	0.512	2%		4.04			360	0.401			1		
DTC015A	SURG-8M		problems	1	0.503	1%		4.16			360	0.443			1		
DTC020A	SURG-8M		problems	2	0.501	1%		4.12			375	0.295			1		
ITC781	SYNFUEL				0.516	4%		44.04			360	0.714			7		
ITC784	SYNFUEL				0.508	8%		86.55			360	0.746	330		7		
ITC785	SYNFUEL				0.260	6%		44.85			360	0.599	345		7		
ITC786	SYNFUEL				0.492	6%		72.84			270	0.635	135		7		
ITC788	SYNFUEL				0.474	6%		92.11			360	0.717	300		7		
ITC795	SYNFUEL				0.531	8%		46.06			360	0.743			8		
ITC796	SYNFUEL				0.590	8%		97.63			360	0.596	255		8		
ITC799	SYNFUEL		problems	2	0.614	8%		96.84			360	0.839	315		8		
ITC801	SYNFUEL		Don't model	9	0.610	7%		41.25			420	0.880			8	9	
ITC805	SYNFUEL		Don't model	9	0.588	8%		90.75			360	0.772	345		8	9	
ITC807	SYNFUEL		Don't model	9	0.475	3%		69.64	3%		300	0.523	195		8	9	
ITC963	SYNEXH		data sparse	2	0.469	11%		5.41			390	0.830			10		
ITC965	SYNEXH		Don't model	9	0.465	11%		4.81			360	0.865	330		10	9	
ITC967	SYNEXH		Don't model	9	0.238	22%		5.33			360	0.594	195		10	9	
ITC968	SYNEXH		Don't model	9	0.470	11%		7.50			360	0.857	150		10	9	
ETC355	SPECIAL				0.000			4.40	3%						2	no	no
DTC040A	SPECIAL				0.001	0%		3.90			375	0.020			1		
DTC040B	SPECIAL				0.001	0%		3.95			375	0.027			1		
ETC354	SPECIAL		Do not model	9	0.000			5.03	4%						2	no	no
EC402	SPECIAL		Reject	99				292.88							0	2	no
EC725	SPECIAL		Don't model	9											1	3	no
ITC640	SPECIAL		don't model. 3-part run	9							420	0.531		o	5	9	
ITC429	REJECT		reject	99	0.000			1.59	11%		120	0.065	60		1	3	no
Modelability Codes																	

			Initial NOx			Carbon			Run time	Max O3		(See below for codes)			
RunID	Classification	Data base status	ppm	unc		ppmC	unc		(min)	(ppm)	(min)	Cond-itions	Char. set	Model-able	Inp File
EC															
1	Chamber parameters not assigned for this set of conditions.														
2	Characterization set not defined														
2	Insifficient run conditions defined to create model input file														
ITC															
1	Chamber parameters not assigned for this set of conditions														
2	Characterization set not defined														
3	Insufficient run conditions defined to create model input file														
4	Simulation failed for SAPRC-90 mechanism and software														
9	Simulation succeeded, but recommended not to model run.														
Others															
no	Not modelable														
Special Conditions Codes															
EC															
d	Dry														
lt	Low Temperature														
ht	High Temperature														
vn	Vacuum injected NOx														
uv	Varied UV - different Pyrex filter														
n	Reactant injected in moddle of run														
ITC															
nb	New bag														
ri	Reactant injected during run														
hl	100% lights														
md	Multi-day. Lights off at night, on during day														
ht	Unusually high temperature.														
o	Other -- see main sheet														
DTC															
rh	50% RH														
Characterixation Sets															

			Initial NOx			Carbon			Run time	Max O3		(See below for codes)			
RunID	**Classification**	**Data base status**	**ppm**	**unc**		**ppmC**	**unc**		**(min)**	**(ppm)**	**(min)**	**Cond-itions**	**Char. set**	**Model-able**	**Inp File**
EC															
1	T, RH in normal range														
2	Low T														
3	High T														
1x	Low RH (Second digit indicates T.)														
ITC															
1-12	Same as ITC Bag number.														
ETC															
1	First bag, before vacuum injected NOx														
2	First bag, vacuum injected NOx														
3	Third bag, vacuum injected NOx														
DTC															
1	Normal (dry)														
2	50% RH														
XTC															
1	Normal														

TABLE A-2.

UNC DATABASE AVAILABLE FEBRUARY 1997

mo/day/yy	General Description & NOx	RED SIDE VOC	BLUE SIDE VOC
au0877	Matched HC at 0.49 ppm NO_x	RED : 1.5 ppmC Propene	BLUE: 1.5 ppmC Propene
de2677	HC Reactivity 0.4 ppm NO_x	RED : 2.96 ppmC Propene	BLUE: 3.82 ppmC Acetaldehyde
jl1877	HC Reactivity at 0.52 ppm NO_x	RED : 1.16 ppmC Formaldehyde	BLUE: 0.97 ppmC Acetaldehyde
jl2077	Delta HC at 0.29 ppm NO_x	RED : 0.65 ppmC Propene	BLUE: 1.23 ppmC Propene
jl2777	HC Reactivity at 0.55 ppm NO_x	RED : 1.0 ppmC Formaldehyde	BLUE: 0.55 ppmC Acetaldehyde
jl2877	Delta HC at 0.53 ppm NO_x	RED : 1.1 ppmC Formaldehyde	BLUE: 2.2 ppmC Formaldehyde
my1877	HC Reactivity at 0.36 ppm NO_x	RED : 1.87 ppmC Acetaldehyde	BLUE: 0.92 ppmC Formaldehyde
no0977	Delta HC at 0.55 ppm NO_x	RED : 3.76 ppmC Propene	BLUE: 1.92 ppmC Propene
no1277	HC Reactivity at 0.46 ppm NO_x---MO	RED : 2.00 ppmC Ethene--See IC Warning N	BLUE: 1.80 ppmC Acetaldehyde
no1977	HC Reactivity at 0.52 ppm NO_x	RED : 3.78 ppmC Ethene	BLUE: 3.82 ppmC Acetaldehyde
no2077	HC Reactivity at Delta NO_x	RED : 4.37 ppmC Ethene	BLUE: 3.92 ppmC Acetaldehyde
oc1877	Delta HC at 0.49 ppm NO_x	RED : 3.89 ppmC Ethene	BLUE: 1.89 ppmC Ethene
oc2277	HC Reactivity at 0.52 ppm NO_x	RED : 3.69 ppmC Propene	BLUE: 8.10 ppmC n-Butane
oc2477	HC Characterization at 0.48 ppm NO_	RED : 3.69 ppmC Propene	BLUE: Background---See IC
st1977	Delta HC at 0.39 ppm NO_X	RED : 1.00 ppmC Formaldehyde	BLUE: 0.68 ppmC Formaldehyde
au1478	CO Characterization at 0.54 ppm NO_	RED : Background	BLUE: 48.2 ppm CO---See IC
au1578	HC Reactivity at 0.55 ppm NO_x	RED : 1.45 ppmC Propene	BLUE: 1.58 ppmC Ethene
au1678	HC Reactivity at 0.65 ppm NO_x	RED : 1.56 ppmC Propene	BLUE: 3.91 ppmC Toluene
au1778	Delta HC at 0.70 ppm NO_x	RED : 0.96 ppmC Acetaldehyde	BLUE: 4.00 ppmC Acetaldehyde
au1878	Delta HC at 0.49 ppm NO_x	RED : 0.74 ppmC Propene	BLUE: 2.88 ppmC Propene
au2178	HC Reactivity at 1 ppm NO_x	RED : 1.39 ppmC Ethene	BLUE: 1.28 ppmC Propene
au2378	Matched HC at 0.5 ppm NO_x	RED : 2.93 ppmC Ethene	BLUE: 2.97 ppmC Ethene
au2478	Matched HC at Delta NO_x	RED : 58.00 ppmC n-Butane	BLUE: 56.30 ppmC n-Butane
au2578	Delta HC at 0.52 ppm NO_x	RED : 13.26 ppmC n-Butane	BLUE: 26.62 ppmC n-Butane
fe2778	HC Reactivity at Delta NO_x	RED : 3.95 ppmC Propene	BLUE: 1.90 ppmC Acetaldehyde
ja1078	HC Reactivity at 0.48 ppm NO_x	RED : 3.25 ppmC Propene	BLUE: 4.35 ppmC Ethene
ja2878	HC Characterization at 0.42 ppm NO_	RED : 3.19 ppmC Propene	BLUE: Background
ja2978	HC Characterization at 0.44 ppm NO_	RED : 3.2 ppmC Propene	BLUE: Background
jl0178	HC Reactivity at Delta NO_x	RED : 1.45 ppmC Ethene	BLUE: 1.54 ppmC Propene
jl2178	Delta HC at 0.23 ppm NO_x	RED : 7.3 ppmC n-Butane	BLUE: 15.7 ppmC n-Butane
jl2278	Delta HC at 0.55 ppm NO_x	RED : 8.36 ppmC n-Butane	BLUE: 17.27 ppmC n-Butane
jl2478	Delta HC at 0.96 ppm NO_x	RED : 2.97 ppmC Propene	BLUE: 1.47 ppmC Propene
jl3078	HC Reactivity at 0.48 ppm NO_x	RED : 1.32 ppmC Ethene	BLUE: 1.25 ppmC Propene
jn1678	HC Reactivity at 0.64 ppm NO_x	RED : 3.97 ppmC Ethene	BLUE: 2.00 ppmC Propene
jn1878	HC Reactivity at 0.36 ppm NO_x	RED : 2.27 ppmC n-Butane, 0.75 ppmC Prop	BLUE: 3.28 ppmC UNCMIX77
jn2178	HC Reactivity at 0.36 ppm NO_x	RED : 2.03 ppmC UNCMIX77	BLUE: 1.58 ppmC n-C4,.54ppmCPrp
mr0678	HC Reactivity at Delta NO_x	RED : 3.77 ppmC Propene	BLUE: 1.80 ppmC Acetaldehyde
mr3178	HC Characterization at 0.49 NO_x: U	RED : 3.82 ppmC Propene	BLUE: 2.00 ppmC Acetaldehyde E
no0278	Delta HC at 0.56 ppm NO_x	RED : 3.52 ppmC Propene	BLUE: 1.41 ppmC Propene
no0778	HC Reactivity at 0.45 ppm NO_x	RED : 1.34 ppmC Propene	BLUE: 2.67 ppmC Ethene

TABLE A-2 Continued.

oc0378	HC Reactivity at 0.5 ppm NO_x	RED : 0.98 ppmC Ethene	BLUE: 0.14 ppmC n-C4, 1.36 ppmC Prop
oc1278	HC Reactivity at 0.48 ppm NO_x	RED : 1.26 ppmC Acetaldehyde, 0.20 ppmC	BLUE: 1.33 ppmC Propene
oc1878	HC Reactivity at 0.46 ppm NO_x	RED : 3.12 ppmC Ethene	BLUE: 1.52 ppmC Propene
oc2078	Delta HC at 0.46 ppm NO_x	RED : 1.39 ppmC Propene	BLUE: 3.65 ppmC Propene
oc2178	Matched HC at 0.51 ppm NO_x, Delta	RED : 3.50 ppmC Propene	BLUE: 3.45 ppmC Propene
oc2278	Matched HC at 0.49 ppm NO_x	RED : 1.38 ppmC Propene	BLUE: 1.38 ppmC Propene
oc2578	HC Reactivity at 0.44 ppm NO_x	RED : 1.16 ppmC Acetaldehyde, 0.2 ppmC E	BLUE: 1.22 ppmC Propene
st1478	HC Reactivity at 0.30 ppm NO_x	RED : 2.24 ppmC Toluene	BLUE: 0.97 ppmC Ethene
st1878	DEMO:HC Reactivity at Matched NO_x	RED : 2.98 ppmC Ethene	
st1978	HC Substitution at 0.69 ppm NO_x	RED : 1.88 ppmC Ethene	BLUE: 0.34 ppmC Ethene,2.07ppmC Formal
au0179	HC Reactivity at 0.35 ppm NO_x, Del	RED : 1.91 ppmC Acetaldehyde	BLUE: 1.00 ppmC Formaldehyde
au0279	HC Reactivity at 0.21 ppm NO_x	RED : 1.49 ppmC Propene	BLUE: 1.01 ppmC Formaldehyde
au0579	HC Reactivity at Delta NO and 0.13	RED : 4.11 ppmC Ethene	BLUE: 1.21 ppmC Formaldehyde
au1379	Delta HC at Delta NO_x	RED : 4.4 ppmC Propene	BLUE: 0.57 ppmC Propene
au1679	HC Reactivity at 0.44 ppm NO_x	RED : 1.42 ppmC Propene	BLUE: 0.17 ppmC Ethen,1.30 ppmC Acetal
jl2979	Matched HC, CO One Side, at 0.50 pp	RED : 1.99 ppmC Propene -- After Sunrise	BLUE: 1.88 ppmC Propene, 11.98 ppm CO
jn1279	HC Reactivity at 0.50 ppm NO_x	RED : 0.83 ppmC Propene	BLUE: 0.53 ppmC Propen,0.80 ppmC Aceta
jn1379	HC Reactivity at 0.45 ppm NO_x	RED : 2.74 ppmC Propene	BLUE: 2.73 ppmC Propen,3.16 ppmC Tolue
jn1479	HC Reactivity at 0.45 ppm NO_x	RED : 1.82 ppmC Propene, 0.112 Propane	BLUE: 1.80 ppmC Propen, 0.153 Propane,
jn2079	HC Reactivity at 0.18 ppm NO_x	RED : 6.23 ppmC n-Butane	BLUE: 6.00 ppmC MEK
jn2779	HC Reactivity at 0.33 ppm NO_x	RED : 5.85 ppmC Benzaldehyde	BLUE: 15.54 ppmC Toluene
jn2979	Matched HC at 0.45 ppm NO_x, Delta	RED : 4.10 ppmC Propene	BLUE: 4.05 ppmC Propene
my2179	Delta HC at Background NO_x	RED : 2.81 ppmC Acetaldehyde	BLUE: 0.83 ppmC Acetaldehyde
oc0979	HC Reactivity at 0.20 ppm NO_x	RED : 14.35 ppmC n-Butane	BLUE: 14.23 ppmC n-Pentane
oc1479	Matched HC at 0.50 ppm NO_x	RED : 2.92 ppmC Propene	BLUE: 2.94 ppmC Propene
oc1879	HC Reactivity at 0.20 ppm NO_x	RED : 15.92 ppmC 2,3-Dimethylbutane	BLUE: 13.84 ppmC n-Butane
oc2079	HC Reactivity at 0.22 ppm NO_x	RED : 13.50 ppmC MEK	BLUE: 12.00 ppmC 2,3-Dimethylbutane
oc2479	Matched HC at 0.46 ppm NO_x	RED : 3.55 ppmC Propene	BLUE: 3.55 ppmC Propene
au0180	DYNM-STAT Reactivity--Matched HC, D	RED : 0.46 ppmC Ethene, 0.23 ppmC trans-	BLUE: 0.48 ppmC Ethen,0.23 ppmC trans-
au0880	HC Reactivity at 0.42 ppm NO_x, Del	RED : 1.90 ppmC Acetaldehyde	BLUE: 0.85 ppmC Biacetyl
au0980	HC Reactivity at 0.47 ppm NO_x, Del	RED : 40.00 ppmC Acetone	BLUE: 36.46 ppmC Aceton,1.0 ppmC Forma
au2680	Delta HC at 0.47 ppm NO_x	RED : 1.00 ppmC Ethene	BLUE: 0.50 ppmC Ethene
au2780	HC Reactivity, Matched CO at 0.50 p	RED : 2.25 ppmC Toluene, 100 ppm CO	BLUE: 1.91 ppmC Propene, 100 ppm CO
jl1680	Delta HC at 0.18 ppm NO_x	RED : 4.01 ppmC Isoprene	BLUE: 1.97 ppmC Isoprene
jl1780	Delta HC at 0.46 NO_x	RED : 0.98 ppmC Isoprene	BLUE: 2.58 ppmC Isoprene
jl2580	Delta HC at 0.25 ppm NO_x	RED : 1.02 ppmC a-Pinene	BLUE: 0.94 ppmC a-Pinene
jl3080	HC Reactivity at 0.18 ppm NO_x	RED : 3.78 ppmC Toluene	BLUE: 2.23 ppmC o-Xylene
jn0480	HC Reactivity at 0.18 ppm NO_x	RED : 4.80 ppmC Acetone	BLUE: 3.80 ppmC MEK
jn1480	HC Reactivity at 0.21 ppm NO_x	RED : 2.30 ppmC a-Pinene, 0.90 ppmC Isop	BLUE: 1.70 ppmC a-Pinene
jn1580	Delta HC at 0.22 ppm NO_x	RED : 1.22 ppmC a-Pinene	BLUE: 0.80 ppmC a-Pinene
no0380	Night O3 Methacrolein vs Methylviny	RED : 3.6 ppmC Methacrolein	BLUE: 3.7 ppmC Methylvinylketone
oc0980	Night O3 Isoprene vs O3 only	RED : 5.0 ppmC Isoprene	BLUE: Background
au0581	HC Reactivity at 0.45 ppm NO_x	RED : 1.60 ppmC Methacrolein	BLUE: 1.50 ppmC Methylvinylketone
au1381	HC Reactivity at 0.47 ppm NO_x	RED : 1.98 ppmC Methylvinylketone	BLUE: 1.89 ppmC Methacrolein
au1481	HC Reactivity at 0.28 ppm NO_x, Del	RED : 1.0 ppmC Methylvinylketone	BLUE: 1.5 ppmC Methacrolein

TABLE A-2 Continued.

au2681	HC Substitution at 0.24 ppm NO_x	RED : 1.46 ppmC UNCMIX80, 0.56 ppmC SIMA	BLUE: 1.37 ppmC SIMMIX1,0.58 ppmC SIMA
au2781	HC Substitution at 0.23 ppm NO_x, D	RED : 2.11 ppmC SIMMIX1	BLUE: 1.43 ppmC SIMMIX1,0.58ppmC SIMAR
au3181	HC Reactivity at 0.24 ppm NO_x, Del	RED : 2.15 ppmC SIMMIX1	BLUE: 1.97 ppmC UNCMIX80
jl0981	HC Substitution at 0.40 ppm NO_x	RED : 1.97 ppmC UNCMIX80	BLUE: 1.44 ppmC UNCMIX80,0.54ppmC m-Xy
jl1581	HC Substitution at 0.27 ppm NO_x	RED : 1.56 ppmC Butane, 0.66 ppmC Propen	BLUE: 1.22 ppmC Butane,0.49ppmC Propen
jl1881	HC Substitution at 0.26 ppm NO_x	RED : 1.55 ppmC Butane, 0.58 ppmC Propen	BLUE: 1.12 ppmC C4, 0.46 ppmC Propen
jl2081	HC Substitution at 0.42 NO_x	RED : 1.24 ppmC UNCMIX80, 0.54 ppmC m-Xy	BLUE: 1.21 ppmC UNCMIX80,0.56ppmC Tolu
jl2181	Delta HC at 0.24 ppm NO_x	RED : 2.00 ppmC UNCMIX80	BLUE: 1.33 ppmC UNCMIX80
jl2281	HC Substitution at 0.26 ppm NO_x	RED : 2.40 ppmC UNCMIX80	BLUE: 1.83 ppmC UNCMIX80,0.88ppmC m-Xy
jl2381	HC Reactivity at 0.43 ppm NO_x	RED : 1.42 ppmC Isoprene	BLUE: 1.49 ppmC Formaldehyde
jn2981	HC Substitution at 0.19 ppm NO_x	RED : 1.22 ppmC UNCMIX80, 0.27 ppmC Tolu	BLUE: 1.53 ppmC UNCMIX80,
oc0181	HC Reactivity at 0.40 ppm NO_x	RED : 0.90 ppmC Biacetyl	BLUE: 0.75 ppmC Methylglyoxal
oc1481	HC Substitution at 0.28 ppm NO_x	RED : 2.60 ppmC UNCMIX80, 0.71 ppmC m-X	BLUE: 2.72 ppmC UNCMIX80,0.71ppmC 1,2,
st0281	Delta HC at 0.24 ppm NO_x, Delta DP	RED : 2.04 ppmC UNCMIX80, 0.43 ppmC SIMA	BLUE: 1.62 ppmC UNCMIX80,0.75ppmC SIMA
st0381	HC Substitution at 0.23 ppm NO_x, D	RED : 1.97 ppmC UNCMIX80, 0.46 ppmC SIMA	BLUE: 1.78 ppmC UNCMIX80,0.53ppmC SIMA
st0981	Matched HC at 0.2 ppm NO_x: STAT On	RED : 1.02 ppmC Isoprene--STAT	BLUE: 1.00 ppmC Isoprene--DYNM
st1081	HC Substitution at 0.25 ppm NO_x	RED : 2.78 ppmC UNCMIX80, 0.70 ppmC SIMA	BLUE: 1.02 ppmC UNCMIX80,0.50ppmC SIMA
st1281	HC Substitution at 0.25 ppm NO_x, D	RED : 1.70 ppmC UNCMIX80, 0.55 ppmC SIMA	BLUE: 1.14 ppmC UNCMIX80,0.40ppmC SIMA
st1481	HC Reactivity at 0.25 ppm NO_x	RED : 1.58 ppmC UNCMIX80, 0.61 ppmC m-Xy	BLUE: 1.65 ppmC UNCMIX80,0.52ppmC Tolu
st2081	HC Reactivity at 0.23 ppm NO_x	RED : 1.62 ppmC UNCMIX80, 0.65 ppmC COMA	BLUE: 1.57 ppmC UNCMIX80,0.51ppmC SIMA
st2481	HC Reactivity at 0.23 ppm NO_x, Del	RED : 1.29 ppmC n-Butane, 0.52 ppmC Prop	BLUE: 0.89 ppmC n-Butane,0.36ppmC Prop
st2881	HC Reactivity at 0.40 ppm NO_x, Del	RED : 1.80 ppmC Biacetyl	BLUE: 1.50 ppmC Methylglyoxal
st2981	HC Substitution at 0.24 ppm NO_x	RED : 1.95 ppmC UNCMIX80, 0.53 ppmC Tolu	BLUE: 1.98 ppmC UNCMIX80,0.48ppmC m-Xy
au0282	Delta CO at 0.4 ppm NO_x	RED : 0.56 ppm CO	BLUE: 45.4 ppm CO
au0382	Delta Auto Exhaust, Delta CO at Del	RED : 2.5 ppmC Auto Exhaust, 18.4 ppm CO	BLUE: 1.3 ppmC Auto Exhst Cryo-Inject,
au0682	Delta Auto Exhaust, Delta CO at 0.3	RED : 1.4 ppmC Auto Exhaust Direct-Injec	BLUE: 1.1 ppmC Auto Exhst Cryo-Inject
au0782	Matched Auto Exhaust, Matched CO at	RED : 1.48 ppmC Auto Exhaust	BLUE: 1.45 ppmC Auto Exhst Cryo-Inject
au2082	Delta CO at 0.41 ppm NO_x	RED : 0.40 ppm CO	BLUE: 50.0 ppm CO
au2282	CO Characterization: Blue Side at 0	RED : Background	BLUE: 40.4 ppm CO
au2382	Delta CO at 0.43 ppm NO_x	RED : 0.234 ppm CO	BLUE: 46.47 ppm CO
au2482	HC Reactivity at 0.32 ppm NO_x	RED : 2.1 ppmC Propionaldehyde	BLUE: 1.9 ppmC Acetaldehyde
au2782	HC Reactivity at 0.43 ppm NO_x; Red	RED : 1.99 ppmC o-Xylene	BLUE: 2.99 ppmC Toluene
de0782	HC Substitution at 0.19 ppm NO_x	RED : 2.47 ppmC UNCMIX82, 0.9 ppmC COMAR	BLUE: 3.49 ppmC UNCMIX82
jl0182	Matched Auto Exhaust, Matched CO at	RED : 3.5 ppmC Auto Exhaust, 73 ppm CO	BLUE: 3.6 ppmC Auto Exhaust, 75 ppm CO
jl0382	O_3 Decay at Background NO_x: DAY 1	RED : 0.47 ppm O3	BLUE: 0.52 ppm O3
jl0482	Continued O_3 Decay at Background N	RED : Day-Old Conditions left from O3 De	BLUE: Day-Old Cond left from O3 De
jl0682	HC Substitution at 0.23 ppm NO_x	RED : 1.4 ppmC SIMMIX, 0.89 ppmC Propylb	BLUE: 1.4 ppmC SIMMIX,0.80ppmC Toluene
jl0882	HC Substitution at 0.30 ppm NO_x	RED : 0.89 ppmC SIMARO, 0.33 ppmC Prope	BLUE: 1.03 ppmC COMARO,0.28ppmC Prope
jl1582	HC Substitution at 0.57 ppm NO_x	RED : 1.7 ppmC Auto Exhaust, 0.5 ppmC m-	BLUE: 1.8 ppmC Auto Exhst, 0.4 ppmC To
jl1782	Two Day Matched HC at Background NO	RED : 0.52 ppmC HCHO	BLUE: 0.58 ppmC HCHO
jl1882	0.49 ppm NO_x Added to Continued HC	RED : Day-Old HCHO and CO Decay--Continu	BLUE: Day-Old HCHO & CO Decay--Continu
jl1982	HC Reactivity at 0.29 ppm NO_x	RED : 2.1 ppmC UNCMIX82, 0.6 ppmC COMARO	BLUE: 2.1 ppmC SIMMIX, 0.6 ppmC COMARO
jl2682	HC Substitution at 0.30 ppm NO_x, D	RED : 2.0 ppmC UNCMIX82, 0.87 ppmC n-Pro	BLUE: 2.0 ppmC UNCMIX82,0.92ppmC Ethyl
jl2782	HC Substitution at 0.30 ppm NO_x	RED : 2.2 ppmC UNCMIX82, 0.91 ppmC m-Xyl	BLUE: 2.2 ppmC UNCMIX82,0.92ppmC n-Pro

TABLE A-2 Continued.

jl2882	HC Substitution at 0.30 ppm NO_x	RED :	2.1 ppmC UNCMIX82, 0.87 ppmC n-Pro	BLUE:	2.1 ppmC UNCMIX82,0.87ppmC 1,2,4
jn0682	Two Day Background Characterization	RED :	Background	BLUE:	Background
jn0782	Matched HC added to Day-Old O_3, De	RED :	1.0 ppmC Acetaldehyde into Day-Old	BLUE:	1.0 ppmC Acetal'd into Day-Old
jn0882	HC Substitution at 0.28 ppm NO_x	RED :	2.25 ppmC UNCMIX80, 0.74 ppmC Ethy	BLUE:	2.28 ppmC UNCMIX80,0.78ppmC Tolu
jn0982	HC Substitution at 0.29 ppm NO_x	RED :	0.64 ppmC Propene, 1.98 ppmC n-But	BLUE:	0.62 ppmC Propene,1.96ppmC n-But
jn1482	HC Reactivity at 0.3 ppm NO_x	RED :	3.1 ppmC Acetaldehyde	BLUE:	3.1 ppmC Propionaldehyde
jn1582	HC Substitution at 0.3 NO_x	RED :	3.4 ppmC UNCMIX82	BLUE:	2.5 ppmC UNCMIX82,0.9ppmC COMARO
jn1682	Background Air Characterization: DA	RED :	Background	BLUE:	Background
jn1782	0.41 ppm NO_x Added to Continued Ch	RED :	Day-old Background	BLUE:	Day-old Background
jn2582	Matched Auto Exhaust at 0.65 ppm NO	RED :	0.555 ppmC Direct AutoExhaust from	BLUE:	0.555 ppmC Direct AutoExhst from
jn2782	Delta CO at 0.45 NO_x	RED :	54.8 ppm CO	BLUE:	0.3 ppm CO
jn2982	Matched AutoExhaust at 0.25 ppm NO_	RED :	2.46 ppmC AutoExhaust, 60 ppm CO	BLUE:	2.48 ppmC AutoExhaust, 55 ppm CO
jn3082	Matched AutoExhaust at 0.32 ppm NO_	RED :	2.84 ppmC Direct AutoExhaust from	BLUE:	3.13 ppmC Direct AutoExhst from
no1582	HC Reactivity at 0.18 NO_x	RED :	2.51 ppmC SIMMIX2	BLUE:	2.74 ppmC UNCMIX82
oc0182	HC Reactivity at 0.78 ppm NO_x	RED :	1.7 ppmC Methylglyoxal	BLUE:	0.5 ppmC Glycolaldehyde
oc0382	Delta HC at 0.25 ppm NO_x	RED :	2.75 ppmC SIMMIX2	BLUE:	1.56 ppmC SIMMIX2
oc0682	Matched AutoExhaust from Different	RED :	1.97 ppmC Direct AutoExhaust from	BLUE:	1.95 ppmC Direct AutoExhst from
oc0882	Matched 0.30 ppm NO_x Decay	RED :	Background	BLUE:	Background
oc2782	HC Reactivity at 0.4 ppm NO_x	RED :	4.5 ppmC Toluene	BLUE:	2.8 ppmC o-Xylene
oc2882	HC Reactivity at 0.5 ppm NO_x	RED :	1.0 ppmC Biacetyl	BLUE:	1.0 ppmC Methylglyoxal
st0382	HC Reactivity at 0.30 NO_x	RED :	5.03 ppmC propylnitrate	BLUE:	5.04 ppmC butylnitrate
st0482	Matched HC: DYMN HC and NO_x One Si	RED :	DYNM 1.1 ppmC Propene	BLUE:	STAT 1.1 ppmC Propene
st0582	CO Characterization at 0.49 ppm NO_	RED :	Background	BLUE:	50 ppm CO
st0682	Delta HC at 0.45 ppm NO_x	RED :	2.3 ppmC Toluene, 0.5 ppmC o-Xylen	BLUE:	1.9 ppmC Toluene,1 ppmC o-Xylen
st0782	Delta HC at 0.47 ppm NO_x	RED :	2.47 ppmC Toluene, 0.42 ppmC o-Xyl	BLUE:	2.0 ppmC Toluene,1.02ppmC o-Xyl
st0882	Delta HC at 0.48 ppm NO_x	RED :	3.01 ppmC Toluene, 1.7 ppmC o-Xyle	BLUE:	3.80 ppmC Toluene,0.9ppmC o-Xyle
st1382	DYMN HC and STAT NO_x One Side; STA	RED :	1.1 ppmC Propene--DYNM	BLUE:	1.1 ppmC Propene--STAT
st1482	Matched HC at 0.62 ppm NO_x	RED :	1.64 ppmC Propene	BLUE:	1.64 ppmC Propene
st1682	HC Substitution at 0.42 ppm NO_x	RED :	2.28 ppmC UNCMIX82, 0.93 ppmC Ethy	BLUE:	2.20 ppmC UNCMIX82,0.93ppmC m-Xy
st1782	Matched AutoExhaust at 0.25 ppm NO_	RED :	2.16 ppmC AutoExhaust--Direct Inje	BLUE:	2.42 ppmC AutoExhst--Cryocondens
st1882	HC Substitution at 0.38 ppm NO_x	RED :	2.2 ppmC UNCMIX82, 0.91 ppmC o-Xyl	BLUE:	2.2 ppmC UNCMIX82,0.89ppmC m-Xyl
st2482	HC Reactivity at 0.33 ppm NO_x	RED :	2.2 ppmC SIMMIX2	BLUE:	3.1 ppmC UNCMIX82
st2982	Matched AutoExhaust--Different Cars	RED :	1.72 ppmC Direct AutoExhaust from	BLUE:	1.74 ppmC Direct AutoExhst from
au0183	HC Reactivity at 0.38 pm NO_x	RED :	4.6 ppmC Toluene	BLUE:	2.6 ppmC o-Xylene
au0683	CO Reactivity One Side Only, at 0.3	RED :	50.2 ppm CO	BLUE:	Background
au1183	Delta HC, Delta CO at 0.23 ppm NO_x	RED :	2.1 ppmC Auto Exhaust from 79 Vola	BLUE:	0.7 ppmC Auto Exhst from 79 Vola
au1983	HC Reactivity at 0.37 NO_x	RED :	4.6 ppmC Isopentane	BLUE:	4.0 ppmC 2,2,4-Trimethylpentane
au2283	STAT and DYNM HC Both: STAT NO_x On	RED :	STAT--0.49 BUT/PROP, 0.55 m-Xylene	BLUE:	STAT-0.48 BUT/PROP,0.55 Toluene;
au2683	STAT HC and NO_x One Side; DYNM HC,	RED :	0.5 ppmC STAT Propene, 1.2 ppmC ST	BLUE:	0.5 ppmC DYNM Propen,1.2 ppmC DY
jl0283	Matched AutoExhaust--2 CARS, Delta	RED :	1.6 ppmC Direct AutoExhaust from C	BLUE:	1.7 ppmC Direct AutoExhst from V
jl0883	Matched AutoExhaust--2 CARS, Delta	RED :	1.7 ppmC 72 Direct AutoExhaust fro	BLUE:	1.7 ppmC 79 Direct AutoExhst fro
jl0983	STAT and DYNM HC Both, STAT NO_x On	RED :	STAT 0.688 BUT/PROP,0.58m-Xylene	BLUE:	STAT 0.643 BUT/PROP, 0.55 Toluene;
jl1583	Matched Auto Exhaust at 0.35 NO_x;	RED :	2.19 ppm AutoExhst from Premium	BLUE:	2.25 ppm AutoExhaust from Regular
jl1783	STAT HC One Side, DYNM HC Other; ST	RED :	1.0 ppmC STAT Propene	BLUE:	1.0 ppmC DYNM Propene

TABLE A-2 Continued.

jl2183	STAT HC and NO_x One Side; DYNM HC	RED :	1.1 ppmC STAT Propene	BLUE:	1.1 ppmC DYNM Propen,0.035 ppm S
jl2483	DAYTIME NO_x Decay: 0.31 ppm NO_x O	RED :	Background	BLUE:	Background
jl2683	Matched HC, Delta CO	RED :	1.0 ppmC Acetaldehyde, 54.9 ppm C	BLUE:	0.97 ppmC Acetaldehyde
jl2783	CO Characterization: One Side Only	RED :	48.6 ppm CO	BLUE:	Background
jl2983	Matched STAT HC at STAT NO_x Both;	RED :	STAT 1.09 ppmC Propene, DYNM Dilut	BLUE:	STAT 1.09 ppmCPropen, DYNM Dilut
jl3183	STAT HC and STAT NO_2 One Side; DYN	RED :	1.09 ppmC STAT Propene	BLUE:	1.09 ppmC DYNM Propene
jn1483	STAT HC and NO_x One Side; DYNM HC	RED :	STAT--1.75 BUT/PROP, 0.85 ppmC STA	BLUE:	DYNM--1.75 BUT/PROP,0.85ppmC DYN
jn2783	STAT HC and NO_x One Side; DYNM HC	RED :	DYNM--1.95 BUT/PROP, 0.93 ppmC Tol	BLUE:	STAT--1.95 BUT/PROP,0.93ppmC Tol
oc0483	HC Reactivity at 0.26 NO_x, Delta C	RED :	2.6 ppmC AutoExhaust, 15.9 ppm CO	BLUE:	2.2 ppmC SynAuto-From Individual
oc0683	DYNM Dilution: STAT HC at STAT 0.36	RED :	2.8 UNCMIX82, 0.85 AROMATIC100683R	BLUE:	2.7 UNCMIX82,0.83ARO-100683B
oc0783	HC Reactivity at 0.35 ppm NO_x	RED :	1.9 ppmC UNCMIX82, 0.75 ppmC COMAR	BLUE:	2.7 ppmC SynAuto
oc1783	DYNM Reactivity: STAT and DYNM HC a	RED :	STAT 1.122 ppmC Propyl, 0.871 ppmC		ppmC Isopen,0.997 ppmC 2,2,4-TMP
st1283	DYNM Delta HC: Stat and Dynm HC at	RED :	STAT 1.08 ppmC UNCMIX82, DYNM 0.4		o-Xyl,0.60ppmC Isopen,0.50 ppmC
st2383	HC Reactivity at 0.38 ppm NO_x	RED :	1.47 ppmC 1-Butene	BLUE:	1.63 ppmC Propene
st2583	Delta HC at 0.45 ppm NO_x	RED :	1.63 ppmC 1-Butene	BLUE:	2.88 ppmC 1-Butene
st2783	HC Reactivity at 0.45 ppm NO_x	RED :	1.59 ppmC 1-Butene	BLUE:	1.59 ppmC t-2-Butene
au0484	HC Substitution at 0.36 NO_x	RED :	1.25 ppmC SynAuto	BLUE:	0.81 ppmC SynAuto,0.32 ppm MeOH,
au0584	Delta HC at 0.35 ppm NO_x	RED :	0.93 ppmC SynAuto	BLUE:	1.33 ppmC SynAuto
au0684	Delta HC at 0.35 NO_x	RED :	2.29 ppmC SynAuto	BLUE:	3.29 ppmC SynAuto
au0784	HC Substitution at 0.38 NO_x	RED :	1.36 ppmC SYNAUTO	BLUE:	0.89 ppmC SYNAUTO,0.30 ppm MeOH,
au0884	HC Substitution at 0.35 NO_x	RED :	2.52 ppmC SynAuto, 0.79 ppm MEOH,	BLUE:	3.73 ppmC SynAuto
au0984	HC Substitution at 0.38 NO_x	RED :	1.30 ppmC SYNAUTO	BLUE:	0.87 ppmC SYNAUTO,0.26 ppm MeOH,
au2284	HC Substitution at 0.32 NO_x, Delta	RED :	3.21 ppmC SYNURBAN	BLUE:	2.14 ppmC SYNURBN,0.87 ppm MeOH,
au2384	HC Reactivity at 0.40 ppm NO_x	RED :	2.999 ppmC methyl-benzyl-Quinone	BLUE:	3.136 ppmC trans-2-Butene
au2584	HC Substitution at 0.35 ppm NO_x	RED :	0.81 ppmC SYNURBAN, 0.30 ppm MeOH,	BLUE:	1.12 ppmC SYNURBAN
jn2684	HC Reactivity at 0.4 NO_x	RED :	2.70 ppmC o-Xylene	BLUE:	2.95 ppmC m-Xylene
jn2784	HC Reactivity at 0.34 ppm NO_x	RED :	1.99 ppmC m-Xylene, 0.25 ppmC Ethe	BLUE:	4.91 ppmC Toluene,0.25 ppmC Ethe
oc0484	Delta HC at 0.36 NO_x	RED :	2.07 ppmC Propene	BLUE:	1.02 ppmC Propene
oc0584	Delta HC at 0.37 NO_x	RED :	3.13 ppmC Ethene	BLUE:	1.80 ppmC Ethene
oc1184	HC Reactivity at 0.35 NO_x	RED :	2.86 ppmC Ethene	BLUE:	2.25 ppmC Propene
oc1284	HC Reactivity at 0.7 NO_x	RED :	2.7 ppmC Ethene	BLUE:	1.9 ppmC Propene
oc1584	Matched HC, Delta CO at 0.021 NO_x,	RED :	1.0 ppmC Acetaldehyde, 0.3 ppm CO	BLUE:	1.0 ppmC Acetaldehyde, 50 ppm CO
st0184	HC Substitution at 0.3 ppm NO_x, De	RED :	2.68 ppmC SYNURBAN, 0.97 ppm MeOH	BLUE:	3.26 ppmC SYNURBAN
st0384	HC Substitution at 0.35 ppm NO_x	RED :	1.11 ppmC SYNURBAN	BLUE:	0.80 ppmC SYNURBAN,0.264ppm MeOH
st0884	Delta HC at 0.33 ppm NO_x, Delta DP	RED :	1.92 ppmC SYNAUTOURBAN	BLUE:	2.84 ppmC SYNAUTOURBAN
st1784	HC Substitution at 0.35 ppm NO_x	RED :	2.31 ppmC SynAutoUrban	BLUE:	1.54 ppmC SynAutoUrbn,0.57 ppm M
st1984	Delta HC at 0.35 NO_x, Delta DP	RED :	4.38 ppmC SYNAUTOLIQ	BLUE:	2.69 ppmC SYNAUTOLIQ
st2184	HC Reactivity at 0.35 ppm NO_x, Del	RED :	2.39 ppmC SynAuto Without HCHO	BLUE:	2.43 ppmC SynAuto, 0.13 ppm HCHO
au2985	HC Substitution at 0.4 ppm NO_x	RED :	2.0 ppmC UNCMIX85; 0.69 ppmC Tolue	BLUE:	2.0 ppmC UNCMIX85;0.26ppmC Tolue
jn2685	Delta HC at 0.30 ppm NO_x	RED :	2.27 ppmC SYNURBAN	BLUE:	3.10 ppmC SYNURBAN
jn2885	HC Substitution at 0.38 NO_x, Delta	RED :	2.39 ppmC SYNURBAN	BLUE:	1.47 ppmC SYNURBAN,0.58ppm MeOH,
oc0185	HCHO Substitution at 0.15 ppm NO_x	RED :	2.85 ppmC UNCMIX85, 0.15 ppmC HCHO		
st0485	HC Reactivity at 0.4 NO_x	RED :	3.105 ppmC AroMix1	BLUE:	3.061 ppmC AroMix2
jl0886	Delta HCHO at 0.17 NO_x	RED :	0.54 ppm Formaldehyde	BLUE:	1.03 ppm Formaldehyde

TABLE A-2 Continued.

jl0986	Delta Ethene at 0.3 ppm NO_x	RED : 0.93 ppmC Ethene	BLUE: 2.10 ppmC Ethene
jl1386	HC Reactivity at 0.29 NO_x	RED : 0.63 ppmC Propene	BLUE: 1.13 ppmC Ethene
oc2886	O_3 DYNM Injected into STAT Ethene	RED : 2.47 ppm Final O3 from DYNM Inject	BLUE: 2.47 ppm Finl O3 frm DYNM Injct
au0988	Delta HC at 0.32 NO_x	RED : 0.89 ppmC Ethene	BLUE: 1.75 ppmC Ethene
au1088	Delta HC at 0.32 NO_x	RED : 1.70 ppmC Ethene	BLUE: 3.35 ppmC Ethene
au1288	Delta HC at 0.58 NO_x	RED : 0.78 ppmC Propene	BLUE: 1.59 ppmC Propene
au1688	HC Reactivity at 0.39 NO_x	RED : 0.80 ppmC Formaldehyde	BLUE: 1.94 ppmC Ethene
au1788	HC Reactivity at 0.36 ppm NO_x	RED : 4.926 ppmC Toluene	BLUE: 1.715 ppmC m-Xylene
au1888	Delta HC at 0.38 ppm NO_x	RED : 3.31 ppmC SYNAUTO	BLUE: 1.92 ppmC SYNAUTO
jl0688	Delta HC at 0.35 NO_x	RED : 3.16 ppmC Ethene	BLUE: 0.57 ppmC Ethene
jl1588	Delta HCHO at 0.3 ppm NO_x	RED : 0.85 ppmC Formaldehyde	BLUE: 0.43 ppmC Formaldehyde
jl2588	NITE RUN--DYNM O_3, NO_x Both Sides	RED: 1.85 ppm O3	BLUE: 1.17 ppm O3, 3.10 ppmC Propene
jl2888	NITE RUN---O_3 DYNM Injection into	RED: 0.881 ppm Final O3 from DYNM Injec	BLUE: 4.41 ppmC STAT 1-Buten,0.362 ppm
st0788	HC Reactivity at 0.36 NO_x	RED : 1.34 ppmC Propene	BLUE: 1.35 ppmC 1-Butene
st1288	Matched HC at 0.32 ppm NO_x	RED : 4.52 ppmC n-Butane	BLUE: 4.47 ppmC n-Butane
st1588	Matched HC at 0.33 ppm NO_x	RED : 8.6106 ppmC n-BUTANE	BLUE: 9.1186 ppmC n-BUTANE
st2288	CO in Red Side at 0.40 ppm NO_x: Wa	RED : Background	BLUE: 50 ppm CO
st2388	CO in Blue Side at 0.8 ppm NO_x Bot	RED : Background	BLUE: 50 ppm CO
st2788	HCHO at Background NO_x Blue Side O	RED : Background	BLUE: 1.29 ppm HCHO
st2888	Day-Old HC One Side; 0.6 ppm NO_x A	RED : 0.0	BLUE: 0.1056 ppm HCHO
au0389	Delta Ethylene at 0.32 ppm NO_x [Re	RED : 1.06 ppmC Ethylene	BLUE: 1.907 ppmC Ethylene
au0290	Delta Methane	RED : 500 ppm Methane	BLUE: 250 ppm Methane
au0390	Delta methane continued	RED : Aug 2, 1990 continued	BLUE: Aug 2, 1990 continued
au2790		RED :	BLUE:
au2890		RED : 2 ppmC Ethylene (Jul 9, 1986 BLUE	BLUE: 1 ppmC Ethylene(Jul9,1986 RED)
oc1690		RED : 2 ppmC Propylene	BLUE: 3 ppmC Ethene
oc1790		RED : 3 ppmC Ethylene	BLUE: 2 ppmC Propylene
oc1890		RED : Background	BLUE: 4 ppmC Ethylene
oc1990		RED : 2nd Day of Oct 18, 1990	BLUE: 2nd Day of Oct 18, 1990
oc2090		RED : 3rd Day of Oct 18, 1990	BLUE: 3rd Day of Oct 18, 1990
oc2190		RED : 4th Day of Oct 18, 1990	BLUE: 4th Day of Oct 18, 1990
st0590		RED : 2 ppmC Ethene	BLUE: 1 ppmC Ethene
st0790	Delta Methane	RED : 250 ppm Methane	BLUE: 500 ppm Methane
st1790	NO RUN: NO2 PHOTOLYSIS MEASUREMENTS	RED : BACKGROUND	BLUE: BACKGROUND
st1890	NO RUN: NO2 PHOTOLYSIS MEASUREMENTS	RED : BACKGROUND	BLUE: BACKGROUND
st1990	NO RUN: NO2 PHOTOLYSIS MEASUREMENTS	RED : BACKGROUND	BLUE: BACKGROUND
st2590		RED : 2 ppmC Propylene	BLUE: 3 ppmC Ethylene
st2790		RED : 250 ppmC Ethane	BLUE: 500 ppmC Ethane
au0991	CRC Run Number 5	RED : 2 ppmC SynUrb/SynIAG	BLUE: 2 ppmC SynUrb/SynM85
au1691	CRC Run 5-- 6:1 SynUrb/SynIAG:NO_x	RED : 1.97 ppmC SynUrb/SynIAG	BLUE: 1.67 ppmC SynUrb/SynM85
au1791	CRC Run Number 5 (second day)	RED : 2 ppmC SynUrb/SynIAG	BLUE: 2 ppmC SynUrb/SynM85
au2191	CRC Run 6-- 6:1 SynUrb/SynM85:NO_x	RED : 2.91 ppmC SynUrb/SynM85	BLUE: 3.17 ppmC SynUrb/SynIAG
au2291	2nd Day	RED : 2.85 ppmC SynUrb/SynM85 (second da	BLUE: 3.06 ppmC SynUrb/SynIAG (2nd da
au2391	Run C3-- CO vs Methane	RED : 100 ppm CO	BLUE: 500 ppm methane

TABLE A-2 Continued.

au3091	Run 4-- 4.5:1 SynUrb/SynIAG:NO_x vs	RED : 1.54 ppmC SynUrb/SynIAG	BLUE: 1.55 ppmC SynUrb/SynM85
au3191	CRC Run Number 4.2, additional NO (	RED : 1.54 ppmC SynUrb/SynIAG (second da	BLUE: 1.55 ppmC SynUrb/SynM85 (2nd da
jl2191	Run C1-- Delta Methane	RED : 500 ppmC Methane	BLUE: 250 ppmC Methane
jl2391	CRC Run 8--6:1 SynM85/NO_x vs 6:1 S	RED : 2.013 ppmC SynM85	BLUE: 2.135 ppmC SynIAG
jl2491	CRC Run 8--9:1 SynIAG/NO_x vs 9:1 S	RED : 3.033 ppmC SynIAG	BLUE: 2.937 ppmC SynM85
oc0191	junk	RED : junk	BLUE: junk
oc0791	junk	RED : junk	BLUE: junk
oc1091	Matched Run at 0.35 ppm NO_x	RED : 3.0 ppmC Ethene	BLUE: 3.0 ppmC Ethene
oc1391	Delta Methyl Ethyl Ketone	RED : 30 ppmC MEK	BLUE: 15 ppmC MEK
oc2391	Background	RED : Background	BLUE: Background
oc2491	Run #3-- 9:1 SynUrb/SynM85:NO_x vs	RED : 3.05 ppmC SynUrb/SynM85	BLUE: 3.03 ppmC SynUrb/SynIAG
oc2591		RED : Background	BLUE: Background
oc2691	CRC Run 1-- 4.5:1 SynUrb/SynIAG:NO_	RED : 1.47 ppmC SynUrb/SynIAG	BLUE: 1.45 ppmC SynUrb/SynM85
st0291	Run 10-- 4.5:1 SynUrb/SynIag/HCHO:N	RED : 1.47 ppmC SynUrb/SynIAG+HCHO	BLUE: 1.44 ppmC SynUrb/SynM85+HCHO
st0391	Run 11-- 6:1 SynUrb/SynM85/HCHO:NO_	RED : 2.04 ppmC SynUrb/SynM85+HCHO	BLUE: 2.04 ppmC SynUrb/SynIAG+HCHO
st0491	Run 8-- 6:1 SynIAG:NO_x vs 6:1 SynM	RED : 2.09 ppmC SynIAG	BLUE: 2.03 ppmC SynM85
st0591	Run 9-- 6:1 SynM85:NO_x vs 6:1 SynU	RED : 2.12 ppmC SynM85	BLUE: 2.00 ppmC SynUrb
st0891	CRC Run 11-- 6:1 SynUrb/SynIAG/HCHO	RED : 2.01 ppmC SynUrb/SynIAG+HCHO	BLUE: 1.94 ppmC SynUrb/SynM85+HCHO
st0991	CRC Run 11-- 6:1 SynUrb/SynIAG/HCHO	RED : 1.89 ppmC SynUrb/SynIAG+HCHO	BLUE: 1.87 ppmC SynUrb/SynM85+HCHO
st1091	Run 7-- 6:1 SynUrb:NO_x vs 6:1 SynI	RED : 2.10 ppmC SynUrb	BLUE: 1.97 ppmC SynIAG
st1291	Run 7-- 6:1 SynIAG:NO_x vs 6:1 SynU	RED : 2.17 ppmC SynIAG	BLUE: 2.20 ppmC SynUrb
st1591	Run 2-- 6:1 SynUrb/SynM85:NO_x vs 6	RED : 2.14 ppmC SynUrb/SynM85	BLUE: 2.12 ppmC SynUrb/SynIAG
st1791	Run 2-- 6:1 SynUrb/SynIAG:NO_x vs 6	RED : 2.14 ppmC SynUrb/SynIAG	BLUE: 2.16 ppmC SynUrb/SynM85
st1891	Run C1a- Matched Methane	RED : 500 ppm Methane	BLUE: 500 ppm Methane
st2191	Delta n-butane	RED : 10 ppmC Butane	BLUE: 20 ppmC Butane
st2291	Junk	RED : 10 ppmC Butane; 1 ppmC Ethylene	BLUE: 20 ppmC Butane; 1 ppmC Ethylene
st2991	Dual Isoprene	RED : 6 ppmC Isoprene	BLUE: 2 ppmC Isoprene
st2991f	Dual Isoprene	RED : ppmC Isoprene	BLUE: ppmC Isoprene
st3091	N-butane	RED : Junk	BLUE: Junk
au1092	CRC Run C1-- Delta Methane	RED : 500 ppm Methane	
au1192	Run 14-- 3.8:1 SynUrb:NO_x vs 3.8:1	RED : 1.288 ppmC SynIAG, without aromati	BLUE: 1.217 ppmC SynUrb, w/o aromati
au1992	CRC Run 20-- 6:1 SynAOF:NO_x vs 6:1	RED : 2.13 ppmC SynAOF	BLUE: 2.09 ppmC SynIAG
au2492	CRC Run 20-- 6:1 SynAOF:NO_x vs 6:1	RED : 2.15 ppmC SynAOF	BLUE: 2.12 ppmC SynIAG
au2592	CRC Run 17-- 6:1 SynUrb/SynAOF:NO_x	RED : 2.08 ppmC SynUrb/SynAOF	BLUE: 2.05 ppmC SynUrb/SynIAG
au3092	CRC Run 15-- 3:1 SynUrb Aromatic:NO	RED : 1.125 ppmC SynUrb(Aromatic)	BLUE: 1.082 ppmC SynIAG(Aromatic)
au3192	CRC Run 18-- 9:1 SynUrb/Synamot:NO_	RED : 3.29 ppmC SynUrb/Synamot	BLUE: 3.12 ppmC SynUrb/SynIAG
jl0792	CRC Run C2--Delta Carbon Monoxide R	RED : 100 ppm CO	BLUE: 250 ppm CO
jl0892	Matched CRC Run-- 6:1 SynUrb:NO_x	RED : 2.55 ppmC SynUrb	BLUE: 2.54 ppmC SynUrb
jl0992	CRC Run C4-- Matched 6:1 SynUrb:NO_	RED : 2.45 ppmC SynUrb	BLUE: 2.58 ppmC SynUrb
jl1092	CRC Run 2-- 6:1 SynUrb/SynIAG:NO_x	RED : 2.08 ppmC SynUrb/SynIAG	BLUE: 2.06 ppmC SynUrb/SynM85
jl1392	Run 6:1 SynUrb:NO_x vs CARTER Mix:N	RED : 2.0 ppmC CARTER Mix	BLUE: 2.0 ppmC SynUrb
jl1492	Run 11- 6:1 SynUrb/SynIAG:NO_x vs 6	RED : 2.0 ppmC SynUrb/SynM85/HCHO(3x)	BLUE: 2.0 ppmC SynUrb/SynIAG
jl1592	CRC Run 11--6:1 SynUrb/SynIAG:NO_x	RED : 2.12 ppmC SynUrb/SynM85+HCHO(x3)	BLUE: 2.24 ppmC SynUrb/SynIAG
jl3092	CRC Run C1--Delta Methane	RED : 500 ppm Methane	BLUE: 250 ppm Methane

TABLE A-2 Continued.

jl3192	2nd Day 500 ppmC Methane vs 250 ppm	RED : 500 ppm Methane	BLUE: 250 ppm Methane
jn0192	Delta MEK Run	RED : 16 ppmC MEK	BLUE: 8 ppmC MEK
jn0892	Delta MVK	RED : 2.1 ppmC MVK	BLUE: 7.7 ppmC MVK
jn1892	Delta Butane Run	RED : 39 ppmC Butane	BLUE: 20 ppmC Butane
jn2192	HCHO Run	RED : 1 ppmC HCHO	BLUE: 0.5 ppmC HCHO
jn2392	Propylene Run (Matched)	RED : 1 ppmC Propylene	BLUE: 1 ppmC Propylene
jn2592	Delta Isoprene	RED : 2.94 ppmC Isoprene	BLUE: 5.99 ppmC Isoprene
jn2892	Methacrolein Run	RED : 7.8 ppmC Methacrolein	BLUE: 2.0 ppmC Methacrolein
my2292	Delta Butane Run	RED : 40 ppmC Butane	BLUE: 20 ppmC Butane
my2392	Delta Butane Run	RED : 37 ppmC Butane	BLUE: 18 ppmC Butane
oc0292	CRC Run 2-- 6:1 SynUrb/SynM85:NO_x	RED : 1.80 ppmC SynUrb/SynM85	BLUE: 1.94 ppmC SynUrb/SynIAG
oc1392	CRC #21	RED : Drying	BLUE: Drying
oc1492	CRC Run 21-- 6:1 SynAOF:NO_x vs 6:1	RED : 2.07 ppmC SynAOF	BLUE: 2.03 ppmC SynM85
oc2292	CRC Run 3-- 9:1 SynUrb/SynIAG:NO_x	RED : 3.32 ppmC SynUrb/SynIAG	BLUE: 3.49 ppmC SynUrb/SynM85
oc2492	CRC Run C1-- Delta Methane	RED : 250 ppmC Methane	BLUE: 500 ppmC Methane
oc2792	CRC Run 11-- 6:1 SynUrb/SynM85+HCHO	RED : 2.07 ppmC SynUrb/SynM85+HCHO(3x)	BLUE: 2.44 ppmC SynUrb/SynIAG
st0192	CRC Run 10-- 4.5:1 SynUrb/SynIAG:NO	RED : 1.55 ppmC SynUrb/SynM85+HCHO(3x)	BLUE: 1.49 ppmC SynUrb/SynIAG
st0292	CRC Run 1-- 4.5:1 SynUrb/SynIAG:NO_	RED : 1.48 ppmC SynUrb/SynM85	BLUE: 1.48 ppmC SynUrb/SynIAG
st0790	Delta Methane	RED : 250 ppm Methane	BLUE: 500 ppm Methane
st1592	Isoprene Run (Delta NOx)	RED : 1.5 ppmC Isoprene	BLUE: 1.5 ppmC Isoprene
au0593	Isoprene One Side + O3 both sides:	RED : 0.0 ppmC Isoprene	BLUE: 5.0 ppmC Isoprene
au1193	Matched 250 ppm CO	RED : 250 ppm CO	BLUE: 250 ppm CO
au1693	Acetone vs Ethane in SynUrb	RED : 1 ppm Ethane 1 ppm SynUrb	BLUE: 1 ppm Acetone 1 ppm SynUrb
au1993	CNG vs IAG in SynUrb	RED : 1 ppm SynCNG 1 ppm SynUrb	BLUE: 1 ppm SynIAG 1 ppm SynUrb
au2393	Delta Ethylene	RED : 2.039 ppmC Ethylene	BLUE: 0.981 ppmC Ethylene
au2493	Propylbenzene vs Ethylbenzene	RED : 1.45 ppmC propylbenzene	BLUE: 1.45 ppmC ethylbenzene
au3093	Delta CO	RED : 250 ppm CO	BLUE: 100 ppm CO
jl0893	Toluene	RED : 2.07 ppmC Toluene	BLUE: 1.03 ppmC Toluene
jl1393	m-Xylene	RED : 0.93 ppmC m-Xylene	BLUE: 0.50 ppmC m-Xylene
jl1593	1,2,4 trimethylbenzene	RED : 0.5 ppmC 1,2,4 trimethylbenzene	BLUE: 0.25 ppmC 1,2,4 trimethylbenzene
jl2193	Delta 1,2,4 trimethylbenzene	RED : 0.43 ppmC 1,2,4 trimethylbenzene	BLUE: 0.25 ppmC 1,2,4 trimethylbenzene
jl2893	m/o-Xylene	RED : 0.41 ppmC o-Xylene	BLUE: 0.48 ppmC m-Xylene
jl3093	CO	RED : 100 ppm CO	BLUE: 100 ppm CO
jn0893	Isoprene One Side and O3 0.3 ppm hr	RED : 2.0 ppmC Isoprene	BLUE: Background
jn1093	Matched Isoprene & Ozone: Night; Me	RED : 2.0 ppmC Isoprene & 100 ppmC Methy	BLUE: 2.0 ppmC Isoprene
jn1193	Isoprene & Ozone Night Run	RED : 5.0 ppmC Isoprene	BLUE: 2.5 ppmC Isoprene
jn1793	Delta Isoprene	RED : 4.7 ppmC Isoprene	BLUE: 2.4 ppmC Isoprene
jn2393	Matched Propylene	RED : 1.0 ppmC Propylene	BLUE: 1.0 ppmC Propylene
no0380	Night O3 Methacrolein vs Methylviny	RED : 3.6 ppmC Methacrolein	BLUE: 3.7 ppmC Methylvinylketone
oc0693	Toluene vs m-Xylene	RED : 1.935 ppmC Toluene	BLUE: 0.803 ppmC m-Xylene
oc0980	Night O3 Isoprene vs O3 only	RED : 5.0 ppmC Isoprene	BLUE: Background
st1093	CNG vs IAG in SynUrb	RED : 1 ppm SynUrb + 1 ppm SynCNG	BLUE: 1 ppm SynUrb + 1 ppm SynIAG
st1393	Toluene vs m-Xylene	RED : 0.789 ppmC m-Xylene	BLUE: 1.909 ppmC Toluene
st1593	Isoprene with O3 ramped Inject Both	RED : 2.5 ppmC Isoprene with 773 ppmC Cy	BLUE: 2.5 ppmC Isoprene

TABLE A-2 Continued.

st2093	500 vs 250 Methane	RED : 250 ppm Methane	BLUE: 500 ppm Methane
st2393	SynCNG/SynURB vs SynIAG/SynURB	RED : 1.5 ppmC SynURB + 1.5 ppmC SynIAG	BLUE: 1.5 ppmC SynURB+1.5 ppmC SynCNG
st2893	Matched NOx; Added 250 ppm CO	RED : High NO2 + 100 ppm CO + 150 ppm CO	BLUE: High NO+100 ppm CO + 150 ppm CO
st2993	Cyclohexane and DMDO Night Run	RED : Background	BLUE: 12 ppmC Cyclohexane+0.43 DMDO
st3093	Cyclohexane and DMDO	RED : Background	BLUE: 12 ppmC Cyclohexane+0.43 ppmV DM
au0194	SynCNG vs SynIAG in SynURB/NOx	RED : 0.50 ppmC Toluene + 0.25 ppmC m-Xy	BLUE: 0.25 ppmC Toluene+0.17 ppmC m-Xy
au0394	SynE85B vs SynIAG in SynURB/NOx	RED : 1.0 ppmC SynE85B + 1.0 ppmC SynURB	BLUE: 1.0 ppmC SynIAG+1.0 ppmC SynURB
au0494	SynE85E vs SynIAG in SynURB/NOx	RED : 1.0 ppmC SynE85E + 1.0 ppmC SynURB	BLUE: 1.0 ppmC SynIAG+1.0 ppmC SynURB
au0794	SynE85E vs SynIAG in SynURB/NOx	RED : 1.0 ppmC SynE85E + 1.0 ppmC SynURB	BLUE: 1.0 ppmC SynIAG+1.0 ppmC SynURB
au0894	SynE85B vs SynIAG in SynURB/NOx	RED : 1.0 ppmC SynURB + 1.0 ppmC SynE85E	BLUE: 1.0 ppmC SynURB+1.0 ppmC SynIAG
au0994	SynE85E-Acetaldehyde vs SynIAG in S	RED : 1.0 ppmC SynURB + 1.0 ppmC SynE85E	BLUE: 1.0 ppmC SynURB+1.0 ppmC SynIAG
au1194	SynE85E vs SynIAG in SynURB/NOx	RED : 1.0 ppmC SynURB + 1.0 ppmC SynE85E	BLUE: 1.0 ppmC SynURB+1.0 ppmC SynIAG
au1294	SynE85E vs SynIAG in SynURB/NOx	RED : 0.75 ppmC SynE85E + 0.75 ppmC SynU	BLUE: 0.75 ppmC SynIAG+0.75 ppmC SynU
au2394	SynE85E vs SynIAG in SynURB/NOx	RED : 0.75 ppmC SynURB + 0.75 ppmC SynIA	BLUE: 0.75 ppmC SynURB+0.75 ppmC SynE8
au2494	SynE85E vs SynIAG in SynURB/NOx	RED : 1.5 ppmC SynIAG + 1.5 ppmC SynURB	BLUE: 1.5 ppmC SynE85E+1.5 ppmC SynURB
au2594	SynE85E vs SynIAG in SynURB/NOx	RED : 1.5 ppmC SynURB + 1.5 ppmC SynIAG	BLUE: 1.5 ppmC SynURB+1.5 ppmC SynE85E
au2694	SynCNG vs SynIAG in SynURB/NOx	RED : 1.5 ppmC SynCNG + 1.5 ppmC SynURB	BLUE: 1.5 ppmC SynIAG+1.5 ppmC SynURB
au2994	250 ppm CO vs 250 ppm CO; staggered	RED : 250 ppm CO and 0.33 ppm NOx early	BLUE: 250 ppm CO and 0.33 ppm NOx late
au3194	250 ppm CO vs 100 ppm CO; matched N	RED : 250 ppm CO	BLUE: 100 ppm CO
jl0194	Matched Propene/NOx	RED : 1.5 ppmC Propylene	BLUE: 1.5 ppmC Propylene
jl0894	Toluene vs m-Xylene with NOx	RED : 0.52 ppmC m-Xylene	BLUE: 0.93 ppmC Toluene
jl1594	Matched Toluene/Xylene/NOx	RED : 0.50 ppmC Toluene + 0.25 ppmC Xyle	BLUE: 0.50 ppmC Toluene+0.25 ppmC Xyle
jl2094	Matched Toluene/Xylene/NOx	RED : 0.47 ppmC Toluene + 0.21 ppmC Xyle	BLUE: 0.42 ppmC Toluene+0.21 ppmC Xyle
jl2594	SynCNG vs SynIAG in SynURB/NOx	RED : 1.0 ppmC SynCNG + 1.0 ppmC SynURB	BLUE: 1.0 ppmc SynIAG+1.0 ppmC SynURB
oc0994	Equal Mass SynURB/SynE85 vs SynURB/	RED : Equal Mass SynURB + SynE85	BLUE: Equal Mass SynURB + SynIAG
oc0994k	Equal Mass SynUrb/SynE85 vs SynUrb/	RED : Equal Mass SynUrb/SynE85	BLUE: Equal Mass SynUrb/SynIAG
oc1294		RED : Stepped CO with NO	BLUE:
oc1394		RED : Stepped CO with NO	BLUE:
oc1894	Toluene vs m-Xylene	RED : 3.0 ppmC m-Xylene	BLUE: 4.0 ppmC Toluene
st0894	SynE85E vs SynIAG	RED : 2.0 ppmC SynIAG	BLUE: 2.0 ppmC SynE85
st0994	SynE85E vs SynURB	RED : 2.0 ppmC SynE85	BLUE: 2.0 ppmC SynURB
st1194	SynE85E vs SynURB	RED : 2.0 ppmC SynURB	BLUE: 2.0 ppmC SynE85E
st1294	Matched SynURB	RED : 2.0 ppmC SynURB	BLUE: 2.0 ppmC SynURB
st1494	SynURB vs SynURB/SynE85	RED : 1.0 ppmC SynURB + 1.0 ppmC SynE85E	BLUE: 2.0 ppmC SynURB
st1594	SynURB vs SynURB/SynE85 (no EtOH)	RED : 1.0 ppmC SynURB + 1.0 ppmC SynE85E	BLUE: 2.0 ppmC SynURB
st1994	Night Isoprene + O3 matched; one si	RED : 5.0 ppmC Isoprene + O3	BLUE: 5.0 ppmC Isoprene+O3; 600 ppm CO
st2094	Night Isoprene + O3 matched; one si	RED : 5.0 ppmC Isoprene + O3	BLUE: 5.0 ppmC Isoprene+O3; 600 ppm CO
st2494	SynURB/SynLPG vs SynURB/SynIAG	RED : 1.0 ppmC SynURB + 1.0 ppmC SynLPG	BLUE: 1.0 ppmC SynURB+1.0 ppmC SynIAG
st2794	SynURB/SynLPG vs SynURB/SynIAG	RED : 1.0 ppmC SynURB + 1.0 ppmC SynLPG	BLUE: 1.0 ppmC SynURB+1.0 ppmC SynIAG
st2894	SynURB/SynE85(+EtOH) vs SynURB/Syn	RED : 1.0 ppmC SynURB + 1.0 ppmC SynE85	BLUE: 1.0 ppmC SynURB+1.0 ppmC SynIAG
ap1895	1-butene vs t-2-butene	RED : 8 ppmC 1-Butene	BLUE: 8 ppmC t-2-butene
ap2095	Isobutylene vs t-2-butene/Ethene	RED : 8 ppmC IsoButylene	BLUE: 4 ppmC t-2-butene&2 ppmC Ethylen
ap2695	cis-2-butene vs 1-butene	RED : 8 ppmC 1-butene	BLUE: 8 ppmC cis-2-butene
ap2895	Ethylene vs Propylene	RED : 4 ppmC Ethylene	BLUE: 6 ppmC Propylene

TABLE A-2 Concluded.

au0195	Matched Ethylene;	RED : 2 ppm Ethylene	BLUE: 2 ppm Ethylene
au0395	Matched Ethylene;	RED : 1 ppm p-Xylene	BLUE: 1 ppm 1,3,5-Trimethylbenzene
au3095	Matched Ethylene;	RED : 1 ppm m-Xylene	BLUE: 1 ppm Toluene
fe2495	cis-2-butene vs isobutylene	RED : 8 ppmC cis-2-butene	BLUE: 8 ppmC isobutylene
jl1495	CO test: Molecular Sieve	RED : 100 ppm Non-Filtered CO	BLUE: 100 ppm Filtered CO(13x molsiev
jl2695	CO test: Molecular Sieve	RED : 2 ppm Propene	BLUE: 2 ppm Propene
jn1395	MATCHED ACROLEIN + OZONE WITH ETHYL	RED : ACROLEIN + ETHYLENE +O3	BLUE: ACROLEIN + O3
jn1495	MATCHED ACROLEIN + OZONE WITH ETHYL	RED : ACROLEIN + ETHYLENE +O3	BLUE: ACROLEIN + O3
jn1895	Matched O3 Injection Equal to Jun 1	RED : O3 Injection	BLUE: O3 Injection
jn1995	CO test: Molecular Sieve	RED : Non-Filtered CO	BLUE: Filtered CO
my2495	1-Butene vs cis-2-butene	RED : 10 ppmC 1-Butene	BLUE: 10 ppmC cis-2-Butene
my2595	Ozone and 1-Butene Night	RED : Ozone 1-Butene	BLUE: Ozone Only
my3195	CO test: Molecular Sieve	RED : Non-Filtered CO	BLUE: Filtered CO
oc0395	Matched CO and NOx; One CO filtered	RED : 250 ppm CO Filtered	BLUE: 250 ppm CO Non-filtered
oc1295	Delta Methane matched NOx	RED : 300 ppm CH4	BLUE: 600 ppm CH4
st0195	Aromatic run; Matched NOx	RED : 1 ppm 1,2,4-tri-methylbenzene	BLUE: 1 ppm o-Xylene
st1195	Aromatic run; Matched NOx	RED : 3 ppm Benzene plus 1 ppm HCHO	BLUE: 3 ppm Benzene
st1295	Propene vs Ethene run; Matched NOx	RED : 1 ppm Propene	BLUE: 1 ppm Ethene
st1995	Propene vs Ethene run; Matched NOx	RED : 6.12 ppmC Propene	BLUE: 4.00 ppmC Ethene
st2895	Benzene + HCHO vs Ethylbenzene run;	RED : 3 ppm Benzene + 1 ppm HCHO	BLUE: 1.5 ppm Ethylbenzene